DEWATERING OF MICROALGAE USING FLOCCULATION AND ELECTROCOAGULATION

A thesis submitted in fulfillment of the requirement of the degree of
Doctor of Philosophy by

Nyomi Uduman

Bachelor of Science

Bachelor of Chemical Engineering (Hons.)

Department of Chemical Engineering

Monash University

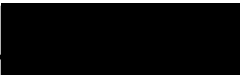Clayton Victoria Australia

October 2012

DECLARATION

Declaration for thesis based or partially based on conjointly published or unpublished work

In accordance with Monash University Doctorate Regulation 17 / Doctor of Philosophy regulations the following declarations are made:

I hereby declare that this thesis contains no material which has been accepted for the award of any other degree or diploma at any university or equivalent institution and that, to the best of my knowledge and belief, this thesis contains no material previously published or written by another person, except where due reference is made in the text of the thesis.

The core theme of the thesis is DEWATERING OF MARINE MICROALGAE USING FLOCCULATION AND ELECTROCOAGULATION. The ideas, development and writing up of all the papers in the thesis were the principal responsibility of Nyomi Uduman, the candidate, working within the Department of Chemical Engineering under the supervision of Dr. Andrew Hoadley and Dr. Michael Danquah.

The inclusion of co-authors reflects the fact that the work came from active collaboration between researchers and acknowledges input into team-based research.

Signed: ███████████ ...

Date: ......01|10|12...............

I

ACKNOWLEDGEMENTS

THESIS SUMMARY

Sustainable development and environmental protection has become a major global concern. Biofuels are an alternative transport fuel that can reduce the consumption of non renewable carbon resources and greenhouse gas emissions. Biodiesel is a type of biofuel that is made from renewable lipid containing biological resources and is non toxic. Current feedstocks for biodiesel production include vegetable oils and animal fats, which are vital components of the human food chain, and this makes them less suitable for biofuel production. Lipid-containing microalgal biomass is another feedstock for biodiesel production and has the potential to replace the conventional sources. Microalgae could have many advantages over traditional feedstocks, such as fast photosynthetic growth rates and high lipid content, and these have triggered interest in microalgae bioprospecting. However, one of the main disadvantages of microalgae-to-biofuel process engineering is the high energy consumption and operational costs associated with the culture dewatering stage for biomass creation. This is due to the small size of microalgae cells and the extremely dilute nature of the microalgae culture even at the late exponential phase of the cultivation process. In order to make biodiesel production from microalgae sources commercially viable, the dewatering step must be technologically and economically effective. Current dewatering technologies such as centrifugal recovery and filtration are highly energy intensive. Cell aggregation induced by either flocculation or coagulation is another commonly used dewatering technique that has the advantage of using less energy under optimum conditions. These techniques have found numerous applications in industrial wastewater treatment, and hence could have a potential application for microalgae removal.

The work conducted in this research investigated two dewatering techniques for microalgae under the umbrella of bioseparation by induced cell aggregation; flocculation and electrocoagulation. A series of batch experiments were carried out under varying experimental conditions using two marine microalgae species; *Chlorococcum sp.* and *Tetraselmis sp.* The key assessment criterion, the microalgae

recovery, was quantified by determining the amount of microalgae recovered, that is, the amount of microalgae that settled due to flocculation or floated due to electrocoagulation.

Two types of flocculants were used in this research; polyelectrolytes and aluminium sulphate (alum). All flocculants were able to achieve successful microalgae flocculation to varying degrees. Contrary to literature, the results from this research showed that anionic and non-ionic polyelectrolytes were able to adequately flocculate marine microalgae. It was also found that alum flocculation was possible at doses that were comparable to those used for freshwater microalgae flocculation, where previous literature had stated that the doses required for marine microalgae flocculation required were in the range of 5 to 10 times larger. The polyelectrolyte flocculants were able to achieve up to 90 % recovery at doses between 2 to 10 mg/L. Alum was able to achieve up to 99 % recovery at doses under 100 mg/L. Flocculation recovery was seen to increase with pH, and the zeta potential showed that the microalgae become more electropositive with decreasing pH. The recovery of microalgae was also seen to increase with increasing temperature.

Electrocoagulation was carried out with two sacrificial anode materials; aluminium and ferritic stainless steel type 430, and a carbon inert anode. The maximum recovery obtained was 99, 90 and 38 % for electrocoagulation with the stainless steel 430, aluminium and carbon anodes, respectively. In order of efficiency, the optimum anode was aluminium, stainless steel 430 and then carbon. The microalgae recovery increased with increasing applied voltage and electrocoagulation time. The valencies of dissolved metal ions from the anode were investigated for multivalent species and confirmed with a metallic and ionic mass balance of the dissolution and electrocoagulation process. The pH of the solution did not appear to have a significant effect on recovery. The zeta potential of the microalgae after electrocoagulation was seen to become more electropositive with increasing experimental run time. An increase in temperature increased recovery whilst a reduction in salinity resulted in reduced microalgal recovery.

The theory of the mechanism of electrocoagulation was proven with the results of the experimental work conducted in this research. Evidence was shown of the three main steps involved in the electrocoagulation mechanism; coagulation, charge neutralisation and flotation. The results demonstrated that coagulation of microalgae occurs in the bulk of solution, and not at a specific location such as in the vicinity of an electrode. The rate limiting step of the electrocoagulation process was found to be the rate of coagulation of microalgae cells, induced by the binding of metal ions onto the microalgae surface.

A mathematical model was developed in order to predict the recovery of microalgae at predetermined electrocoagulation conditions such as the applied current, time, microalgae species and electrode material. The mathematical model was able to accurately predict microalgae recovery for all microalgae systems. This model made it possible to optimise the electrocoagulation process for conditions that required a low energy demand and accomplished high microalgae recovery. These optimum conditions enabled a comparison between alum flocculation and the aluminium anode electrocoagulation. Such a comparison is interesting as the two processes have a similar flocculation mechanism.

A techno-economic and carbon assessment was performed on the unit operation of microalgal culture dewatering operation as part of the microalgal biodiesel production process. This involved estimating the operation costs, carbon dioxide emissions and energy consumption. Three different dewatering technologies were investigated; centrifugation, electrocoagulation/centrifugation and alum flocculation/centrifugation. The analysis showed that both electrocoagulation and flocculation require significantly less energy to dewater in comparison to centrifugation. However, when the energy to produce the raw materials was taken into account, electrocoagulation was found require a greater energy demand. The operational cost of continual replacement of the anodic material significantly increased the overall economics of electrocoagulation compared to alum flocculation. In terms of energy requirements, carbon dioxide emissions and overall costs, alum flocculation showed to be the most promising dewatering technique

with genuine potential to be used as the main dewatering technology in microalgae sourced biodiesel production.

Future work may involve the investigation of electrocoagulation as a continuous process and also the combination of alum flocculation and electrocoagulation as a single dewatering method.

CONTENTS

Nomenclature

A_0 Initial mass of microalgae at time zero (g)

A_∞ Mass of unflocculated microalgae at infinite time (g)

b Mass ratio of metal ions used for coagulation per gram of microalgae

BOD   Biological Oxygen Demand (ppm)

COD   Chemical Oxygen Demand (ppm)

D Diameter (m)

DC   Direct Current (A)

dE Change in energy

dM Change in mass

E^o Electrode potential (V)

e^- Electron

EOM   Extracellular Organic Matter

F   Faradays Constant

FBRM   Focused Beam Reflectance Measurement

fps   Frames Per Second

g   Gravitational acceleration (m/s^2)

i Current (A)

k' Rate constant

k Rate constant

M Relative molecular weight (g/mol)

m Mass (g)

m_{H_2} Mass of hydrogen gas (g)

m_{floc} Mass of flocs (g)

n Amount (mol)

N Agitator speed (s^{-1})

N_p Power number

ppm   Parts Per Million

r Radius (m)

Re   Reynolds number

rpm   Revolutions per minute

t Time (s)

TSS   Total Suspended Solids (ppm)

v/v   Volume/Volume

w Quantity of electrode material dissolved (g)

w/v   Weight/Volume

v Velocity (m/s)

V Volume (L)

x Mass of hydrogen gas used per mass of microalgae floc (g)

x_{21} Amount of hydrogen where the density of flocs equal the critical density (g)

y Fraction of microalgae that does not flocculate

z Number of electrons in Faradays law equation

ρ_C Critical density (kg/m^3)

ρ_{floc}^{0} Density of floc at time zero (kg/m^3)

ρ_{fluid} Density of sea water (kg/m^3)

ρ_{H_2} Density of hydrogen (kg/m^3)

ρ_{sphere} Density of floc (kg/m^3)

μ Viscosity of microalgae (Ns/m^2)

σ Standard deviation

List of Figures

List of Tables

CHAPTER 1 INTRODUCTION AND BACKGROUND

Lack of sustainable practices and environmental degradation are major issues of our world today, and it has become a global goal to reduce anthropological carbon dioxide emissions contributing to the greenhouse effect and thus global warming. One of the chief sources of energy is petroleum, which has the major disadvantage of creating atmospheric pollution. (Hossain, A. B. M. S. 2008; Antoni, D. et al. 2007) 90 % of transport fuels are hydrocarbon sourced and with the depleting reserves of oil the search for alternative fuels becomes more and more imperative (Shirvani, T. et al. 2011). Thus a reduction in transportation emissions can play a significant role in the reduction of total greenhouse gas emissions.

Biodiesel is an alternative fuel that is made from renewable biological sources which include vegetable oils and animal fats. Biodiesel is non toxic and biodegradable and has a low emission profile (Ma, F. and Hanna, M. A. 1999; Demirbas, A. and Karslioglu, S. 2007). The particular importance of biodiesel in today's society is that it can be a potential replacement for petroleum derived diesel fuel, which is also becoming unsustainable due to depleting supplies (Demirbas, A. and Demirbas, M. F. 2011; Scott, S. A. et al. 2010; Danquah, M.K. et al. 2009; Chisti, Y. 2007). The increasing prices of crude oil and the growing political instability in oil producing countries is another factor which places emphasis on the need to look into other sources of transport fuel (Antoni, D. et al. 2007).

Vegetable oils and animal fats are currently being used as feedstocks to produce biodiesel. However these sources also provide a valuable food commodity for human consumption. The competition between food and fuel may lead to an increase in their price, which is a great concern where there is insufficient food to satisfy global requirements (Bull, J. J. and Collins, S. 2012; Chisti, Y. 2007).

Microalgae is another source of oil to that of vegetable oils or animal fats which can be converted into biodiesel. Microalgae are able to photosynthetically convert

carbon dioxide into algal biomass. The use of microalgae to create biodiesel has many advantages over the currently used biodiesel production sources. Microalgal crops, unlike other oil crops, are able to grow extremely fast (Shirvani, T. et al. 2011). Microalgae can be grown throughout the year and can be harvested continuously on non-agricultural land, even in arid regions of the world. Some species of oil producing microalgae can make use of water that is not suitable for conventional agriculture (Shirvani, T. et al. 2011; De La Noue, J. and De Pauw, N. 1988). Unlike other sources of biodiesel, the demand for a large area of land is greatly reduced when using microalgae. An example of the productivity of algae is that it is estimated that with further optimisation, microalgae can realistically produce approximately 40 tonnes per hectare per year of oil at a large scale, which is significantly greater than the yield of oil achievable with land based crops. (Stephenson A. L. et al. 2010)

1.1 Microalgae Sourced Biodiesel Production

Figure 1.1 shows a flow diagram of the main steps involved in the microalgae sourced biodiesel production process.
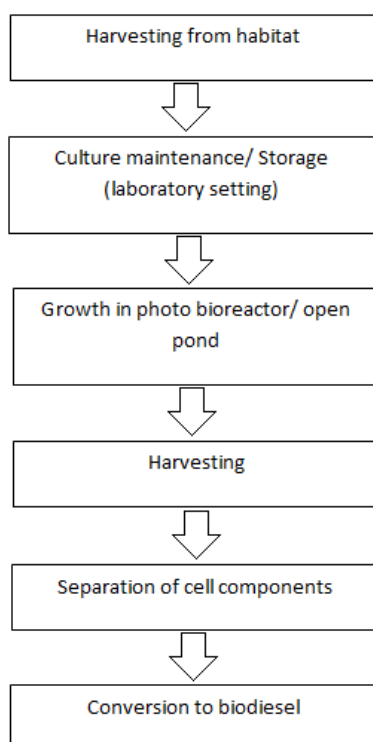
Figure 1. 1. A flow diagram showing steps in microalgal biodiesel production.

(Sander, K. and Murthy, G. S. 2010).

The first stage includes the growth and culturing of the microalgae. The large-scale production of microalgal biomass is generally a continuous system where fresh culture medium is fed at a constant rate while microalgal broth is continuously removed.

Microalgae grow via photosynthesis. Light, carbon dioxide, water and a growth medium (inorganic salts, vitamins and elemental materials such as nitrogen and phosphorus) are required for photosynthetic growth. The temperature of the system must generally stay between 20 to 30 °C. Agitation is also an important aspect of microalgal cultivation because it helps to avoid sedimentation, photoinhibition, nutrient limitation, thermal stratification and increases the light conversion efficiency (De La Noue, J. and De Pauw, N. 1988).

A review by Shelef, G. et al. (1984) describes the harvesting and dewatering step as a method that concentrates the microalgae from a dilute suspension of approximately 0.02 - 0.06 wt % total suspended solids (TSS) to 15 - 25 wt % TSS or more. There are many available techniques that can be used for microalgae dewatering, all of which are explored in section 1.3.

In the lipid extraction step (separation of cell components in figure 1.1), the microalgal biomass is exposed to an eluting extraction solvent which permeates and extracts the lipid molecules out of the microalgal cellular matrices. Microalgal lipid extraction generally uses either an organic solvent or supercritical carbon dioxide as an extraction solvent. Chloroform/methanol (2/1 v/v) is the most frequently used organic solvent mixture, however, the use of hexane/isopropanol (3/2 v/v) is highly attractive due to its low-toxicity (Halim, R. et al. 2011). Once the lipids are separated from the cell debris and the extraction solvent, it is then converted into biodiesel via transesterfication. It should be noted that this method is an only used as an analytical procedure and is not relevant to full scale microalgae extraction.

The main reaction involved in the production of biodiesel is a transesterfication (or alcoholysis) reaction, as seen in figure 1.2. The transesterfication reaction involves

the displacement of an alcohol from an ester by another alcohol. The oil used to make biodiesel is made of triglycerides. In the case of microalgae sourced biodiesel, these triglycerides are sourced from the microalgal lipid stores. The reaction proceeds in a stepwise manner where the triglycerides are converted first to diglycerides, then to monoglycerides and finally into glycerol (Ma, F. and Hanna, M. A. 1999; Chisti, Y. 2007; Demirbas, A. and Karslioglu, S. 2007). After each reaction step, a mole of ester is produced. The transesterfication reactions are reversible; however the reaction equilibrium is always conditioned to produce more biodiesel and glycerol (Ma, F. and Hanna, M. A. 1999).
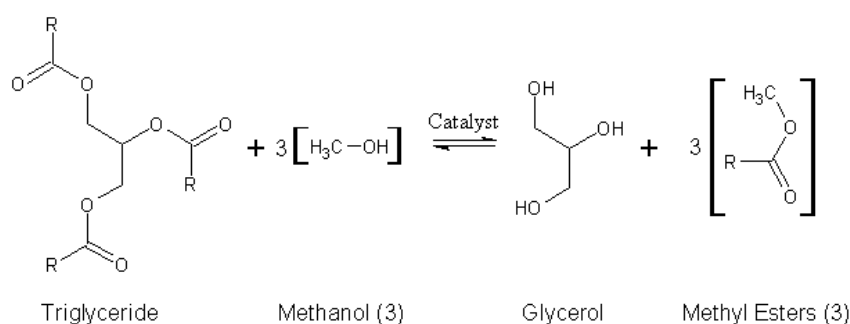
Figure 1. 2. Transesterfication reaction of oil into biodiesel.
R represents hydrocarbon groups.

The reaction is catalysed either by acids, alkalis or lipase enzymes. Alkali-catalysed transesterfication has been found to be about 4000 times faster than the same amount of acid catalyst used in transesterfication (Fukuda, H. et al. 2001; Chisti, Y. 2007). Low conversion of transesterfication reactions may occur due to side saponification reactions (the formation of soap), a process which occurs in the presence of water molecules and free fatty acids. Saponification results in catalyst consumption and a reduction in catalytic potency (Ma, F. and Hanna, M. A. 1999; Chisti, Y. 2007; Demirbas, A. and Karslioglu, S. 2007). To prevent this reduction in overall conversion, the oil and alcohol should be dried and have a minimum amount of free fatty acids (Chisti, Y. 2007).

The main factors that affect transesterfication reaction are the molar ratio of triglycerides to alcohol, the presence and type of catalyst, the reaction temperature,

process time, and the amount of free fatty acids and water molecules in the oils and fats (Ma, F. and Hanna, M. A. 1999). The biodiesel product is finally recovered by washing with water in order to remove the glycerol and excess methanol.

1.2 Limitations to the Biodiesel Production Process

The main obstacle that stands in the way of broad commercialisation of biodiesel (made from conventional sources such as vegetable oils and animal fats) is the related high costs due to the high priced feedstocks (Wright, L. 2006; Li, X. et al. 2007). In the case of microalgal feedstocks, Ma, F. and Hanna, M.A. (1999) state that the limitations are due to the high energy and cost of the processing steps. Pushparaj, B. et al. (1993) and Oh, H. et al. (2001) have concluded that harvesting and dewatering is the major problem that limits the commercialisation of algal biodiesel, and that 20 – 30 % of the total cost of biomass production is accountable to microalgal cell recovery. It is therefore necessary to improve the scale up and remove the economic constraints of the harvesting and dewatering process in order to be able to commercialise fully the use of microalgae in biodiesel production.

1.3 Conventional Microalgae Dewatering Techniques

The following section reviews the dewatering techniques that are available for microalgae cell recovery, and focuses on the methods which are able to recover microalgae and also their associated advantages and disadvantages. Each technique is able to concentrate the microalgae to varying extents. From the information presented, it will become clear that it is difficult for any one dewatering step to achieve a 100 fold increase in solids content. Therefore most processes must involve two or more dewatering steps in order to obtain the desired final microalgae concentration.

1.3.1 Centrifugation

Centrifugation is a separation process that uses centrifugal forces to separate solids and liquids. The separation is based on the particle size and density difference of the medium components. A study conducted by Moraine, R. et al. (1980) found that high speed centrifugation was a reliable and effective recovery technique for microalgae. Laboratory centrifugation tests were carried out on pond effluent at 500 - 1000 g and showed that 80 - 90 % could be recovered in 2 - 5 min. Although centrifugation is an effective method of microalgal recovery, the main disadvantage found was the high investment and operating costs that were required.

Centrifugal recovery was evaluated in a review by Grima, E.M. et al. (2003). This review compared different applications of centrifugation for the harvesting of microalgae and concluded that although centrifugal recovery is highly energy intensive, it is rapid and is a preferred method for microalgal cell recovery. Work by Knuckey, R.M. et al. (2006) states that, although centrifugation is a successful dewatering method, exposure of microalgal cells to high gravitational and shear forces can damage cell structure. Also, processing of large volumes of culture could be time consuming and costly. Becker, E. (1995) states that due to the high capital costs, high energy and operating costs connected to centrifugation, the dewatering method is only suitable for high value products. In relation to biodiesel, which is regarded a high value product; centrifugation is still not feasible for commercial use, because in order to reduce the market price of the biofuel to something that is competitive to the current fuel prices, the overall cost of the process must be reduced.

1.3.2 Flocculation

Flocculation is a recovery technique that involves the use of a chemical flocculant in order to induce coagulation of the microalgae cells. Flocculation will be discussed extensively in chapter 2. The main costs associated with flocculation are those needed to purchase the flocculants. The energy required to flocculate microalgae is also quite low, with only a small amount needed for the mixing of the flocculant into

the microalgae system. Flocculation studies by Pushparaj, B. et al. (1993) and Lee, S.J. et al. (1998) concluded that harvesting of microalgal cells by flocculation was a superior method to conventional harvesting methods such as centrifugation and flotation because it allowed for treatment of large quantities of microalgal culture, as well as being able to be applied to a wide range of species. Although flocculation has proven to be successful for concentrating microalgae, the method alone may not be sufficient. Moraine, R. et al. (1979) indicated that microalgal flocs have a specific gravity close to and even below that of water when exposed to light, releasing photosynthetic oxygen. This means that sedimentation of microalgal flocs may not be possible and methods combining flocculation with other techniques such as flocculation-flotation and flocculation-centrifugation may need to be considered. This however is not a significant problem since a two-step dewatering process is generally required in order to achieve the desired microalgal concentration, of 15 - 25 wt % TSS.

1.3.3 Filtration and Screening

This method of separation utilises a permeable medium through which a suspension is passed. The permeable medium retains the solids and allows the liquid to pass through. Figure 1.3 shows a schematic diagram of a tangential flow filtration system.

Screening involves passing the suspension through a screen with a specific pore size. The solid particles that are larger than the screen pore size are retained whilst the liquid phase passes through the screen. Microstrainers and vibrating screen filters are the two main types of screens used for microalgae harvesting (Shelef, G. et al. 1984). Microstrainers are described by Wilde, E.W. et al. (1991) as rotating filters with fine mesh screens and a continual backwash. The flow-through rate of the filter determines how much culture medium is processed per microstrainer unit and is the key factor that determines the overall cost. The flow-through rate (and cost of the unit) is determined by the size of the screen openings. The size of the screen opening will be dependent on the species of microalgae. Larger microalgal species will require larger openings, resulting in faster flow rates and a lower cost. The

concentration of microalgae is another factor that influences the efficiency of the process. A high microalgal concentration can result in blocking of the screen whilst a low microalgal concentration can result in inefficient capture (Wilde, E. W. et al. 1991). A study by Middlebrooks, E.J. et al. (1974) stated the limitations of microstrainers to include incomplete solids removal and difficulty in handling solids fluctuations.

A review by Shelef, G. et al. (1984) investigated filtration as a dewatering technique. The review states that filtration requires a pressure drop to be applied across the system in order to force the fluid through the filter. The extent of pressure required for the medium determines which type of driving force is used; gravity, vacuum, pressure or centrifugal. There are two main types of filtration; surface filters (where the solids are deposited on the filter medium in a thin film or cake) and depth filters/deep bed filters (where the solids are deposited within the filter medium) (Shelef, G. et al. 1984). Moraine, R. et al. (1990) suggest that one of the major problems associated with filtration is that media that are fine enough to retain the microalgae tend to bind and therefore require regular backwashes. This results in a decrease in the amount of microalgal concentrate.

Grima, E.M. et al. (2003) conducted a review on the process options available for the recovery of microalgal biomass. They found that filtration methods that operate under pressure or vacuum are suitable for recovering microalgal species with large cell size, but are inadequate to recover microalgal species with sizes approaching bacterial dimensions (in the range of micrometers).

1.3.4 Tangential Flow Filtration / Cross Flow Filtration

In tangential flow filtration, the medium flows tangentially across a membrane. The retentate is recirculated across the membrane, keeping the cells in suspension and minimising fouling. Particles with sizes smaller than the pores of the membrane are able to pass through whilst those larger in size are retained. The type of membrane used in this process may be an ultrafiltration membrane or microporous membrane,

and both are available in a wide range of pore sizes or molecular weight cut-offs (Petrusevski, B. et al. 1995).

As Grima, E.M. et al. (2003) reported, microfiltration and ultrafiltration are possible alternatives that could be used to recover microalgae. Advantages of tangential flow filtration over other recovery techniques such as conventional filtration, centrifugation, flocculation and sedimentation is that better filtration rates can be achieved to completely remove debris and microalgal cells. Petrusevski, B. et al. (1995) conducted a study on the suitability of tangential flow filtration for the recovery of microalgae. The tangential flow filtration system included a membrane with pore size of 0.45 μm. It was found that the system could successfully recover large volumes of microalgal culture, with the overall microalgal biomass recovery being 70 - 89 %. It was also found that the system was able to preserve the structure and properties such as motility and negative surface charge of the microalgal biomass.

The costs involved in this technique are related with pumping and membrane replacements (Rossignol, N. et al. 1999). Large scale recovery of microalgae using this technique can be restricted due to continuous fouling and subsequent replacement of the membranes.
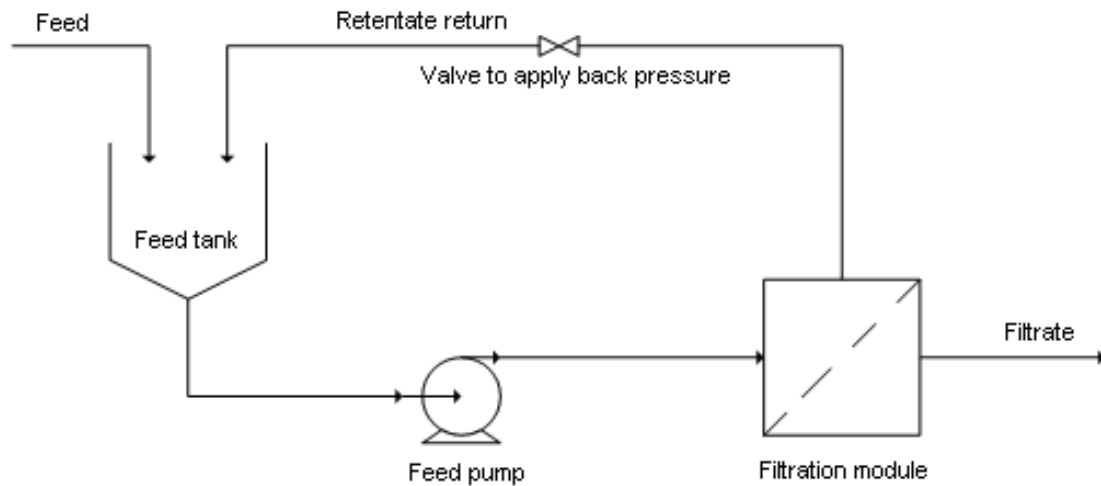
Figure 1. 3. Schematic diagram of a simple tangential flow filtration system.
The microalgal culture and recycled retentate is pumped from the feed tank to the filtration module.
The filtrate carries onto the next step of the process while the retentate is returned back to the feed
tank.

1.3.5 Gravity Sedimentation

Gravity sedimentation is a technique that separates a feed suspension into a concentrated slurry and clear liquid. Harvesting by sedimentation at natural gravity can be accomplished via lamella separators and sedimentation tanks. The microalgal suspension is pumped continuously whilst the slurry is removed discontinuously. The main form of energy required is that needed to pump the slurry. Flocculants can be added in order to increase the microalgal separation and the rate of sedimentation. Sedimentation tanks are not used widely in the industry, but are a reliable method to concentrate microalgal suspensions to 1.5 % TSS (Mohn, F. H. 1980). Separation of microalgae by sedimentation tanks is an inexpensive process. However without the addition of flocculants, the reliability is low (Shelef, G. et al. 1984).

The density of microalgal particles play an important role in the success of solids removal by gravity settling. Calculations performed by Edzwald, J.K. (1993) show that microalgae particles with low density do not settle well and are poorly removed by settling.

1.3.6 Flotation

Flotation can be described as a physiochemical type of gravity separation in which air or gas is bubbled through a solid-liquid suspension and the gaseous molecules are attached to the solid particles. These particles are carried to the surface of the liquid and accumulate as float, which can be removed. The size of the particles is important in flotation; the smaller the particle size the more likely the particle can be levitated by the bubbles. A particle diameter of less than 500 μm can be used for flotation (Matis, K. A. et al. 1993). Another important parameter is the particle capture by the bubble. The capturing process can be described as the product of two probabilities: the probability of the collision between a bubble and a particle and the probability of adhesion of the bubble and the particle after collision has occurred. It has been shown that there is a decrease in the probability of collision with decreasing particle size (Matis, K. A. et al. 1993). There are two main types of flotation; dissolved air flotation and dispersed air flotation.

1.3.6-1 Dissolved Air Flotation

Dissolved air flotation is the most widely used flotation technique applied in industrial effluent treatment (Matis, K. A. et al. 1993; Rubio, J. et al. 2002). The process of dissolved air flotation involves the reduction of pressure of a water stream that is pre-saturated with air (at pressures higher than atmospheric). The liquid containing the dissolved air is then injected at atmospheric pressure into a flotation tank through nozzles or needle valves. This generates bubbles that rise through the liquid and carry the suspended solids to the surface, which can then be skimmed off. A portion of the clarified liquid is separated and saturated with air to be recycled back into the flotation tank (Matis, K. A. et al. 1993; Chung, Y. et al. 2000; Rubio, J. et al. 2002).

Microalgae separation by dissolved air flotation have often been combined with chemical flocculation (Bare, W. F. R. et al. 1975) and it is possible to obtain microalgal slurries up to 6 wt % (Bare, W. F. R. et al. 1975; Moraine, R. et al. 1980).

A study carried out by Edzwald, J.K. (1993) looked into the removal of microalgae using dissolved air flotation in comparison to settling. The results showed that microalgae removal by dissolved air flotation required pre-treatment by flocculation. Dissolved air flotation and settling experiments were conducted at identical conditions. It was found that dissolved air flotation was more successful for microalgae removal.
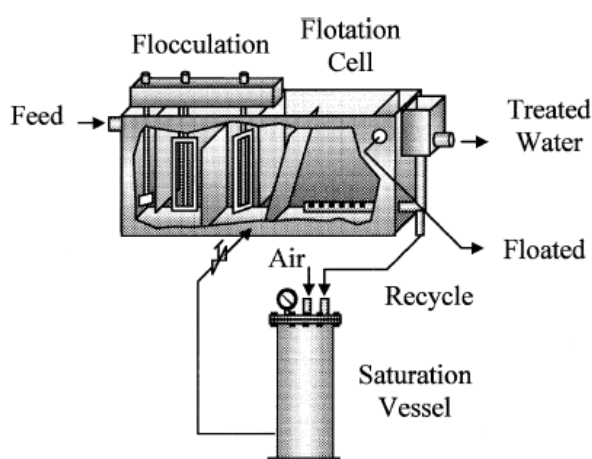
Figure 1. 4. A conventional dissolved air flotation unit (Rubio, J. et al. 2002).

The microalgae culture flows continuously through the unit. Flocculants are added and with mixing, induces microalgal flocculation. The flocculated microalgae reaches the flotation cell where a recycled stream of water is used to introduce dissolved air into the system.

1.3.6-2 Dispersed Air Flotation

Dispersed air flotation involves the formation of bubbles by a high speed mechanical agitator and an air injection system. Gas introduced at the top is mixed with liquid and allowed to pass through a disperser, which creates bubbles ranging from 700 to 1500 μm in diameter (Rubio, J. et al. 2002). Surfactants or collectors are used to prepare the surface of the algae particles for flotation by air bubbles or to encourage microalgae agglomeration. They do this by changing the hydrophobicity of the particle, which will affect the likelihood of microalgae - bubble attachment (Phoochinda, W. et al. 2004).

A dispersed air flotation study was performed by Chen, Y.M. et al. (1998). Three types of surfactant were used as the collectors for microalgae removal: non ionic X-100, cationic CTAB and anionic SDS. Experiments were conducted on the microalgal species *Scenedesmus quadricauda*. The results of the study showed that dispersed air flotation was successful for the removal of *Scenedesmus quadricauda* from water. The most effective collector was the cationic CTAB. The optimum pH range was 5 - 8. It was proposed that the role of the collector ions is to increase the resistance of bubble rupture. They may also migrate to the solid surface and increase the hydrophobicity of the solid particle, which may lead to electrical interactions between the solid particles and the gas bubbles.

1.3.7 Electrocoagulation

Electrocoagulation utilises electric current to separate the microalgae cells from the dilute medium. Electrocoagulation will be discussed in detail in chapter 2. The mechanism of electrocoagulation involves the use of reactive electrodes which are able to produce coagulating ions in situ that induce microalgae - metal ion coagulation. Hydrogen bubbles that are also formed during the process are then able to carry the microalgae - metal ion floc to the surface of the solution. Mollah, M.Y.A. et al. (2004) describe the advantages of using electrochemical processes as being environmentally compatible, versatile, safe, energy efficient and cost effective.

1.4 Potential for Microalgae Biodiesel Commercialisation

In order to make the microalgae sourced biodiesel production process commercially viable, the dewatering step must be optimised for lower cost and energy requirement. Table 1.1 presents a comparison of recovery yield, concentration factor, reliability, cost, energy usage, advantages and disadvantages for each of the dewatering techniques presented in section 1.3.

Table1. 1. Comparison of dewatering techniques.

Dewatering Process	Highest Possible Recovery/Yield	Highest Possible Concentration Factor	Energy Usage	Reliability	Costs involved	Advantages	Disadvantages
Centrifugation	Up to 22 % TSS (Shelef et al. 1984)	120 (Grima et al. 2003)	Very high	Very good	Initial capital cost of centrifuge	Reliable and effective recovery	High operating cost
	80 - 90 % clarification (Moraine et al. 1980)	Self cleaning disk stack centrifuge (Grima et al. 2003)	Self cleaning disk stack centrifuge, 1 kWh/m^3 (Grima et al. 2003)		Cost of depreciation maintenance	Rapid recovery possible	High energy intensive
	> 95 % cell harvest efficiency (Grima et al. 2003)				Operating energy costs		
	Self cleaning disk stack centrifuge, 12% TSS (Grima et al. 2003)		Decanter bowl centrifuge, 8 kWh/m3 (Grima et al. 2003)				
Flocculation	> 95 % removal of microalgae (Ayoub et al. 1986)	200 - 800 (Knuckey et al. 2006)	Very low - only mixing energy required	Very good	Cost of flocculant	Low energy input	Introduction of chemicals into system
		Efficiencies ≥ 80 % (Knuckey et al. 2006)			Mixing energy costs	Can be applied to a wide range of species	May cause contamination
						Recovery of large volumes	Cost of chemical
							Capital cost of dosing equipment

Dewatering Process	Highest Possible Recovery/Yield	Highest Possible Concentration Factor	Energy Usage	Reliability	Costs involved	Advantages	Disadvantages
Filtration and screening (natural filtration)	1 - 6 % TSS (Mohn, F. H. 1980)	15 - 60 (Mohn, F. H. 1980)	Low	Good	Cost of filter/membrane replacement	Suitable for recovering larger microalgae cells	Regular backwashes required
			Vibrating screen filter, 0.4 kWh/m^3 (Mohn, F. H. 1980)		Operating energy costs		Lower microalgae concentrations required to avoid clogging
Filtration and screening (pressure filtration)	5 - 27 % TSS (Mohn, F. H. 1980)	50 – 245 (Mohn, F. H. 1980)	Moderate	Very Good	Cost of filter/membrane replacement		Incomplete solids removal
			Chamber filter press, 0.88 kWh (Mohn, F. H. 1980)		Operating energy costs		Regular replacement of membranes
Gravity Sedimentation	0.5 - 1.5 % TSS (Shelef, G. et al. 1984)	Lamella separator, 16 (Mohn, F. H. 1980)	Very low Lamella separator, 0.1 kWh/m^3 (Mohn, F. H. 1980)	Poor	Initial capital cost of separator	Low energy input	Low reliability without addition of flocculants

Dewatering Process	Highest Possible Recovery/Yield	Highest Possible Concentration Factor	Energy Usage	Reliability	Costs involved	Advantages	Disadvantages
Tangential flow filtration	70 - 89 % microalgal recovery (Petrusevski, B. et al. 1995)	5 - 40 (Petrusevski, B. et al. 1995)	High 1.9 - 2.1 kWh/m3 (Danquah, M. K. et al. 2009)	Good to very good	Cost of filter/membrane replacement and pumping Operating energy costs	Better filtration rates compared to filtration/screening Recovery of large volumes	Continuous fouling of membranes Regular replacement of membranes
Flotation	Dissolved air flotation, 1 - 6 % TSS (Shelef, G. et al. 1984) Dispersed air flotation, 90 % microalgae removal (Chen, Y. M. et al. 1998)	N/A	Moderate 0.6 - 1.5 kW/m3 (Higgins, M. J. and Novak, J. T. 1997)	Good to very good	Cost of flocculant, replacement of electrodes Operating energy costs	Reliable recovery	Requires pre treatment with flocculation Replacement of electrodes
Electrocoagulation	> 90 % microalgae removal (Poelman, E. et al. 1997)	N/A	Low 0.3 kWh/m3 (Poelman, E. et al. 1997)	Very good	Cost of replacement of electrodes Operating energy costs	Energy efficient Cost effective	Replacement of electrodes

From table 1.1, it can be seen that although each technique can achieve adequate microalgae recovery, for the majority of techniques one step alone is not sufficient to dewater the microalgae to the desired concentration required for further processing. The two most promising techniques are clearly flocculation and electrocoagulation. In comparison to the others, these two techniques have a low energy requirement and minimal costs. They can obtain microalgal recoveries of above 90 % and have few disadvantages. Electrocoagulation with marine microalgae also has the advantage of increasing the conductivity of the overall solution, thus requiring a lower energy requirement. For these reasons, flocculation and electrocoagulation were chosen as the dewatering techniques to be investigated in this research.

1.5 Research Aims

It is clear that if microalgae sourced biodiesel was to become a feasible alternative fuel, the limitations involved in the process must be removed or at the least reduced to a significant degree. There are obvious advantages in the use of marine microalgae species over freshwater microalgae species for use as a biodiesel feedstock, such as not consuming freshwater resources. The specific aims of this research were to critically review the literature, the dewatering of marine microalgae using flocculation, the dewatering of marine microalgae using electrocoagulation, the development of a mathematical model and performing a techno - economic carbon assessment. The detailed literature review was performed in order to outline the research gaps found in the literature to date. The optimum recovery conditions of the chosen dewatering techniques were determined, and also whether these techniques are realistically able to reduce the energy and cost of the dewatering process. The choice of dewatering techniques was the two processes that showed the most potential for process optimisation. A mathematical model was developed that produced the expected recovery of microalgae, amount of coagulation and amount of settling. A techno - economic carbon assessment performed in order to determine the feasibility of the dewatering techniques in a commercial scale.

1.6 Structure of Thesis

This thesis was structured in a traditional manner starting with a literature review in chapter 2, where a detailed discussion was undertaken including information and data on the preceding and current research in flocculation and electrocoagulation studies. The result of the literature review revealed that little successful work had been performed on marine microalgae flocculation and electrocoagulation. This brought upon the proposal for the research aims and led to the design of a series of batch flocculation and electrocoagulation experiments using the two marine microalgae species*.*

The materials and methods are described in chapter 3, and include the characteristics of the two marine microalgae species, the different experiments that were conducted, as well as procedures and equipment used. Chapter 4 details the results and discussion of all flocculation work. Chapter 5 presents the experimental electrocoagulation results, along with the related discussion. All results are expressed in graphical or tabular format. Chapter 6 provides an explanation of the mathematical model and the experimental results and discussion that correspond to the main steps involved in the mechanism of electrocoagulation. Chapter 7 examines a techno-economic study of the dewatering stage of the biodiesel production process. This chapter investigates the comparison of three types of dewatering; flocculation/centrifugation, electrocoagulation/centrifugation and centrifugation. The energy required, carbon dioxide emissions and cost were compared and discussed, giving further exploration to the possibility of commercialism. Chapter 8 provides the final conclusions to the research and responds to whether the research aims were achieved. Suggestions are made for possible future directions of the research.

CHAPTER 2 LITERATURE REVIEW

2.1 Introduction

Numerous studies have found that microalgae have definite advantages over conventional biofuel sources. However, broad commercialisation of microalgae sourced biofuel has been restrained due to high costs of operation during processing. One particular processing step with high operational costs is harvesting and dewatering and this is mainly due to the dilute nature of microalgal cultures. The high cost of these step inflict high operational costs to the overall process. Thus, the unit operation of harvesting and dewatering is a major factor affecting the viability of algae-based fuels. Sander, S. and Murthy, G.S. (2010) performed a life cycle assessment on microalgae sourced biodiesel and concluded algae dewatering was the most significant energy sink in the process and that there was a need for new dewatering technologies in order to make the process a sustainable, commercial reality.

Microalgal harvesting is performed extensively in water treatment and biofuel production. The purpose for microalgal harvesting in biofuel production differs from that in water treatment. Removal of undesirable microalgae in the water treatment industry involves a progressive reduction in both microalgal chemical oxygen demand (COD) and biological oxygen demand (BOD) to values below their discharge limits. In contrast, for biodiesel production, microalgae need to be concentrated as much as possible, to simplify the lipid extraction step that follows. Although the objectives are different, the harvesting techniques involved may be the same. One difference is that for biodiesel production, the microalgae biomass is required for further processing; therefore, the dewatering method used must not contaminate or be toxic to this processing system, and similarly the water medium would normally be recycled and therefore any residual toxic compounds would not be acceptable. Microalgal harvesting involves the concentration of dilute microalgal suspensions, typically 0.02 - 0.06 wt % TSS into a slurry or paste with concentrations of 15 - 25

wt % TSS or more depending on the target process objective (Shelef, G. et al. 1984). From Figure 2.1, it can be seen that it is possible to obtain the desired microalgal concentration by a one or a two-step harvesting process. The latter involves a primary harvesting step that forms a slurry of 2 - 7 wt % TSS followed by a secondary dewatering step which produces an algal paste of 15 - 25w t % TSS. The concentration obtained in the harvesting steps is crucial to the overall process as it influences the subsequent processing steps (Mohn, F. H. 1980; Shelef, G. et al. 1984).
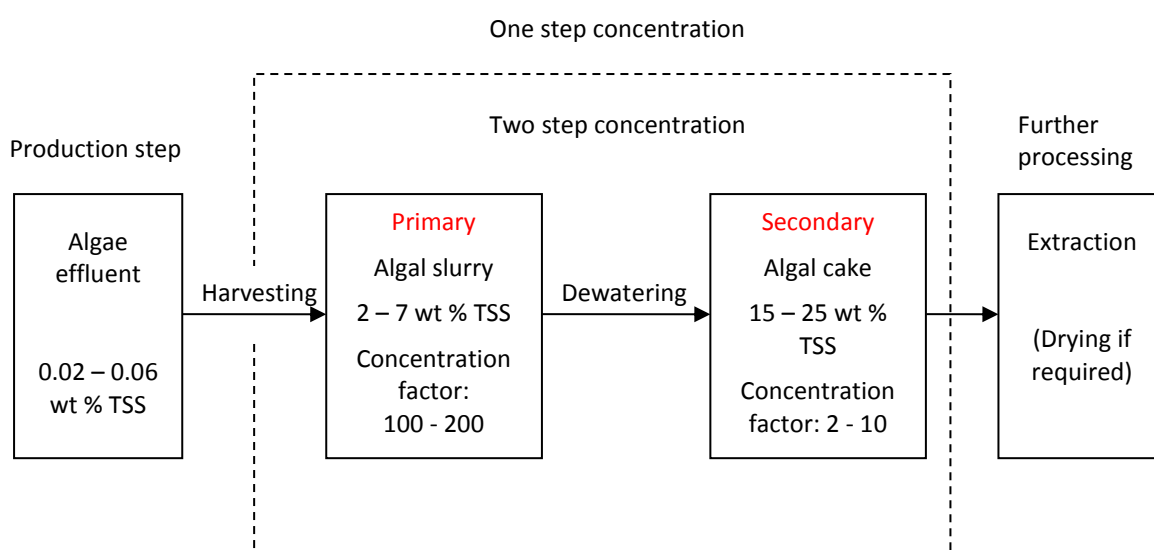
Figure 2. 1. Schematic presentation of microalgal production and processing.

A colloidal dispersion is described by Everett, D.H. (1988) as a system which consists of a dispersed phase distributed uniformly in a finely divided state in a dispersion medium. Hunter, R.J. (2001) states that colloids can avoid aggregation and have stability when the particles have the same electric charge and therefore repel each other on approach. This mechanism is referred to as electrostatic stabilisation (Hunter, R. J. 2001). When the attractive forces of a particle overweigh the repulsive forces, the colloid dispersion is unstable and coagulation occurs. Aragon, A.B. et al. (1992) describe microalgae systems as behaving as colloidal particles due to the microalgae cells having charged surfaces.

Edzwald, J.K. (1993) and Vlaski, A. et al. (1997) state that microalgae can generally be considered as particles whose stability is due to:

20

(i)   Surface charge (which is electronegative in the range from pH 2.5 - 11.5)

(ii)   Steric effects (due to water molecules bound to the microalgal surface)

(iii)   Adsorbed macromolecules or extracellular organic matter (EOM)

When compared to other particles in suspension, microalgae have the disadvantage that they are composed of several species with different characteristics such as size, shape and motility that can influence their behaviour towards treatment. This makes them more difficult to characterise and to name one single technique as the best for microalgal recovery (Vlaski, A. et al. 1997). For example, Vlaski, A. et al. (1997) quote a flagellated microalgal species *Rhodomonas spp.* as being noted to escape floc material via motility mechanisms.

Several techniques for the dewatering of microalgal cultures have been developed including centrifugation, flocculation, filtration and screening, gravity sedimentation, flotation and electrocoagulation. These techniques rely on microalgal properties that simplify the harvesting and recovery process. Borowitzka, M.A. (1992) describe these properties to include large cell size, high specific gravity compared to the medium and reliable auto-flocculation or induced flocculation.

From earlier the discussion on the potential commercialisation of the microalgal biodiesel production process by the optimisation of the dewatering stage, it was established that the dewatering techniques to be investigated in this research are flocculation and electrocoagulation. These techniques are reviewed in this literature review along with a comparative study of their performance.

2.1.1 Quantitative Evaluation of Dewatering Performance

The performance of each dewatering technique can be quantitatively evaluated by the following factors:

- The solid content of the recovered microalgae - water slurry. This can be described in terms of the concentration factor or the amount of total suspended solids. For example, a microalgae solution can be concentrated

21

from a dilute solution to up to 12 wt % TSS or a concentration factor of 120 using centrifugation (Grima, E. M. et al. 2003).

- The recovery/yield of microalgal biomass. This refers to the amount of recovered microalgae as a percentage of total processed microalgae. For example, dispersed air flotation can achieve 90 % microalgae recovery which means that 90 % of the total solids content (on a mass basis) in the original microalgae solution has been recovered in the final slurry (Chen, Y. M. et al. 1998).

- The consumption of energy required for the operation (for techniques that involve the use of electrical power). The energy required for dewatering is generally quoted in kWh/m^3 of microalgal suspension or kWh/kg of microalgae recovered.

The main methods of measuring the amount of microalgae recovered include UV-VIS absorbance and gravimetric concentration measurements of the resulting microalgae - water slurry. These protocols can be viewed in detail in Appendix A.1.4 and A.2.1.

2.2 Dewatering Technologies

2.2.1 Flocculation

Flocculation is the process where a solute particle in a solution forms an aggregate called a floc. Flocculation occurs when the solute particles collide and adhere to each other (Gregory, J. 1989; Pieterse, A. J. H. and Cloot, A. 1997). Chemicals called flocculants are usually added to induce flocculation. Tenney, M.W. et al. (1969) state that most microalgal cells have a size range between 5 - 50 μm, and they can form stable suspensions with a chemically reactive cellular surface that has a net negative surface charge due to the ionisation of functional groups. As mentioned earlier, the stability of the microalgal colloidal system will be dependent on the charge of the microalgae cells. If the cells have a net negative charge, they will repel each other and avoid coagulation; hence the solution will be stable. Therefore, in agreement

22

with Tenney, M.W. et al. (1969) the stability of these microalgal suspensions will be dependent on the forces that interact between the particles themselves and between the particles and water.

There are two main types of flocculants; inorganic flocculants and organic polyelectrolyte (polymer) flocculants. Flocculation studies by Pushparaj, B. (1993) tested many different flocculants for use in microalgal flocculation and the most effective was found to be aluminium sulphate followed by cationic polyelectrolytes.

2.2.1-1 Polyelectrolyte (Polymer) Flocculants

Polyelectrolyte flocculants are described by Stumm, W. And Morgan, J.J. (1981) as polymeric flocculants that include ionic and non ionic species, natural and synthetic polymers. The mechanism of microalgal flocculation by polyelectrolyte flocculants can be explained by a combination of charge neutralisation and particle bridging. The extent of each depends on the charge density and the chain length of the polyelectrolyte. The flocculation mechanism involves the attachment of the polyelectrolyte molecule on the microalgal surface by electrostatic forces or chemical forces (atomistic interactions such as hydrogen bonding). The polyelectrolyte is able to adsorb onto the surface of the microalgae due to one or a combination interactions such as coulobmic, dipole-dipole, hydrogen bonding or van der Waals interactions. Akers, R.J. (1975) describes polyelectrolyte bridging to occur in 3 stages:

1.   Dispersion of the polyelectrolyte into the solution phase.

2.   Adsorption of the polyelectrolyte at the interface.

3   Compression of the adsorbed polyelectrolyte at the interface and collision of these particles to form bridges, which leads to floc generation.
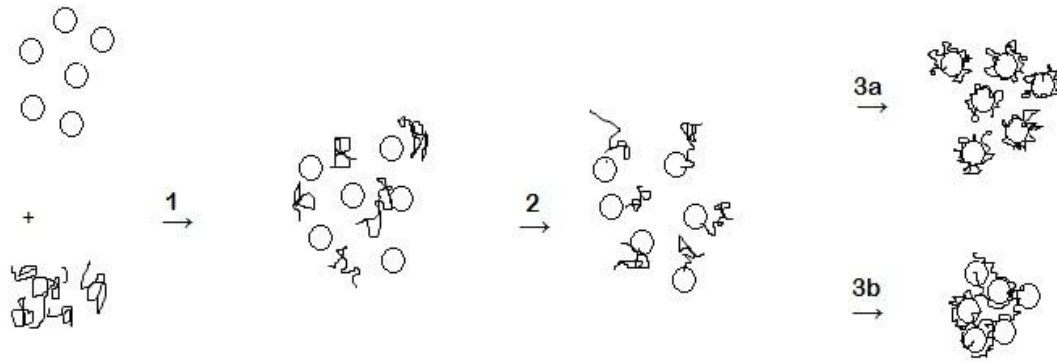
Figure 2. 2. Schematic diagram of flocculation due to particle bridging (Akers, R. J. 1975).

The polyelectrolyte can stick to certain points on the microalgal surface but have its tail trail out into the solvent. This results in polyelectrolyte segments attached to the microalgal surface as trains, separated from one another by loops which extend into the solution and end in a tail. It is possible for the loops and tails of the polyelectrolyte to attach to similar parts of other polyelectrolytes and form bridges; resulting in a three dimensional matrix (Tenney, M. W. et al. 1969; Evans, D. F. and Wennerstrom, H. 1999).
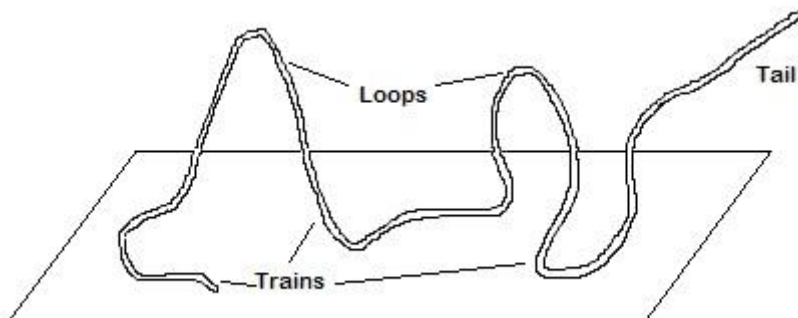
Figure 2. 3. Schematic diagram of polyelectrolyte adsorbed onto a surface (Hunter, R. J. 2001).
In some cases the polyelectrolyte adsorbs only at one point or over a very limited region with the remainder as a random coil in solution. Polyelectrolytes adsorbing onto an oppositely charged surface may be bonded so frequently that they lie essentially on the surface.

Bernhardt, H. and Clasen, J. (1994) proposed that the stability of a colloidal and finely dispersed system is determined by the negative charge density of the particle surface and that the adsorption coagulation with charge neutralisation forms the

basis of destabilisation of the colloidal system and its aggregation within the flocculation process. The dosage of positively charged flocculant is dependent on; the amount of negative charge in the dispersed system, the surface charge density, the total cell surface area, the cell counts per volume and the charge density of the cationic flocculant. Bernhardt, H. and Clasen, J. (1994) stated that functional groups on microalgal cell walls are important because they induce the formation of negative charge centres on the cell surfaces. The functional groups are mostly carboxyl groups and these influence the iso-electric point of the microalgae cells in the aqueous medium. The concentration and reactivity of these functional groups can vary with growth phase and metabolic conditions of the microalgae. This variation directly affects the negative charge density of the microalgae and therefore influences the adsorption of organic polyelectrolytes or inorganic iron and aluminium hydroxo complex flocculants.

Tenney, M.W. et al. (1969) states that the extent of microalgal flocculation is determined by the degree of coverage of the microalgal surface by the polyelectrolyte. If less than the optimum concentration of polyelectrolyte is added, it will result in inadequate bridging which may not be able to withstand shear forces due to any agitation. If there is too much coverage by the polyelectrolyte, it can cause electrostatic or steric hindering of bridging. Electrostatic hindering refers to difficulty in bridging due to the abundance of electrostatic charges. Steric hindering refers to difficulty in bridging due to the overall structure of the microalgae-polyelectrolyte aggregation.

The adsorption of polyelectrolyte flocculants onto the microalgae surface can be demonstrated from the results obtained in a study of microalgae flocculation with polyelectrolytes performed by Tenney, M.W. et al. (1969). Flocculation was performed on fresh water microalgae using synthetic organic polyelectrolytes. Using the standard jar test, the extent of microalgal flocculation was determined by measuring the turbidity of the suspension after 1 h of settling. Cationic polyelectrolyte polyamine was found to flocculate the algae successfully at an optimum dose of 2.5 mg/L. Figure 2.4 shows the results from flocculation with

cationic polyelectrolyte Dow, C-31 on *Chlorophyta.* Figure 2.4, part c shows the relationship between the concentration of the polyelectrolyte added (the dose) and the concentration measured in solution. The difference between the two curves represents the concentration of the polyelectrolyte that is attached to the microalgal surface. From the figure, it can be seen that up to a polyelectrolyte concentration of around 3 mg/L, all of the polyelectrolyte is attached to the microalgal surface. Above this concentration, there is increasing amounts of polyelectrolyte observed in the solution, with the curves eventually becoming parallel, which indicates the microalgae surface from that point is completely covered by the polyelectrolyte. Figure 2.4, part d represents the extent of microalgal surface coverage as a function of the increasing polyelectrolyte dose. Optimal flocculation is observed at around 50 % surface coverage.
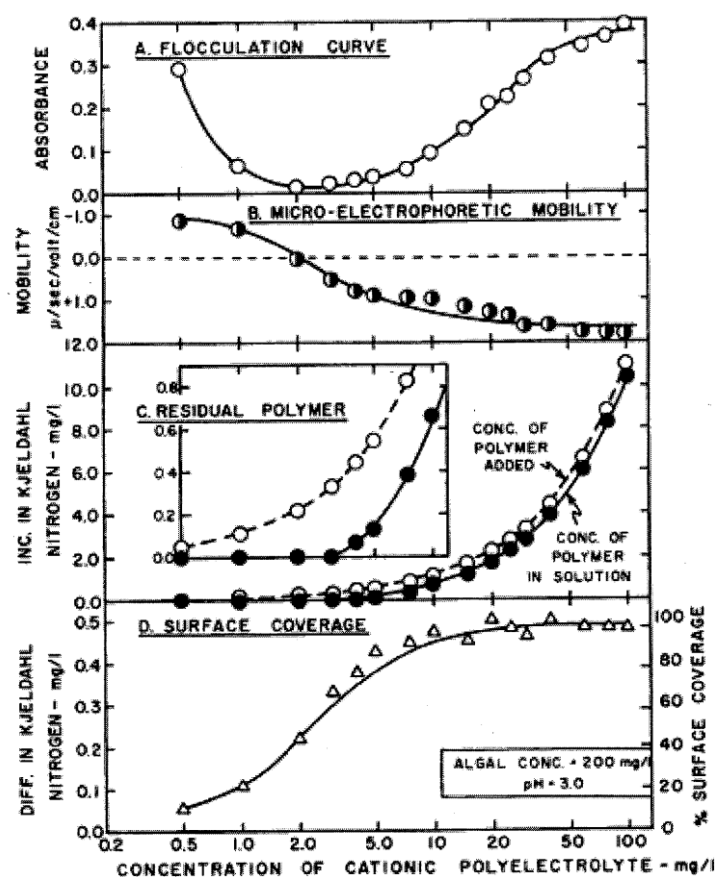
Figure 2. 4. Flocculation of *Chlorophyta* with cationic polyelectrolyte Dow, C-31 (Tenney, M. W. et al. 1969).

Polyelectrolyte flocculants can either be cationic, anionic or non-ionic. Shelef, G. et al. (1984) conducted a review on microalgae harvesting and processing techniques. Polyelectrolyte flocculants that were reviewed are listed in table 2.1, with optimal dose and pH values.

Table 2. 1. Different flocculants and their optimal dose and pH for microalgal flocculation (Shelef, G. et al. 1984).

Type or Class	Flocculant	Optimal Dose (mg/L)	Optimal pH
	Alum	80 - 250	5.3 - 5.6
Inorganic	Ferric Sulphate	50 - 90	3.0 - 9.0
	Lime	500 - 700	10.5 - 11.5
	Purifloc	35	3.5
	Zetag 51	10	> 9
Polymeric	Dow 21M	10	4.0 - 7.0
	Dow C31	1 - 5	2.0 - 4.0
	Chitosan	100	8.4

Tilton, R.C. et al. (1972) performed a study on flocculation of microalgae with synthetic polyelectrolytes and found that in general, increasing the molecular weight of a polyelectrolyte flocculant led to a lower optimal dose required.

The effect of pH was also demonstrated in a study by Tenney, M.W. et al. (1969) who found that the most effective flocculation with cationic polyelectrolytes was achieved at low pH levels. This is because at low pH levels, there is reduced electrostatic repulsion between colloids and this leads to a greater chance of polyelectrolyte bridging due to expansion of the polymer chains. The concentration of microalgae can vary the microalgal surface area, which will determine the dose of flocculant required. The composition of the microalgal culture media can also affect the flocculation process. It was also found that the concentration of hydrogen ions (pH) can affect the action of the polyelectrolyte (such as the degree of ionisation, charge density and the extent of coiling) and the surface charge density of the microalgae.

Another influential factor is the size of the flocs formed during flocculation. As the density of microalgae is close to that of water, flocculation can lead to the formation of flocs with low relative densities (especially when the concentration of the flocculant is low). Therefore, as stated by Ezwald, J.K. (1993), floc sizes in excess of 100 μm are required to achieve effective sedimentation. The addition of high molecular weight bridging polyelectrolytes can further increase floc size and lead to an improvement in microalgal settling (Briley, D. S. and Knappe, D. R. U. 2002).

Since charge neutralisation is one of the methods for encouraging microalgal flocculation, the charge of the polyelectrolytes is a very important factor that affects the microalgae flocculation. Studies conducted by Bernhardt, H. and Clasen, J. (1991) have shown that due to the negatively charged microalgae surface, anionic polyelectrolytes do not exert much influence if used as the sole flocculant. Early studies conducted on anionic and non-ionic polyelectrolytes did not achieve successful microalgal flocculation (Tenney, M. W. et al. 1969; Bernhardt, H. and Clasen, J. 1991). Figure 2.5 shows flocculation results from a study conducted by Tenney, M.W. et al. (1969) of *Chlorophyta* with anionic polyelectrolyte Dow, A-21. The increase in negative micro-electrophoretic mobility observed gives evidence to the fact that the anionic polymer is able to attach to the microalgal surface.
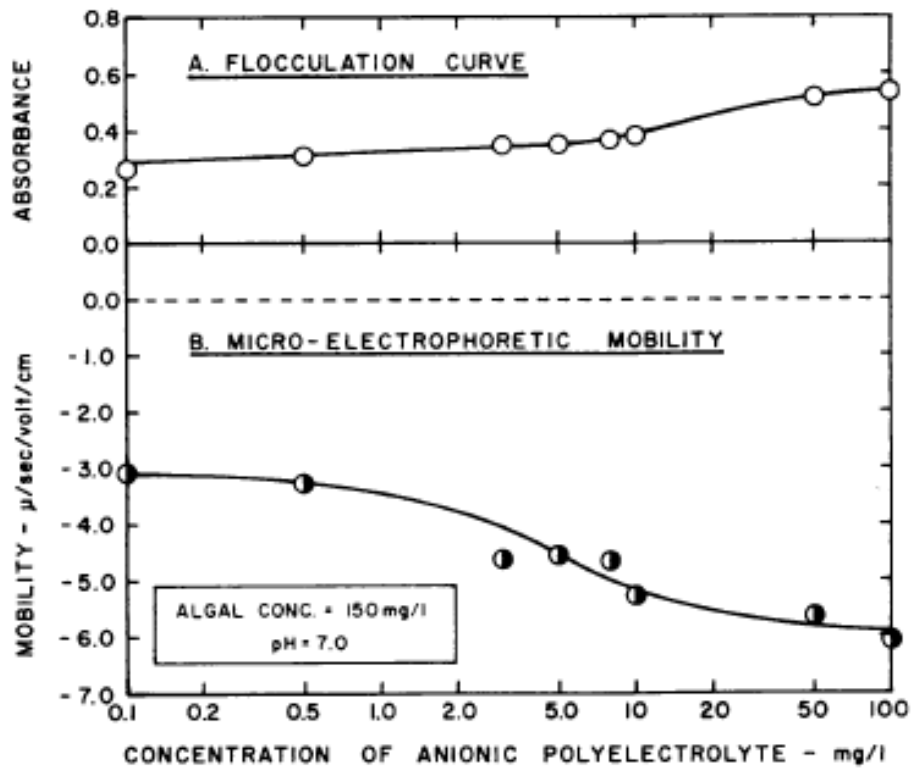
Figure 2. 5. Flocculation of *Chlorophyta* with anionic polyelectrolyte Dow, A-21 (Tenney, M. W. et al. 1969).

Figure 2.6 is taken from the same study and shows the flocculation of *Chlorophyta* with non-ionic polyelectrolyte Nalco N-670. Figure 2.6, part c shows the measurement of the residual polyelectrolyte concentration. This figure indicates that the non-ionic polyelectrolyte is being adsorbed onto the microalgae surface in a similar manner to the cationic polyelectrolyte (shown in figure 2.4).
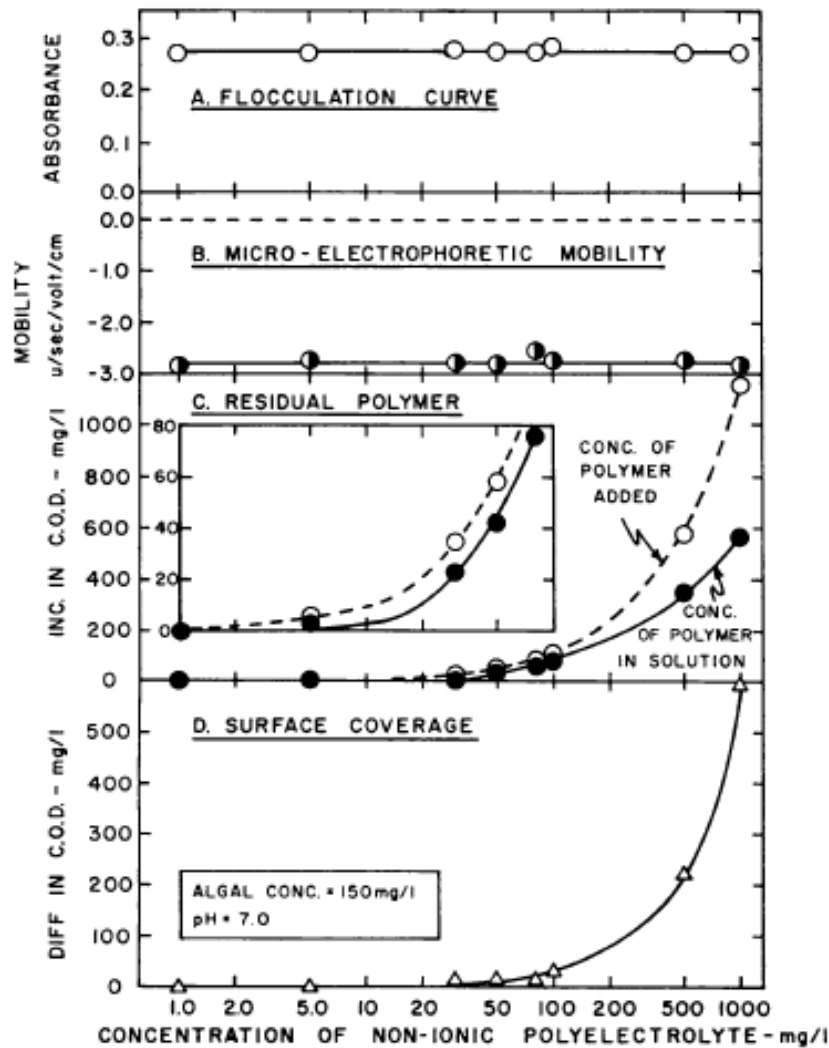
Figure 2. 6.   Flocculation of *Chlorophyta* with non-ionic polyelectrolyte Nalco N-670 (Tenney, M. W. et al. 1969).

As explained by Tenney, M.W. et al. (1969), the inability of flocculation with anionic polyelectrolytes is due the repulsion between like charges or by polymer segments being unable to bridge between particles due to insufficient length. From the data obtained from the study, it is apparent that the mechanism of anionic and non-ionic polyelectrolyte bonding onto the microalgal surface is a result of chemical forces (hydrogen bonding, interactions with cations on the colloid surface or anion interchange with adsorbed ions such as OH^-) rather than electrostatic forces.

2.2.1-2 Inorganic Flocculants

Early studies on algal flocculation have shown that microalgae can be successfully flocculated when their surface charges are neutralised. Charge neutralisation refers to a state where the net electrical charge of the microalgal particle has been cancelled due to adsorption of an equal amount of the opposite charge. The mechanism of microalgal flocculation with inorganic flocculants is charge neutralisation, provided the microalgae are small and approximately spherical (Bernhardt, H. and Clasen, J. 1991). In order for microalgae to be flocculated by inorganic flocculants, the pH needs to be low enough to form cationic hydrolysis products (Briley, D. S. and Knappe, D. R. U. 2002).
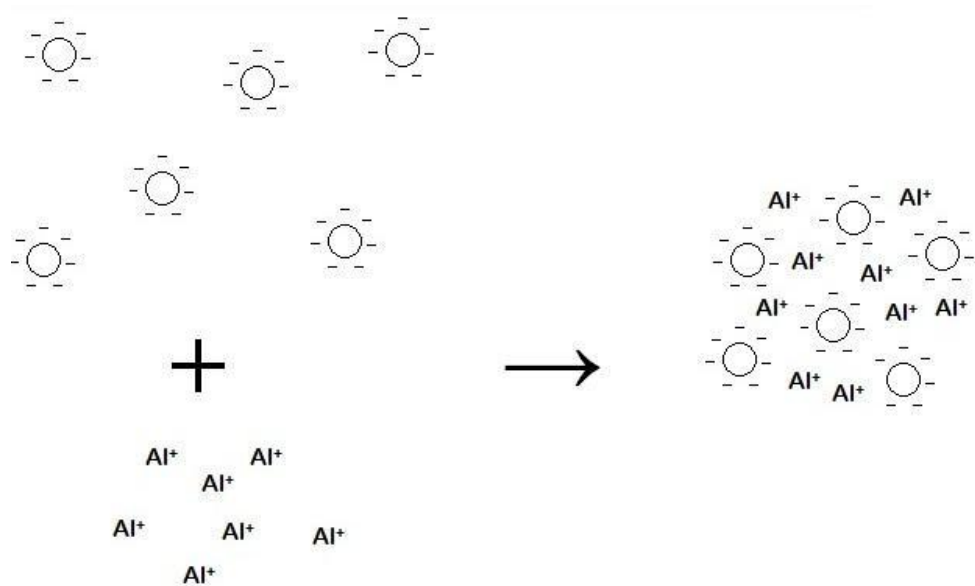
Figure 2. 7. Schematic diagram of flocculation due to charge neutralisation with a positively charged aluminium species.

Alum flocculation studies were conducted by Friedman, A.A. et al. (1977). From figure 2.8, it can be seen that at pH's between 7.5 and 9, alum proved to be an effective flocculant.
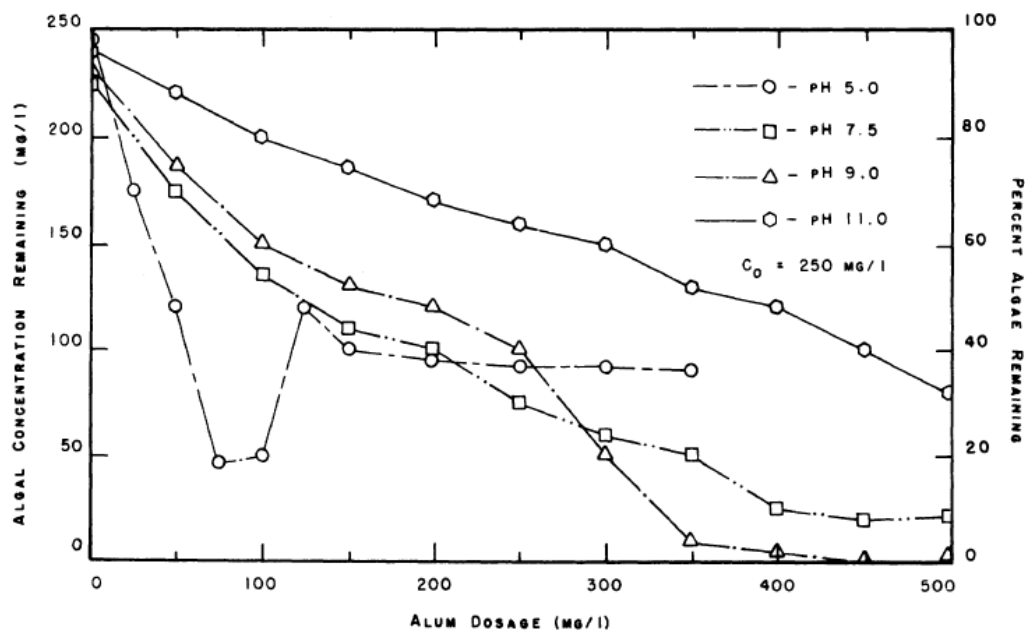
Figure 2. 8. Microalgae flocculation with alum (Friedman, A. A. et al. 1977).

Shelef, G. et al. (1984) conducted a detailed review on inorganic flocculants. The optimal dose and pH of certain inorganic flocculants can be viewed in table 2.1. Inorganic flocculants are able to form polyhydroxy complexes at an appropriate pH. The inorganic flocculants reviewed were alum ($Al_2(SO_4)_3.18H_2O$), ferric sulphate and lime. The sources of data were from flocculation experiments using jar tests (batch flocculation experiments) or using a pilot scale apparatus. It was found that alum displayed a superior flocculating ability compared to ferric sulphate in terms of the optimal dose of flocculant, pH and quality of water slurry obtained (Moraine, R. et al. 1980). Lime was found to have good flocculation ability but the flocculant could only be used for microalgal cultures that had magnesium concentrations above 10 mg/L (Folkman, Y. and Wachs, A. M. 1973). The sludge formed from the flocculation process also contained a greater amount of lime than microalgae. A study by Ayoub, G.M. et al. (1986) also observed that lime treatment used to induce flocculation in microalgal suspensions was more effective, if the original suspension already contained magnesium or calcium ions.

32

2.2.1-3 Combined Flocculation

The combined flocculation process is a multi-step flocculation process using more than one type of flocculant. The combined flocculation process was studied by Mc Garry, M.G. (1970) with the use of alum in combination with polyelectrolyte flocculants. As was found in previous studies, anionic and non-ionic polyelectrolytes were found to be unsuccessful when used both alone and in conjunction with alum, for flocculating microalgae. From figure 2.9, it can be seen that with the aid of cationic polyelectrolytes, the flocculation of microalgae with alum can be significantly improved, with increasing doses of both alum and cationic polyelectrolyte resulting in higher concentrations of settled microalgae.
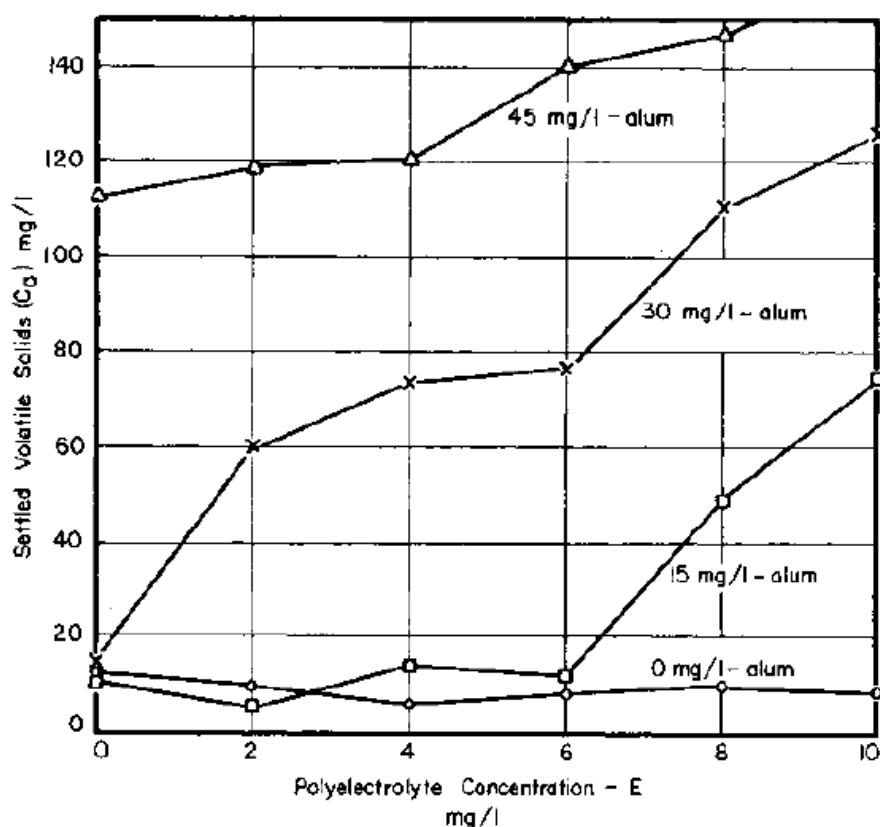
Figure 2. 9. Effect of alum combined with polyelectrolyte flocculation on settled volatile microalgae solids (McGarry, M. G. 1970).

The combined flocculation process was also studied by Sukenik, A. et al. (1988) . Two approaches were studied: the use of both organic polyelectrolyte and inorganic

33

flocculants and the treatment of microalgal cultures with oxidants preceding the flocculation process. The sequential addition of chitosan (polymeric) and alum or ferric chloride (inorganic) flocculants improved the overall degree of flocculation as well as reduced the dosage of inorganic flocculant required (figure 2.10). Although at high ionic strengths, chitosan found to be unable to bridge between microalgal particles, it was assumed to adsorb to the microalgal cell surface and reduce the charge, predisposing the microalgal cells to flocculation by the inorganic flocculant thus reducing the dose.
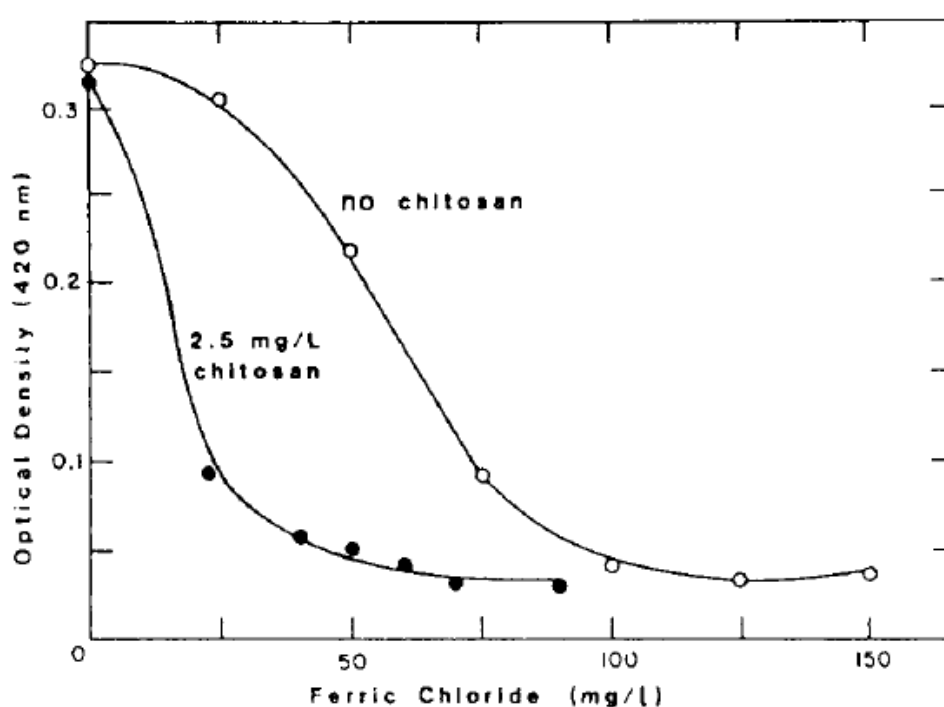
Figure 2. 10. Chitosan addition to *I. galbana* flocculation with ferric chloride (Sukenik, A. et al. 1988).

Ozone was used as a pre-treatment to flocculation because it was thought that it would reduce microalgal motility, change cell surface characteristics and improve flocculation. From figure 2.11, it can be seen that even at low doses of ferric chloride, pre-treatment with ozone has a significant effect on flocculation efficiency.

34
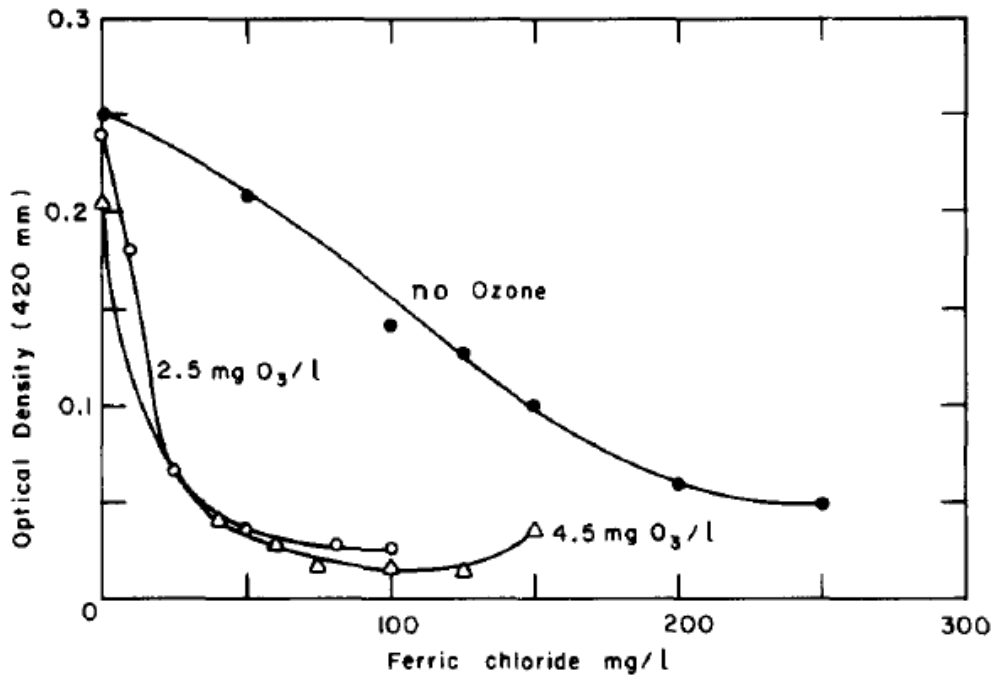
Figure 2. 11. *I. galbana* pretreatment with ozone followed by flocculation with ferric chloride (Sukenik, A. et al. 1988).

2.2.1-4 Auto-flocculation and pH Induced Flocculation

Auto-flocculation is the spontaneous floc formation and settling of microalgae. This type of flocculation is associated with an increase in pH due to photosynthetic carbon dioxide consumption and the formation of inorganic precipitates. It is proposed that aside from the precipitation of inorganics, the formation of microalgal aggregates can be explained by excreted organic macromolecules, inhibited release of microalgae daughter cells and aggregation between microalgae and bacteria. Sukenik, A. and Shelef, G. (1984) investigated auto-flocculation in outdoor ponds and also in the laboratory. In the outdoor pond experiments, microalgal species *Sc. dimorphus* was grown autotrophically for seven days at a constant pH of 7 by the addition of carbon dioxide. On the eighth day, the pond agitation and carbon dioxide supply was stopped. Auto-flocculation proceeded with an increase in pH due to continued carbon dioxide consumption by the photosynthetic activity of the culture. It was observed that the microalgae aggregated into flocs and settled at the bottom of the pond. The laboratory experiments also found that auto-flocculation could be simulated by changing the alkaline conditions to that required for auto-flocculation.

35

The mechanism for auto-flocculation is the supersaturation state of the culture medium (with respect to calcium and phosphate ions) due to the increase in pH. This supersaturation causes initial nucleation of calcium phosphate precipitation that is promoted by the microalgal cells acting as the solid surface. The calcium phosphate precipitate is positively charged (in the presence of excess calcium ions) and so is adsorbed and reacts with the negatively charged microalgal cells resulting in agglomeration.

Similar studies have been conducted in the water treatment industry using alkalising agents such as lime or sodium hydroxide to raise the pH levels required to embark on chemical flocculation in microalgae. A study conducted by Semerjian, L. and Ayoub, G.M. (2003) also showed that the use of alkalising agents successfully resulted in microalgae flocculation due to the precipitation of calcium and magnesium hydroxides.

Ayoub, G.M. et al. (1986) investigated pH induced freshwater microalgal flocculation with the addition of sea water into the medium. The results showed that the presence of sea water significantly increased microalgal cell removal. It is believed that the calcium carbonate flocs have a negative charge, whilst the magnesium hydroxide flocs have a positive charge. Since microalgal cells have a negative charge, the magnesium hydroxide flocs are responsible for the majority of cell removal due to charge destabilisation.

Although this method of flocculation seems inexpensive and simple, it is pointed out by Benemann, J. and Oswald, W. (1996) that flocculation induced by environmental stresses such as extreme pH, temperature or nutrient depletion is considered too unreliable to be economical on a commercial scale. Furthermore, it is stated by Higgins, M.J. and Novak, J.T. (1997) that the increased presence of sodium in a marine environment would reduce the exocellular protein that is responsible for flocculation.

2.2.1-5 Microbial Flocculation

Microbes have been studied extensively for use as flocculating agents (Toeda, K. and Kurane, R. 1991; Lee, S. H. et al. 1995; Lian, B. et al. 2008). A study by Lee, A.K. et al. (2009) investigated the feasibility of microbial flocculation for marine microalgae harvesting. Organic carbon was used as the substrate for the growth of microbes that were used in situ for flocculation of *P. carterae.* Successful flocculation was achieved and maximum recovery was obtained with 0.1 g/L substrate and a mixing time of 24 h. It was found that the efficiency of recovery of microalgae increased with mixing time. An increase in mixing time also resulted in an increase in the number of bacteria and an increase in the probability of collisions between particles. Microbial flocculation is seen as a promising technique as there is no need for addition of metallic flocculants, the microalgae cells are not damaged during the process and it may be possible to reuse the media.

2.2.1-6 Marine Microalgal Flocculation

The majority of work done on microalgae flocculation has been on freshwater species. Alum has been studied extensively as a flocculant for freshwater microalgae removal (Van Vuuren, L. R. J. and Van Duuren, F. A. 1965; McGarry, M. G. 1970; Friedman, A. A. et al. 1977). These studies have found that effective flocculation of freshwater microalgae is possible with alum at low and near neutral pH. Microalgae growth in a high ionic strength marine environment has been studied over the years. The effect of ionic strength on the flocculation using cationic polymers has been studied in general (Tricot, M. 1984) and also for use in microalgae (Sukenik, A. et al. 1988). Bilanovic, D. and Shelef, G. (1988) found that the high salinity of the marine environment inhibited flocculation with polyelectrolytes. Figure 2.12 shows the poor results obtained for marine microalgal flocculation compared to freshwater for all flocculant types tested. Effective flocculation was attained at salinity levels lower than 5 g/L. The reduced effectiveness of cationic polymers to induce microalgae flocculation in sea and brackish waters is explained by Bilanovic, D. and Shelef, G. (1988) to be primarily attributed to the effect of medium ionic strength on the

configuration and dimension of the polyelectrolyte. At high ionic strength, the polyelectrolyte shrinks to its smallest dimensions, and fails to bridge between algal cells (Bilanovic, D. and Shelef, G. 1988).
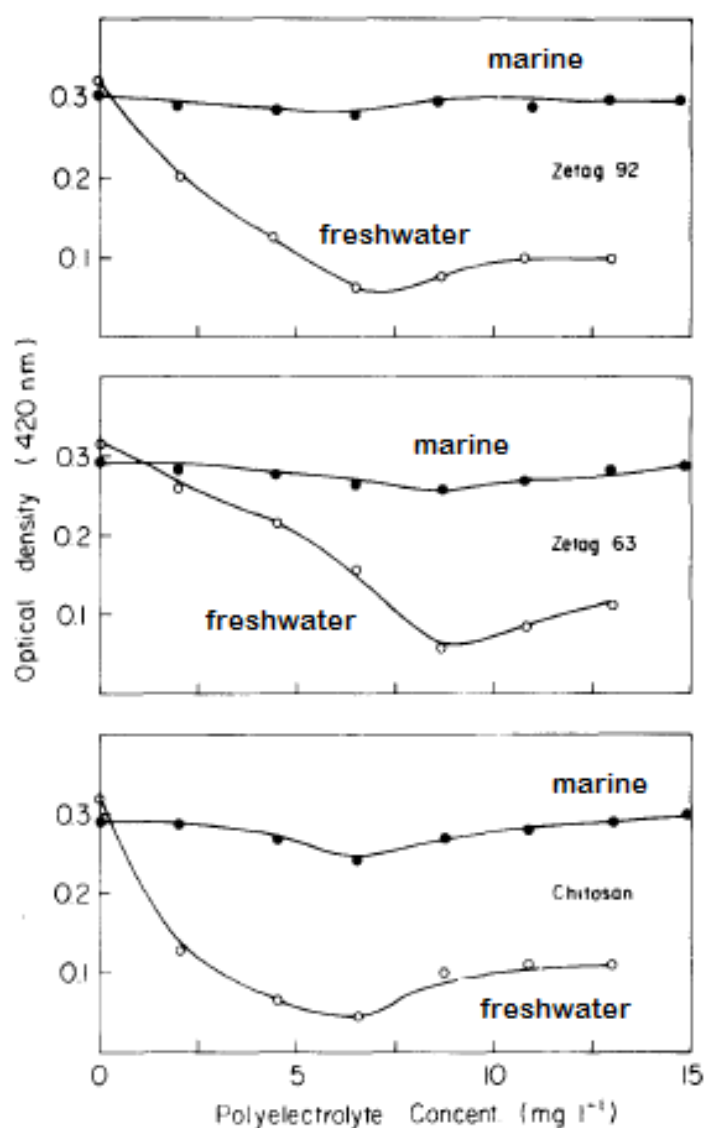
Figure 2. 12. Flocculation of marine and freshwater microalgae from the species of the genera *Chlorella* with synthetic and natural cationic polyelectrolyte: Zetag 92, Zetag 63 and Chitosan (Bilanovic, D. and Shelef, G. 1988).

The possibility of flocculating marine microalgae species using inorganic flocculants ferric chloride and alum was studied by Sukenik, A. et al. (1988). Flocculation was performed on marine microalgae species *Isochrysis galbana* and *Chlorella stigmatophora.* The optimal dosage required to flocculate marine microalgae was

found to be in the order of 5 to 10 times higher than that for freshwater microalgae. The optimal dose for the two inorganic flocculants was also seen to increase significantly with an increase in the ionic strength of the media. Figure 2.13 shows the difference between the recovery efficiency of ferric chloride flocculation on marine and freshwater microalgae species. The optical density measured for the freshwater species is significantly lower than that for the marine species. Table 2.2 illustrates the considerable difference between optimum doses for marine and freshwater microalgal flocculation. It is proposed that the high salinity of the marine microalgae species interferes with the flocculation process by reducing the chemical activity of the flocculant and masking functionally actives sites of the flocculants (Sukenik, A. et al. 1988).
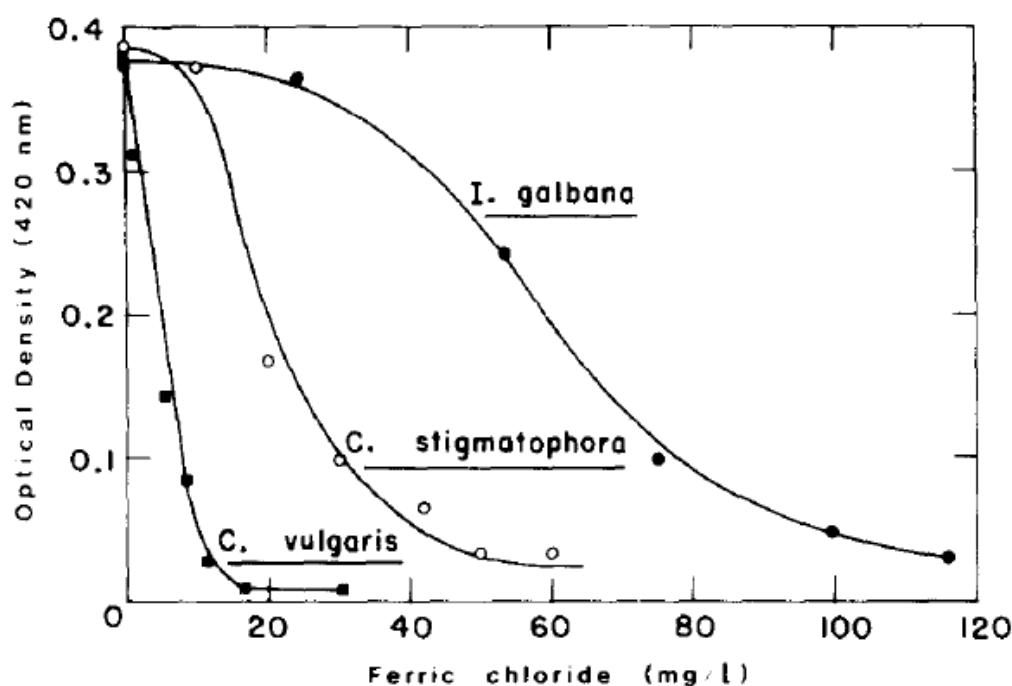
Figure 2. 13. Flocculation of marine microalgal species *(lsochrysis galbana and Chlorella stigmatophora)* and freshwater microalgal species *(Chlorella vulgaris)* with ferric chloride (Sukenik, A. et al. 1988).

Table 2.2. Optimal dosage of inorganic flocculants for marine and freshwater microalgal flocculation (Sukenik, A. et al. 1988).

Culture Medium	Microalgal Species	Optimal Dose for Flocculation (mg/L)	
		Alum	Ferric Chloride
Marine	I. galbana	225 ± 21	120 ± 15
	C. stigmatophora	140 ± 15	55 ± 9
Freshwater	C. vulgaris	25 ± 4	11 ± 4

2.2.2 Electrocoagulation (Electrolytic Coagulation)

Electrocoagulation is described by Mollah, M.Y.A. et al. (2004) as versatile, environmentally compatible, safe, selective, cost effective and amenable to automation. The main disadvantage of electrocoagulation is the need to regularly replace the sacrificial anode. The process medium also requires a minimum conductivity depending on the reactor design. If chlorides are present, some toxic chlorinated organic compounds may also be formed in situ. Gao, S. et al. (2010b) state that there are also many factors that can influence the efficiency of the electrocoagulation process. These include the electrode material, the current density, medium temperature and pH and any coexisting ions.
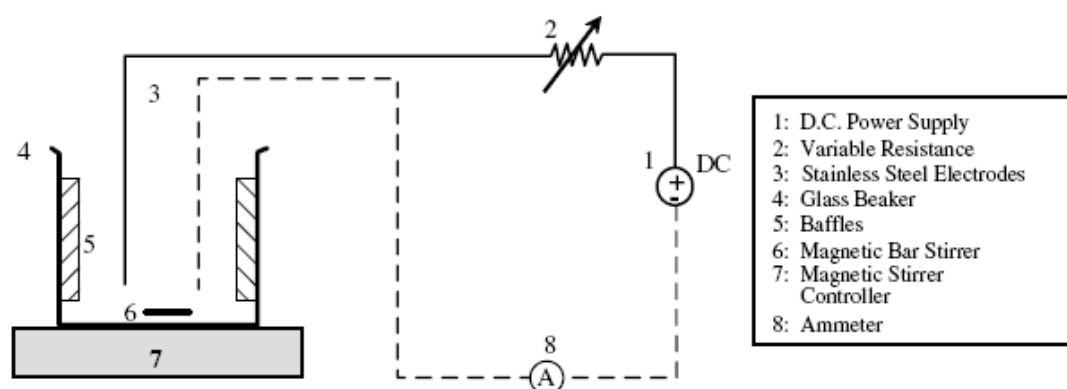
Figure 2. 14. Schematic diagram of the electrocoagulation process (Bukhari, A. A. 2008).

Aragon, A.B. et al. (1992) describe the electrocoagulation process as involving the use of chemical and physical mechanisms to separate microalgal mass from the water based medium. It is based on the fact that microalgae are able to behave as

colloid particles and therefore move in an electric field. In this process, electrolysis is utilised in order to separate the algae cells from the dilute medium.

Reactive electrodes are used which are usually connected to an external DC power source. The electrodes produce coagulating ions in situ which induce microalgae coagulation. The flocs that form from electrocoagulation are fairly large and contain less bound water. (Mouedhen, G. et al. 2008)

The process takes places in three successive stages as described by Mollah, M.Y.A. et al. (2004), Bukhari, A.A. (2008) and Ghernaout, D. et al. (2008):
1. Formation of coagulants by electrolytic oxidation of the sacrificial electrode.
2. Destabilisation of the contaminants, particulate suspension, and breaking of emulsions. This step includes compression of the diffuse double layer around the charged species by the interaction of ions generated by oxidation of the sacrificial anode. Also, charge neutralisation (resulting in a zero net charge) of the ionic species present in the media by counter ions produced by the electrochemical dissolution of the sacrificial anode and floc formation as a result of electrostatic attraction between particles.
3. Aggregation of the destabilised phases to form flocs followed by flotation.

Iron or aluminium is most commonly used as the sacrificial anode material. Studies have shown that aluminium electrodes are more efficient than iron (Gao, S. et al. 2010b) and stainless steel (Aragon, A. B. et al. 1992) electrodes. During electrolysis, iron or aluminium is dissolved from the anode, generating ions that almost immediately hydrolyse to polymeric iron or aluminium hydroxide. Coagulation results from the interaction of the metal cations with the negative algae particles that migrate toward the anode due to electrophoretic motion. Water is hydrolysed which produces hydrogen bubbles at the cathode and under certain conditions oxygen bubbles at the anode. These bubbles are able to carry the flocculated particles to the surface through their natural buoyancy. It is believed that smaller bubbles are able to provide a greater surface area for attachment of particles which results in better separation efficiency for the entire process (Alfafara, C. G. et al.

2002; Mollah, M. Y. A. et al. 2004; Azarian, G. H. et al. 2007). Jimenez, A. et al. (2010) conducted a study on the production of hydrogen bubbles for electroflotation processes and found that the pH can have a strong influence on the bubble size and production. For pH values above 2 - 3, gas bubbles in solution typically carry a negative charge.

The amount of electricity that passes through the electrolytic solution determines how much metal is dissolved into the solution. This is stated in papers by Mollah, M.Y.A. et al. (2004), Azarian, G.H. et al. (2007) and Bukhari, A.A. (2008), and can be described by the following equation that has been derived from Faraday's law:

$$w = \frac{itM}{zF}$$
(2.1)

Where w is the quantity of electrode material dissolved (g), i is the current (A), t is the time in s, M is the relative molar mass of the electrode concerned, z is the number of electrons in the oxidation/reduction reaction and F is the Faraday's constant.

The generation of bubbles and dosage of coagulant produced is determined from the current density. The current density also strongly influences mixing of the solution and mass transfer at the electrodes. Holt, P.K. et al. (2005) and Murugananthan, M. et al. (2004) looked into bubble particle interaction. They state that the probability of particle-bubble collision is greater if the bubble and particle size are similar. The bubbles that are generated from electrolysis are very small (ranging from 15 to 80 µm) and vary depending on current density and pH. At a neutral pH, hydrogen bubbles are at their smallest. The material of the electrodes also affects the bubble size of the hydrogen bubbles. Oxygen bubble size increases with pH. Bubble size has also been observed to decrease with increasing current intensity (Murugananthan, M. et al. 2004).

When a potential is applied to a simple electrocoagulating reactor set up from an external power source, the anode will undergo oxidation while the cathode will experience reduction. The electrochemical reactions include: (where M refers to the metal of the electrode) (Mollah, M. Y. A. et al. 2004):

At the anode:

$$M_{(s)} \rightarrow M_{(aq)}{}^{n+} + ne^- \qquad (2.2)$$

$$2H_2O_{(l)} \rightarrow 4H^+{}_{(aq)} + O_{2(g)} + 4e^- \qquad (2.3)$$

At the cathode:

$$M_{(aq)}{}^{n+} + ne^- \rightarrow M_{(s)} \qquad (2.4)$$

$$2H_2O_{(l)} + 2e^- \rightarrow H_{2(g)} + 2OH^- \qquad (2.5)$$
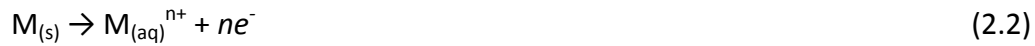
If iron is used as the sacrificial anode metal, two different mechanisms are proposed for the production of metal hydroxides (Zaroual, Z. et al. 2006; Bukhari, A. A. 2008):

Mechanism 1:

$$2Fe \rightarrow 2Fe^{2+} + 4e^{--} \qquad (2.6)$$

$$2Fe^{2+} + 5H_2O + 0.5O_2 \rightarrow 2Fe(OH)_{3(s)} + 4H^+ \qquad (2.7)$$

Mechanism 2:

$$2Fe \rightarrow 2Fe^{2+} + 4e^- \qquad (2.8)$$

$$Fe^{2+} + 2OH^- \rightarrow Fe(OH)_{2(s)} \qquad (2.9)$$
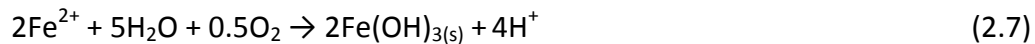
Iron ions can exist in the ferrous state, where the iron carries two positive charges (equation 2.9) or the ferric state, where iron carries three positive charges (equation 2.7). The ferric state is referred to as the oxidised state and is much less soluble in water than the ferrous state. Bukhari, A.A. (2008) states that if the iron is present in the ferrous state, then it can be concluded that the dominant mechanism of particle removal is charge neutralisation. This means that increased removal of microalgae would be observed as the coagulant dose increases.

If aluminium is used as the sacrificial anode material, the main reactions that occur are (Khemis, M. et al. 2006; Kobya, M. et al. 2006; Mouedhen, G. et al. 2008):

At the anode:

$$Al \rightarrow Al^{3+} + 3e^- \tag{2.10}$$

At the cathode:

$$2H_2O + 2e^- \rightarrow H_2 + 2OH^- \tag{2.11}$$

If the anode potential is high, secondary reactions may occur that evolve oxygen:

$$2H_2O \rightarrow O_2 + 4H^+ + 4e^- \tag{2.12}$$

Aluminium ions produced in equation 2.10 immediately undergo spontaneous hydrolysis reactions that produce various monomeric species according to the sequence (equations written without co-ordinated water molecules) (Mouedhen, G. et al. 2008):

$$Al^{3+} + H_2O \rightarrow Al(OH)^{2+} + H^+ \tag{2.13}$$

$$Al(OH)^{2+} + H_2O \rightarrow Al(OH)_2^+ + H^+ \tag{2.14}$$

$$Al(OH)^{2+} + H_2O \rightarrow Al(OH)_3 + H^+ \tag{2.15}$$
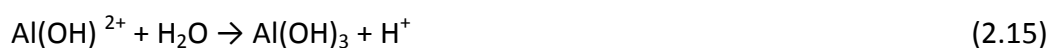
Dimeric, trimeric and polynuclear hydrolysis can also occur giving products such as $Al_2(OH)_2^{4+}$, $Al_3(OH)_4^{5+}$, $Al_6(OH)_{15}^{3+}$, $Al_7(OH)_{17}^{4+}$, $Al_8(OH)_{20}^{4+}$, $Al_{13}O_4(OH)_{24}^{7+}$, $Al_{13}(OH)_{34}^{5+}$.

The amount of aluminium ions that are produced during electrolysis is greater than the theoretical value that can be calculated from Faraday's law, as mentioned by Lee, W. and Pyun, S. (1999) and Mouedhen, G. et al. (2008). This is due to the pitting corrosion that causes metal dissolution at the anode by the chloride ions present in the medium. The reactions at the anode (equations 2.13 to 2.15) make the vicinity of the anode acidic, where as the reaction at the cathode (equation 2.11) make the vicinity at the cathode alkaline. The mechanism of action of the generated

aluminium species is charge neutralisation and sweep flocculation. The magnitude and significance of these mechanisms is dependent on pH and coagulant dose.

After electrocoagulation with aluminium electrodes, a change is observed in solution pH. When the initial pH is acidic, the pH is seen to increase due to hydrogen evolution at the cathode and/or the exchange of anions in solution such as Cl^- and SO_4^{2-} with OH^- in $Al(OH)_3$ to free OH^-. When the initial pH is alkaline, the pH is seen to drop, explained by oxygen evolution and/or the dissolution reactions of aluminium and its hydroxide as $[Al(OH)_4]^-$ being alkalinity consumers. (Murugananthan, M. et al. 2004; Mouedhen, G. et al. 2008)

A study by Aragon, A.B. et al. (1992) compared the efficiency of conventional microalgae recovery by flocculation with aluminium sulphate $[Al_2(SO_4)_3.18H_2O]$ and electrocoagulation. The microalgae used for the experiments consisted of a mix of 80 % *Scenedesmus acutus* and 20 % *Chlorella vulgaris*. The experiment conducted for the flocculation was the standard jar test. For the electrolytic experiments, the electrode material was aluminium and had a total active surface area of 54 cm^2. Samples were taken from the bottom of the experimental vessel at periodic time intervals and the absorbance measured in order to determine the microalgae concentration. The experiment was performed at various current densities and potential differences. Figure 2.15 shows the results obtained for the electrolysis experiments. The figure clearly shows the influence that the applied current can have on the removal percentage of the microalgae. It is concluded from the results that electrolysis techniques are more effective than flocculation. This decision was based on the fact that electrolysis had a lower cost (the cost of energy was lower than the cost of flocculants), had a shorter time for separation to occur, and a lower probability that the recovered microalgae would be contaminated with metallic hydroxides.
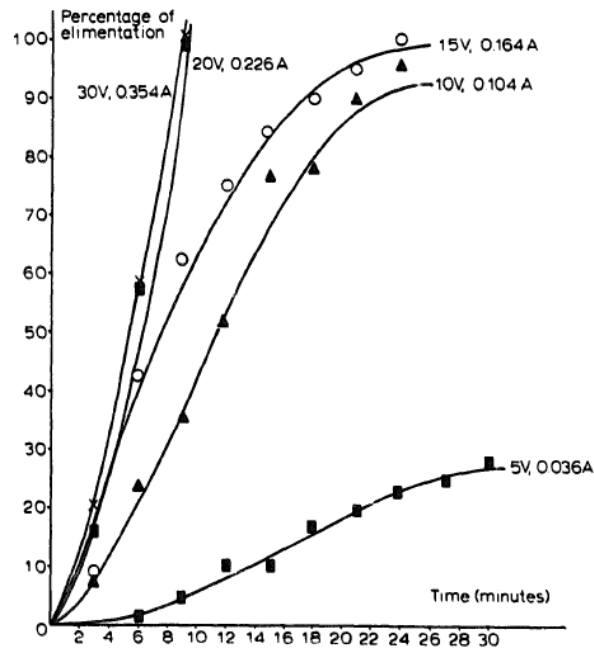
Figure 2. 15. Percentage of microalgae removal versus time for different currents with microalgae mix 80 % *Scenedesmus acutus* and 20 % *Chlorella vulgaris* (Aragon, A. B. et al. 1992).

Aragon, A.B. et al. (1992) found that there is a relationship between the potential difference applied and the time needed for electrolysis to occur to achieve a certain level of microalgal separation. This relationship was further demonstrated by Azarian, G.H. et al. (2007) who studied the effect of continuous flow electrocoagulation for the removal of microalgae from wastewater. The experiments consisted of five aluminium electrodes in the shape of flat plates (three anodes, two cathodes). The choice of electrode material was based on the fact that electrode dissolution would introduce a flocculant into the system. The removal of microalgae was determined from chlorophyll a and TSS measurements. Figure 2.16 shows the removal of chlorophyll a and TSS with increasing electrical power input. The results showed that applying higher power inputs led to and increased microalgae removal rate. An increase in power also resulted in a decrease in the time required to achieve separation as well as an increase in the amount of flocculating agent produced. Using a higher power also resulted in an increase in temperature. The change in pH was insignificant.
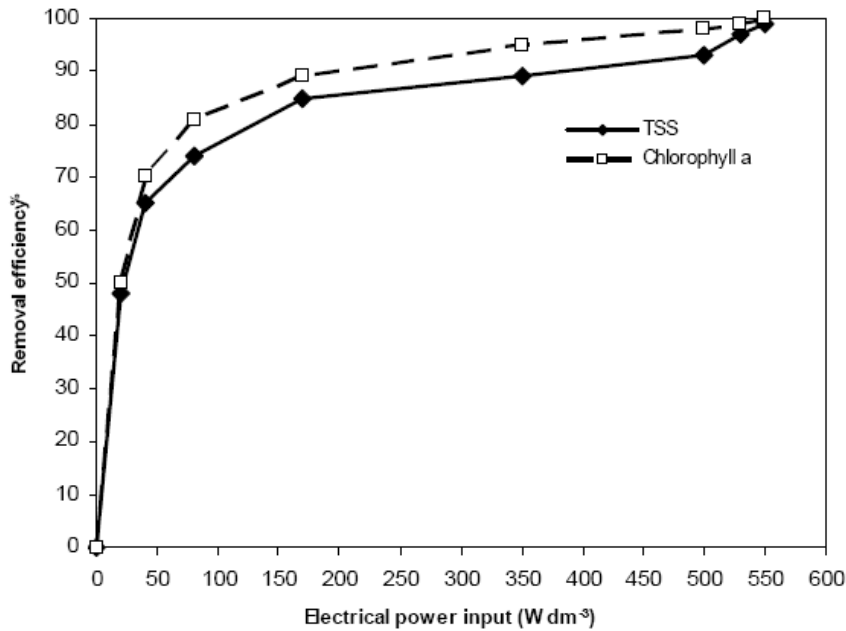
Figure 2. 16. Chlorophyll a and TSS removal efficiencies at different electrical power inputs with a retention time of 10 minutes (Azarian, G. H. et al. 2007).

Aragon, A.B. et al. (1992) also studied the affect of microalgae concentration on electrocoagulation. It was found that higher removal efficiencies could be obtained when the initial concentration of chlorophyll a (i.e. concentration of microalgae) was high. This can be explained due to the fact that the amount of colloids present in the solution is not adequate for the formation of solids. Higher concentrations of microalgae increase the probability of interactions between particles, which will give better a better flocculation result.

A study conducted by Poleman, E. et al. (1997) investigated electrolytic flocculation of freshwater microalgae. The experiments were carried out in a 100 L vessel with electrodes arranged vertically. Different set-ups were tested with varying distance between cathode and anode, voltages and current densities. The results showed that electrolytic flocculation was successful in removing microalgae from dilute suspensions, having removed 80 - 95 % of microalgae in 35 min. Decreasing the voltage led to slower microalgae removal rate but it had the advantage of consuming less energy. Decreasing the total surface area of the electrodes and increasing the distance between electrodes also consumed less energy. For microalgae

concentrations varying between 2.7 and 36.1 mg dry mass/L, energy consumptions were 122.2 and 9.1 kWh/kg, respectively.

Alfafara, C.G. et al. (2002) investigated electrolytic microalgae removal in batch and semi continuous reactors. Microalgae was obtained from lake water, with the dominant species being *Microcystis sp.* The electrodes used were polyvalent aluminium alloy for the anode and titanium alloy for the cathode. Carbon anodes were also used to determine the amount of removal that could be achieved without the coagulation that occurs from metal dissolution. The removal of microalgae was determined from chlorophyll a measurements. The results obtained were similar to that obtained in studies by Aragon, A.B. et al. (1992), showing a higher chlorophyll a removal at a shorter time with a higher electrical power input.

The idea behind replacing the aluminium anode with carbon is that the metal dissolution step does not occur for carbon, as it is inert. This means that the only mechanism of microalgae removal is the bubble-particle interaction and flotation. Alfafara, C.G. et al. (2002) discovered that the rate of chlorophyll a removal was less efficient and much slower with the carbon electrodes due to the removal mechanism being electro-flotation alone. Figure 2.17 shows the comparison of microalgae removal using polyvalent aluminium and carbon anodes. These results emphasise the importance of the flocculation mechanism in the electrocoagulation process.
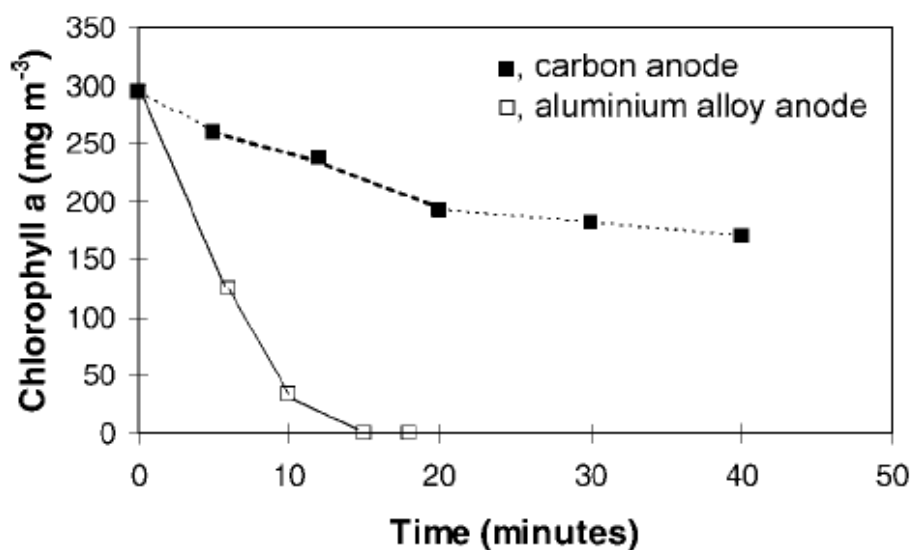
Figure 2. 17. Comparison of microalgae removal using polyvalent aluminium alloy and carbon anodes (Alfafara, C. G. et al. 2002).

The effect of mixing speed was also investigated by Alfafara, C.G. et al. (2002). A reduction in removal was observed at higher mixing speeds (550 rpm). This can be explained by higher shear forces which may destroy the microalgae flocs or disperse the gas bubbles which normally entrap the flocs.

An investigation on electrocoagulation treatment for the removal of total suspended solids from wastewater was conducted by Bukari, A.A. (2008). Stainless steel electrodes were used at various current and contact times. It was found that at lower current of 0.05 A and 0.1 A, the removal efficiency increased as the amount of iron generated in the system increased. This is consistent with the charge neutralisation mechanism, where removal increases as the coagulant dose increases. The results obtained at higher currents (0.2, 0.4 and 0.8 A) suggest that the dominant mechanism of particulate removal is sweep floc coagulation where the coagulant forms a precipitate which settles by gravity and collides with and drags colloids down with them. Chlorine is able to be used as an oxidant to convert ferrous iron into insoluble ferric iron. The wastewater in the study contained high concentrations of chlorine ions. At higher currents, more chlorine gas is produced, which results in the conversion of ferrous iron to insoluble ferric iron. This may affect sweep floc coagulation. Murugananthan, M. et al. (2004) has shown that the use of

49

iron electrodes at higher potentials favours the formation of Fe(III) ions. Precipitation of Fe(III) hydroxides have a better coagulating ability than Fe(II) hydroxides (Zaroual, Z. et al. 2006).

A study by Gao, S. et al. (2010a) investigated the effect of chloride ions for microalgae removal with electrocoagulation using aluminium electrodes. The species of microalgae used was a freshwater species, *M. aeruginosa.* The presence of chlorine ions was found to increase the performance of the electrocoagulation process. This is said to be due to the fact that chloride ions are able to increase the electrical conductivity of the medium, which means that the process would then require a lower applied voltage to run. If aluminium electrodes are used, an insulating film of alumina (Al_2O_3) may form on the electrodes which causes increased resistance and requires a greater current density to be applied. It also inhibits the dissolution of Al^{3+} and electron transfer (Lee, W. and Pyun, S. 1999; Wang, C. et al. 2009). The presence of chloride ions promotes the breakdown of this alumina film through pitting corrosion (Mouedhen, G. et al. 2008). Oxidation of chloride ions into active chlorine species (chlorine, hypochlorus acid, hypochlorite) can occur which may improve removal of certain pollutants by oxidation. Oxidation can also result in the inactivation of microalgae cells.

It was also found by Gao, S. et al. (2010a) that the concentration of Al^{3+} in the absence of Cl^- was lower than the theoretical value. This may be due to the competition between Al^{3+} ion dissolution and O_2 evolution at the anode. The formation of alumina on the anode surface may also inhibit the dissolution of Al^{3+} as well as electron transfer, which can decrease the current efficiency.

The zeta potential after electrocoagulation was also monitored by Gao, S. et al. (2010a). The zeta potential can be used as a measurement of the amount destabilization of microalgae cells. The higher the degree of destabilisation, the more likely flocculation will occur. The zeta potential was measured after electrocoagulation. The results can be seen in figure 2.18 and show that with increasing electrolysis time, the zeta potential became more positive. It was also

50

observed that the rate of increase of the zeta potential with electrolysis time increased as the concentration of Cl⁻ increased from 1 to 5 mM, where as the rate slowed down when the concentration of Cl⁻ was further increased to 8 mM. According to Canizares, P. et al. (2008) and Trompette, J.L. and Vergnes, H. (2009), this may be due to the fact that Cl⁻ ions can be absorbed onto the surface of aluminium hydroxide species, which increases the negative charge of the aluminium hydroxide precipitates under alkaline condition. Or the positive charges of the aluminium hydroxide hydrolysis species may be reduced due to the increase in concentration of Cl⁻ ions.
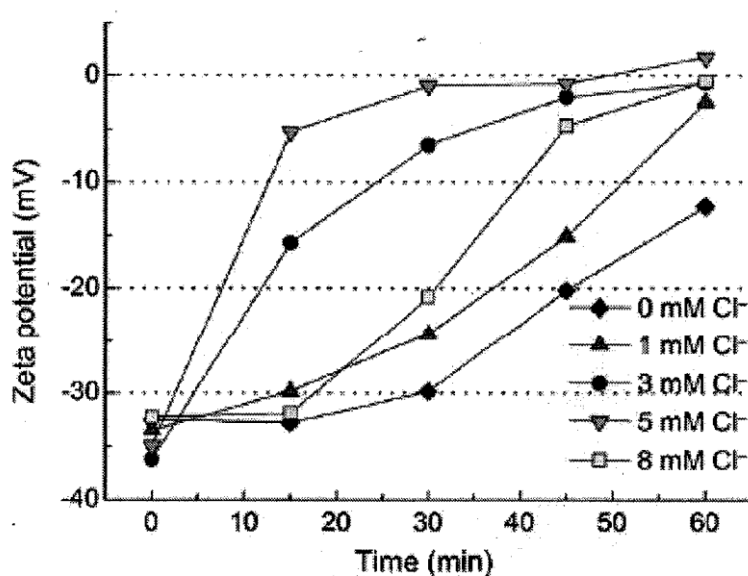
Figure 2. 18. Zeta potential with time for electrocoagulation with *M. aeruginosa* at varying Cl⁻ concentrations (Gao, S. et al. 2010a).

The equations relating to chloride ion oxidation are: (Gao, S. et al. 2010a)

$$2Cl^- \rightarrow Cl_2 + 2e^- \tag{16}$$

$$Cl_2 + H_2O \rightarrow HOCl + H^+ \, Cl^- \tag{17}$$

$$HOCl \rightarrow H^+ + OCl^- \tag{18}$$
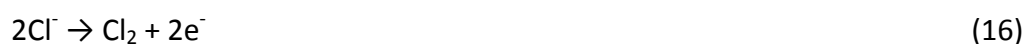
Gao, S. et al. (2010a) found that the efficiency of algae removal during electrocoagulation can be significantly improved in the presence of Cl⁻. Active chlorine is generated in the presence of Cl⁻ and the amount of active chlorine increased with time and initial Cl⁻ concentration. This also had the effect of

inactivating the algae cells. The Cl⁻ ions in the solution were also able to increase the amount of Al^{3+} release, which can be explained by pitting corrosion and the removal of the oxide film due to the presence of the Cl⁻ ions. The Cl⁻ ions also had the added effect of reducing the magnitude of the zeta potential of the algae to values closer to zero, which further destabilises the particles, leading to coagulation.

A study was conducted by Vandamme, D. et al. (2011) on freshwater microalgae *Chlorella vulgaris* and marine microalgae *Phaeodactylum tricornutum.* Electrocoagulation was carried out using iron and aluminium electrodes. Optimal recovery of marine microalgal species was obtained above 80 % at a run time of 30 min and current density 3 mA/cm². The result can be explained by the increase in coagulant dosage i.e. metal dissolution that occurs with increasing the applied current and run time. Visual observation of the process showed the formation of brown-green precipitates when using the iron electrode and a milky precipitate when using the aluminium electrode. The efficiency of electrocoagulation was seen to decline with increasing pH for both microalgae species.
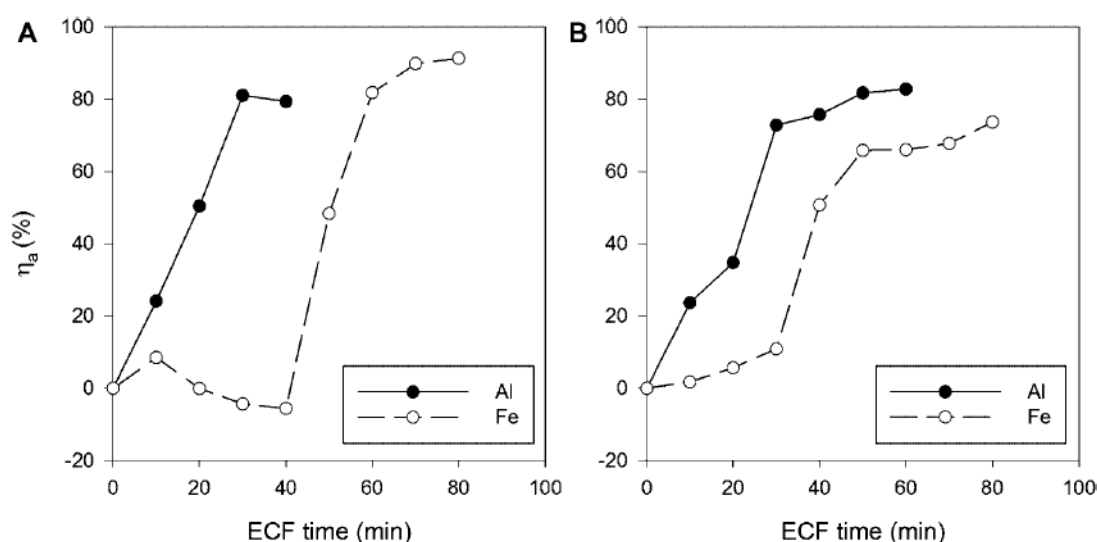
Figure 2. 19. Microalgae recovery as a function of electrocoagulation time using different electrodes. (A) *Chlorella vulgaris,* (B) *Phaeodactylum tricornutum,* 3 mA/cm² (Vandamme, D. et al. 2011).

2.2.3 Combined Flocculation and Electrocoagulation

A study by Can, O.T. et al. (2006) investigated the effect of electrocoagulation with aluminium anodes coupled with flocculating agents such as alum and PAC, for the treatment of textile wastewater. PAC is a pre-polymerised Al(III) chemical that contains a range of hydrolysis and polymeric species which are relatively large and carry a high cationic charge. Their enhanced surface activity and improved charge neutralising capacity may make them more effective at a comparatively lower dose than alum. The results from this study (figure 2.20) found that the coupling of alum and PAC to electrocoagulation resulted in a significant improvement on the percentage of COD removal. The results showed that the combination of techniques resulted in an increase in performance and rate of electrocoagulation, and a reduction in operating costs and electricity consumption. For an operating time of 5 min, the COD removal rate was improved from 23 % with electrocoagulation alone to 78 % with combined flocculation (addition of 0.8 kg PAC/m^3) and electrocoagulation.
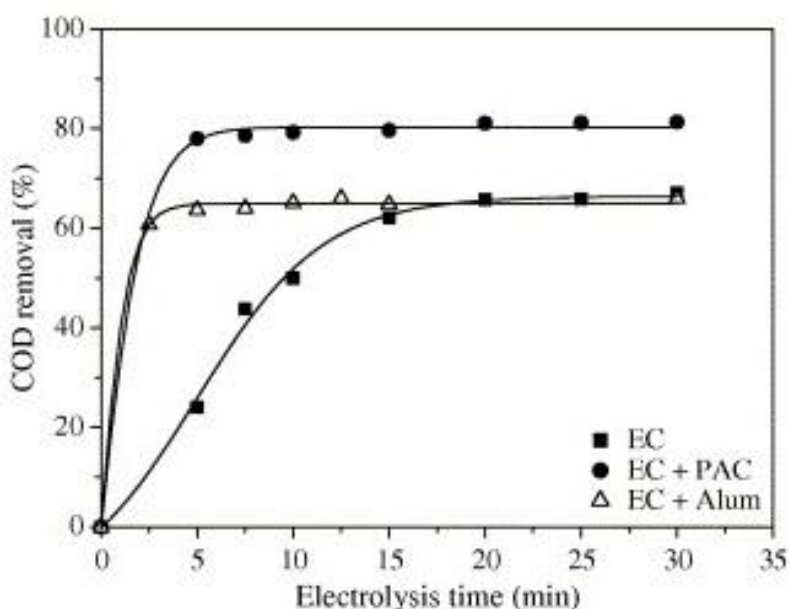
Figure 2. 20. Percentage COD removal with time for electrocoagulation, electrocoagulation coupled with PAC and electrocoagulation coupled with alum (Can, O. T. et al. 2006).

2.3 Research Gaps

A large number of studies have been completed on the harvesting and recovery techniques of microalgal cells in dilute suspensions. The choice of which harvesting technique to use depends on the characteristics of the microalgal species and the final product desired. Desired microalgal properties that simplify harvesting are large cell size, high specific gravity compared to the medium and reliable auto-flocculation (Borowitzka, M. A. 1992). In addition to these, the optimum harvesting method chosen for a particular microalgal species should have minimum energy requirements and be as economical as possible. The main harvesting techniques are summarised in chapter 1. It was concluded from chapter 1 that the most promising dewatering techniques were flocculation and electrocoagulation due to their relatively low cost and energy requirements. The literature review detailed the work that has been conducted thus far on both flocculation and electrocoagulation. The gaps in the research are presented below.

Freshwater microalgae flocculation has been thoroughly studied over many years. However, there is a dearth of information and comparative studies for marine microalgae. With growing concern about freshwater resources in many parts of the world, further research on the processing of marine microalgae would be very beneficial. Flocculation efficiency in saline water is contradictory. Optimum flocculation parameters and real time monitoring of the flocculation process for marine microalgal species is lacking in the preceding research that has been done to date.

Electrocoagulation with marine microalgal species has also only been studied very briefly. The saline environment would serve to increase the conductivity and reduce the power input compared to that of freshwater, making the technique a suitable candidate for further research. The theory of the mechanism of electrocoagulation has been reported extensively, however no exact evidence or investigations into the rate limiting step of the process or experimentally proving the theories have been published to date. Current electrocoagulation research, having focused mainly on

the percentage of recovery of microalgae, the efficiency of electrodes and energy demand of the process, lack data on the dissolving metal such as mass balances in the system, evidence of the valency of species dissolving from the anode material, the amount of metal required for effective coagulation and the amount of metal remaining in the separated and recovered microalgae. Current literature lacks investigation and analysis of the hydrogen produced in the system; such as the percentage of bubbles used for flotation. There has also been no work published that involves the development of a mathematical model for predicting batch electrocoagulation recovery.

CHAPTER 3 MATERIALS AND METHODS

3.1 Characteristics of the Microalgae

The microalgae species used in the experimental work are *Chlorococcum sp.* and *Tetraselmis sp*. Both are a marine microalgae species and have approximately equal cell size and characteristics. *Chlorococcum sp*. is an indigenous Australian microalgae species and *Tetraselmis sp.* was obtained from CSIRO Microalgae Research Centre (Hobart Australia). The two species differ in cell shape and structure. *Tetraselmis sp*. have flagella and are motile where as *Chlorococcum sp.* are not. The significant difference in shape, structure, growth characteristics and motility of the two microalgae species enables a species comparison of flocculation and flotation separation efficiency. Table 3.1 shows the main microalgae properties of microalgae species *Chlorococcum sp. a*nd *Tetraselmis sp.* Figure 3.1 shows a microscope image of microalgae species *Chlorococcum sp. a*nd *Tetraselmis sp..*

The exact choice of microalgae species used was outside the scope of this research. The work was conducted in collaboration with Biomax Pty Ltd, who made the decision to use *Chlorococcum sp.* and *Tetraselmis sp.* based on the fact that their research showed that both species had adequate lipid stores that made them suitable for use in biodiesel production.

Table 3. 1. Microalgae properties of *Chlorococcum sp.* and *Tetraselmis sp.*

	Chlorococcum sp.	Tetraselmis sp.
Dry weight concentration (g/L)	0.3 (electrocoagulation work) 0.6 (flocculation work)	0.6 (electrocoagulation work) 0.3 (flocculation work)
pH of microalgae cells in culture media	9.17	8.34
Conductivity of microalgae cells in culture media (mS/cm)	42.83	47.08
Approximate cell size range (µm)	10 (diameter)	10 (width)
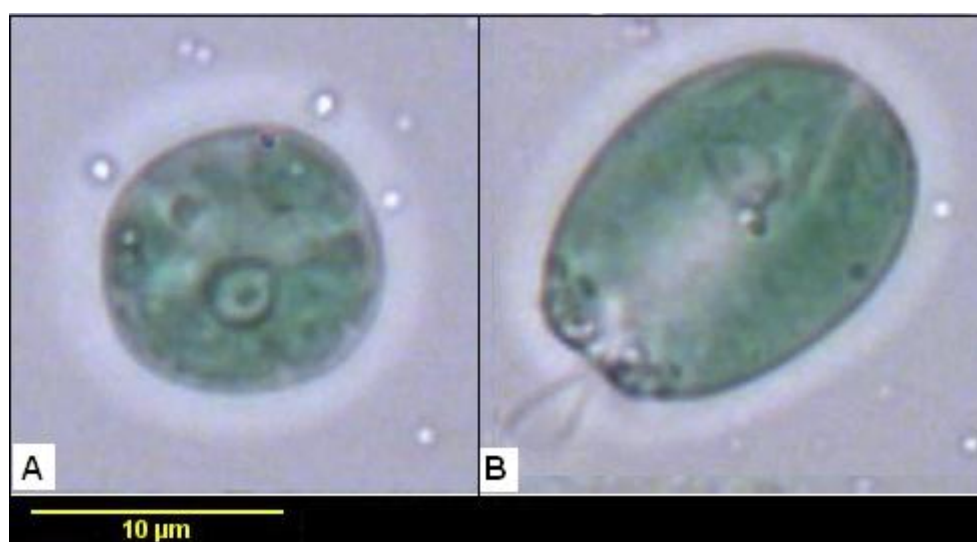
Figure 3. 1. Microscope image of microalgae species. A) *Chlorococcum sp.* at x 100 magnification, B) *Tetraselmis sp*. at x 100 magnification.

[1] There was a transition period for the changing of the flue gas/ compressed air mixture to only compressed air. The exact period is not known; therefore this data is presented to the best of my knowledge.

3.2 Microalgae Culture Description

Laboratory scale semi-continuous microalgal photobioreactor bags with a maximum volume of 100 L were used to cultivate marine microalgal cells from the genus *Chlorococcum sp*. and *Tetraselmis sp*. (figure 3.2). The temperatures of the cultures were between 17 - 24 °C, corresponding to ambient temperatures between 20 - 28 °C. The source of carbon for the microalgae growth was initially from carbon dioxide supplied from aeration with a flue gas (sourced from Monash University engineering boiler house) and a compressed air mixture (20:80). However, this was later changed to 100 % air with a nominal CO_2 concentration of 0.03 vol % [1]. The microalgae used for flocculation work was grown with the flue gas/ compressed air mixture and the electrocoagulation work was done with microalgae grown with compressed air only. The sparging of the flue gas/compressed air mixture served as a means for obtaining uniform mixing of the microalgae culture.

The harvested cultures were stored at room temperature after collection and were tested within 120 h. Both microalgae mediums had a salinity of 30 g/L. All experiments were performed with cells from a single harvest, at the stationary phase. This was done to ensure the same growth phase and storage conditions and to nullify any variations that could result from differences in culture conditions. Please refer to appendix A.1.3 for details on microalgae harvesting.
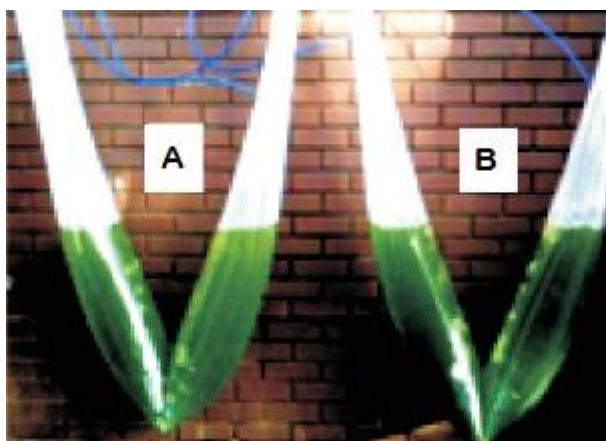
Figure 3. 2. Microalgae bioreactor bags: A) *Chlorococcum sp.* B) *Tetraselmis sp.*

58

3.3 Flocculation – Jar Stirrer Test

The polyelectrolyte flocculants investigated were obtained from two Australian chemical manufactures; Nalco and Ciba. A range of cationic, anionic and non-ionic polyelectrolytes were acquired. Please refer to table 3.2 for details. The alum flocculant was obtained from Australian chemical manufacturer Orica.

Table 3. 2. Charge density and molecular weight properties of polyelectrolyte flocculants.

Polyelectrolyte flocculant	Manufacturer	Charge density	Molecular weight
71303	Nalco	low/medium cationic	medium
71305	Nalco	low cationic	medium/high
71301	Nalco	medium cationic	medium/high
82230	Nalco	low/medium anionic	medium/high
Magnafloc 156	Ciba	medium anionic	high
Magnafloc 155	Ciba	low/medium anionic	high
Magnafloc 351	Ciba	non ionic	high

The flocculation experiments were carried out in 1 L batch jar tests. A desired dose of the flocculant was added into the microalgae solution. For polyelectrolyte flocculants, the mixture was agitated at 200 rpm for 10 s for a fast mix followed by a slow mix for 10 min at 50 rpm. The polyelectrolyte mixing conditions were determined experimentally by performing flocculation experiments at varying mixing conditions to obtain the optimum settings. Please refer to appendix A.3.1 for details. For alum flocculation, the mixture was agitated at 100 rpm for 1 min for a fast mix followed by a slow mix for 4 min at 60 rpm. The alum mixing conditions were taken from Mc Garry, M.G. and Tongkasame, C. (1971) as the mixing conditions that would give adequate dispersion of alum into the solution. The flocculated microalgae was then left to settle for 30 min. A sample of the solution was pipetted from a fixed

height in the jar corresponding to a volume of 0.8 L. The absorbance of this sample was measured using a UV-VIS-2450 spectrophotometer (Shimadzu, Australia). Please refer to Appendix A.1.4 for details. The absorbance of settled microalgae was also measured at a fixed height. The recovery of microalgae was calculated as the percentage mass of microalgae flocculated and settled compared to the total mass of microalgae in the system.

3.4 Electrocoagulation

Electrocoagulation was carried out in a 300 ml rectangular vessel with electrodes made of flat stainless steel (L × W × H = 120 × 1 × 20 mm). The electrodes were mounted along two opposite walls in the vessel, 48 mm apart. A laboratory power supply (1 - 15 V) was used to apply the electric current. Figure 3.3 shows a schematic diagram of the electrocoagulation cell, and figure 3.4 shows a real image of the electrocoagulation cell. Electrocoagulation experiments were performed under batch conditions with varying duration at: (1) specific voltages: (2) at specific currents. Figure 3.5 shows a schematic diagram of the electrocoagulation experimental set up. After cessation of the electric current, the vessel was left standing for 15 min to allow the concentrated microalgae to float to the surface (15 min was chosen as it allowed adequate time for the flotation of all flocs). Figure 3.6 shows the floated microalgae layer after electrocoagulation. Three distinct sections exist in a side elevation view of the culture; the floated microalgae concentrate, the seawater supernatant with less suspended microalgae cells, and the settled microalgae. The size of each layer varies depending on the applied current and time. The concentration of each microalgae sample was then measured at 570 nm via absorbance with a UV-VIS-2450 spectrophotometer (Shimadzu, Australia). The microalgae recovery of the system was calculated as the percentage of microalgae that had floated to the surface in comparison to the total mass of microalgae in the system.

Due to the imposition of the current, the cathode material is inert. The material chosen for the cathode was ferritic stainless steel type 430. Ferritic stainless steels

are relatively cheap, are magnetic, have a body centered cubic atomic structure and have similar mechanical properties to carbon steel, although less ductile. The chromium content in ferritic steels is limited to about 28 % (Schweitzer, P. A. 2007).

The different materials investigated for the anode were ferritic stainless steel type 430, aluminium and carbon (graphite). Ferritic stainless steel and aluminium both act as sacrificial anodes when an electrical circuit is completed, and will dissolve into the solution as either Fe or Al ions. Both metals have a passive state where they are protected by an oxide layer. However, when sufficient voltage is applied, they both become active and are able to dissolve. Ferritic stainless steel has a disadvantage that both iron and chromium will be dissolved and chromium is toxic. However, from metal concentration analysis of microalgae after electrocoagulation, the percent of chromium was found to be insignificant (please refer to Appendix A.3.2). Aluminium is one of the most abundant elements and is known for its low density, and is generally considered to be safe. It is also soft, lightweight, ductile and malleable metal and is non magnetic. Graphite has a layered, planar structure where the carbon atoms are arranged in a hexagonal lattice. Graphite is able to conduct electricity and is highly diamagnetic. Graphite does not act as a sacrificial anode; hence it will not dissolve into the microalgal solution when an electric current is applied.

Table 3. 3. Anode material properties.

Material	Half Cell Reaction	E° (Volts)	Cost (USD/kg)	Reference
Aluminium	$Al^{3+}_{(aq)} + 3e^- \leftrightarrow Al_{(s)}$	-1.66	2.2	(Metal News 2011)
Stainless steel	$Fe^{2+}_{(aq)} + 2e^- \leftrightarrow Fe_{(s)}$	-0.44	1.98	(Metal News 2011)
Carbon	No reaction (inert)	-	2.5	(Northern Graphite 2011)
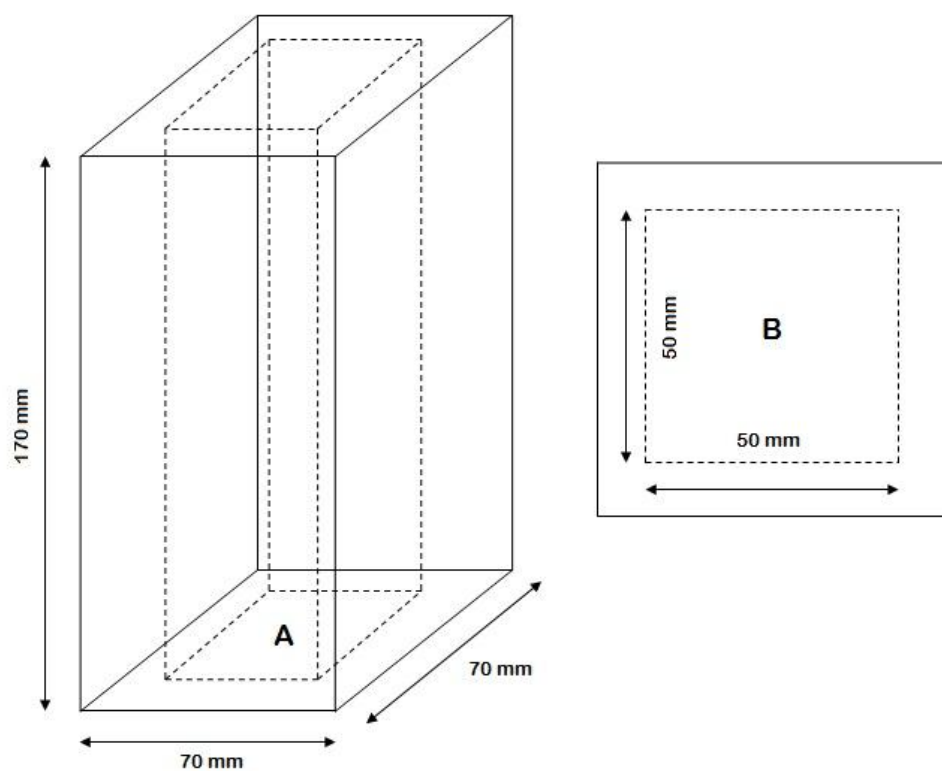
Figure 3. 3. Schematic diagram of electrocoagulation cell: A) side view, B) top view.
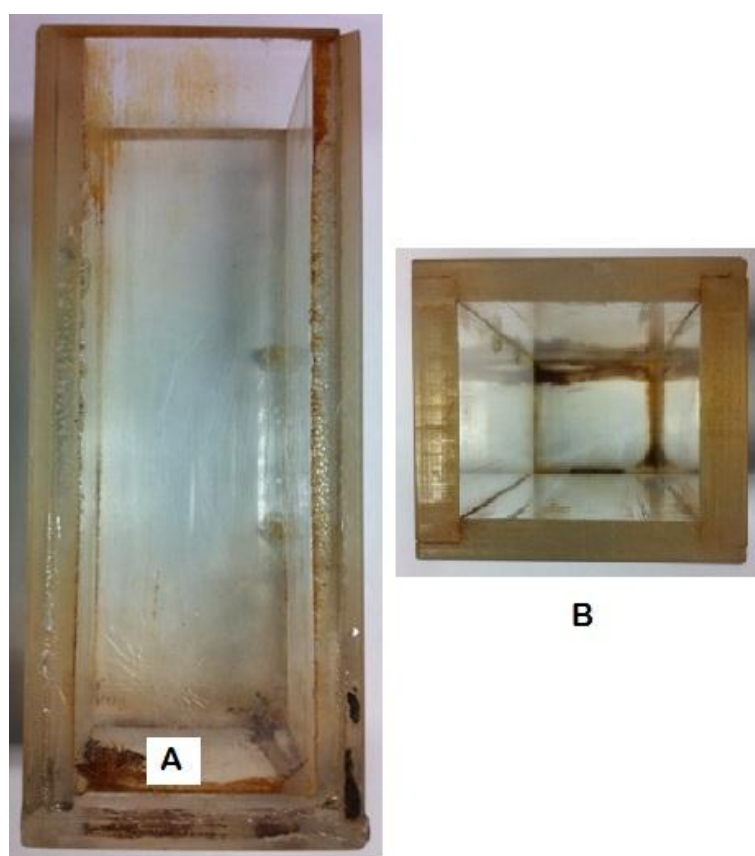
Figure 3. 4. Image of electrocoagulation cell: A) side view, B) top view.
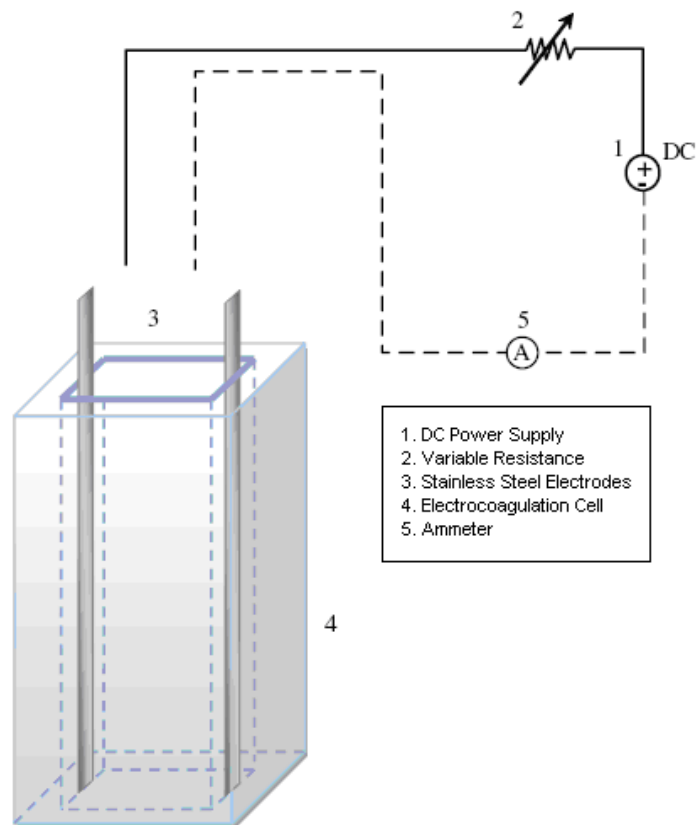
Figure 3. 5. Schematic diagram of electrocoagulation set up.
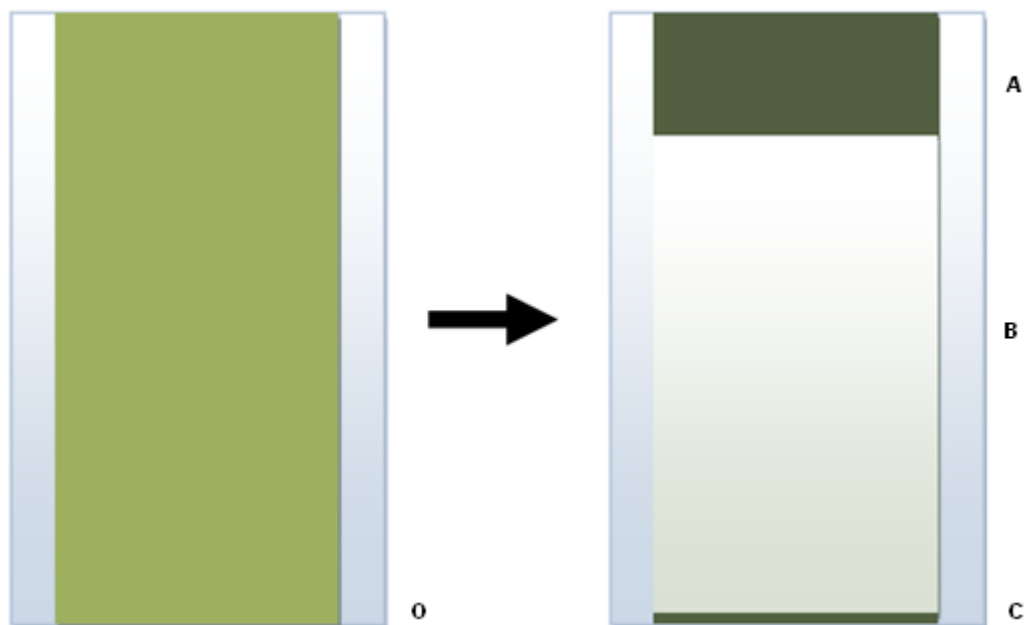
Figure 3. 6. Schematic diagram of sample before and after electrocoagulation.

A) Floated microalgae concentrate, B) Seawater supernatant with minimal remaining microalgae, C) Settled microalgae, O) Original microalgae before electrocoagulation.

3.5 Focused Beam Reflectance Measurement

A Focused Beam Reflectance Measurement probe (or FBRM probe) (Mettler Toledo, Australia) was used to estimate the algae size distribution by determining the chord size distributions of the fresh microalgae species. The FBRM operates by scanning a highly focused laser beam (with a wavelength of 780 nm) at a fixed speed across particles in suspension. A chord is determined from laser reflectance and is a characteristic dimension of the particle in the flow field perpendicular to the laser probe. Based on the manufacturer's recommendations, the mixer speed was set at 400 rpm. The time duration of the backscattered light from each particle is measured and multiplied by the velocity of the scanning laser (Blanco, A. et al 2002; Heath, A.R. et al. 2002). The size and number of particles are given in terms of the chord length, which is calculated from the time the particle takes to pass through the laser beam. For a spherical particle the average chord length is less than the particle diameter, because chords can be obtained that do not pass through the centre of the particle. Therefore, the FBRM only provides an estimate of the particle size and its main use is in showing the difference in particle size distribution due to the processing conditions.
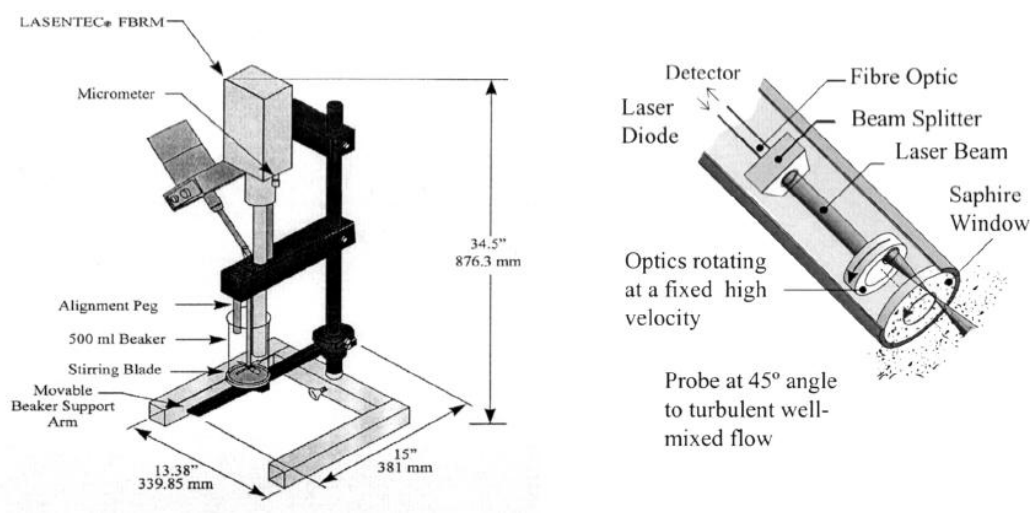
Figure 3. 7. Schematic diagram of FBRM setup (Blanco, A. et al. 2002).

The FBRM was used to estimate the size distribution of the microalgae. Figure 3.8 shows the FBRM distribution of *Chlorococcum sp.* and *Tetraselmis sp.* The distribution shows a higher range of counts per second for *Chlorococcum sp.* which indicates a higher microalgae culture concentration. The importance of the distribution to this research is that it shows that the chord distribution of both species is similar, meaning that differences observed in flocculation and flotation will not be due to any differences in microalgae cell size. The single cells are around 10 microns, as shown in figure 3.8. Due to the differences in growth kinetics of the two species, the concentration of *Tetraselmis sp.* and *Chlorococcum sp.* were not identical. Figure 3.8 shows that the counts per second values for *Tetraselmis sp.* is half that of *Chlorococcum sp.*, showing the difference in concentration between the species. Figure 3.9 shows the counts per second values divided by the dry weight concentration of each microalgae species. From the figure, it can be seen that apart from varying concentrations, the size distributions of both microalgae species are similar.
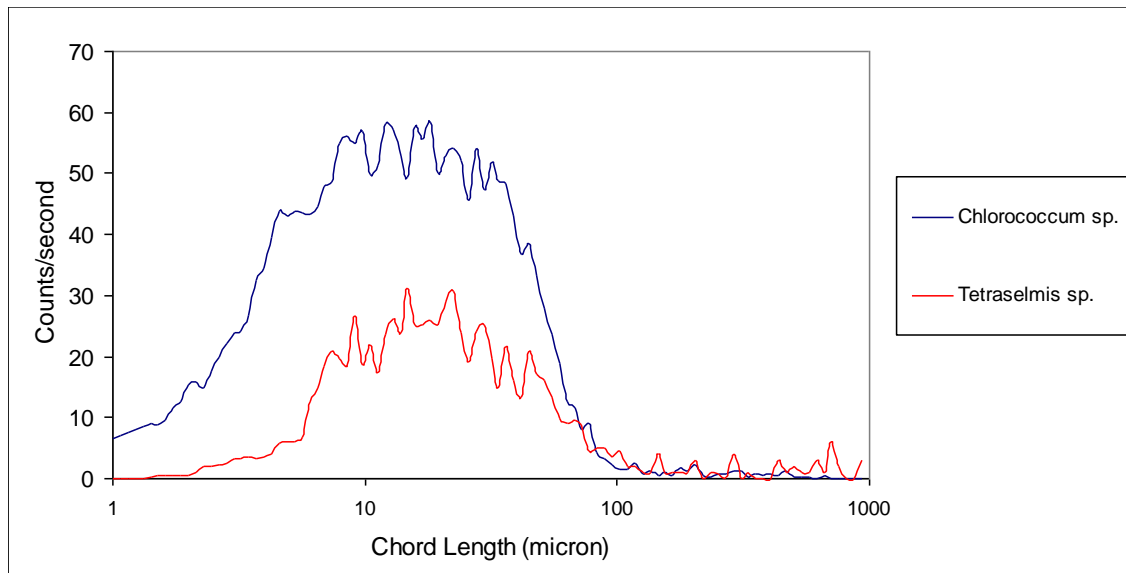
Figure 3. 8. FBRM analysis – distribution of chord length versus counts per second for freshly harvested *Chlorococcum sp.* at dry weight concentration 0.6 g/L and *Tetraselmis sp.* at dry weight concentration 0.3 g/L.
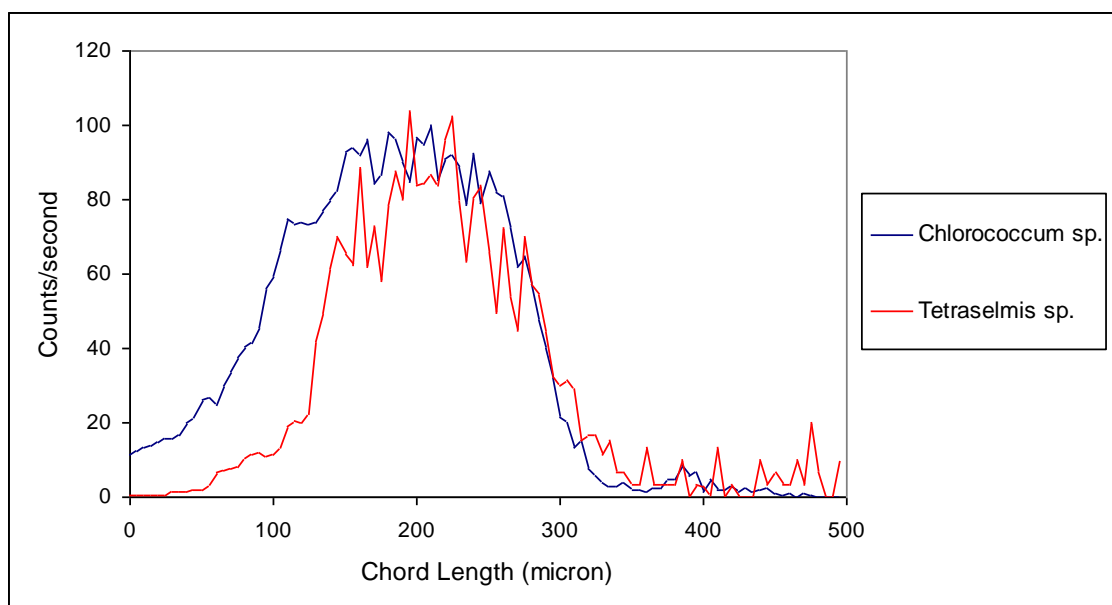
Figure 3. 9. FBRM analysis – distribution of chord length versus counts per second divided by microalgae dry weight concentration, for freshly harvested *Chlorococcum sp.* and *Tetraselmis sp.*

The FBRM was used in this research to observe the flocculation process in real time and to determine the efficiency of flocculation. For real time flocculation, the flocculant was added to a sample of microalgae, and the particle counts per second was measured with time. This resulted in a graph showing the change in particle size of the microalgae, which can be seen in chapter 4. To measure the efficiency of the flocculation process, the FBRM was used to obtain particle distributions of the microalgae before and after flocculation. This resulted in a graph showing the difference in particle counts per second versus the particle size of the sample, which can be seen in chapter 4. The FBRM instrument can measure a maximum particle size of 1000 μm, but this was not an issue as the flocs that formed did not exceed 500 μm.

3.6 Zeta Potential

The Zeta Potential of the microalgae was measured in folded capillary cells with a sample size of approximately 1 ml. The measurements were conducted before and after electrocoagulation on undiluted samples with a Zetasizer Nano ZS (Malvern, Australia). The Zetasizer Nano ZS can measure the Zeta Potential of particles with

diameters from 3.8 nm to 100 μm. The instrument can accept samples with concentrations from 0.1 ppm to 40 % w/v, at temperatures up to 120 °C. Measurements were taken in triplicate to ensure reproducibility and a quality factor was provided by the instrument for each measurement that gave confidence in the data obtained. If there was not sufficient agreement, the results were not kept.

3.7 Temperature

The temperature of the medium was varied in order to investigate the effect on flocculation efficiency or electrocoagulation removal efficiency. The temperature was increased to the desired temperatures using a stirred hot plate, or decreased by allowing it to cool in a refrigerator at 4 °C.

3.8 pH

The pH of the medium was varied in order to investigate the effect on flocculation efficiency or electrocoagulation removal efficiency. The pH of microalgae was adjusted to more alkaline conditions using 1 molar sodium hydroxide or acidic using 1 molar hydrochloric acid. The pH was measured using a pH probe connected to a digital pH meter (TPS Pty Ltd, Australia).

3.9 Salinity

The salinity of the microalgae was changed from 100 % (which corresponded to the typical salinity of the media) to salinity values that were reduced by dilution with de-ionised water, given in table 3.4. This was done in order to observe the effect of salinity on electrocoagulation removal efficiency. The salinity of the microalgae was measured based on the electrical conductivity of the solution using a conductivity probe connected to a conductivity meter (TPS Pty Ltd, Australia).

Table 3. 4. Salinity of microalgae with addition of de ionised water.

% Microalgae	% De-ionised water	Concentration of culture media (g/L)
100	0	30
80	20	24
50	50	15
20	80	6

3.10 Capture of Bubble-Floc Aggregations

The flotation of the microalgae flocs due to bubble attachment was observed using a high speed camera (MotionPro Y3 of Integrated Design Tools, Inc., Germany). The camera is capable of capturing 2560 × 2048 images at a shutter speed of 5000 fps. The shutter speed was calibrated periodically. The cell used for these experiments was a mini cell (L × W × H = 100 × 80 × 2 mm). The mini cell was used because the camera required adequate light to pass through the cell in order to clearly capture the bubble/floc images. Please refer to Appendix A.3.6 for details of mini cell and camera set up.

3.11 Microalgae Cell Viability

The microalgae cell viability (health of microalgae cells) after increasing the temperature or after applying the electric current was measured with a PAM-210 Chlorophyll Fluorometer (WALZ, Germany). This instrument induces the chlorophyll in the microalgae to emit photons by the exposure of blue light into the microalgae solution. The higher wavelength of red light is emitted due to the fluorescence and then measured. The instrument gives the output measurement as a yield, with inactive chlorophyll (dead algae) giving a low yield. A similar method for determining microalgae cell viability using a PAM-210 Chlorophyll Fluorometer is given by Franco, M.C. et al. (2011).

CHAPTER 4 FLOCCULATION OF MARINE MICROALGAE

4.1 Background and Purpose

Flocculation followed by a settling process has a low energy input, but can be expensive if the flocculant is costly and the dosage is high. However, most microalgal systems rely on cheap flocculants such as ferric chloride, aluminium sulphate, chitosan and various polyelectrolytic flocculants (Grima, E. M. et al. 2003). This makes flocculation a potentially viable option for microalgae dewatering.

Studies conducted on flocculation using marine microalgal species have not been successful. Sukenik, A. et al. (1988) achieved no success with polyelectrolyte flocculation of marine microalgae with salinity up to 36 g/L. Further studies by Bilanovic, D. and Shelef, G. (1988) found that by decreasing the salinity of the microalgae media the flocculation efficiency of all cationic polyelectrolytes increased. Flocculation with inorganic flocculants such as alum has also proven to be successful with freshwater microalgae species (Moraine, R. et al. 1980; Shelef, G. et al. 1984). However, with marine microalgae species, the optimal dosage required of alum was found to be 5 - 10 times greater than that of freshwater microalgae (Sukenik, A. et al. 1988).

The aim of the flocculation research is to investigate flocculation with marine microalgae species *Chlorococcum sp.* and *Tetraselmis sp.* and to determine optimum flocculation conditions for the different flocculant types.

4.2 Flocculation Results

4.2.1 Jar Stirrer Testing with Polyelectrolyte Flocculants

The jar stirrer tests determined the optimum dose of each flocculant and the corresponding microalgae recovery obtained. The optimum dose for each flocculant

is presented in table 4.1. The optimum dose of flocculant was chosen as the dose which gave the highest recovery amount. Figure 4.1 shows the range of recoveries for *Chlorococcum sp.* obtained for non-ionic flocculant Magnafloc 351. Error bars were calculated from triplicate measurements. Please refer to Appendix A.1.5 for optimum recovery results for all flocculants. From the figure, it can be seen that a dose of 10 mg flocculant/L algae is clearly the optimum dose. The recovery of microalgae refers to the relative mass of flocculated microalgae compared to the total mass of microalgae in the system. The term mg flocculant /mg algae refers to the mass of flocculant required per mass of microalgae in the jar. The term mg flocculant /mg flocculated algae refers to the mass of flocculant that was used per mass of flocculated microalgae product.
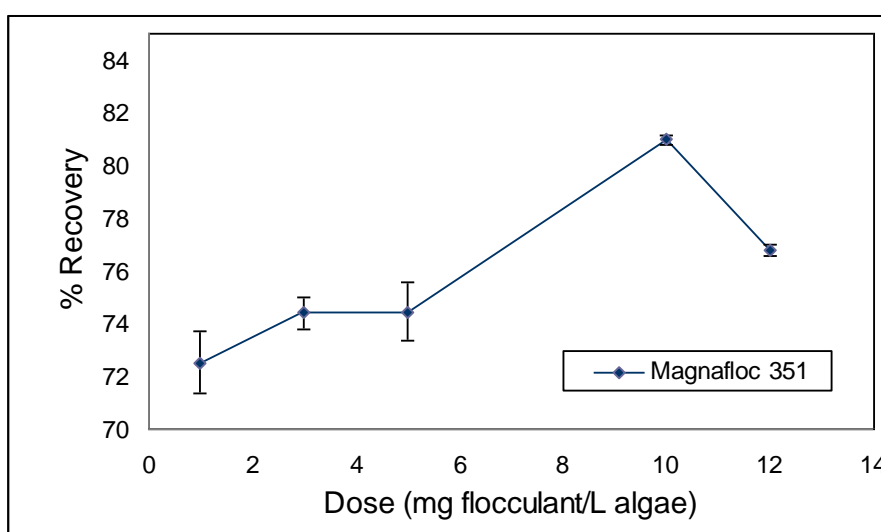
Figure 4. 1. Percentage recovery of *Chlorococcum sp.* with varying dose of non-ionic polyelectrolyte Magnafloc 351.

Figures 4.2 and 4.3 show the percentage recovery obtained for flocculation of *Chlorococcum sp.* and *Tetraselmis sp.* with the different polelectrolyte flocculants. For both species of microalgae, the cationic polyelectrolyte flocculants 71303 and 71305 were found to be highly effective. For *Chlorococcum sp.*, these two polyelectrolyte flocculants gave the highest microalgae recovery of 89.9 ± 0.2 % at a dose of 4 mg/L for 71303 and 85.3 ± 0.5 % at a dose of 3 mg/L for 71305. For *Tetraselmis sp.*, the microalgae recovery obtained was 88.6 ± 0.5% at a dose of 10

mg/L for 71303 and 86.9 ±0.3 % at a dose of 8 mg/L for 71305. This measures well with the flocculant doses used in freshwater microalgae flocculation studies, with the optimum dose ranging from 2.5 mg/L for a cationic polyamide (Tenney, M. W. et al. 1969) to 10 mg/L for a cationic polyacrylamide Zetag 51 (Moraine, R. et al. 1980).

For flocculation of *Chlorococcum sp.*, the non-ionic polyelectrolyte Magnafloc 351 was observed to be the worst flocculant overall, with the highest optimum dose of 10 mg/L and the second lowest algae recovery of 79.9 ± 0.6 %. However, for flocculation of *Tetraselmis sp.* with the non-ionic polyelectrolyte Magnafloc 351, the recovery obtained was 90 ± 0.6 % with a low optimum dosage of 2 mg/L.

Table 4. 1. Flocculant optimum dose and percentage recovery of *Chlorococcum sp.* (based on an average microalgae concentration of 0.6 g/L) and *Tetraselmis sp.* (based on an average microalgae concentration of 0.3 g/L)

Flocculant (charge)	Microalgae species	Optimum dose (mg flocculant / L algae)	Optimum dose (mg flocculant / g algae)	Optimum dose (mg flocculant / g flocculated algae)	% Recovery
71303	Chlorococcum	4	6.7	7.4	89.9 ± 0.2
(+)	Tetraselmis	10	33.3	37.6	88.6 ± 0.5
71305	Chlorococcum	3	5	5.9	85.3 ± 0.5
(+)	Tetraselmis	8	26.7	30.7	86.9 ± 0.3
71301	Chlorococcum	3	5	6.4	78.0 ± 0.3
(+)	Tetraselmis	8	26.7	32.5	82.0 ± 0.4
82230	Chlorococcum	5	8.3	9.9	84.5 ± 0.3
(-)	Tetraselmis	4	13.3	16.1	82.9 ± 0.3
Magnafloc 156	Chlorococcum	3	5	5.9	84.5 ± 0.4
(-)	Tetraselmis	5	16.7	30.8	54.1 ± 0.6
Magnafloc 155	Chlorococcum	2	3.3	4	83.9 ± 0.6
(-)	Tetraselmis	5	16.7	32.5	51.3 ± 0.4
Magnafloc 351	Chlorococcum	10	16.7	20.9	79.9 ± 0.6
(no charge)	Tetraselmis	2	6.7	7.4	90.0± 0.6
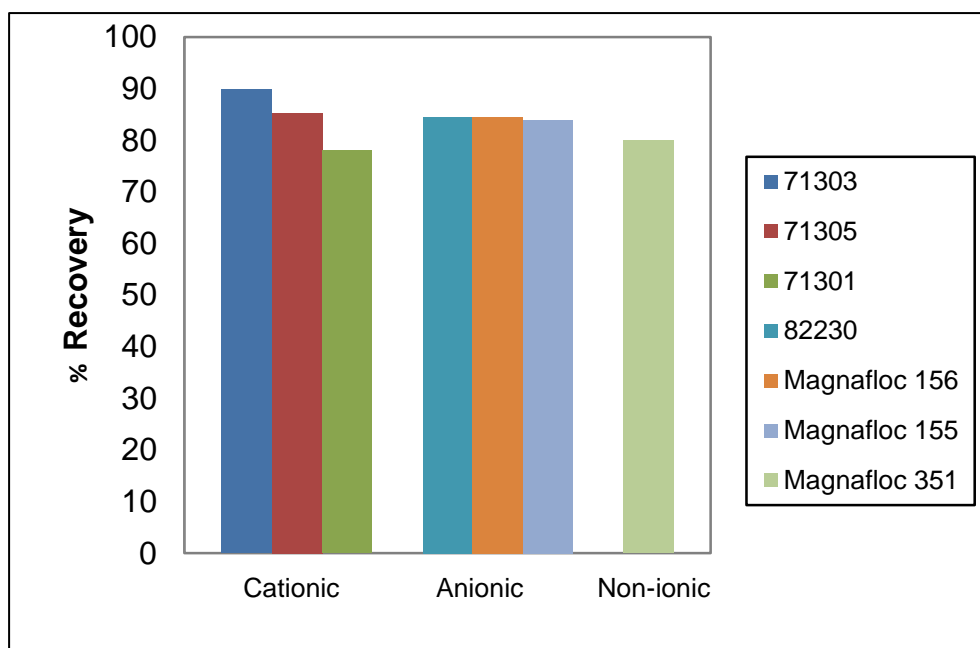
Figure 4. 2. Percentage recovery of *Chlorococcum sp.* with polyelectrolyte flocculants.
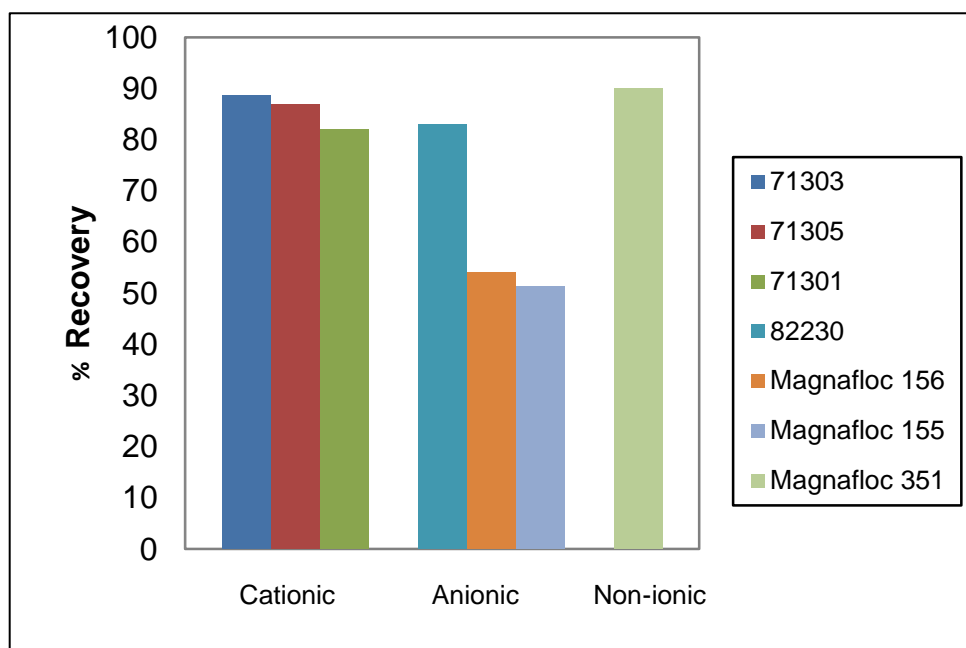
Figure 4. 3. Percentage recovery of *Tetraselmis sp.* with polyelectrolyte flocculants.

4.2.2 Jar Stirrer Testing with Alum

Alum flocculation was carried out at varying doses with both marine microalgae species. Figures 4.4 and 4.5 show the percentage recovery and pH after flocculation with alum for *Chlorococcum sp.* and *Tetraselmis sp.* The optimum dose was determined to be the lowest dose of alum that gave the best microalgae recovery.

An optimum dose of 47 mg alum/L microalgae and 70.5 mg alum/L microalgae was obtained for *Chlorococcum sp.* and *Tetraselmis sp.*, respectively. The pH of the microalgae solution was seen to decrease with increasing dosage of alum.

The optimum flocculation recovery obtained with alum was achieved at flocculation pH (i.e. pH after flocculation) of 6.92 and 6.94 for *Chlorococcum sp.* and *Tetraselmis sp.,* respectively. Studies have found that effective flocculation of freshwater microalgae is possible with alum at low and near neutral pH (Van Vuuren, L. R. J. and Van Duuren, F. A. 1965; McGarry, M. G. 1970; Friedman, A. A. et al. 1977). In a study by Black, A.P. and Chen, C. (1967), effective flocculation with alum was achieved with pH ranging from 6.5 to 7.5 when the alum dose was 10 mg/L or greater. The results from this research show an obvious trend that as the dose of alum increases, the pH of the microalgae solution decreases. This is expected because as more alum is introduced into the system, the positive aluminium species will form compounds with the OH$^-$ ions in the solution, therefore making the solution less alkaline.
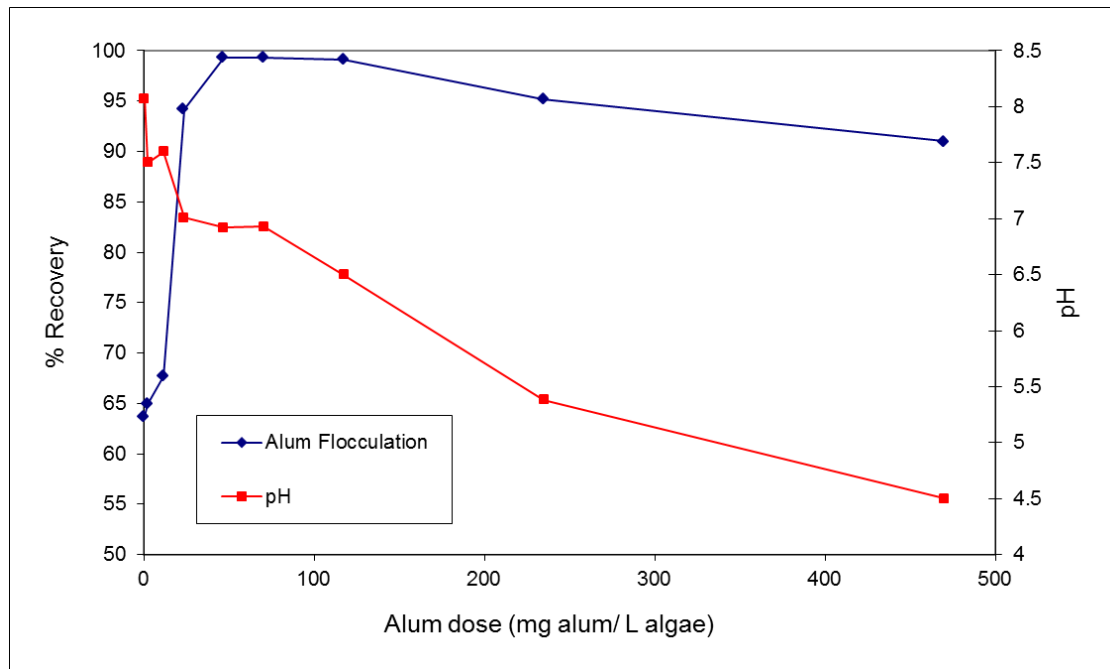
Figure 4. 4. Percentage recovery and pH after flocculation with alum for *Chlorococcum sp.*
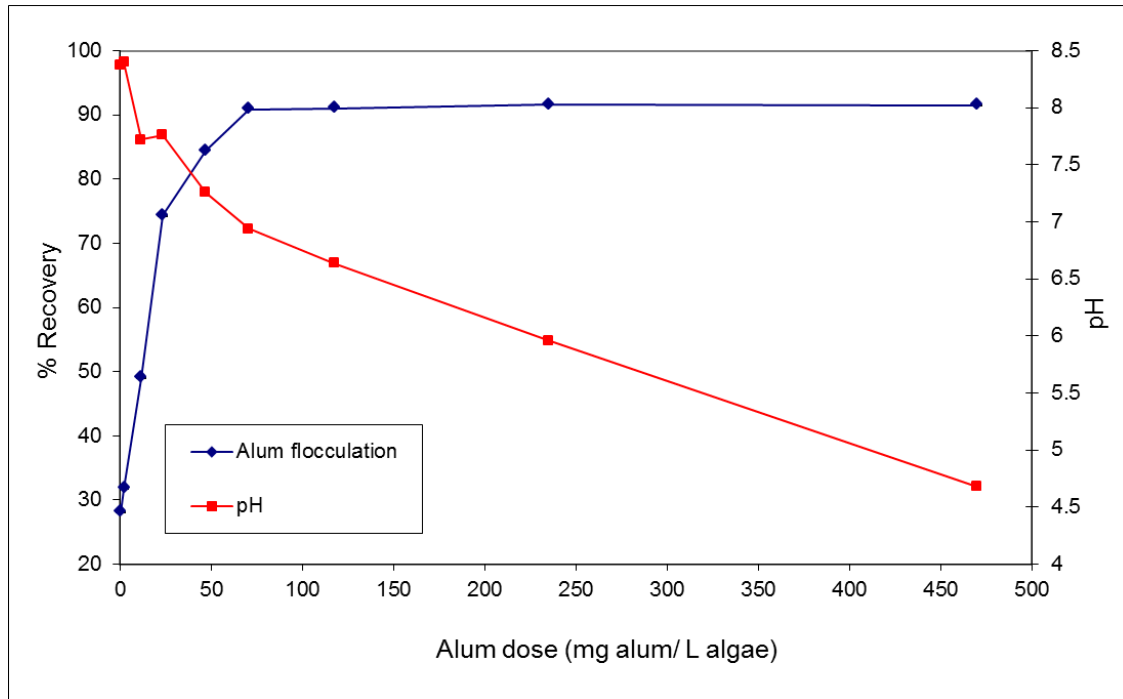
Figure 4. 5. Percentage recovery and pH after flocculation with alum for *Tetraselmis sp.*

4.2.3 Focused Beam Reflectance Measurement

The FBRM allowed for real time analysis of the flocculation process which meant that the microalgal flocculation process could be observed more clearly. Figures 4.6 to 4.8 show the change in counts per second with time after the addition of flocculant. The size distributions are on the basis of the cell chord lengths, which are related to the length of time that the cells spend passing through the laser beam. For a spherical particle, the chord lengths will always be less than the cell's diameter.

It can be seen that immediately after addition of the flocculant (shown as the vertical dashed line), the particle counts in the chord size ranges of less than 10 μm and 10 to 50 μm significantly decrease while those in the chord size range of 150 to 300 μm and 300 to 1000 μm increase. This corresponds to the flocculation process where the smaller sized particles of 10 to 50 μm are agglomerating into larger ones. Consequently after flocculation, there is a decrease in the counts of smaller particles with a simultaneous increase in the counts for the larger particles. These results

75

illustrate that the FBRM instrument is an excellent tool to monitor and graphically observe the flocculation process.

Figure 4.6 shows fluctuations of the counts in the size ranges of <10 μm and 10 - 50 μm after the addition of flocculant to *Chlorococcum sp.* This fluctuation corresponds to the breaking and re-agglomeration of the microalgal flocs due to the shearing forces of the FBRM mixer blades. This fluctuation is not as evident in the flocculation process for anionic flocculants or flocculation with *Tetraselmis sp.* because the flocs that form have a smaller size, and are therefore more able to withstand greater shearing forces.
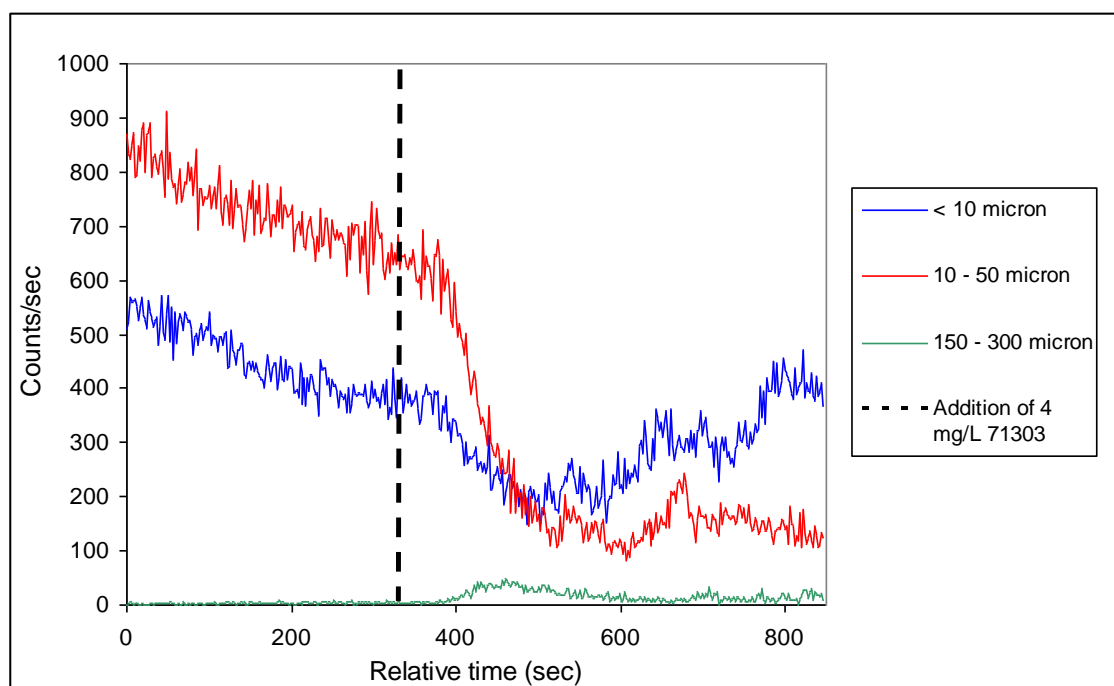
Figure 4. 6. FBRM analysis of *Chlorococcum sp.* – counts per second versus time for flocculation using cationic polyelectrolyte 71303 at 4mg/L for three broad ranges of particle chord size.
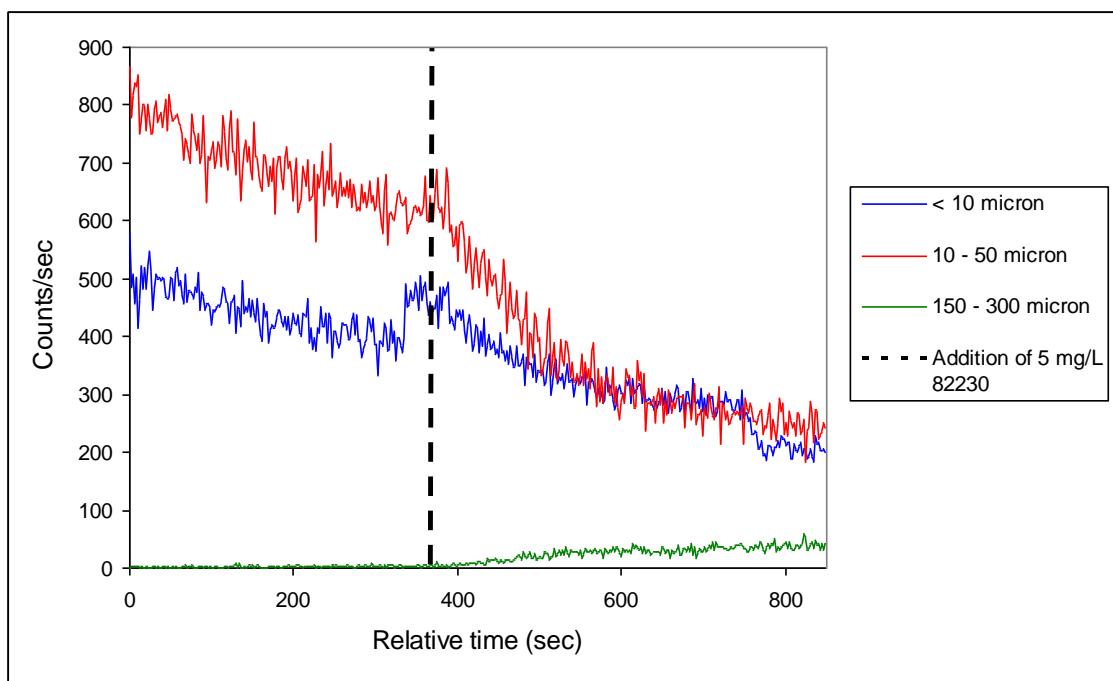
Figure 4. 7. FBRM analysis of *Chlorococcum sp.* – counts per second versus time for flocculation using anionic polyelectrolyte 82230 at 5mg/L for three broad ranges of particle chord size.
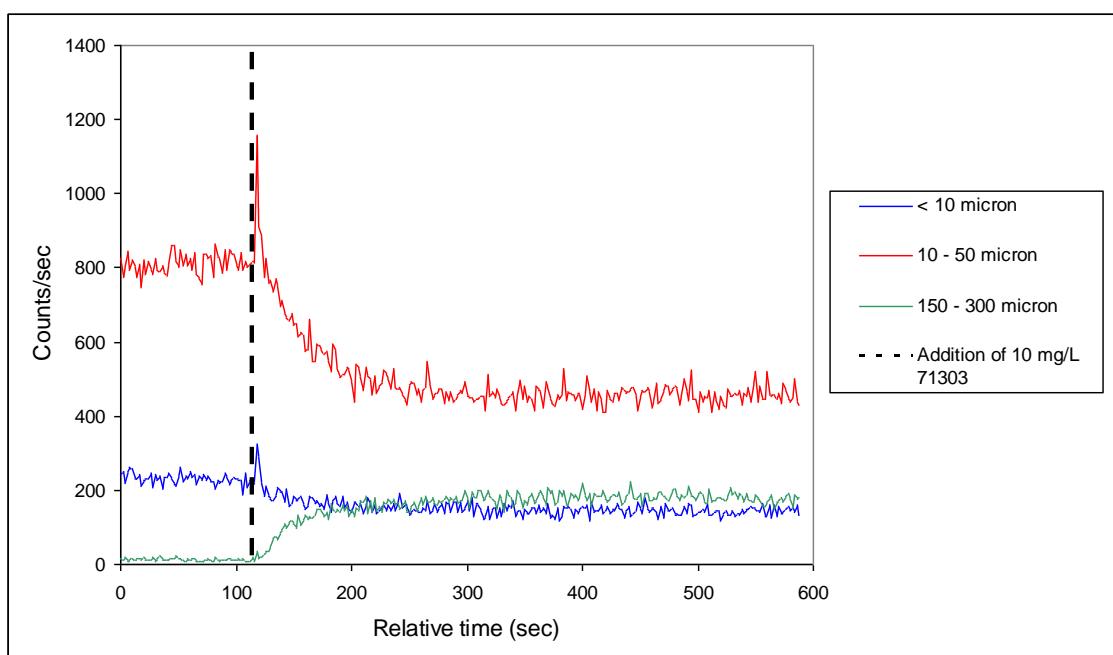
Figure 4. 8. FBRM analysis of *Tetraselmis sp.* – counts per second versus time for flocculation using cationic polyelectrolyte 71303 at 10 mg/L, for three broad ranges of particle chord size.

The flocculation efficiency was also observed using the FBRM. This involved obtaining the FBRM distributions for microalgae before flocculation, i.e. obtaining

77

the fresh microalgae distribution, performing the flocculation jar stirrer experiment, decanting the supernatant after the settling period and then obtaining the distribution of the supernatant. The before and after flocculation distributions were then overlaid to observe the difference in counts per second between the two samples. From figure 4.9, for cationic polyelectrolyte 71303 with *Chlorococcum sp.*, it can be seen that there is a significant difference in the distributions at the optimum dose of 4 mg/L and half the optimum dose of 2 mg/L. The counts per second for flocculation with 2 mg/L is higher than that for 4 mg/L, which indicates a greater number of un-flocculated cells and a lower flocculation efficiency. Figure 4.10 shows a similar efficiency result for flocculation of *Chlorococcum sp.* with 5 mg/L anionic polyelectrolyte 82230. The result from Figure 4.10 further verifies the ability of anionic polyelectrolytes to flocculate marine microalgae. A similar result was obtained for flocculation of *Tetraselmis sp.*, as shown in figure 4.11.
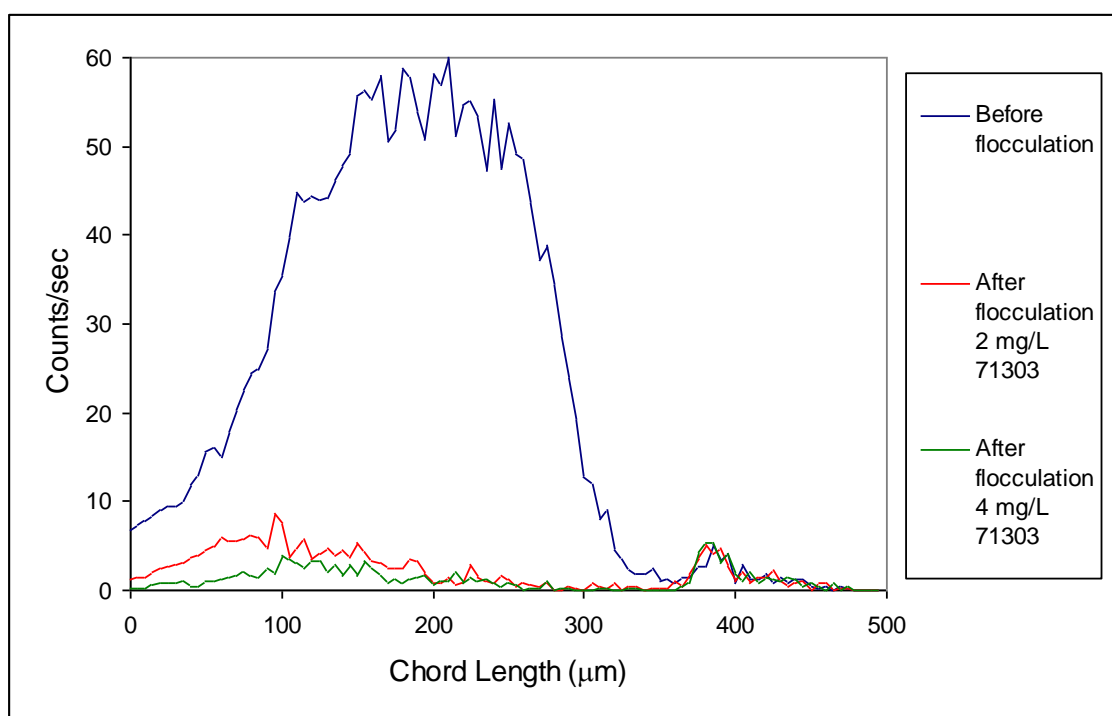
Figure 4. 9. FBRM analysis of *Chlorococcum sp.* – before and after flocculation using cationic polyelectrolyte 71303 at 4 mg/L and 2 mg/L.
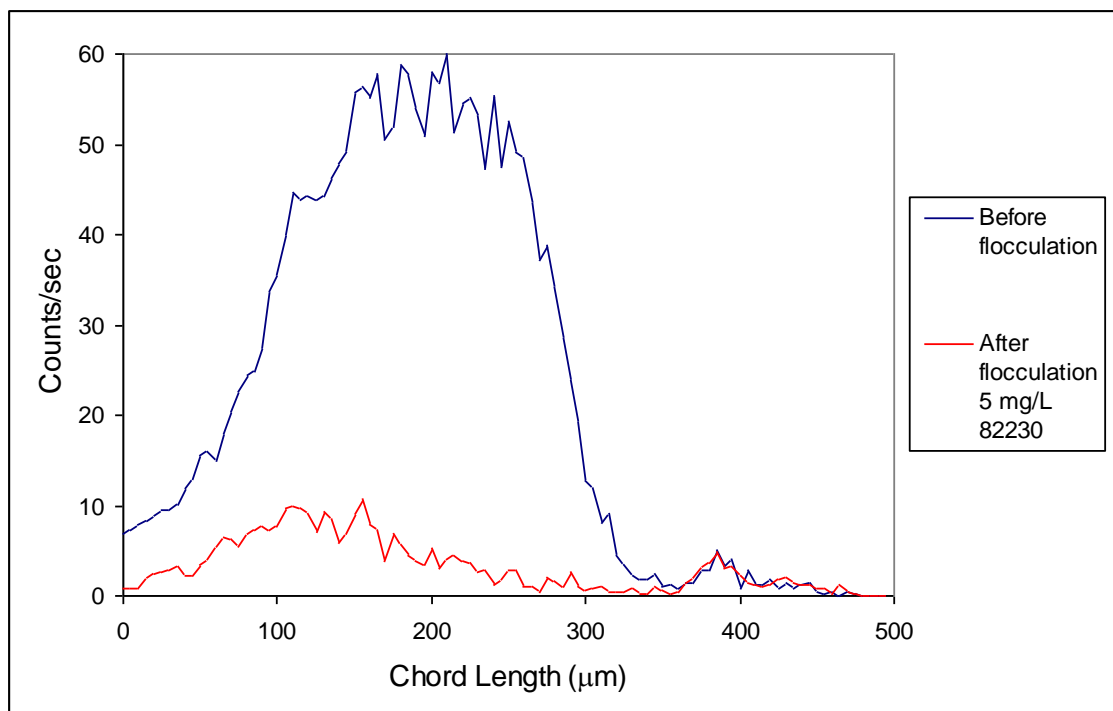
Figure 4. 10. FBRM analysis of *Chlorococcum sp.* – before and after flocculation using anionic polyelectrolyte 82230 at 5 mg/L.
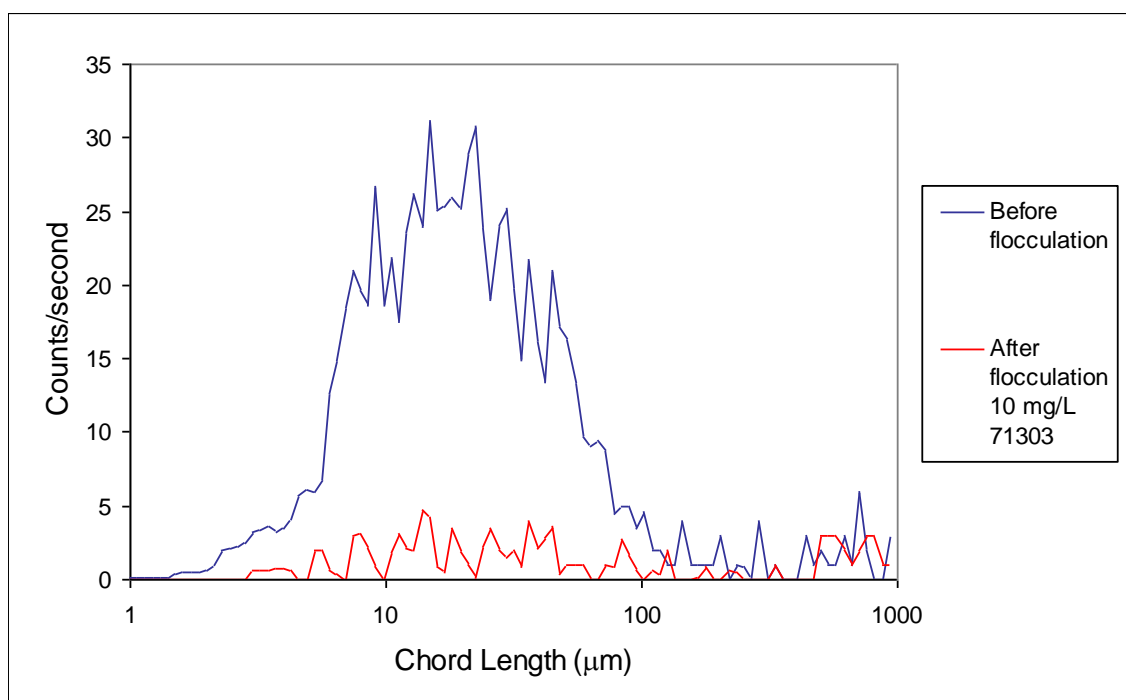
Figure 4. 11. FBRM analysis of *Tetraselmis sp.* – before and after flocculation using cationic polyelectrolyte 71303 at 10 mg/L.

The FBRM results gave weighted average data for counts per second versus time before and after flocculation. The weighted average is an average in which each quantity to be averaged is assigned a weight. These weightings determine the relative importance of each quantity on the average. Figures 4.12 and 4.13 show the difference in particle chord lengths before and after flocculation. It can be seen on both figures that after flocculation occurs, there is a significant increase in counts per second for the size range of 100 to 500 μm due to agglomeration of smaller microalgae particles.
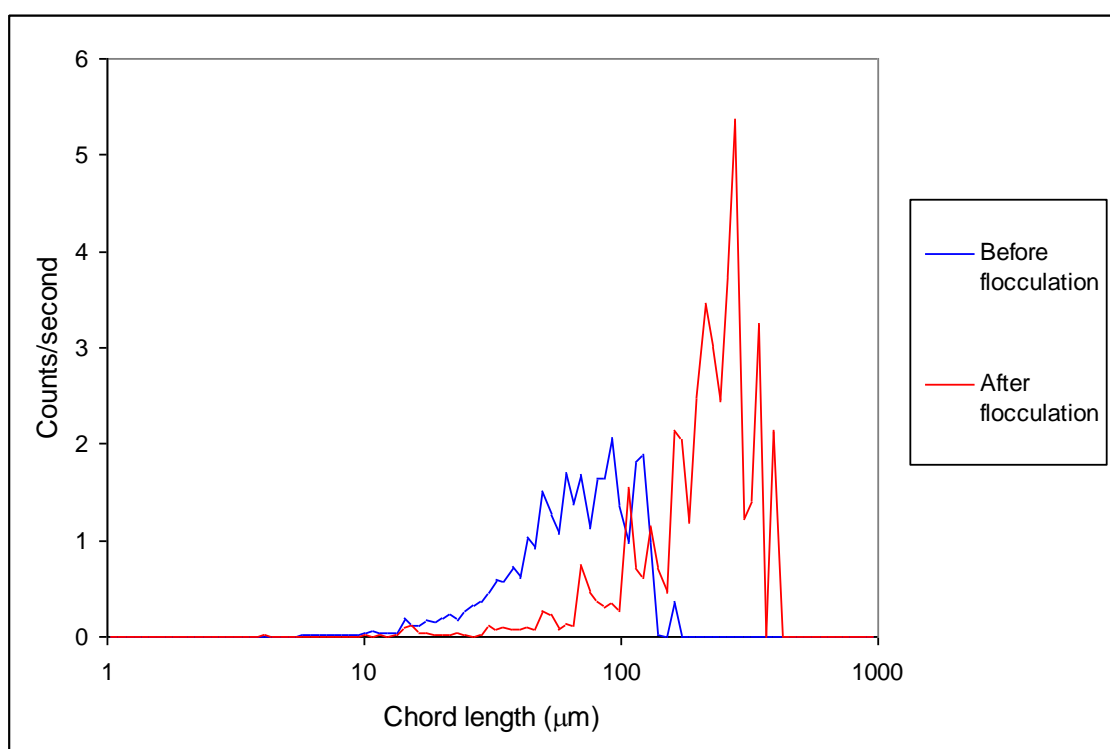
Figure 4. 12. FBRM analysis of *Chlorococcum sp.* – weighted average data for counts per second versus time for flocculation using cationic polyelectrolyte 71303 at 4 mg/L.
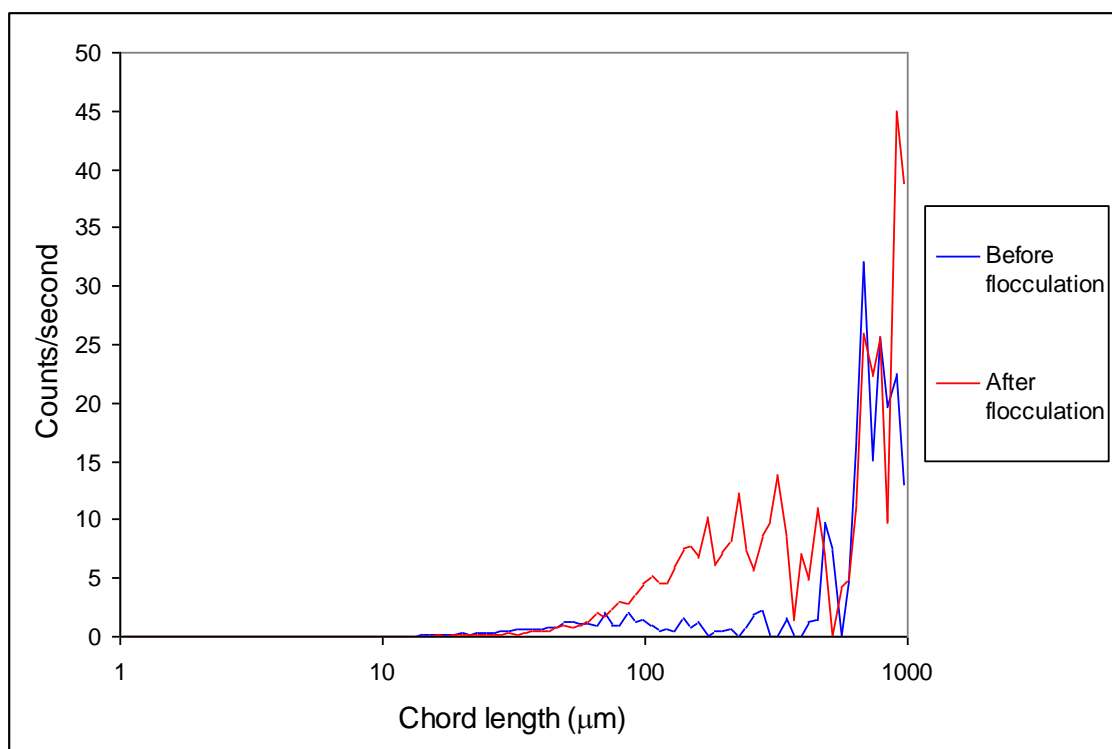
Figure 4. 13. FBRM analysis of *Tetraselmis sp.* – weighted average data for counts per second versus time for flocculation using cationic polyelectrolyte 71303 at 10 mg/L.

4.2.4 pH

The effect of pH on the flocculation of microalgae was determined by performing the flocculation process at pH 4, 6 and 8, respectively of the most successful cationic and anionic polyelectrolyte. Table 4.2 presents the results of microalgae recovery by flocculation at different pH values using the most successful cationic and anionic polyelectrolyte. The results show that the marine microalgal recovery increases with pH, unlike freshwater microalgae which was reported to be the opposite effect of results from previously conducted studies (Tenney, M. W. et al. 1969). Flocculation was not carried out at high alkaline pH because at pH values greater than 10.5 the recovery of the marine microalgae can be achieved very efficiently without the use of polyelectrolyte flocculants. At alkaline pH above 10.5 Mg^{2+} and Ca^{2+} ions present in the salt water media can be made to precipitate and as these cations surround the negatively charged microalgal cells, the precipitate will sweep the algae from the suspension (Ayoub, G. M. et al. 1986; Semerjian, L. and Ayoub, G. M. 2003). Although this is an effective means of removing the algae from solution, in a process where the algae requires further treatment to extract lipids, this is not an attractive

81

option, because an additional step is required in order to separate the microalgae from the precipitate.

4.2.5 Zeta Potential

The zeta potential was measured for each flocculation test for the most successful cationic and anionic polyelectrolyte. It was found that with decreasing pH, the zeta potential of the un-flocculated microalgal solution became more positive (the charge becoming closer to the iso-electric point). This result is expected because the microalgae surface charge becomes more positive as the pH decreases.

Table 4. 2. Percent recovery and zeta potential of un-flocculated algae at varying pH, done at the optimum dose for each flocculant, for *Chlorococcum sp.*

	pH 4		pH 6		pH 8	
Flocculant	% Recovery	Zeta Potential (mV)	% Recovery	Zeta Potential (mV)	% Recovery	Zeta Potential (mV)
71303	86.5	-4.9 ± 1.6	89.8	-6.8 ± 0.6	89.9	-7.04 ± 0.2
82230	56.3	-4.6 ± 0.7	77.5	-7.3 ± 1.5	84.5	-7.64 ± 0.9
Magnafloc 156	54.5	-7.8 ± 0.8	74.3	-12.6 ± 0.4	84.5	-13.08 ± 0.7

4.2.6 Temperature

Temperature was seen to have a noticeable effect on microalgae recovery by flocculation. It was found that the percentage of microalgal recovery increased with temperature (figure 4.14). This can be explained by the theory of collision (Haynie, D. T. 2008). With increasing temperature, there is a greater probability that the polyelectrolyte and microalgae cells will collide due to the increasing mobility of the cellular particles at higher temperature. Increasing the number of collisions increases

the number of possible interactions that can occur, which in turn improves the flocculation rates. The increasing mobility resulting from temperature increase relates to the molecular mobility of the flocculant molecules which results in an increase in flocculant-algae interactions per time, hence productivity and recovery. The settling rates are also improved with increasing temperature due to a greater density difference.

An additional factor is the health and viability of the microalgae. The WALZ PAM-210 chlorophyll fluorometer was used to measure the dimensionless yield of active chlorophyll in the microalgae. It was observed that with increasing temperature, the viability and health of the microalgae cells dropped. Healthy, viable microalgal cells can achieve yields of around 0.6 - 0.7, however at 48 °C (the highest temperature test), the microalgae had an average active chlorophyll yield of only 0.03 for all flocculants, indicating that nearly all the microalgae had been killed. The enhanced recovery results obtained at high temperatures could be due to the fact that dead microalgae are easier to separate. Possible explanations may include a change in the cell charge and/or the excretion of polyelectrolytic substances.
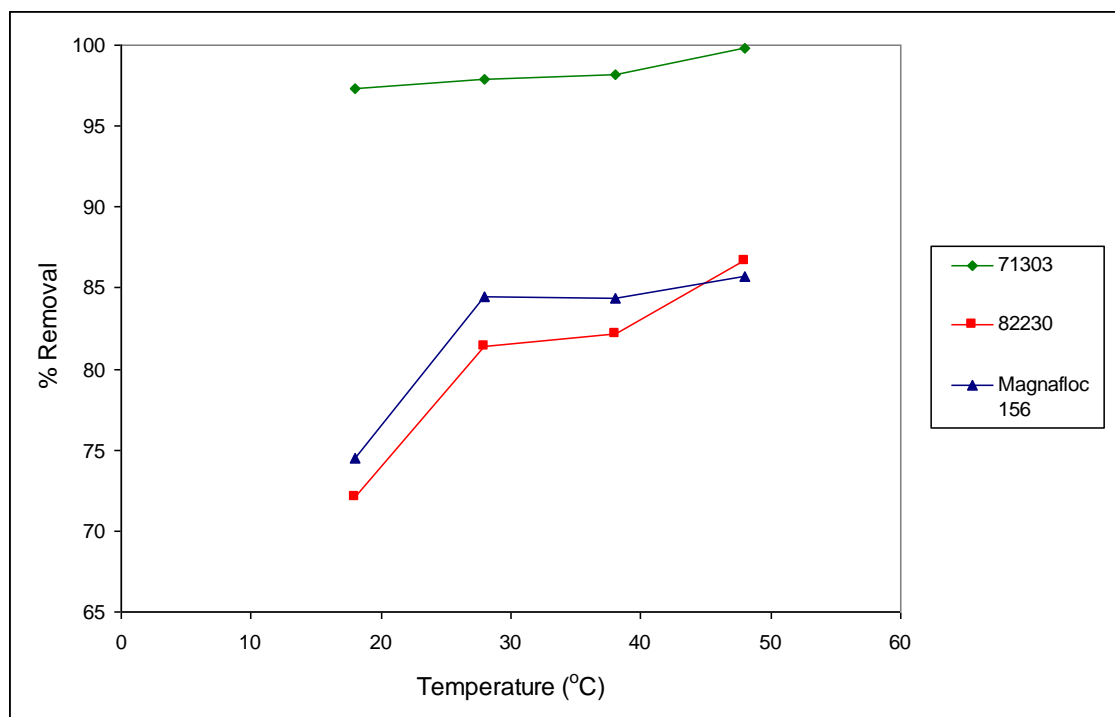
Figure 4. 14. Percentage recovery of microalgae at varying temperatures for *Chlorococcum sp.*

Experiments were performed using the optimum dose for each flocculant.
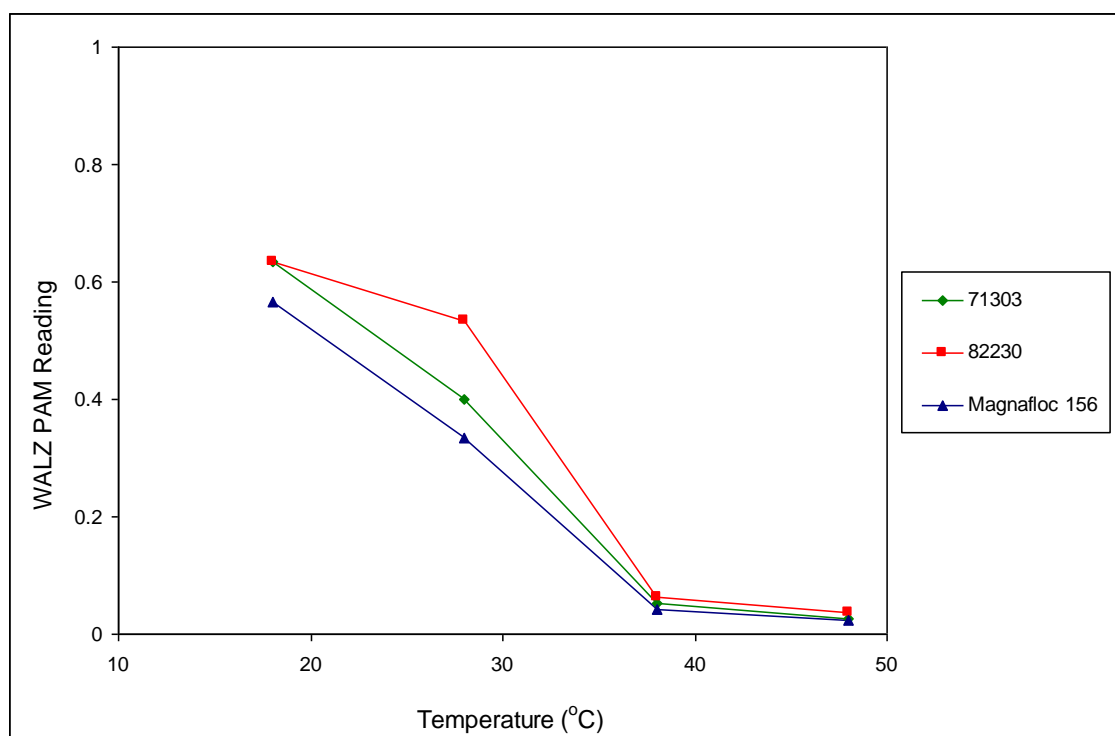
Figure 4. 15. WALZ PAM-210 results with increasing temperature, for flocculation with *Chlorococcum*

sp.

4.3 Discussion of Marine Microalgae Flocculation

The results gathered from the flocculation studies illustrate that all types of flocculants tested were successful in flocculating marine microalgae.

Numerous studies previously conducted on freshwater microalgae found minimal success with anionic and non-ionic polyelectrolytes (Tenney, M. W. et al. 1969; Bernhardt, H. and Clasen, J. 1991). Studies have also shown that the high salinity of the marine environment inhibited flocculation with polyelectrolytes (Bilanovic, D. and Shelef, G. 1988). Contradictory to these studies, it was found that all charge types of polyelectrolyte flocculants were able to achieve adequate flocculation success. The efficiency of the flocculation process is determined by the probability of collision of the polyelectrolyte and microalgal particles, as well as the capability of these particles to stick together once brought together by collision (Pieterse, A. J. H. and Cloot, A. 1997). The mechanism of flocculation is explained by charge neutralisation and polyelectrolyte bridging (Bernhardt, H. and Clasen, J. 1991; Bernhardt, H. and Clasen, J. 1994). The degree to which mechanism dominates depends on the charge density and chain length of the polyelectrolyte. The mechanism of action involves the adsorption of the polyelectrolyte onto the surface of the microalgae.

As described in literature, the mechanism of anionic and non-ionic polyelectrolyte attachment to the microalgae surface is more likely to be governed by hydrogen bonding (Tenney, M. W. et al. 1969; Stechemesser, H. and Dobias, B., editors 2005). Tenney, M.W. et al. (1969) states that the inability of flocculation with anionic polyelectrolytes is due the repulsion between like charges or by polymer segments being unable to bridge between particles due to insufficient length. It is likely that there is a low concentration cationic intermediate layer surrounding the negative microalgae cells, which enables for electrostatic binding of the microalgae and the flocculant. Table 4.3 shows the concentration factor of the flocculated settled microalgae achieved after flocculation with polyelectrolytes, as well as their charge and molecular weight properties. It is known that the higher the molecular weight of

85

the polymer and the stronger the charge density (opposite to that to which the polyelectrolyte must flocculate), the more efficient the flocculation process will be. From table 4.3, it can be seen that the molecular weight for both anionic and non-ionic polyelectrolytes are high, which would aid in flocculation, as the main mechanism involved is due to particle bridging. The charge density of the anionic polyelectrolyte is low to medium, which would reduce the chances of like-charge repulsion.

Table 4. 3. Polyelectrolyte properties and concentration factor for flocculation with *Chlorococcum sp.* and *Tetraselmis sp.*

Flocculant	Charge density	Molecular weight	Final Concentration Factor	
			Chlorococcum sp.	Tetraselmis sp.
71303	low/medium cationic	medium	39.2	133
71305	low cationic	medium/high	38.4	127
71301	medium cationic	medium/high	37.2	117
82230	low/medium anionic	medium/high	35.9	100
Magnafloc 156	medium anionic	high	23.5	93.3
Magnafloc 155	low/medium anionic	high	34.3	80.0
Magnafloc 351	non ionic	high	41.9	140

Although similar removal efficiencies were obtained for each microalgae species, the corresponding doses were very different. In some cases, the optimum dose required for *Tetraselmis sp.* was approximately double that required for *Chlorococcum sp.* (please refer to table 4.1). An explanation lies with the differences in dry weight concentrations of both microalgal species, with *Chlorococcum sp.* being double that of *Tetraselmis sp.* for all flocculation experiments. From table 4.3, it can be seen that

the concentration factor for flocculation with *Tetraselmis sp.* is significantly greater than that for *Chlorococcum sp.* The final settled concentrations achieved after flocculation was similar for both species, however due to the initial concentration of *Tetraselmis sp.* being so low, the concentration factors were calculated to be much higher.

The top five polyelectrolytes can be seen as successful. Although 71303 may be the best flocculant, the next four flocculants have similar recovery efficiencies. Flocculants such as 71305 and Magnafloc 155 have a lower efficiency than 71303, but also use a lower amount of polyelectrolyte per litre of microalgae. Depending on the cost of the flocculant, it may be more advantageous to choose a cheaper flocculant with lower efficiency over an expensive flocculant with slightly higher efficiency. However, it can also be seen in Figure 5.4 that a lower than optimum dose of 71303 can still achieve a better recovery efficiency than the optimum dose of the other flocculants. As these experiments were conducted at a laboratory scale, it would be beneficial to explore their potential at an industrial scale.

Another observation with polyelectrolyte flocculation that was found to be contradictory to literature was the recovery obtained at varying pH. The results showed that microalgal recovery increases with pH, unlike freshwater microalgae which showed the opposite effect in a previous study by Tenney, M.W. et al. (1969). Reducing the pH to acidic conditions brings the freshwater microalgae closer to its iso-electric point and at this point the microalgal cells are more likely to flocculate. This effect is more significant for the anionic flocculants. For marine microalgal species, a higher pH will also affect the precipitation of salts, which has a significant effect on microalgal recovery. The cationic flocculants show a minimal change in microalgae recovery efficiency over the three pH values. This is because the charge neutralisation mechanism for cationic polyelectrolytes persists with changing pH. However, for the anionic polyelectrolytes, decreasing the pH brings an increase in the amount of H^+ ions in solution, which binds to the negatively charged

polyelectrolyte, thus giving it a lower efficacy. The pH variation could also affect the optimum pH range required for successful polyelectrolyte activity.

Alum has been studied extensively as a flocculant for freshwater microalgae removal (Van Vuuren, L. R. J. and Van Duuren, F. A. 1965; McGarry, M. G. 1970; Friedman, A. A. et al. 1977). Sukenik, A. et al. (1988) found that flocculation of marine microalgae required alum doses to be in the order of 5 to 10 times higher than that for freshwater microalgae. It is proposed that the high salinity of the marine microalgae species interferes with the flocculation process by reducing the chemical activity of the flocculant and masking functionally actives sites of the flocculants (Sukenik, A. et al. 1988). The results from this research are contradictory to this statement as the doses of alum obtained are comparable to the optimum range of 25 mg/L as stated by Sukenik, A. et al. (1988) and 80 - 250 mg/L as stated by Shelef, G. et al. (1984), for freshwater microalgae species. Microalgae are a living biological species and there are many factors that may affect their ability to flocculate such as pH, temperature and ionic strength. The difference observed between the research results the literature may be due to specific differences in microalgae characteristics or differences in flocculation parameters between the experiments. The flocculation mixing conditions used by Sukenik, A. et al. (1988) was a fast mix at 80 rpm for 2 min, followed by a slow mix at 20 rpm for 30 min. The mixing conditions for used in this experimental research was taken from literature as the ideal flocculation mixing condition that allowed for adequate dispersion of alum (fast mix at 100 rpm for 1 min, followed by a slow mix at 60 rpm for 4 min). Further differences between the experimental conditions are that the microalgae grown by Sukenik, A. et al. (1988) was grown in 10 L bioreactors using artificial fluorescent light, where as the microalgae grown for this research was grown with natural sunlight, in 100 L bioreactors. Due to a stronger focus on electrocoagulation in this research, alum flocculation was not investigated further; however an explanation to these differences is a potential research aim for future work.

A study by Friedman, A.A. et al. (1977) stated that at low and near neutral pH's, alum proved to be an effective flocculant. This is because in order for microalgae to be

flocculated by inorganic flocculants, the pH needs to be low enough to form cationic hydrolysis products (Briley, D. S. and Knappe, D. R. U. 2002). The alum flocculation results in figure 4.4 and 4.5 show that as the alum is added into the microalgae solution, the pH decreases to an acidic range. As stated, this pH range is ideal for alum flocculation and may be the reason for flocculation success. During alum flocculation, aluminium ions target the surface charge of the microalgae. The membrane surface charge density of the microalgae may be independent of the culture medium, whether freshwater or marine. The marine environment has an effect on the culture conductivity but it is possible it doesn't have an effect on the amount of ions required to flocculate a given microalgal species.

4.4 Flocculation Experimental Conclusions

In early studies of marine microalgae flocculation only cationic polyelectrolytes were shown to be effective. This research shows that batch flocculation tests of cationic, non-ionic and anionic polyelectrolytes can be successful for marine microalgae species, *Chlorococcum sp*. and *Tetraselmis sp*. Optimum flocculation conditions were obtained for each type of flocculant with each microalgae species.

Similar recovery values of microalgae were obtained for both microalgae species, however the optimal dosage required was different. In some cases, the optimum dose required to flocculate *Tetraselmis sp.* was double that needed for *Chlorococcum sp*. This difference can be explained by the difference in cell characteristics between the microalgal species and difference in dry weight concentration. These results however, only hold for the specific conditions. Changes in pH, temperature and ionic strength can significantly affect the flocculation efficiency.

FBRM was used to evaluate the microalgae flocculation process in situ by measuring particle counts and the chord size distribution. This made it possible to graphically observe the changes in particles size of the microalgae during the flocculation process and further proved the flocculation ability of anionic polyelectrolytes.

Alum flocculation was also investigated in this research. It was found that contrary to literature, alum was able to successfully flocculate marine microalgae at comparable doses to freshwater species.

CHAPTER 5 ELECTROCOAGULATION OF MARINE MICROALGAE - RESULTS

5.1 Background and Purpose

From chapters 1 and 2, electrocoagulation of microalgae was determined to be a promising dewatering technique which has several advantages over conventional dewatering methods such as a low energy input and no direct addition of chemicals (as for example those required for the chemical flocculation dewatering technique). Electrocoagulation is versatile, environmentally compatible, safe, selective and often cost effective. The main disadvantage of electrocoagulation is the need to regularly replace the sacrificial anode (Mollah, M. Y. A. et al. 2004). This method of solids separation has been extensively studied for suspended solids in wastewater and there have also been a limited number of studies of this process for the removal of freshwater microalgae (Aragon, A. B. et al. 1992; Alfafara, C. G. et al. 2002; Mollah, M. Y. A. et al. 2004; Azarian, G. H. et al. 2007).

The use of electrocoagulation for dewatering of microalgae results in efficient recovery values. The efficiency of microalgae removal with electrocoagulation can operate in the range of 80 - 95 % (Poelman, E. et al. 1997) and even up to 100 % with electrocoagulation at optimal conditions (Gao, S. et al. 2010b).

The successful results obtained for electrocoagulation with freshwater microalgae species have naturally led to the interest to determine the efficiency of electrocoagulation for marine microalgae. Since marine microalgae are grown in a high salinity medium, the electrical conductivity of the solution is higher than that of freshwater; meaning a lower amount of electrical energy would be required to operate the system.

Three different electrode materials were used in this research; stainless steel 430, aluminium and carbon. During electrocoagulation, the sacrificial anode material dissolves from the anode, generating cations that almost immediately hydrolyse, depending on the pH conditions. Coagulation results from the interaction of the metal cations with the negatively charged microalgae particles migrating towards the anode due to electrophoretic motion. Water is hydrolysed to produce hydrogen bubbles at the cathode and these bubbles are trapped by the flocculated particles and the combined buoyancy is reduced sufficiently to allow the complex to be carried to the surface. (Alfafara, C. G. et al. 2002; Mollah, M. Y. A. et al. 2004; Azarian, G. H. et al. 2007)

The presence of chloride ions in the culture media may influence the effectiveness of the electrocoagulation process. Chloride ions may aid in recovery by oxidising to form active chlorine species such as chlorine, hypochlorus acid and/or hypochlorite that can cause microalgae inactivation via oxidation (Gao, S. et al. 2010a). The presence of chloride ions also increases the conductivity of the microalgae culture, which leads to the process requiring a lower electrical energy input. Chlorine may also have an effect on the motion of flagellated microalgae. Pre-treatment of microalgae with oxidants such as chlorine have shown to completely impede the gliding action of species *Navicula sp.* and *Nitzschia sp.* (Petrusevski, B. et al. 1996).

The aim of this research was to determine the effectiveness of this separation technique, which was quantified based on the removal ratio of the microalgae from the media, the concentration of solids in the separated fraction and the power requirements of the process. The separation efficiency of the different anode materials were determined and compared and the mechanisms associated with electrocoagulation were also verified. As discussed in chapter 3, the choice of electrode material was determined by the cost of electrode material and its ability to produce a coagulating metal ion species.

5.2 Electrocoagulation Results – Constant Voltage

5.2.1 Stainless Steel 430 Cathode/ Stainless Steel 430 Anode

5.2.1-1 Microalgae Recovery by Electrocoagulation

Electrocoagulation experiments were conducted on a range of different voltages and run times. Figure 5.1 shows the measured current density as a function of time after the application of a constant voltage of 5 V for both microalgae species. Figure 5.2 shows the measured voltage as a function of time after the application of a constant current of 1 A for both microalgae species.
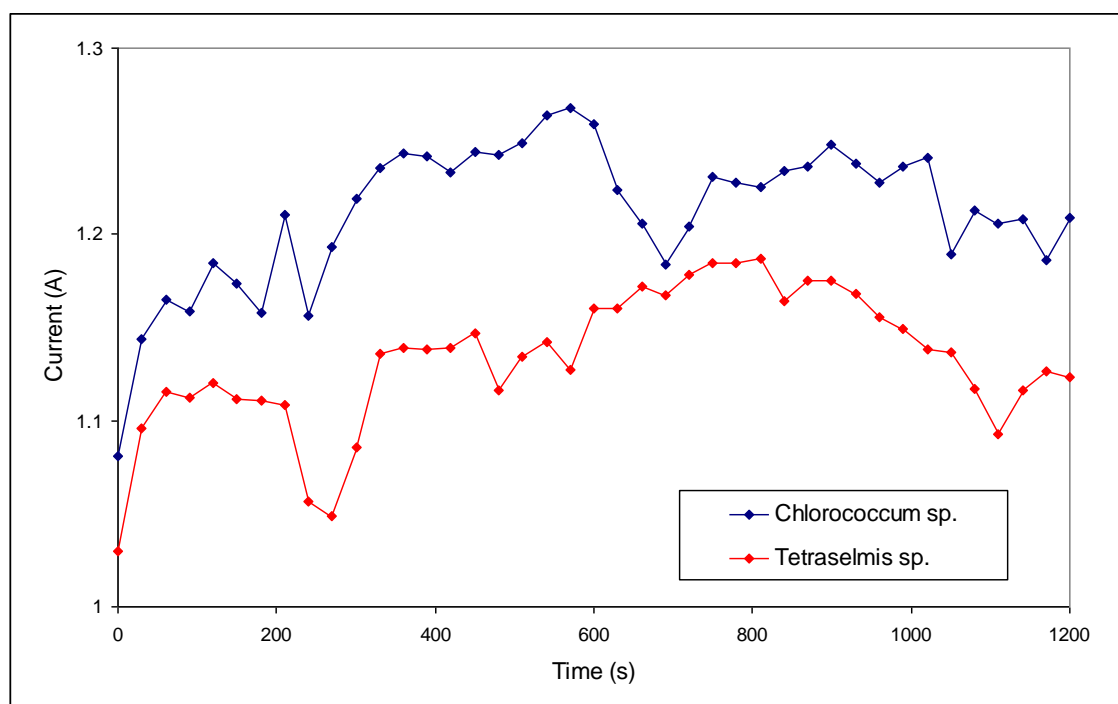
Figure 5. 1. Current versus time for a constant voltage of 5 V for *Chlorococcum sp.* and *Tetraselmis sp.*, with the stainless steel 430 anode.

Figure 5. 2. Voltage versus time for a constant current of 1 A for *Chlorococcum sp.* and *Tetraselmis sp.*, with the stainless steel 430 anode.

Table 5.1 shows the current density readings for the different experimental conditions tested.

Table 5. 1. Current density measured during electrocoagulation for *Chlorococcum sp.* and *Tetraselmis sp.*, with the stainless steel 430 anode.

	Tetraselmis sp.			Chlorococcum sp.		
	8 °C	22 °C	60°C	8 °C	22 °C	60°C
	Current Density (A/cm^2)			Current Density (A/cm^2)		
3V	0.01	0.02	0.03	0.01	0.02	0.03
5V	0.03	0.06	0.09	0.03	0.05	0.07
10V	0.09	0.15	0.23	0.09	0.12	0.20

Table 5.2 provides a log of the experiments conducted on *Chlorococcum sp.* and *Tetraselmis sp.* as well as the final concentration factor and the electrical input required for electrocoagulation in kWh per kg of microalgae removed, in the batch electrocoagulation cell (please refer Appendix A.2.3 for calculations).

Table 5. 2. Electrical input for electrocoagulation flotation experiments with the stainless steel 430 anode.

		Time (s)	Final Concentration Factor	Electrical Input (kWh/kg Microalgae Removed)
	3V	180	3.38	11.8 ± 0.07
		360	7.41	3.49 ± 0.15
		900	21.2	4.31 ± 0.11
Chlorococcum sp.	5V	180	5.70	10.0 ± 0.07
		360	10.5	8.30 ± 0.08
		900	16.7	18.1 ± 0.02
	10V	180	9.71	24.8 ± 0.08
		360	26.9	41.3 ± 0.10
		900	29.7	102 ± 0.12
	3V	180	4.67	1.97 ± 0.09
		360	10.9	0.71 ± 0.62
		900	11.0	0.88 ± 0.01
Tetraselmis sp.	5V	180	8.01	3.58 ± 0.36
		360	8.99	3.78 ± 0.52
		900	18.1	8.31 ± 0.02
	10V	180	14.62	11.7 ± 0.03
		360	15.57	35.7 ± 0.03
		900	24.15	52.8 ± 0.02

Figures 5.3 and 5.4 show the recovery of microalgae for *Chlorococcum sp.* and *Tetraselmis sp.* as a function of the time that the voltage was applied. The maximum recovery obtained was 98 ± 0.12 and 99 ± 0.02 % for *Chlorococcum sp.* and *Tetraselmis sp.,* respectively at electrocoagulation conditions of 10 V and 900 s.

For each voltage, it can be seen that the recovery of microalgae reaches a maximum value and then plateaus. The electrocoagulation results show an increase in microalgae recovery efficiency with voltage and run time. Applying lower voltages and longer times also gave near optimum recovery results. The plateau in recovery observed in the results show that adequate recovery is possible with run times that

are significantly lower than the maximum voltages and run times. Thus, it avoids the issue of possible changes to microalgae structure due to toxicity.
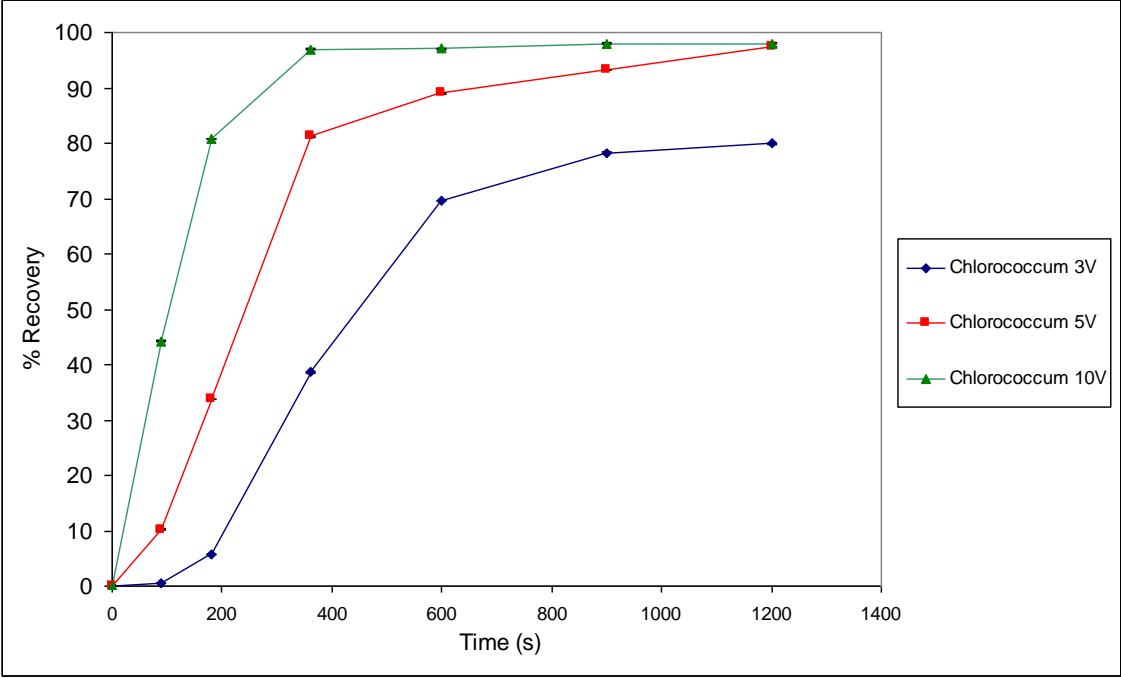
Figure 5. 3. Percentage recovery of *Chlorococcum sp.* during electrocoagulation at different voltages, with the stainless steel 430 anode.
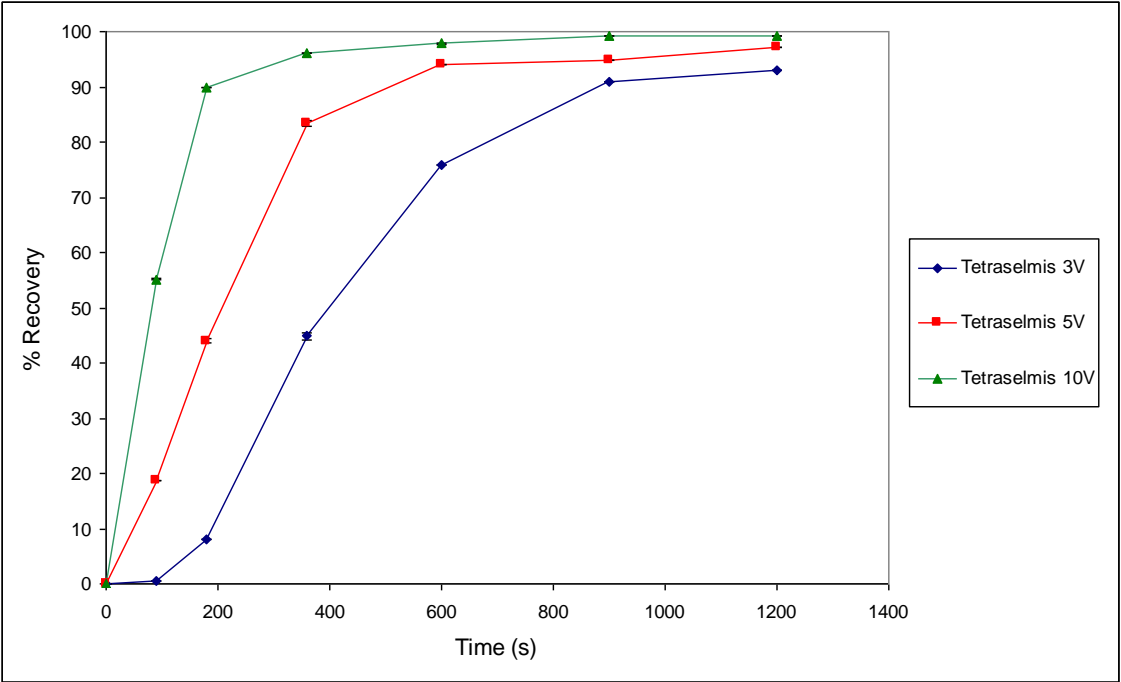
Figure 5. 4. Percentage recovery of *Tetraselmis sp.* during electrocoagulation at different voltages, with the stainless steel 430 anode.

Figure 5.5 shows the change in electrical input per change in kg microalgae removed for the given time periods. It can be seen from the figure that each voltage has a minimum power requirement. (Please refer to Appendix A.2.3 for details on calculations). This minimum corresponds to the point where the rate of recovery starts to slow. It is postulated that after this time, the same energy is being expended generating bubbles at the cathode, but there are fewer and fewer flocs to interact with these bubbles and thus the energy efficiency of the separation drops. Another explanation would be that the ratio of flocs to bubbles increases with time, but after a certain time the average number of bubbles to each floc is above the minimum required. The optimum minimum power required to achieve the greatest microalgal recovery was 3.12 kWh/kg for *Tetraselmis sp.* and 7.09 kWh/kg for *Chlorococcum sp.* at a power input at 5 V. A study by Poleman, E. et al. (1997) conducted electrocoagulation experiments on fresh water blue-green microalgae, green microalgae and diatoms. For microalgae concentrations varying between 2.7 and 36.1 mg dry mass/L, energy consumptions were 122.2 and 9.1 kWh/kg, respectively (Poelman, E. et al. 1997). The difference in the power consumption values between studies can be attributed to the use of freshwater and marine microalgae cultures. Freshwater microalgae species have higher power requirements due to the lower conductivity of the solution.
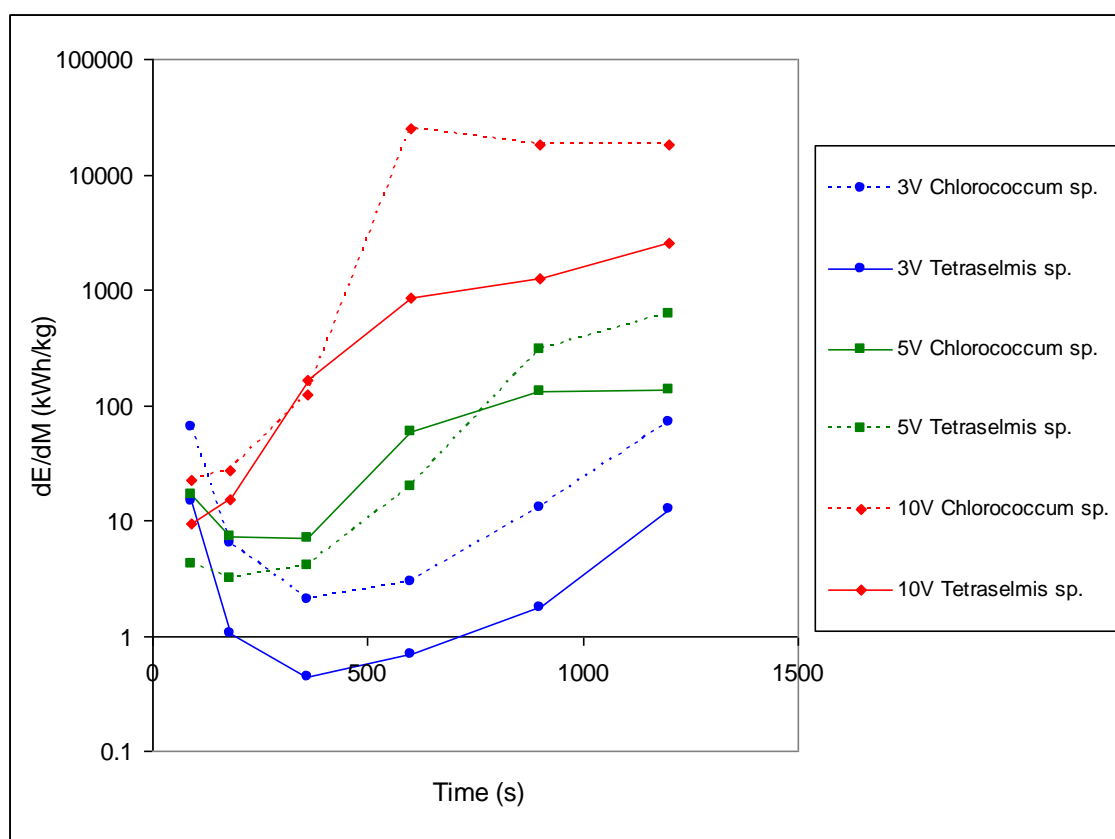
Figure 5. 5. Electrical input per kg microalgae recovered versus time for electrocoagulation flotation experiments, with the stainless steel 430 anode.

5.2.1-2 Effect of Microalgae Salinity on Recovery

Table 5.3 shows the current density obtained for electrocoagulation with varying ratios of microalgae to de-ionised water. It can be seen that the current and current density decrease with the percentage of de-ionised water in an approximately linear manner, which relates directly to the change in electrical conductivity of the media.

Table 5. 3. Initial current density measured during electrocoagulation for *Chlorococcum sp*. and *Tetraselmis sp.* at 3V.

Ratio of Microalgae : De-ionised Water	Chlorococcum sp. Current Density (A/cm^2)	Tetraselmis sp. Current Density (A/cm^2)
20 : 80	0.004	0.003
50 : 50	0.011	0.009
80 : 20	0.017	0.014
100 : 0	0.020	0.020

Figure 5.6 and 5.7 show the recovery of microalgae with time. The results show that reducing the salinity of the microalgal cultures resulted in poor recovery of microalgae. This is explained partly by the reduction in the conductivity of the system, which leads to a reduction in the applied current at the fixed voltage. Lower current will affect the dissolution reaction at the anode, producing a lower amount of coagulant and also a lower production rate of hydrogen bubbles, thus reducing the amount of microalgal aggregation and recovery.
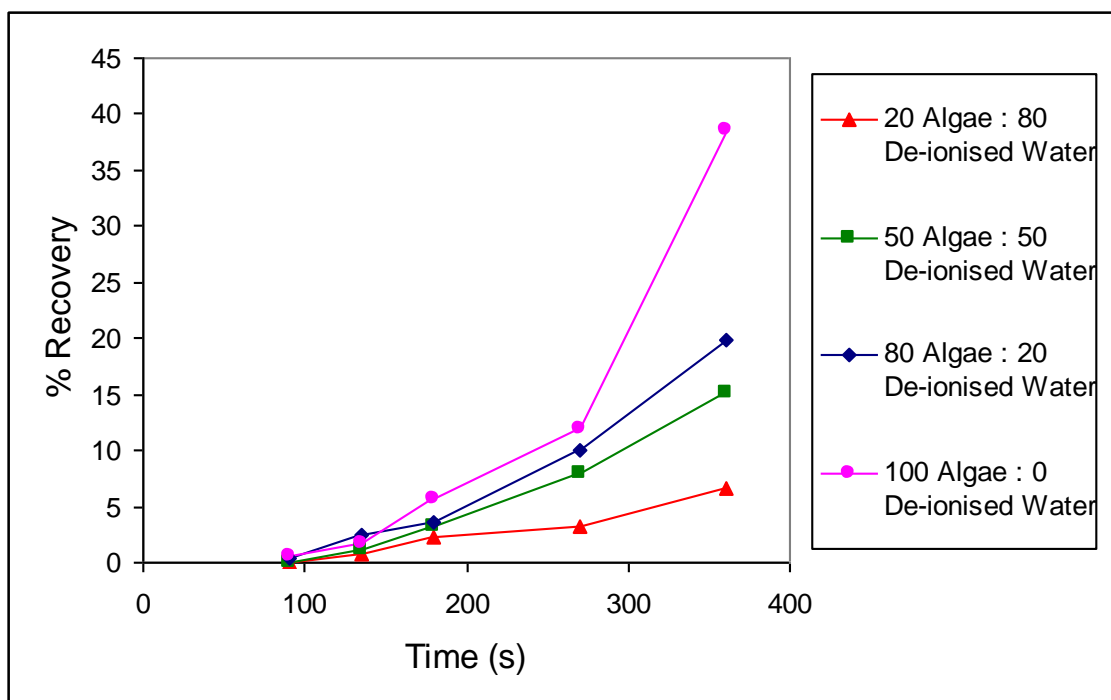
Figure 5. 6. Percentage recovery of *Chlorococcum sp.* versus time during electrocoagulation at 3 V with varying salinity, with the stainless steel 430 anode.
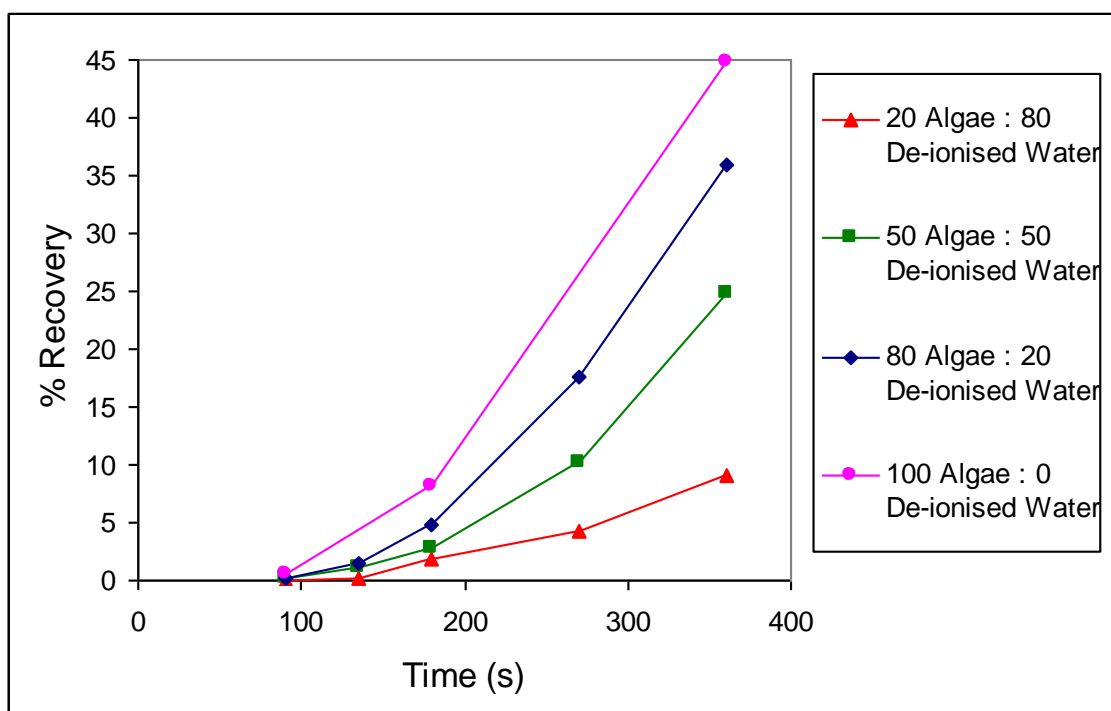
Figure 5. 7. Percentage recovery of *Tetraselmis sp.* versus time during electrocoagulation at 3 V with varying salinity, with the stainless steel 430 anode.

If the electrocoagulation was controlled solely by the current density, and the data was scaled by dividing by the current density, the salinity results should all align to a single curve. Figure 5.8 and 5.9 show the recovery of microalgae with time scaled by dividing by the current density. It can be seen from the figures that for smaller dilutions such as ratios of 80:20 and 50:50 of microalgae: de-ionised water the curves are quite close. But in the case of a 4x dilution as for 20:80 microalgae: de-ionised water, the results do not follow the expected trend. These results indicate that there are other factors which may have an influence on the microalgae recovery. These factors include:

- Changes in the compression of the electrical double layer of the microalgae. This could have an effect on the extent of metal ion adsorption to the microalgae surface; hence affect microalgae coagulation and recovery.

- Changes in the density of the culture media. Sea water is denser than fresh water. An increase in the percentage of de-ionised water will result in a reduction in the relative density of the culture media and the microalgae/bubble complex. This may make it more difficult for the microalgae flocs to float to the surface and hence affect microalgae recovery.

- Changes in the size and possibly the charge of hydrogen bubbles. As will be shown later in figure 5.12, the hydrogen bubble size is affected by the system pH. A change in salinity of the system means that there will be a change in the ions that are present, which could have an impact on the concentration of H^+ and OH^- ions, resulting in a change in system pH. This could have an effect on the extent of flotation of microalgae flocs, hence affect the overall recovery.

It can be seen in figures 5.6 and 5.7 that as the percentage of de-ionised water increases, there is an increase in lag time. The term lag time is described as the time it takes to initiate microalgal recovery. This lag time is discussed in greater detail in chapter 6, section 6.4.2.
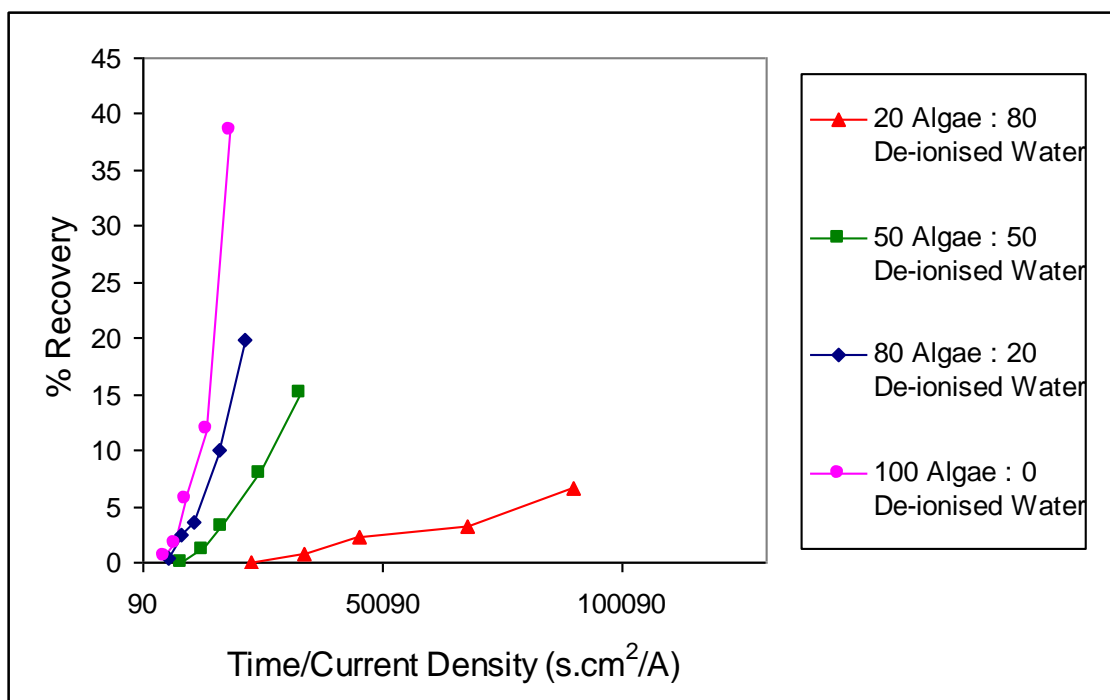
Figure 5. 8. Percentage recovery of *Chlorococcum sp.* versus time/current density during electrocoagulation at 3 V with varying salinity, with the stainless steel 430 anode.
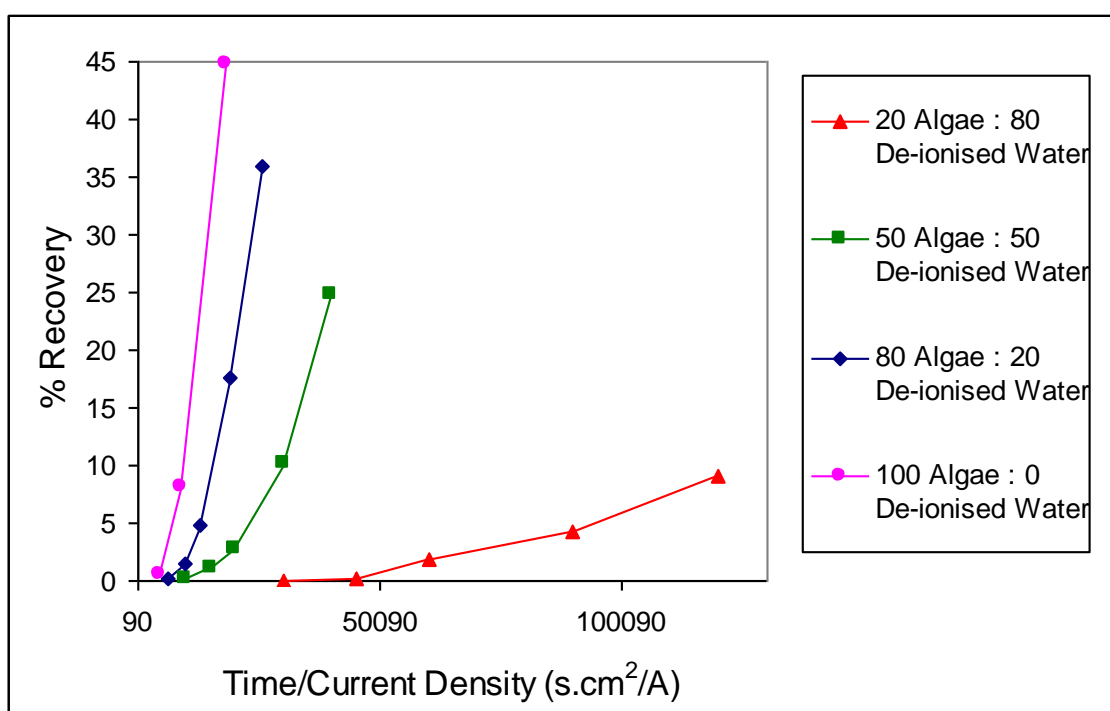
Figure 5. 9. Percentage recovery of *Tetraselmis sp.* versus time/current density during electrocoagulation at 3 V with varying salinity, with the stainless steel 430 anode.

5.2.1-3 Effect of Microalgae Temperature on Recovery

Increasing the temperature of the microalgal culture resulted in greater microalgal recovery efficiency (figures 5.10 and 5.11). This can be explained by the theory of collision (Haynie, D. T. 2008). With increasing temperature, the microalgae cells have greater kinetic energy, therefore the probability of collision and hence agglomeration will increase. Electrical conductivity is also strongly dependent on temperature. With increasing temperature, the electrical conductivity of the microalgae system increases and this in turn allows for a higher current to flow through the system at a given voltage. Higher currents and thus higher bubble formation rates results from an increased conductivity which in turn results in a greater recovery efficiency. Increasing the temperature also favours the kinetics of dissolution of the sacrificial anode, hence affecting the concentration of active coagulants required for agglomeration. A study by Gao, S. et al. (2010b) observed a dramatic increase in microalgae recovery with temperature. This increase in recovery was attributed to collision theory, where as the temperature increases, the microalgae cells gain an increase in particle transport through the reduction of viscosity.

The effect of temperature is important for a number of reasons. It could explain seasonal fluctuations in harvesting efficiency for open air raceway pond systems. It could also be used to improve the energy efficiency overall by thermally heating the solution before harvesting, thereby reducing the electrical power requirements. Low temperature heating could be achieved using waste heat or a renewable source.

The selection of temperature range was done in order to have a range of temperatures that corresponded to extreme conditions, with 5 °C being an extreme low point, 22 °C being the normal experimental operating temperature and 60 °C being an extreme high point.
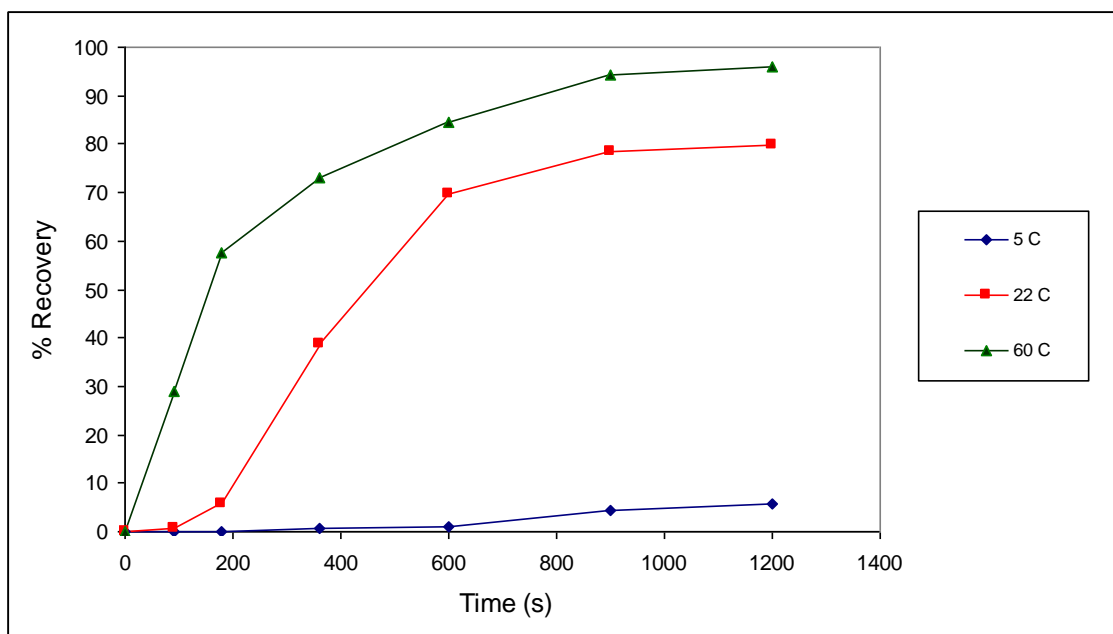
Figure 5. 10. Percentage recovery of *Chlorococcum sp.* during electrocoagulation at 3 V and different temperatures, with the stainless steel 430 anode.
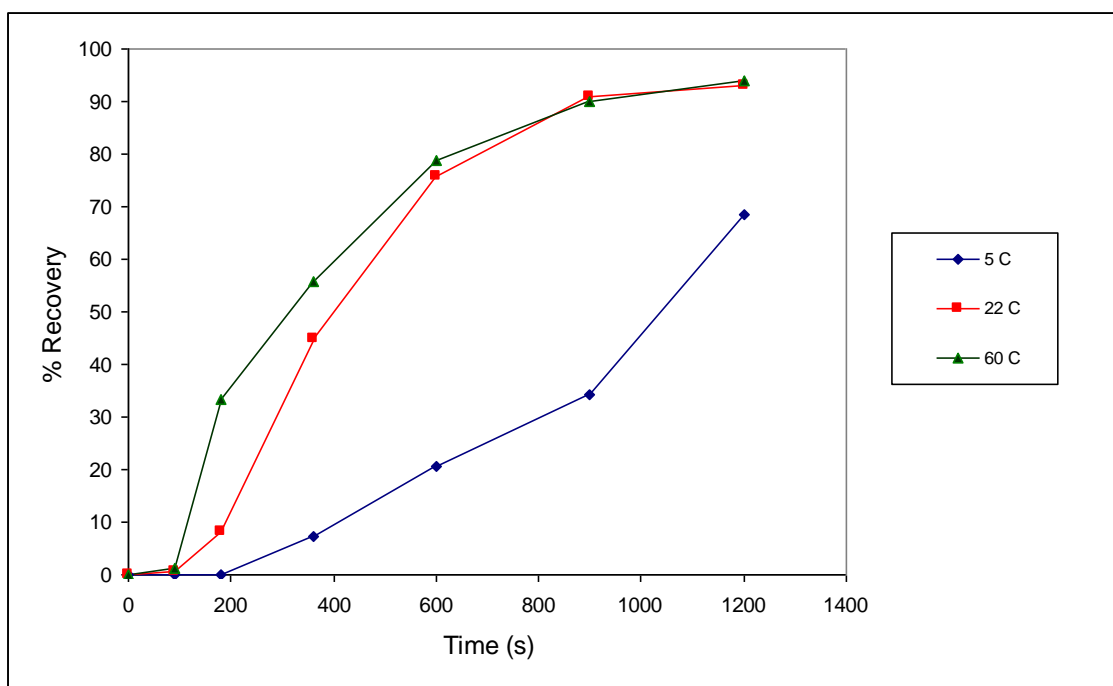
Figure 5. 11. Percentage recovery of *Tetraselmis sp.* during electrocoagulation at 3 V with different temperatures, with the stainless steel 430 anode.

5.2.1-4 Effect of Microalgae pH on Recovery

The starting pH of both microalgae species was varied from 4 to 9 before electrocoagulation was carried out. The results in tables 5.4 and 5.5 show that there was no apparent trend in microalgae recovery due to varying the starting pH. Increasing the applied current and voltage, however, still resulted in increased recovery of microalgae.

Table 5. 4. Affect of initial microalgae pH on recovery for *Chlorococcum sp.*, with the stainless steel 430 anode.

		ph4	ph5	ph7	ph8	ph 9
	Time (s)	% Recovery	% Recovery	% Recovery	% Recovery	% Recovery
3V	90	0.16	0.00	0.20	0.53	0.12
	180	4.56	3.16	11.3	5.74	0.98
	360	14.4	13.4	33.5	38.7	33.7
5V	90	12.3	12.4	25.9	11.7	19.6
	180	38.2	37.9	48.1	61.7	52.0
	360	64.8	67.5	79.6	76.8	83.2
10V	90	47.6	50.2	61.2	52.7	61.0
	180	78.0	77.4	80.7	75.3	81.7
	360	89.9	82.4	91.0	87.0	87.9

Table 5. 5. Effect of initial microalgae pH on recovery for *Tetraselmis sp*, with the stainless steel 430 anode.

	Time (s)	ph4 % Recovery	ph5 % Recovery	ph7 % Recovery	ph8 % Recovery	ph 9 % Recovery
3V	90	0.31	0.00	0.78	0.54	0.00
	180	13.6	12.9	11.0	8.09	4.33
	360	44.4	50.0	39.3	44.9	22.0
5V	90	28.6	21.4	18.4	18.7	22.0
	180	50.0	50.6	37.5	44.0	41.8
	360	83.9	74.9	66.6	83.4	79.3
10V	90	51.8	53.8	52.3	55.2	55.0
	180	84.4	80.3	87.9	89.8	85.1
	360	95.2	95.3	95.6	96.2	94.8

Electrocoagulation was also carried out with salt water media in a mini cell with stainless steel electrodes in order to observe the change in hydrogen bubble size with pH (please refer to Appendix A.3.6 for details on the mini cell). The pH of the salt water media was varied from 2 to 10 using 1 molar hydrochloric acid to increase acidity or 1 molar sodium hydroxide to increase alkalinity. The hydrogen bubbles that evolved were then captured with a high speed camera and analysed with Image J software. Figure 5.12 shows the results obtained, with the hydrogen bubble size increasing with increasing pH. These results tell us that if the hydrogen bubble size is an important factor in the flotation of the floc complex, the starting pH should influence microalgae recovery. The hydrogen bubbles produced in salt water media electrocoagulation have larger diameters than the bubbles produced in microalgae electrocoagulation (please refer to Appendix A.2.8). Assuming the conductivity of marine microalgae culture is the same as the salt water media, the explanation for the difference in bubble size can be attributed to the uniformity of the salt water medium, which allows bubble-bubble collisions and the consolidation of two bubbles into a single bubble. For a heterogeneous system like the microalgal suspension, the presence of microalgal particulates provides a physical barrier to the bubble-bubble

collisions and once the bubbles are trapped by the algae no further agglomeration of bubbles is possible.
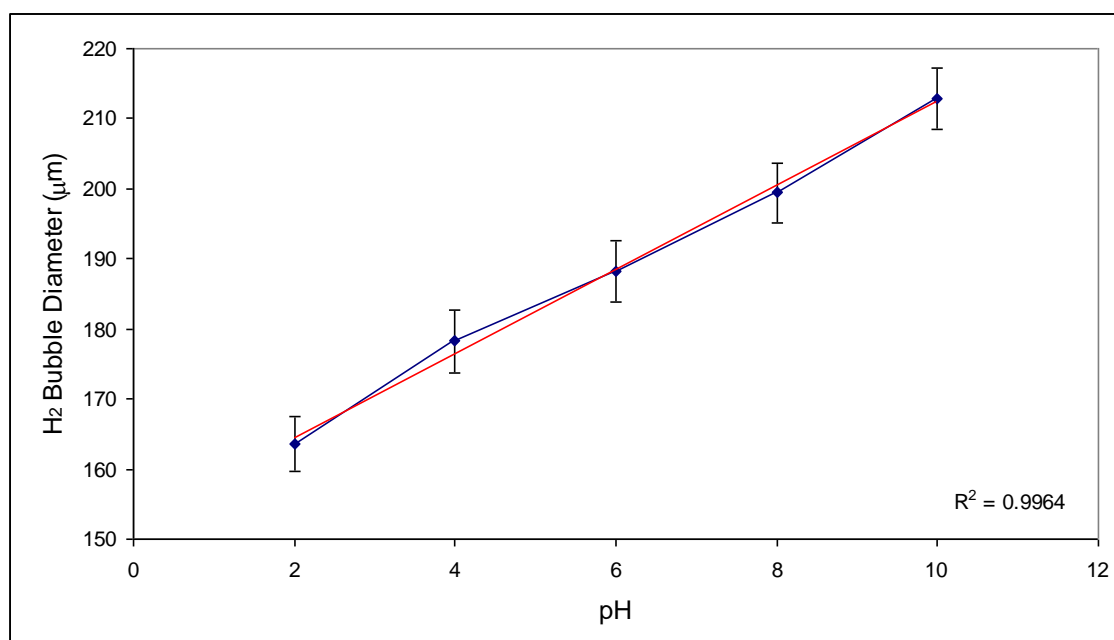
Figure 5. 12. Hydrogen bubble size with changing pH, electrocoagulation of salt water media at 5 V, with the stainless steel 430 anode.

5.2.1-5 Dissolution of Iron

Evidence of the stainless steel electrode being sacrificial (i.e. iron dissolving from the anode) was seen from control electrocoagulation experiments conducted on culture media alone. The culture media is colourless which made it easy to observe any precipitates that form in the microalgae solution. It was observed that green precipitates formed during electrocoagulation and floated to the surface by hydrogen bubbles (figure 5.13). From the colour of precipitate, it can be concluded that the iron species Fe^{2+} dissolves from the anode (Vandamme, D. et al. 2011).

Figure 5. 13. Electrocoagulation performed on salt water media at 5 V, with the stainless steel 430

anode.

5.2.2 Stainless Steel 430 Cathode/ Aluminium Anode

5.2.2-1 Microalgae Recovery by Electrocoagulation

Electrocoagulation experiments were conducted on a range of different voltages and run times for the batch cell using a stainless steel 430 cathode, but now replacing the stainless steel 430 anode with an aluminium anode. Figure 5.14 shows the measured current as a function of time after the application of a constant voltage of 5 V for both microalgae species. Figure 5.15 shows the measured voltage as a function of time after the application of a constant current of 1 A for both microalgae species
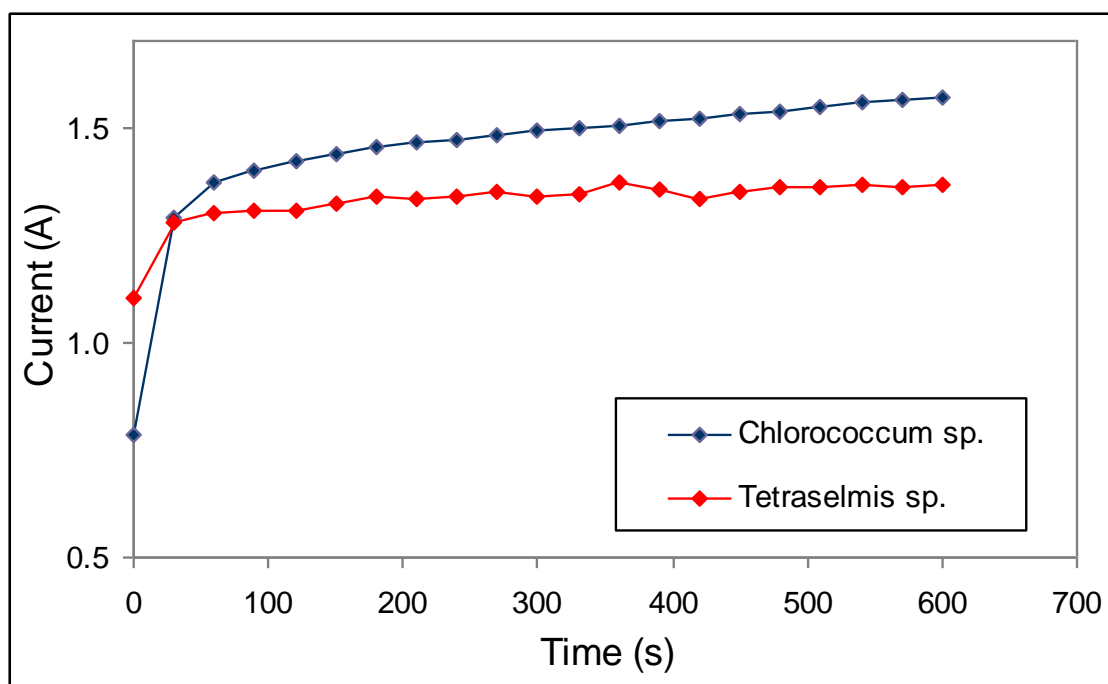
Figure 5. 14. Current versus time for a constant voltage of 5 V for *Chlorococcum sp.* and *Tetraselmis sp.*, with the aluminium anode.
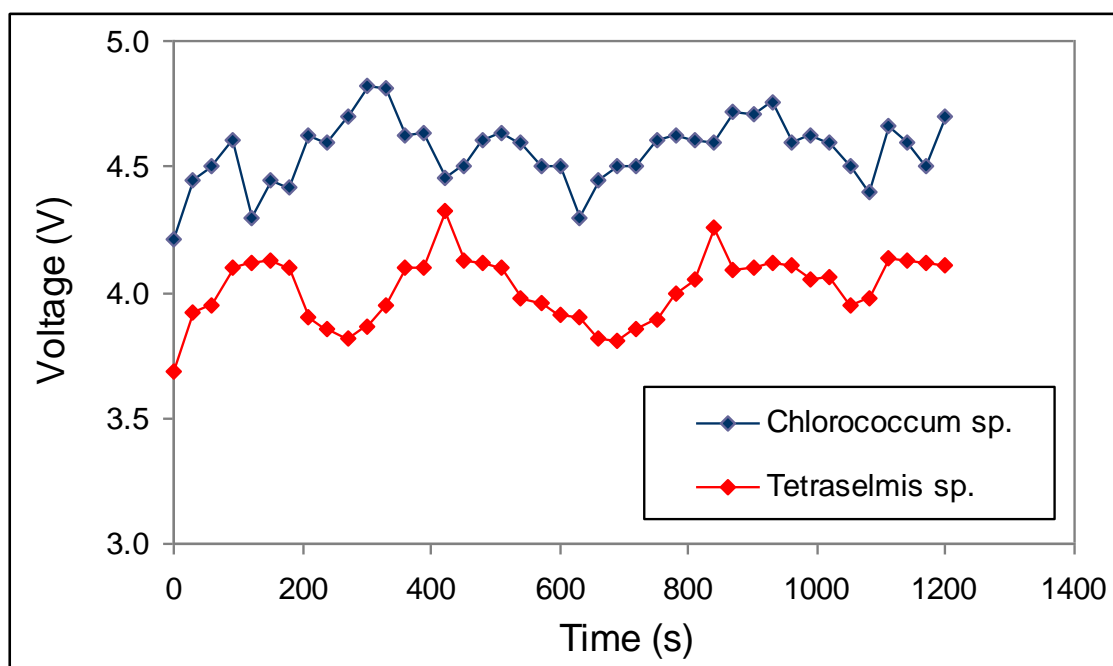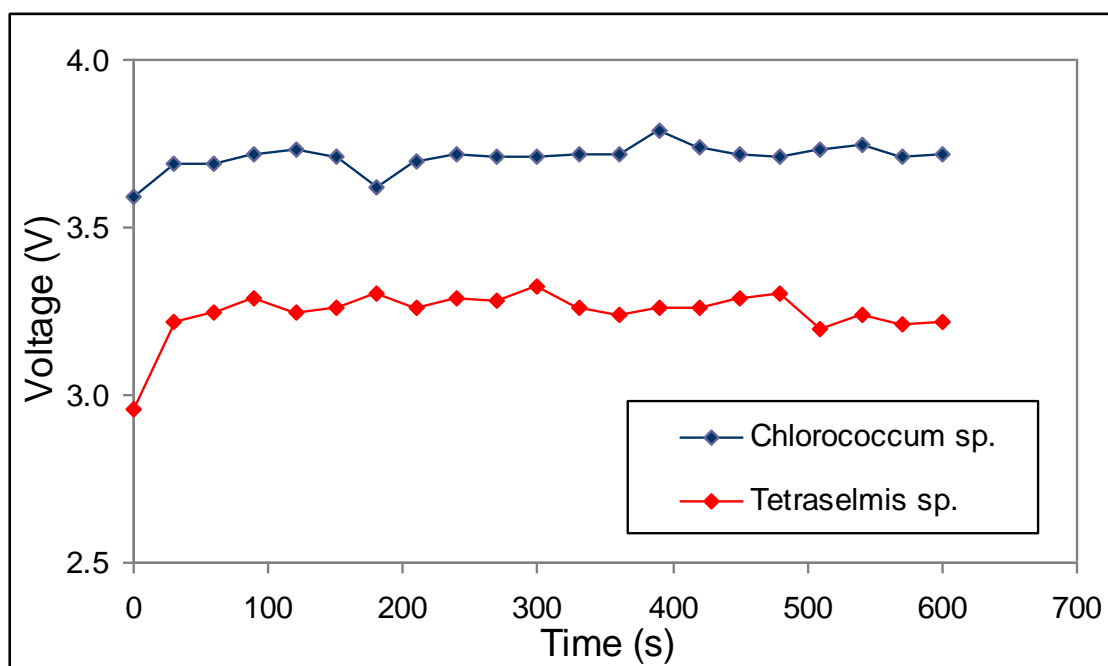
Figure 5. 15. Voltage versus time for a constant current of 1 A for *Chlorococcum sp.* and *Tetraselmis sp.*, with the aluminium anode.

Table 5.6 shows the initial current density readings for the different experimental conditions tested.

Table 5. 6. Initial current density measured during electrocoagulation, with aluminium anode.

	Current Density (A/cm^2)	
	Chlorococcum sp.	**Tetraselmis sp.**
2V	0.010	0.009
3V	0.030	0.024
5V	0.060	0.055

Table 5.7 provides a log of the different experiments conducted on *Chlorococcum sp.* and *Tetraselmis sp.* as well as the final concentration factor and electrical input required for electrocoagulation in kWh per kg of microalgae removed. The electrical input into the system has been calculated from the product of the applied voltage, the average measured current and the time that the voltage is applied (please refer to Appendix A.2.3 for calculations).

110

Table 5. 7. Electrical input for electrocoagulation flotation experiments with the aluminium anode.

		Time (s)	Final Concentration Factor	Electrical Input (kWh/kg Microalgae Removed)
Chlorococcum sp.	2V	180	4.09	0.54 ± 0.08
		360	4.83	0.69 ± 0.03
		600	4.83	1.10 ± 0.06
	3V	180	4.45	1.05 ± 0.05
		360	4.51	2.10 ± 0.06
		600	4.82	3.38 ± 0.06
	5V	180	4.47	3.28 ± 0.04
		360	4.73	6.28 ± 0.05
		600	4.83	10.31 ± 0.04
Tetraselmis sp.	2V	180	13.87	0.18 ± 0.02
		360	14.03	0.24 ± 0.06
		600	14.10	0.42 ± 0.01
	3V	180	14.16	0.41 ± 0.09
		360	14.17	0.74 ± 0.02
		600	14.30	1.25 ± 0.01
	5V	180	13.83	1.41 ± 0.03
		360	13.87	2.75 ± 0.06
		600	14.17	4.58 ± 0.02

The electrocoagulation results for the aluminium anode were similar to that of the stainless steel anode. Figures 5.16 and 5.17 show the percentage of microalgae recovered at different applied voltages and batch run times, for both microalgal species. The recovery of microalgae was seen to increase with applied voltage and time and appears to follow a sigmoidal trend. The recovery obtained for *Tetraselmis sp.* was slightly higher than *Chlorococcum sp*. for all electrocoagulation experiments. This is mainly due to the fact that the concentrations of microalgae for *Tetraselmis sp.* was double that of *Chlorococcum sp.* during all electrocoagulation experiments.

The higher cell density of *Tetraselmis sp.* microalgae provides the coagulant cations with an increased probability to adhere to the cells to form flocs to remove the last few percent of algae.

At lower voltages, a lag phase can be observed before surface accumulation of flocs. This lag phase is more apparent in the stainless steel anode results than the aluminium results. The lag time can be related to the period where there is very minimal flotation of microalgae resulting from insufficient microalgae agglomeration or microalgae-bubble interaction. A study by Holt, P.K. et al. (2002) also describes a lag phase during electrocoagulation experiments.
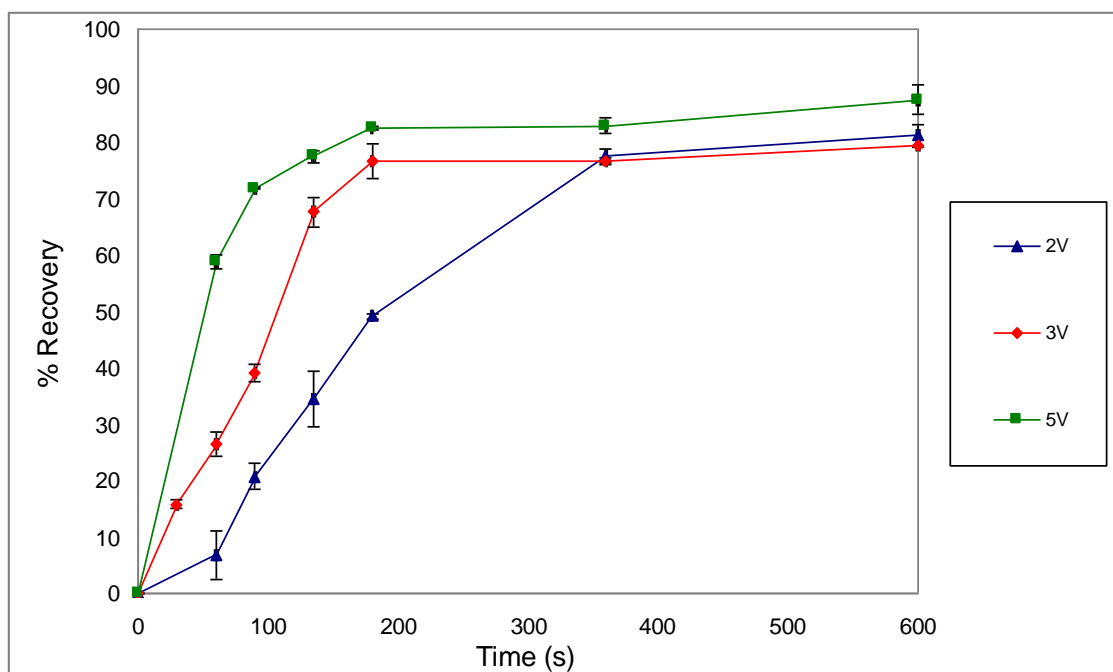
Figure 5. 16. Percentage of microalgae recovery as a function of process time for *Chlorococcum sp.*, with the aluminium anode.
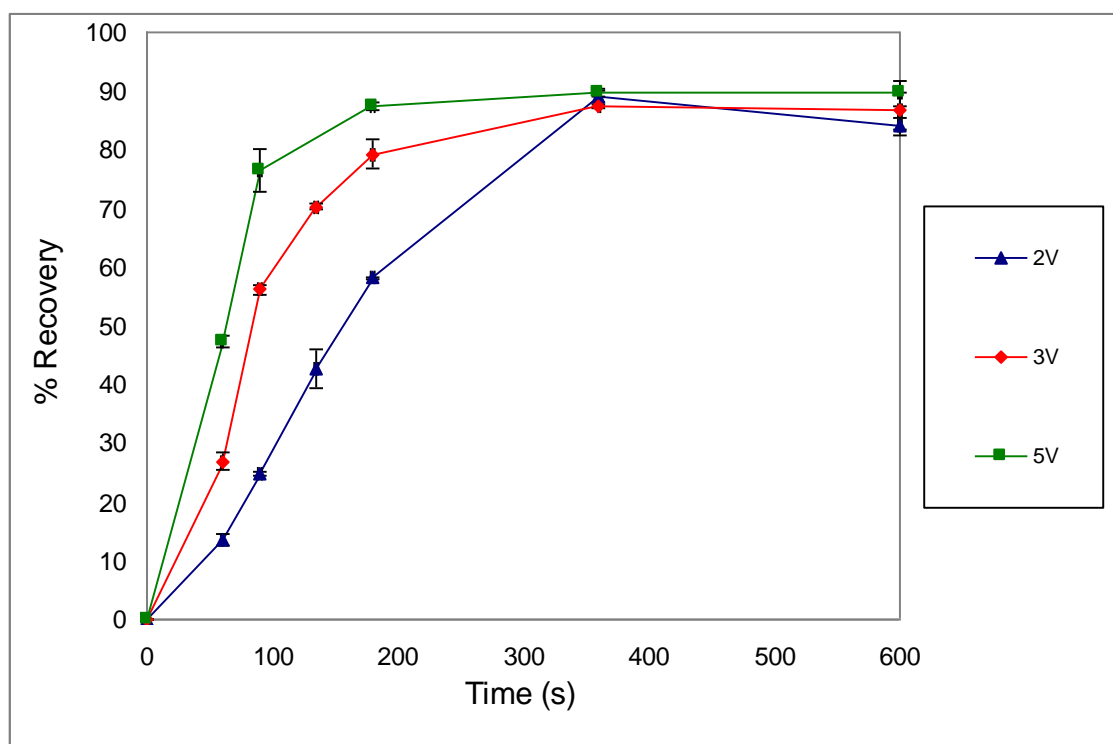
Figure 5. 17. Percentage of microalgae recovery as a function of process time for *Tetraselmis sp.*, with the aluminium anode.

Figure 5.18 shows the change in electrical input per change in kg of recovered microalgae for the given time periods. It can be seen from the figure that each voltage has a minimum power requirement. The minimum corresponds to the point where the rate of recovery starts to slow. After this time, the same energy is being expended to generate bubbles at the cathode, but there are fewer flocs to interact with these bubbles and therefore the energy efficiency of the separation drops. The optimum minimum power required to achieve the greatest microalgal recovery was 0.70 kWh/kg for *Tetraselmis sp.* and 1.53 kWh/kg for *Chlorococcum sp.* at a power input at 5 V.
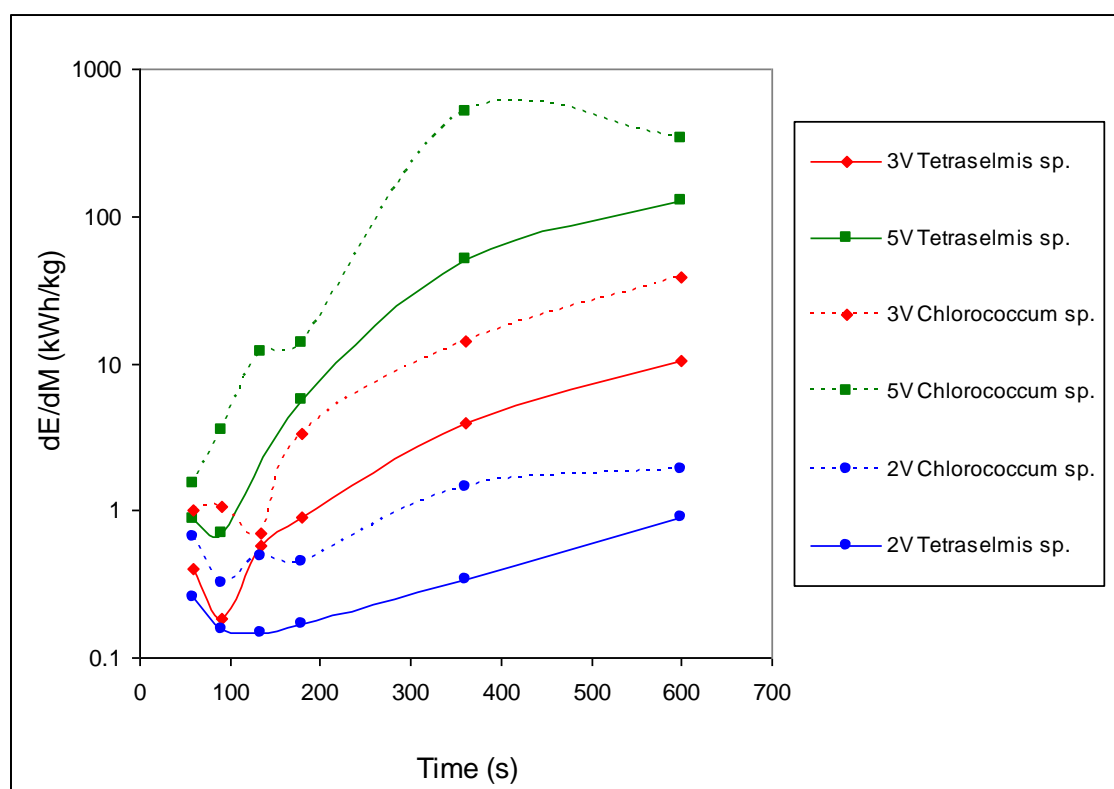
Figure 5. 18. Electrical input per kg microalgae recovered versus time for electrocoagulation flotation experiments, with the aluminium anode.

5.2.2-2 Effect of Batch Volume on Microalgae Recovery

The liquid volume in the cell used in all electrocoagulation experiments was normally 300 ml. Experiments were conducted with varying the liquid volume for constant current density electrocoagulation using an aluminium anode. The results showed

that changes in the liquid volume did not have a significant effect on microalgal recovery, if the current density was kept constant. The larger volumes of microalgae showed slightly better recovery at lower run times, however as the run time increased, all recoveries reached same final value. By keeping the current density constant, the amount of bubbles produced per unit volume of liquid was also constant for the different sample volumes. Please refer to Appendix A.3.7 for details.

5.2.2-3 Effect of Electrocoagulation on Microalgae pH

The pH of the solution after electrocoagulation was observed to decrease with the run time for both microalgae species, as seen in figures 5.19 and 5.20. When the initial pH is alkaline, the drop in pH can be explained by oxygen evolution and/or the dissolution reactions of aluminium and its hydroxide $[Al(OH)_4]^-$ as being alkalinity consumers (Murugananthan, M. et al. 2004; Mouedhen, G. et al. 2008).

It can be seen from figures 5.16 and 5.17 that for electrocoagulation experiments with the aluminium anode, the recovery of microalgae plateaus after 360 s, where as the recovery of microalgae continues to increase with increasing time for electrocoagulation with the stainless steel anode (see figures 5.3 and 5.4). This observation can be attributed to the ineffectiveness of aluminium as a coagulant when the solution pH lies in the acidic range, as seen in figures 5.19 and 5.20 where the pH drops to acidic after 200 s. The ineffectiveness of aluminium at low pH was also reported by Chen, G. (2004) who noted a sharp decrease in suspended solids removal when the pH dropped below 4.
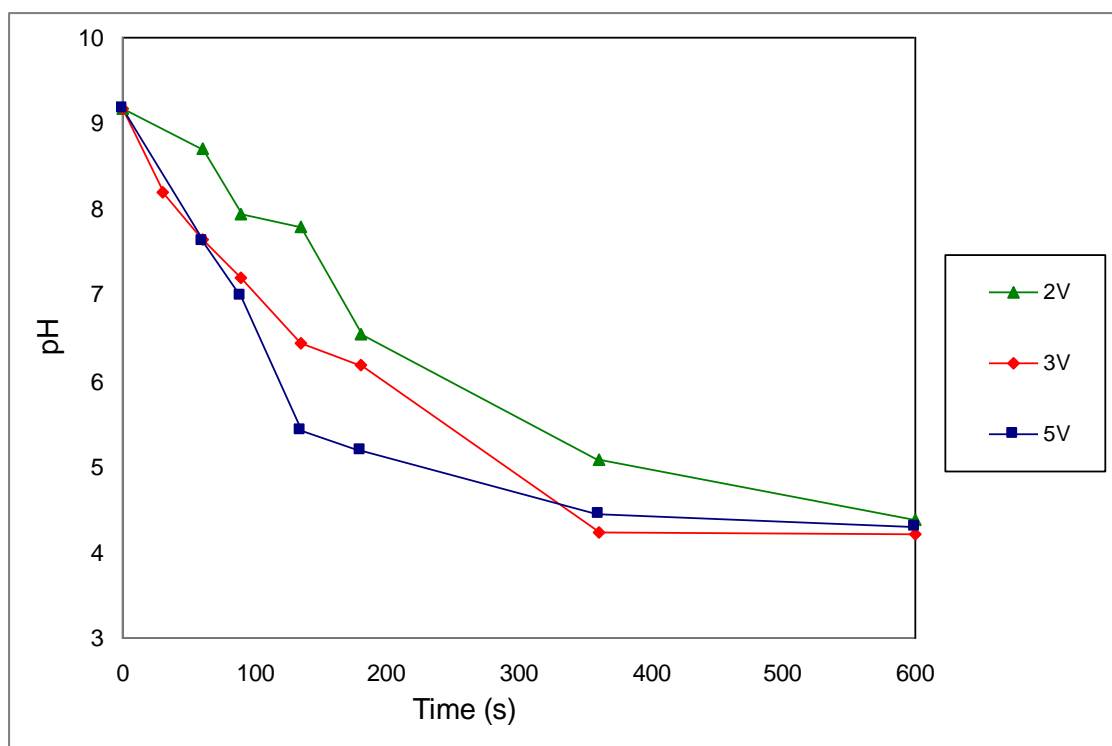
Figure 5. 19. Average pH of supernatant after electrocoagulation for *Chlorococcum sp.*, with the aluminium anode.
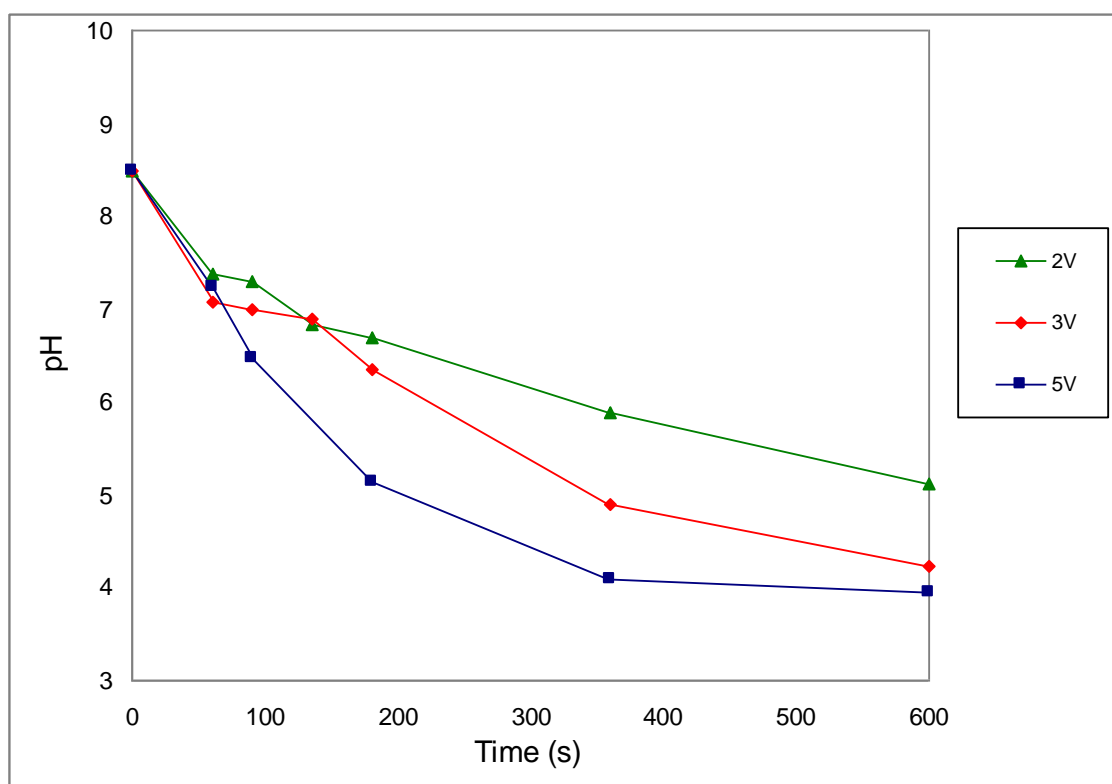
Figure 5. 20. Average pH of supernatant after electrocoagulation for *Tetraselmis sp.*, with the aluminium anode.

116

5.2.3 Stainless Steel 430 Cathode/ Carbon Anode

Carbon was also used as an anode material to further investigate the importance of the coagulation step in the electrocoagulation process. Figure 5.21 shows the measured current with time for a constant voltage of 5 V and the measured voltage with time for a constant current of 1 A.
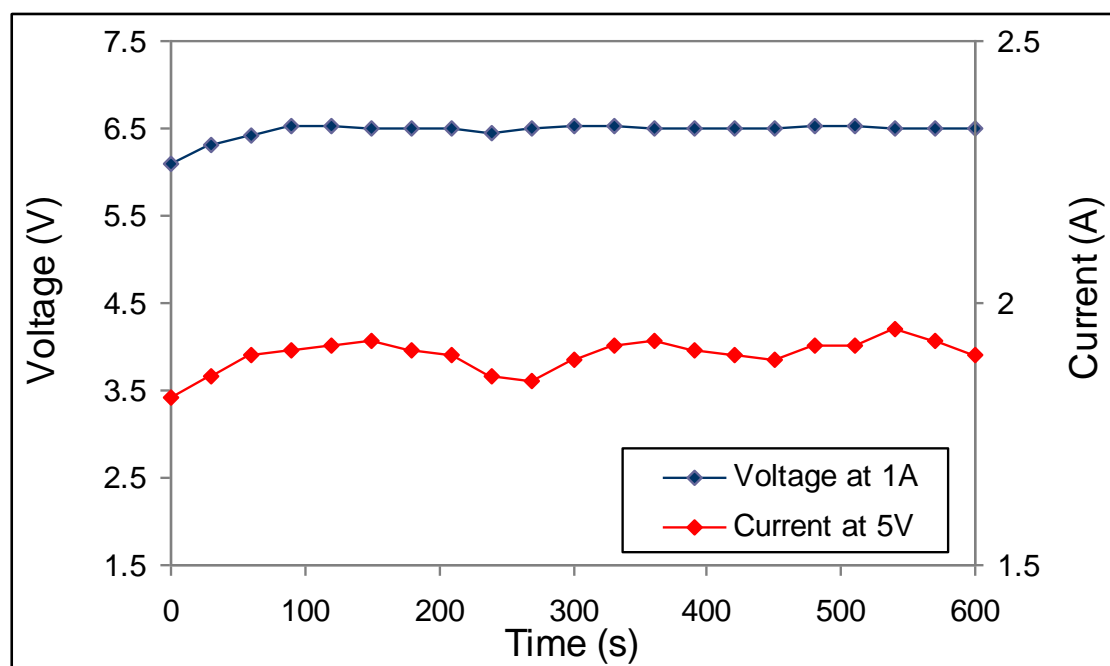
Figure 5. 21. Current at a constant voltage of 5 V and voltage at a constant current of 1A, versus time for *Tetraselmis sp.* with the carbon anode.

The electrocoagulation results obtained show that the recovery of microalgae is poor when using a carbon anode. From figure 5.22, it can be seen that after a run time of 600 s with a voltage of 5 V, the recovery of *Tetraselmis sp.* was only 38.15 %. After electrocoagulation, the majority of microalgae mass was left in suspension or settled to the bottom of the cell. The carbon electrode is a non sacrificial electrode; and therefore no metal is dissolved into the microalgae solution during electrocoagulation. This means that the only mechanism of microalgae removal is the bubble-particle interaction and flotation. The poor recovery results verifies that the microalgae needs to be flocculated in order for the bubbles to efficiently carry them to the surface.

117
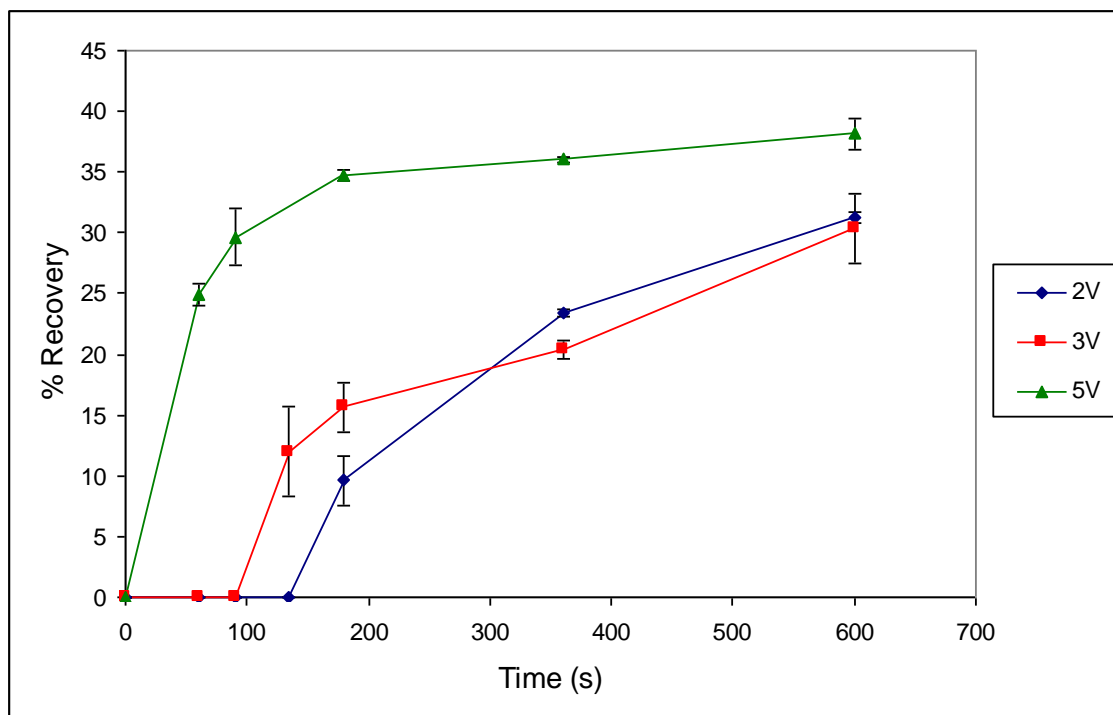
Figure 5. 22. Percentage recovery of *Tetraselmis sp.* during electrocoagulation at different voltages, with the carbon anode.

5.3 Electrocoagulation Results – Constant Current

Electrocoagulation was carried out with each anode material at a constant current of 1 A. This was done in order to have a direct comparison of the electrocoagulation efficiency of the anode materials. Figure 5.23 shows that at constant current, aluminium had the best recovery efficiency. Table 5.8 shows the equivalent voltages achieved with the different anode materials.

All electrocoagulation experiments discussed thus far have been performed with constant voltage. Each different anode metal has a different place on the electrochemical series (please refer to Appendix A.3.5). This means that for each anode material, at a constant voltage, a slightly different amount of electrical current is necessary in order to complete the electrical circuit and begin the anode dissolution reaction. The comparison based on constant current allows the comparison of electrocoagulation efficiency between anode materials. Electrocoagulation was considered to run for consistent electrochemical conditions. The results show that the aluminium anode gave the best recovery, followed by stainless steel and finally, carbon.
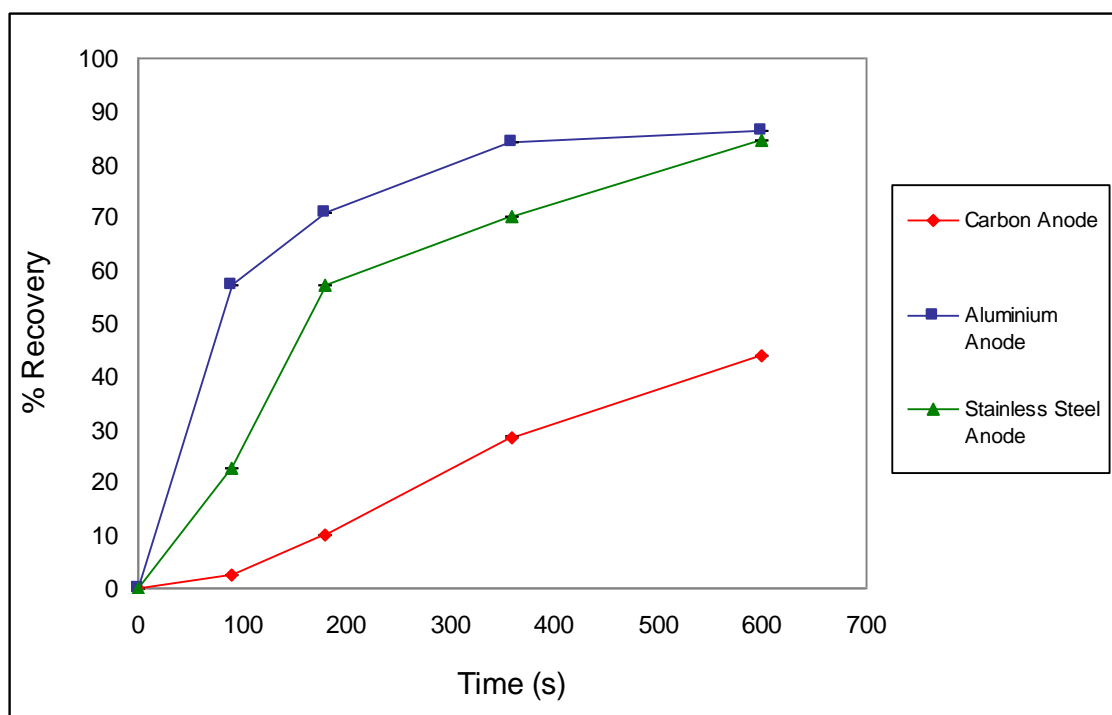
Figure 5. 23. Percentage recovery of *Chlorococcum sp.* with different anode materials at varying times and a constant current of 1 A.

Table 5. 8. Corresponding voltages for electrocoagulation with a constant current of 1 A with *Chlorococcum sp*.

Electrodes	Average voltage at constant current of 1 A (V)
Stainless steel 430 cathode / Stainless steel 430 anode	4.6
Stainless steel 430 cathode / Aluminium anode	3.7
Stainless steel 430 cathode / Carbon anode	6.5

CHAPTER 6 ELECTROCOAGULATION OF MARINE MICROALGAE – DISCUSSION

6.1 Theoretical Mechanism of Electrocoagulation

The theoretical mechanism of electrocoagulation takes place in three successive stages as described by Mollah, M.Y.A et al. (2004), Bukhari, A.A. (2008) and Ghernhout, D. et al. (2008). These stages include:

1. Formation of coagulants by electrolytic oxidation of the sacrificial electrode.

2. Charge neutralisation of the ionic species present in the media by counter ions produced by the electrochemical dissolution of the sacrificial anode.

3. Aggregation of the destabilised phases to form flocs, followed by flotation.
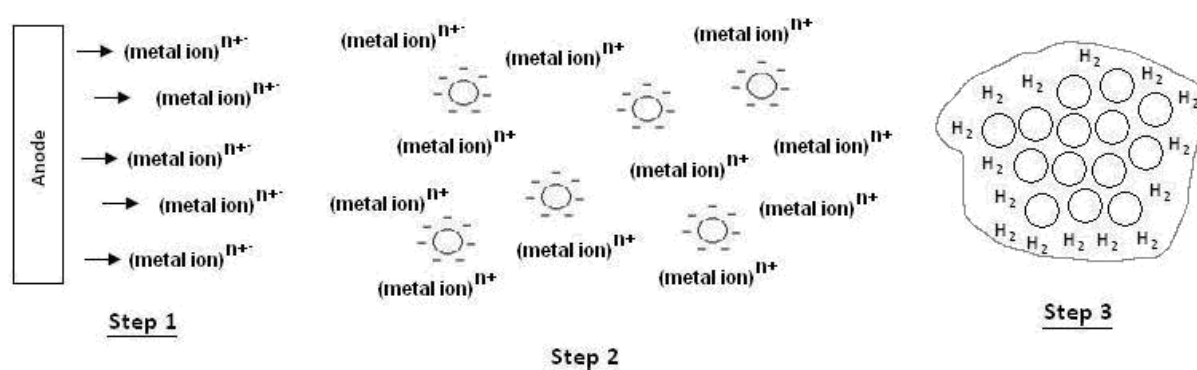
Figure 6. 1. Schematic diagram of the steps involved in mechanism of electrocoagulation.

The electrocoagulation work done in this research was aimed at covering the research gaps outlined in chapter 2. The various studies conducted on electrocoagulation to date have proposed mechanistic steps to promote the understanding of the technology with little experimental validation of these steps. The following work will provide evidence of the theoretical mechanisms described in the literature as well as outline the rate limiting step of electrocoagulation. In addition to this, a mathematical model has been developed to predict the amount of microalgae that can be recovered.

6.2 Development of the Mathematical Model

A mathematical model was developed in order to predict the degree of microalgal recovery with time. The general equations describing the microalgae electrocoagulation process are given by equations 6.1 and 6.2. These equations describe the recovery of microalgae as a two-step process where firstly the microalgae is flocculated due to interaction with metal ions, then these flocs either float to the surface and are recovered due to interaction with hydrogen bubbles, or settle to the bottom of the electrocoagulation cell.

Algae (A) + Metal Ion (B) $\rightarrow$ Flocculated Algae (C) (6.1)

Flocculated Algae (C) + H$_2$ $\rightarrow$ Floated Algae (D) + Settled Algae (E) (6.2)
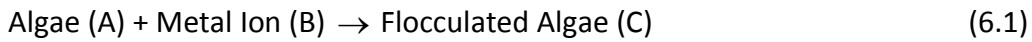
6.2.1 Microalgae Flocculation

The mathematical equation describing the production of flocs resulting from the charge neutralisation of microalgae by the metal ions can be obtained by solving the differential equation for a constant volume batch reactor.

The equation for microalgae coagulation/flocculation can be written as follows:

$$A + bB \xrightarrow{k'} C$$ (6.3)

Where k' is the rate constant and b is a mass ratio of metal ions used for coagulation per gram of microalgae.

Writing this as an nth order differential equation in terms of the change in mass of flocculated algae with time:

$$V \frac{d[C]}{dt} = k'[A]^n[B]$$ (6.4)

Where V is the electrocoagulation batch cell volume (L), [A], [B] and [C] are the concentrations of species A, B and C (g/L) and n is the power for the algae concentration, which is unknown.

By assuming there is no chemical interaction between the hydrogen gas and the liquid in the cell, and negligible volume effect of gas build-up, then the liquid volume will be constant:

$$\frac{dC}{dt} = k[A]^n[B], \qquad \text{where} \quad k = \frac{k'}{V} \qquad (6.5)$$

The concentration of metal ions in the system at any given time will equal the amount of metal ions produced at the anode minus the amount of metal ions that have attached to the microalgae and formed flocs. The amount of metal ions produced can be described by an equation derived from Faraday's law:

$$w = \frac{itM}{zF} \qquad (6.6)$$

Where w is the quantity of electrode material dissolved (g), i is the current (A), t is the time (s), M is the relative molar mass of the electrode concerned (g/mol), z is the number of electrons in the oxidation/reduction reaction, F is the Faradays constant.

Equation 6.5 will asymptote to complete coagulation of the microalgae, but for reasons that will be discussed later in this chapter, the conversion at long electrocoagulation times may not reach 100 %. For this reason the term y is used to define the fraction of microalgae that does not flocculate.

$$y = \frac{A_\infty}{A_0} \qquad (6.7)$$

Where A_∞ is the mass of unflocculated microalgae at infinite time (i.e. at long electrocoagulation time), and A_0 is the initial mass of microalgae at the start (g).

The amount of metal ions that have attached to the microalgae can be obtained from the initial amount of microalgae minus the amount of algae that has not flocculated. This value is then multiplied by constant b, described earlier as a factor relating to the mass of metal ions used for coagulation per gram of microalgae.

Combining the terms, the rate equation becomes:

$$\frac{dC}{dt} = k(A - yA_0)^n \left[\left(\frac{itM}{nF} \right) - b(A_0 - A_0 y - A + yA_0) \right]$$

$$\Rightarrow \frac{dC}{dt} = k(A - yA_0)^n \left[\left(\frac{itM}{nF} \right) - b(A_0 - A) \right] \tag{6.8}$$

Integrating equation 6.8 with the initial conditions A_0 and $C_0 = 0$ in an equation relating the mass of flocculated microalgae (C) with time. However, equation 6.8 can not be integrated directly and therefore an ordinary differential equation solver in MATLAB was used. MATLAB ordinary differential equation solvers are written to solve problems of the form:

$$\frac{dx_1}{dt} = f_1(x_1, x_2, x_3, \ldots, t)$$

$$\frac{dx_2}{dt} = f_2(x_1, x_2, x_3, \ldots, t)$$

$$\frac{dx_3}{dt} = f_3(x_1, x_2, x_3, \ldots, t)$$

....

The specific solver used for the integration of equation 6.8 was *ode45*. This solver uses a variable step Runge-Kutta method to solve differential equations and has a 4th order, medium accuracy.

6.2.2 Flotation and Sedimentation of Flocculated Microalgae

The recovery of microalgae by electrocoagulation is described as the amount of flocculated microalgae that floats to the surface of the cell. Given sufficient time, the flocculated microalgae that do not float to the surface will instead settle to the bottom of the cell. The density of the flocs determines whether they will float or settle. The starting density of the microalgae flocs can be assumed to be similar to that of the sea water media. The attachment of hydrogen gas bubbles reduces the density of the flocs and enables them to float to the surface. There will be a critical density ρ_C where the density of flocs becomes low enough to enable flotation. The critical density was calculated using Stokes law (equation 6.9). The critical density was calculated to be 945 and 974 kg/m^3 for *Chlorococcum sp.* and *Tetraselmis sp.*,

respectively. The critical density was based on the assumption that the radius and rise velocity of microalgae was an average value obtained from experimental data and the density and viscosity of microalgae was similar to that of sea water. The calculation is provided in Appendix A.2.5-2.

$$v = \frac{2r^2(\rho_{sphere} - \rho_{fluid})g}{9\mu}$$
(6.9)

Where v is the velocity of the particle (m/s), r is the radius of the particle (m), ρ_{sphere} and ρ_{fluid} are the densities of floc and microalgae (kg/m^3), μ is the viscosity of the media (Ns/m^2) and g is the acceleration due to gravity (m/s^2). It is assumed that the temperature is room temperature, and the salinity of the microalgae is 30 g/L.

Flocs that do not float are assumed to eventually settle. The mass of floated flocs (D) and settled flocs (E) is described as:

$$D(t) = \sum C(t), \qquad \text{when } \rho_{floc} \leq \rho_C$$
(6.10)

$$E(t) = \sum C(t), \qquad \text{when } \rho_{floc} > \rho_C$$
(6.11)

The density of a floc containing hydrogen bubbles is described by the following equation:

$$\rho_{floc}(t) = \frac{m_{floc} + m_{H_2}}{\dfrac{m_{floc}}{\rho_{floc}^0} + \dfrac{m_{H_2}}{\rho_{H_2}}}$$
(6.12)

Where m_{H_2} and m_{floc} is the mass of hydrogen gas and the mass of flocs excluding the entrained hydrogen bubbles at time t, and ρ_{floc}, ρ_{floc}^0 and ρ_{H_2} are the densities of floc at time t, the floc excluding hydrogen, and the hydrogen gas, respectively (kg/m^3).

From experimental results, it was observed that only a small percentage of hydrogen gas is used for flotation of microalgae flocs. Rearranging equation 6.12 to determine x at the critical density:

$$\left(\frac{\rho_C}{\rho_{floc}^0} + \frac{\rho_C}{\rho_{H_2}} \right) = 1 + x$$

$$x = \left(1 - \frac{\rho_C}{\rho_{floc}^0} \right) \bigg/ \left(\frac{\rho_C}{\rho_{H_2}} - 1 \right) \tag{6.13}$$

where x refers to the mass of hydrogen gas used per mass of microalgae floc.

From experimental results, it was observed that the flocs started to float after an initial period of around of 21 s. The amount of hydrogen used per microalgae floc can be distributed with the amount of flocs (C) as shown in figure 6.2, where x_{21} refers to the amount of hydrogen where the density of flocs equal ρ_C. Figure 6.2 shows a linear distribution of hydrogen amongst the flocs. If the total number of flocs is divided in n packets, then for each packet (i), the quantity of hydrogen per mass of algae would be the linear equation:

$$p(i) = x_{max} - x_{max}(i/n)$$

The maximum amount of hydrogen used per microalgae floc is given by equation 6.14:

$$x_{max} = \left[\frac{m_{H_2}}{m_{floc}} \right]_{max} = \frac{x_{21}}{m_{H2}(t=21)} \times m_{H_2}(t) \tag{6.14}$$

Because the quantity of hydrogen being evolved is constant, $m_{H_2}(t)$ will increase linearly with time and as a consequence x_{max} will also increase linearly with time.
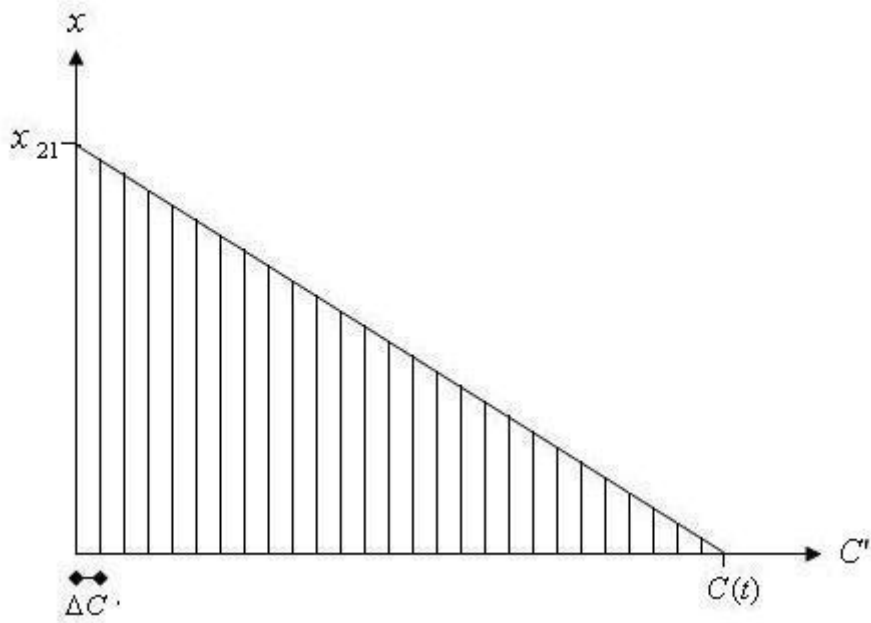
Figure 6. 2. Distribution of hydrogen gas used for flotation with mass of flocs.

The density of each packet (i) can then be calculated as:

$$\rho(i)_{floc} = \frac{1 + p(i)}{\dfrac{1}{\rho_{floc}^{0}} + \dfrac{p(i)}{\rho_{H_2}}} \qquad (6.15)$$

In order to calculate the mass of flocculated algae (C), floated flocs (D) and settled flocs (E), equations 6.8, 6.10, 6.11 and 6.15 must be linked and solved together, as shown in figure 6.3. This was done using MATLAB, with the results giving values for the mass of C, D and E with time (please refer to Appendix A.2.5-4 for MATLAB code).

Step 1

Calculate coagulation of microalgae by solving differential equation:

$$\frac{dC}{dt} = k(A - yA_0)^n \left[\left(\frac{itM}{nF} \right) - b(A_0 - A) \right]$$

Step 2

Calculate floated or settled algae based on the critical density:

$$D(t) = \sum C(t), \qquad \rho_{floc} < \rho_C$$

$$E(t) = \sum C(t), \qquad \rho_{floc} > \rho_C$$
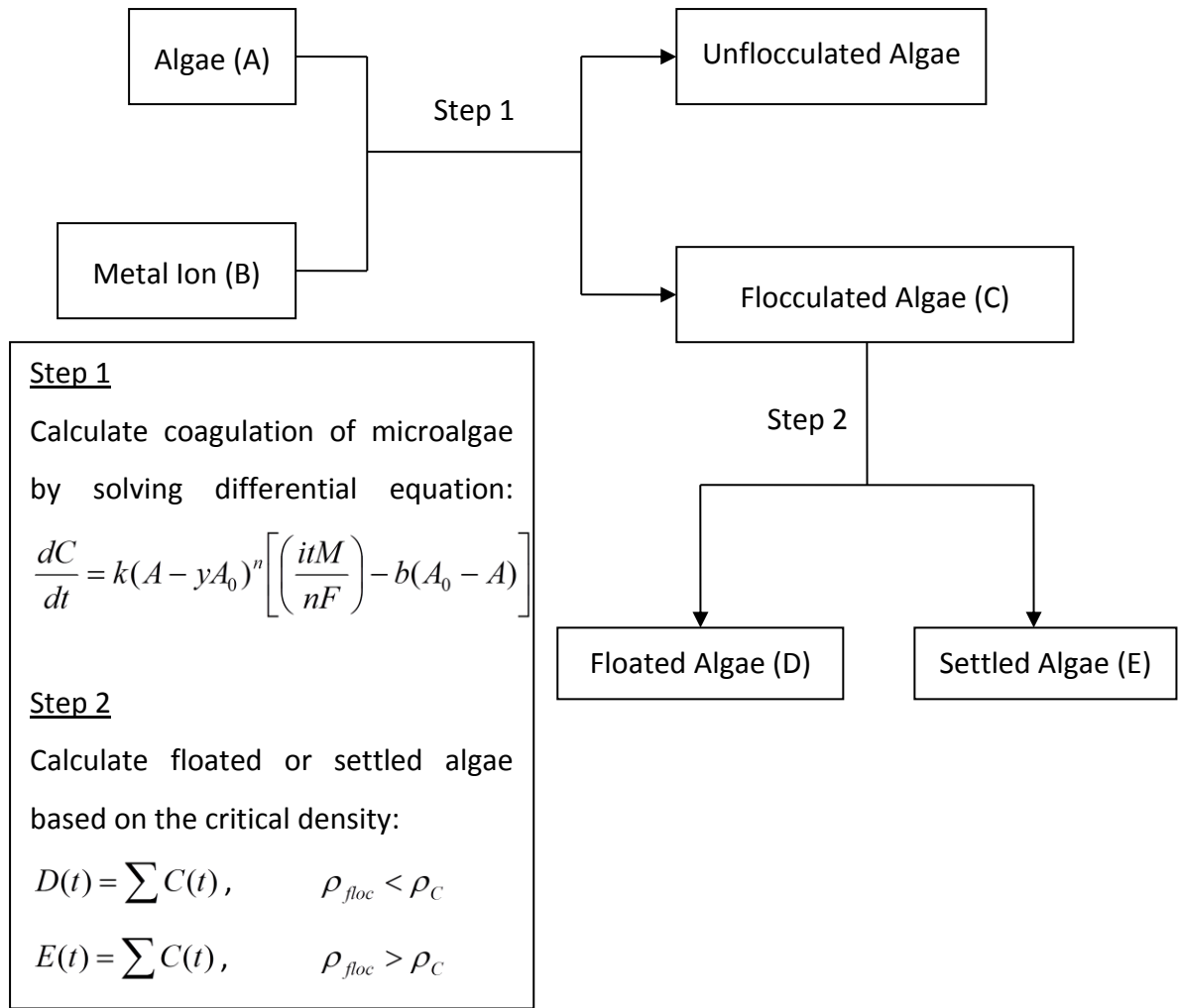
Figure 6. 3. Simplified flow sheet depicting how the model computes results.

Each step in the model had certain associated assumptions and simplifications, listed as follows:

Step 1 - Rate Based Reaction:

- The value of b was taken as the ratio of metal produced per gram of microalgae, obtained from experimental data (see section 6.4.1).
- The volume of the system is constant, assuming there is no chemical interaction between the hydrogen gas and the liquid in the cell, and negligible volume effect of gas build-up.
- The microalgae flocs produced (C) were assumed to be the same size, and thus the variation is taken into account with respect to the hydrogen content (in step 2).

128

- The reaction order of the equation with respect to the microalgae concentration was determined from comparing modelling results for different algae concentrations.

Step 2 - Equilibrium Based Reaction:

- The bubble size was assumed to be the same for all bubbles (see section 6.5.2).
- The number of bubbles per mass of algae was assumed to have a linear distribution.

To predict the recovery of microalgae for a given electrocoagulation run time, the model requires an input of the current applied to the system. Each of the systems studied (*Chlorococcum sp., Tetraselmis sp.*, stainless steel 430 anode, aluminium anode) has a different set of parameters, which are listed in table 6.1. The parameters were obtained by fitting the experimental data into the mathematical model and determining the values which gave the best model fit. The underlying mechanism of action for the model can be separated into two parts; the first part of the model relies on the ability of metal ions to coagulate the microalgae cells and the second part of the model is determined by the distribution of hydrogen bubbles to each of the microalgae flocs.

Table 6. 1. Parameters used for electrocoagulation model.

Microalgae System		k	b	Y	n
Chlorococcum sp.	Stainless steel	2	0.05	0.02	2
	Aluminium	80	0.01	0.10	2
Tetraselmis sp.	Stainless steel	2	0.05	0.02	2
	Aluminium	80	0.01	0.10	2

The first part of the model is a rate based reaction that describes the coagulation of microalgae due to charge neutralisation by the metal ion species. The value of k is the rate at which coagulation occurs and the value of n is the reaction the order with respect to the microalgae concentration. The second part of the model is not based

on the rate of separation, but simply the equilibrium between settling and flotation of the microalgae. Since the hydrogen bubbles only attach to the flocculated microalgae, it is assumed that any unflocculated microalgae will ultimately settle. The p value is directly related to the proportion of the total hydrogen bubbles used to float the flocs, which is based on the x_{21} value. It is a measure of the likelihood that a bubble will collide with the microalgae and become incorporated within the microalgae floc. The higher the value of p the greater the number of hydrogen bubbles attached to the flocs, and thus the lower the density of the floc, making it more likely to rise than settle.

6.3 Formation of Coagulants

During electrocoagulation, the reactive anode dissolves and produces coagulating ions in situ. The rate of dissolution depends on the applied current. The dissolution of iron ions from the stainless steel 430 anode and the aluminium anode was confirmed by performing a metals analysis test on the microalgae after electrocoagulation using plasma mass spectrometry performed by a certified independent laboratory. The weight of the anode before and after electrocoagulation experiments was measured and the anode metal was observed to dissolve linearly with time. Faraday's law was used to calculate the theoretical amount of metal ion dissolution. Faraday's law was also incorporated into the mathematical model to determine metal ion dissolution; hence the amount of metal ion produced from the model is equivalent to the theoretical amount.

Figures 6.4 and 6.5 show a comparison of the measured weight loss and the theoretical mass of iron dissolved from the stainless steel 430 anode for a valency of 2+ and 3+, for both microalgae species. From the figures, it is clear that the experimental mass of iron dissolved agrees in general with the production of ferrous ions (2+ charge). The experimental mass is slightly lower than the theoretical amount and this may be due to the fact that the theoretical curve is calculated based on iron alone dissolving into the system, where as the 430 stainless steel contains 28 % wt chromium. These results, along with the visual observation of ferrous ions green

precipitate shown in chapter 5, confirm that the iron species dissolving from the electrode are in the ferrous state, and is in keeping with work conducted by Vandamme, D. et al. (2011).

Figure 6.6 shows the potential - pH equilibrium diagram for the iron-water system. According to this diagram, at a pH range of 8 - 10, and at -0.44 V (which corresponds to the E^0 value of the ferrous iron dissolution equation), the existing iron species has a valency of 2+. This agrees with the experimental findings; however the result is intended for a simplified iron-water system unlike the more complex stainless steel - seawater system that is present in this research.

Ferrous iron dissolution equation:

$$Fe^{2+}_{(aq)} + 2e^- \rightarrow Fe_{(s)} \tag{6.16}$$
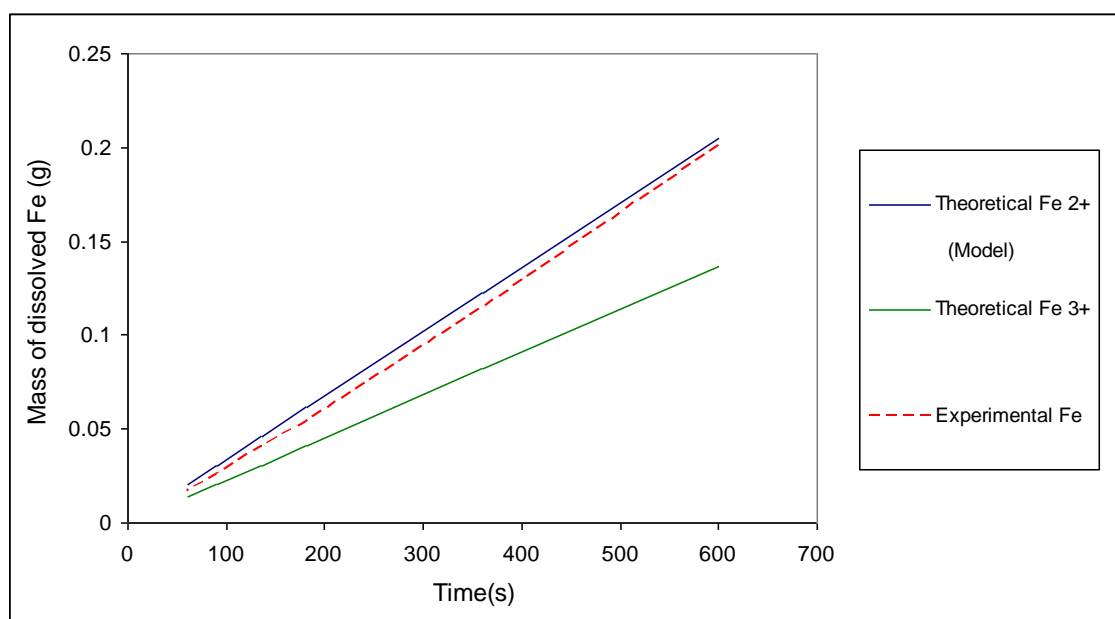
Figure 6. 4. The relationship between the amount of sacrificial anode dissolved (determined both theoretically and experimentally) with respect to time under an applied voltage of 5 V – for *Chlorococcum sp.,* with the stainless steel 430 anode.
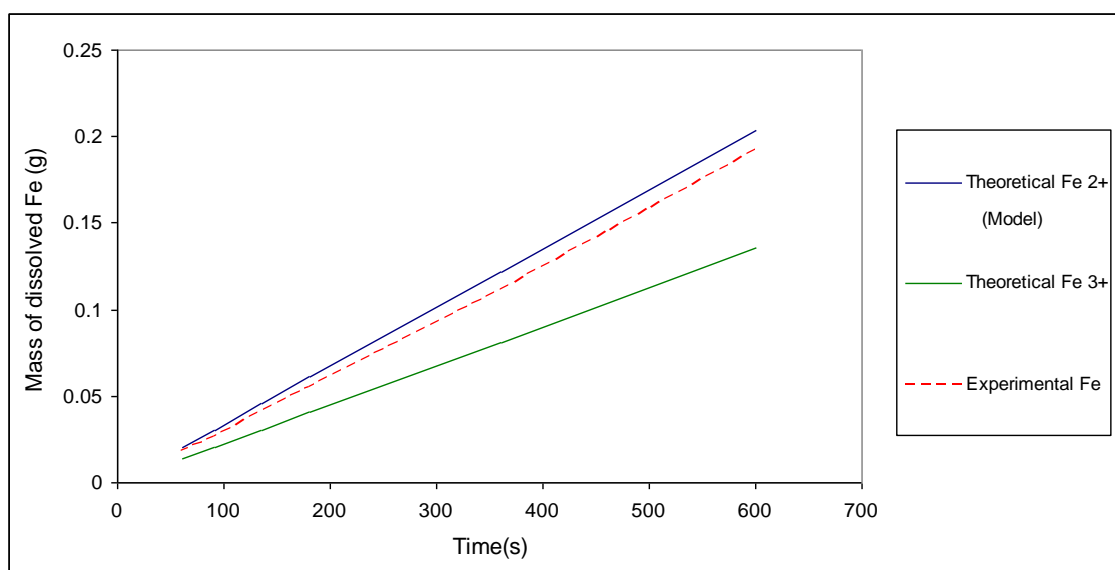
Figure 6. 5. The relationship between the amount of sacrificial anode dissolved (determined both theoretically and experimentally) with respect to time under an applied voltage of 5 V – for *Tetraselmis sp.*, with the stainless steel 430 anode.
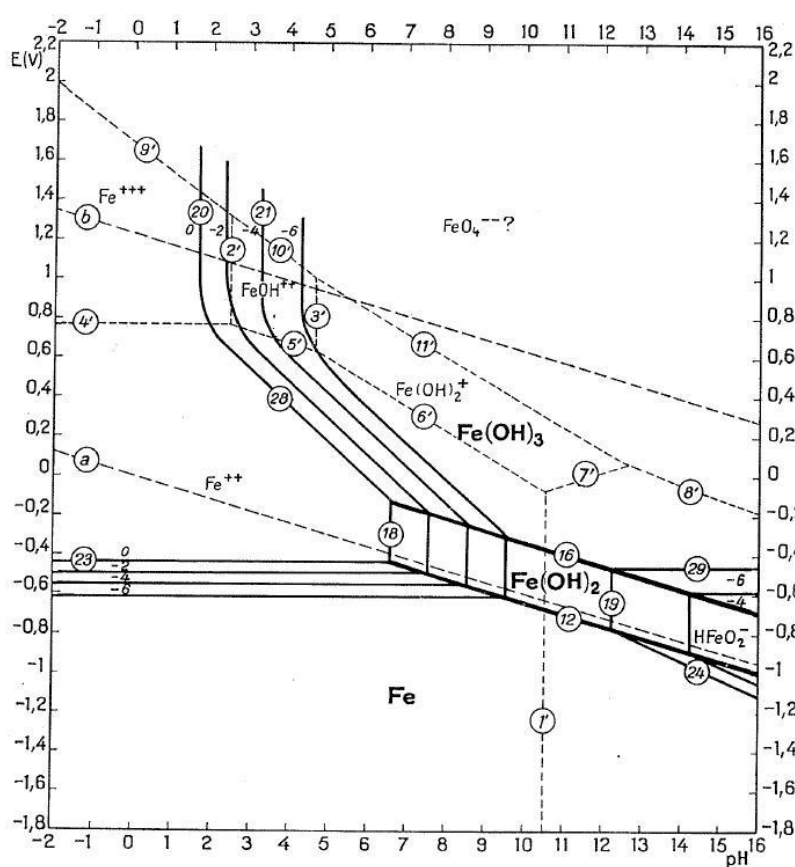
Figure 6. 6. Potential – pH equilibrium diagram for the system iron-water at 25 °C (Pourbaix, M. 1966).

The results obtained indicate that the efficiency of conversion of current into Fe^{2+} (referred to as the current efficiency) is slightly less than 100 %. The most likely explanation is due to the chromium that also dissolves into solution (please refer to Appendix A.3.2 for post electrocoagulation metals analysis results). The calculation of the anode dissolution includes 28 % chromium ($Cr \rightarrow Cr^{3+}$) and, assuming that the chromium phase dissolves at the same rate as iron. Figure 6.7 shows a parity plot of the theoretical and experimental mass of iron and chromium dissolved from the anode material. It can be seen from this figure that the amount of metal dissolved experimentally is close to the adjusted theoretical calculation for stainless 430.

Figure 6.7 shows that there is a small difference in the slope of the parity plot, which over-predicts the dissolution rate initially. A possible explanation is due to the presence of the passive film that coats the stainless steel 430 metal. It may take a certain amount of time after current is applied for the film layer to be removed, which may account for a lower mass to be dissolved.
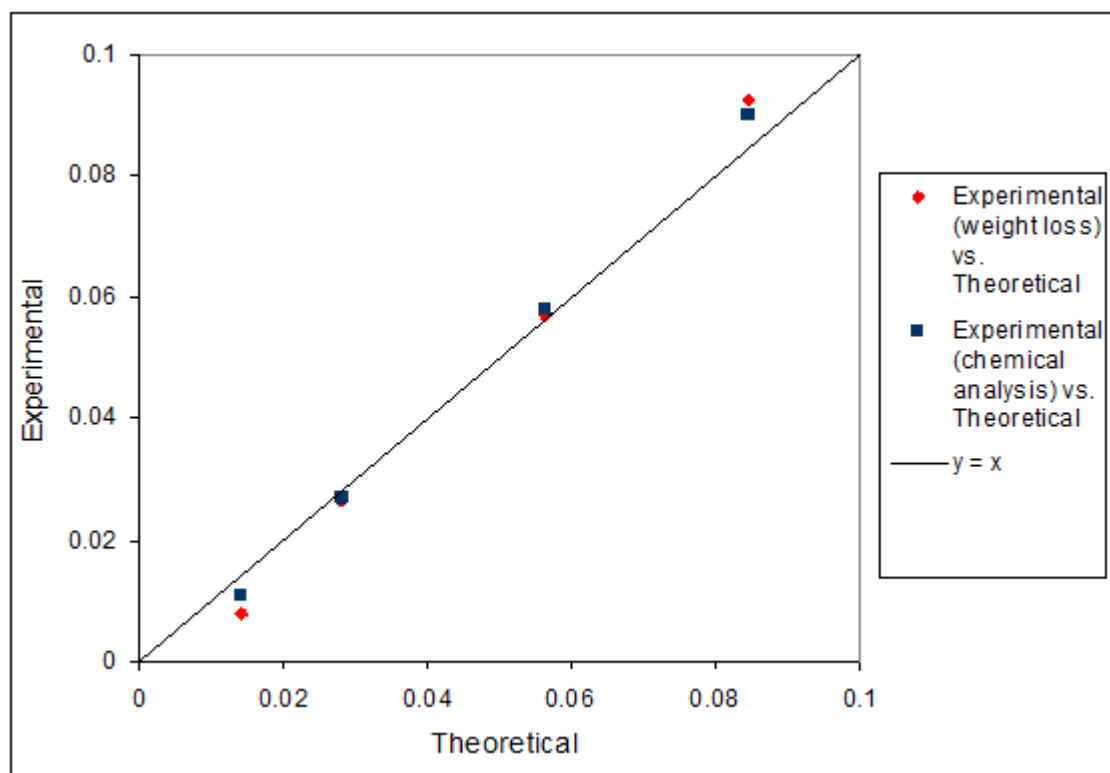
Figure 6. 7. Parity plot showing experimental and theoretical iron dissolution (adjusted for chromium content) at the anode for electrocoagulation under an applied voltage of 5 V, with *Chlorococcum sp*.

133

Figures 6.8 and 6.9 correspond to tests using the aluminium anode. These figures show a comparison of the measured change in anode mass and the mass of theoretical aluminium for a valency of 2+ and 3+ for each microalgal species. The results show that the experimental mass of dissolved aluminium lies between the theoretical values obtained for the 2+ and 3+ ion valencies. It has been reported that the mass of dissolved aluminium is higher than is expected due to the pitting corrosion at the anode by the chloride ions present in the medium (Lee, W. and Pyun, S. 1999; Mouedhen, G. et al. 2008). Therefore, it can be concluded that the aluminium that dissolves from the anode is in the Al^{3+} state, as observed also by Khemis, M. et al. (2006), Kobya, M. et al. (2006) and Mouedhen, G. et al. (2008). Figure 6.10 shows the passivation of aluminium oxide in water. According to this figure, at a pH range of 8-10 and at -1.67 V (which corresponds to the E° value of the Al^{3+} dissolution equation), dissolution of the aluminium solid will occur.

The valency of the aluminium species has significance because it will affect the amount of aluminium that is produced at the anode. As seen in figures 6.8 and 6.9, the actual amount of aluminium dissolution is approximately halfway between the dissolution for Al^{2+} and Al^{3+}. The mathematical model requires the valency of the metal ion as an input. A valency of 2.6 was used (instead of 3), which means that a more realistic amount of aluminium is dissolved at the anode, giving more accurate results.
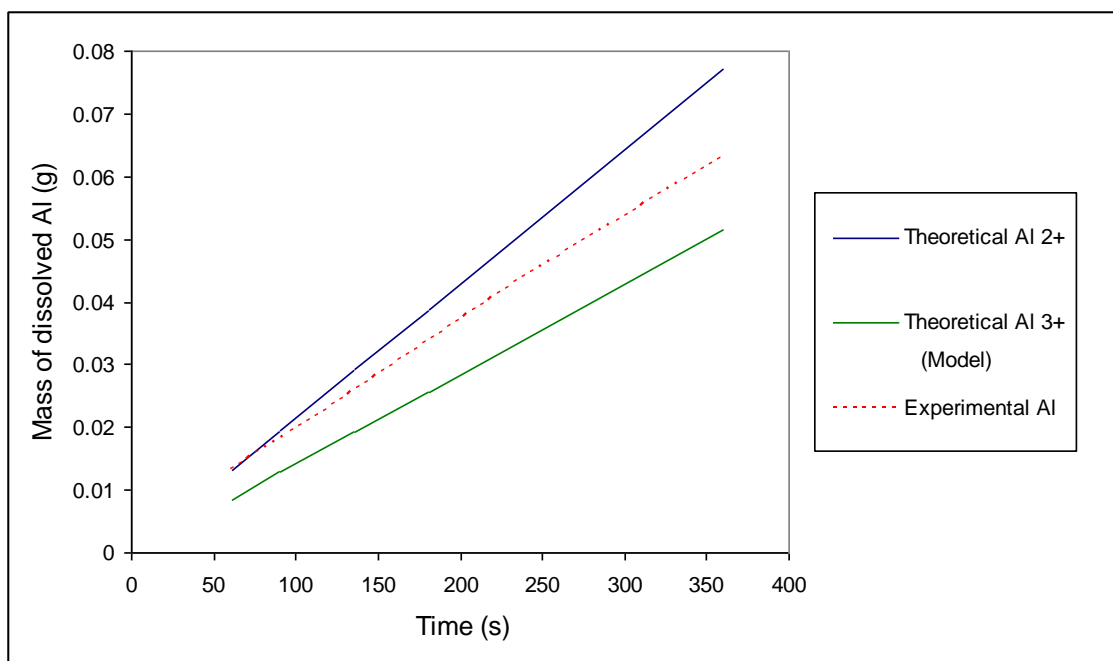
Figure 6. 8. The relationship between the amount of sacrificial anode dissolved (determined both theoretically and experimentally) with respect to time under an applied voltage of 5 V – for *Chlorococcum sp.*, with the aluminium anode.
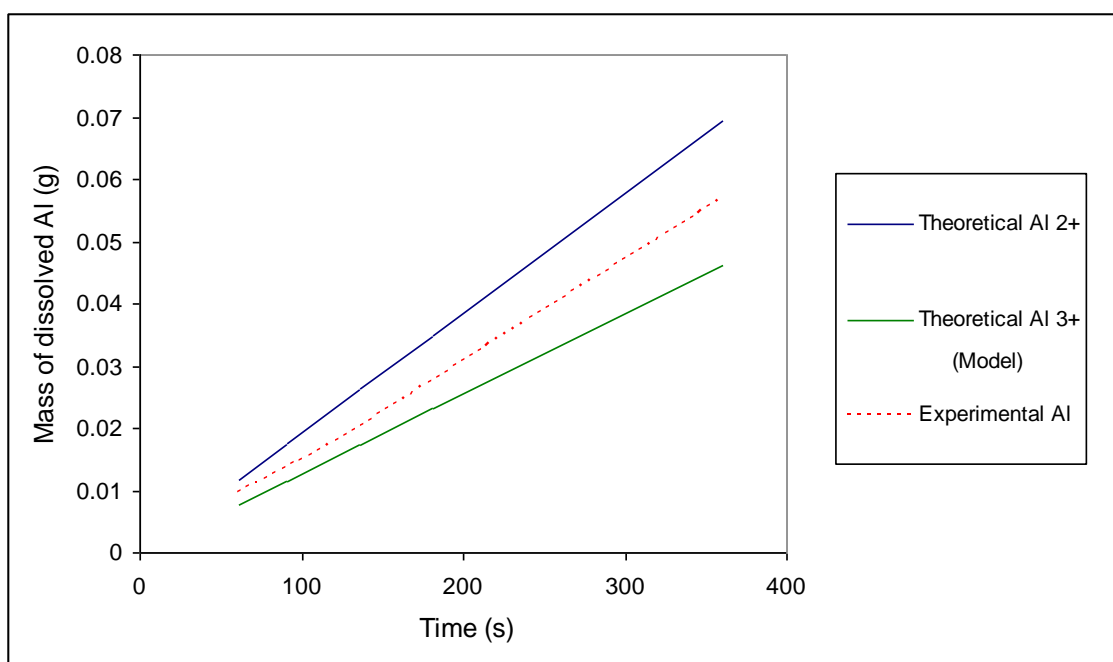
Figure 6. 9. The relationship between the amount of sacrificial anode dissolved (determined both theoretically and experimentally) with respect to time under an applied voltage of 5 V – for *Tetraselmis sp.*, with the aluminium anode.
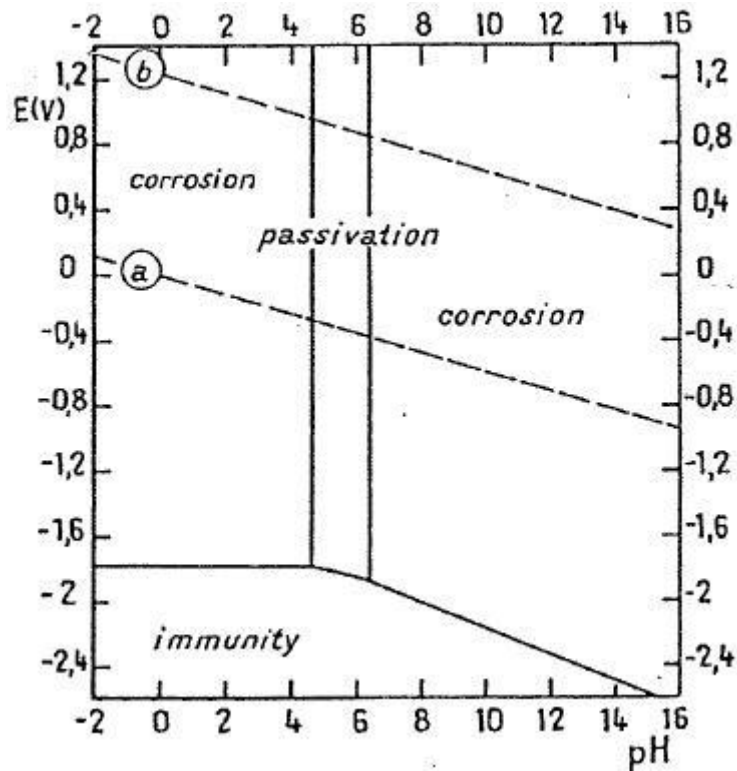
Figure 6. 10. Passivation of $Al_2O_3.H_2O$ (Pourbaix, M. 1966).

Figure 6.11 shows a parity plot of the theoretical and experimental mass of aluminium dissolved from the anode material based on a valency of 2.6+. It can be seen from this figure that the amount of aluminium that is produced experimentally (both from mass change during electrocoagulation and chemical analysis of aluminium) is equal to the theoretical value that can be calculated from Faraday's law with a valency of 2.6+.
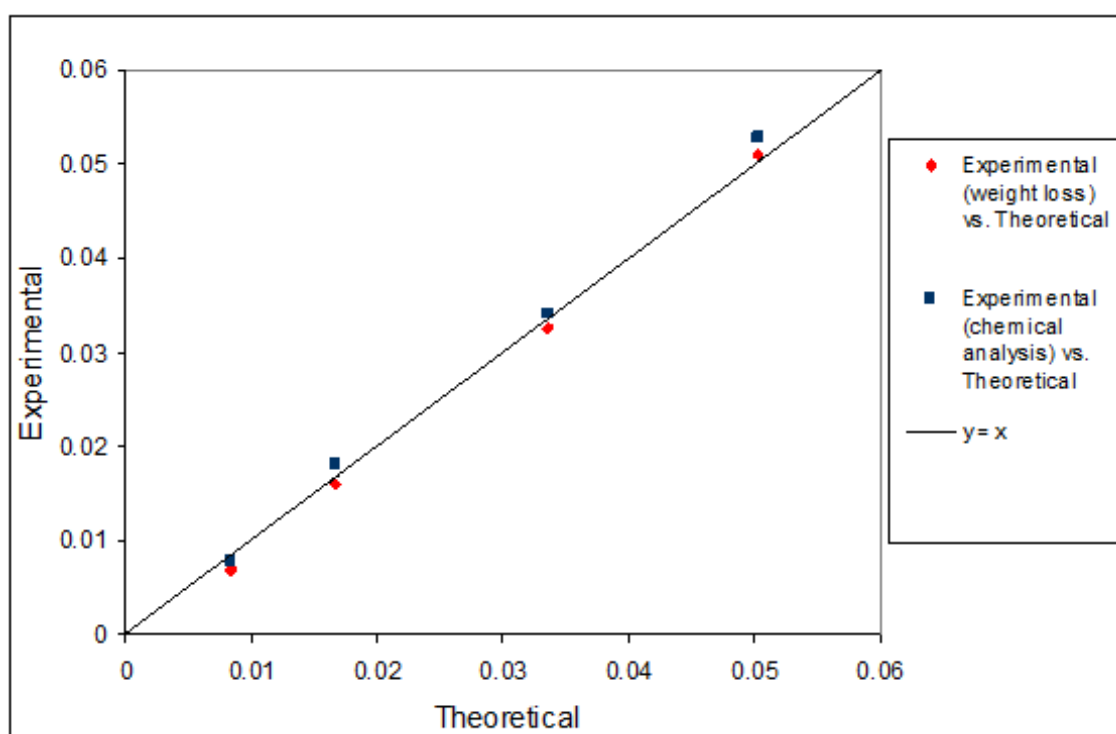
Figure 6. 11. Parity plot showing experimental and theoretical aluminium dissolution at the anode (with theoretical aluminium species having a 2.6+ valency), for electrocoagulation under an applied voltage of 5 V, with *Chlorococcum sp*.

6.4 Charge Neutralisation and Coagulation

6.4.1 Charge Neutralisation and Coagulation Experimental Results

Neutralisation of the negatively charged microalgae must take place in order for coagulation to occur. The neutralisation of the microalgae was monitored by performing zeta potential measurements of the microalgae media after the electrocoagulation process. The zeta potential is a measurement that describes the electrokinetic potential of a colloidal system. The value of the zeta potential is significant, because it can be directly related to the stability of the colloidal system. When the zeta potential is low, attractive forces are able to overcome the repulsive forces and the system may flocculate (Zetasizer Nano series technical notes MRK654-01, Malvern Instruments). Freshly harvested microalgae are negatively charged and have zeta potential values of -8.67 mV and -10.47 mV for *Chlorococcum sp.* and *Tetraselmis sp.*, respectively. These zeta potential values agree with a study

conducted by Henderson, R. et al. (2008) who achieved successful microalgal recovery with flotation at initial zeta potential values ranging from 0 to -15 mV.

Figures 6.12 to 6.14 show the change in zeta potential of the microalgae after electrocoagulation for varying electrolysis times with the stainless steel 430 anode at fixed voltages of 3, 5 and 10 V, for *Chlorococcum sp.* and *Tetraselmis sp.* Figure 6.15 shows the change in zeta potential of *Chlorococcum sp.* after electrocoagulation for varying run times at fixed voltages of 3 and 5 V with the aluminium anode. The results show that at lower electrolysis times, the zeta potential of the microalgae does not deviate significantly from the starting value. The longer the current is applied, the more electropositive the microalgae species become. This means that the system is less stable and attractive forces will dominate leading to particle agglomeration and increased removal efficiency. It is noted that the removal efficiencies and zeta potential measurements with increasing run time for both microalgal species show similar patterns. This can be explained by the similarities in size and charge of both species. It also shows that since the two species have different motility, the motility of microalgae does not have a significant effect on separation efficiency.

For electrocoagulation with both the stainless steel 430 and aluminium anodes, the zeta potential can be seen to plateau to a constant value at longer run times. This point corresponds to the point where the microalgae is fully neutralised and can no longer adsorb any more metal ions. This saturation point indicates that only a certain amount of metal is required to neutralise the negative charge of the microalgae. If more than this amount is dissolved, it is not effective and results in an excess of metal ions present in the system. This result agrees with the alum flocculation results presented in chapter 4. Flocculation with increasing doses of alum resulted in recovery values that increased with dosage to a particular point and then plateaued.
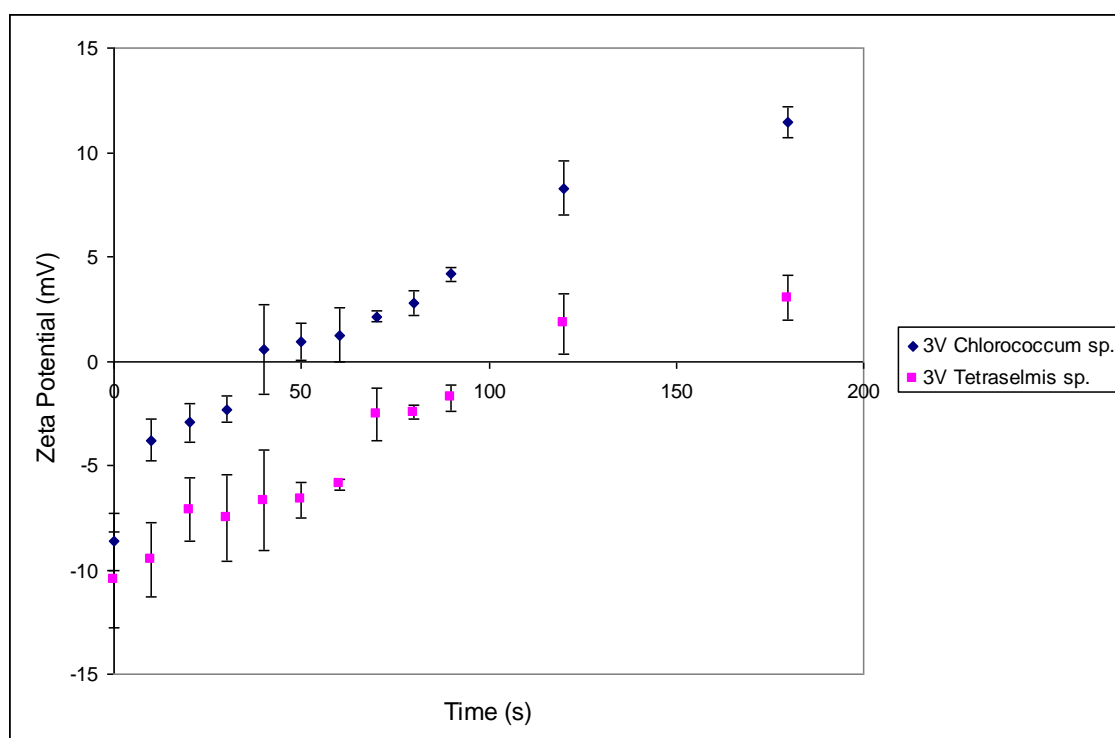
Figure 6. 12. Zeta potential change during electrocoagulation at a fixed voltage of 3 V for
Chlorococcum sp. and *Tetraselmis sp.*, with the stainless steel 430 anode.
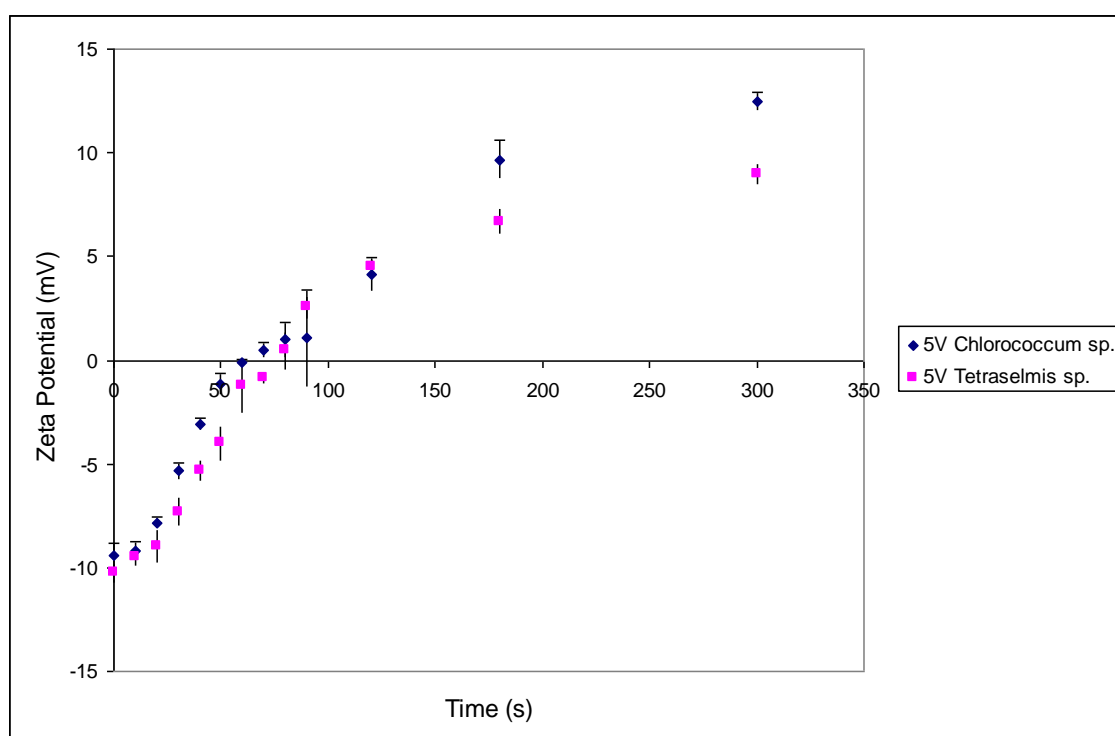
Figure 6. 13. Zeta potential change during electrocoagulation at a fixed voltage of 5 V for
Chlorococcum sp. and *Tetraselmis sp.*, with the stainless steel 430 anode.
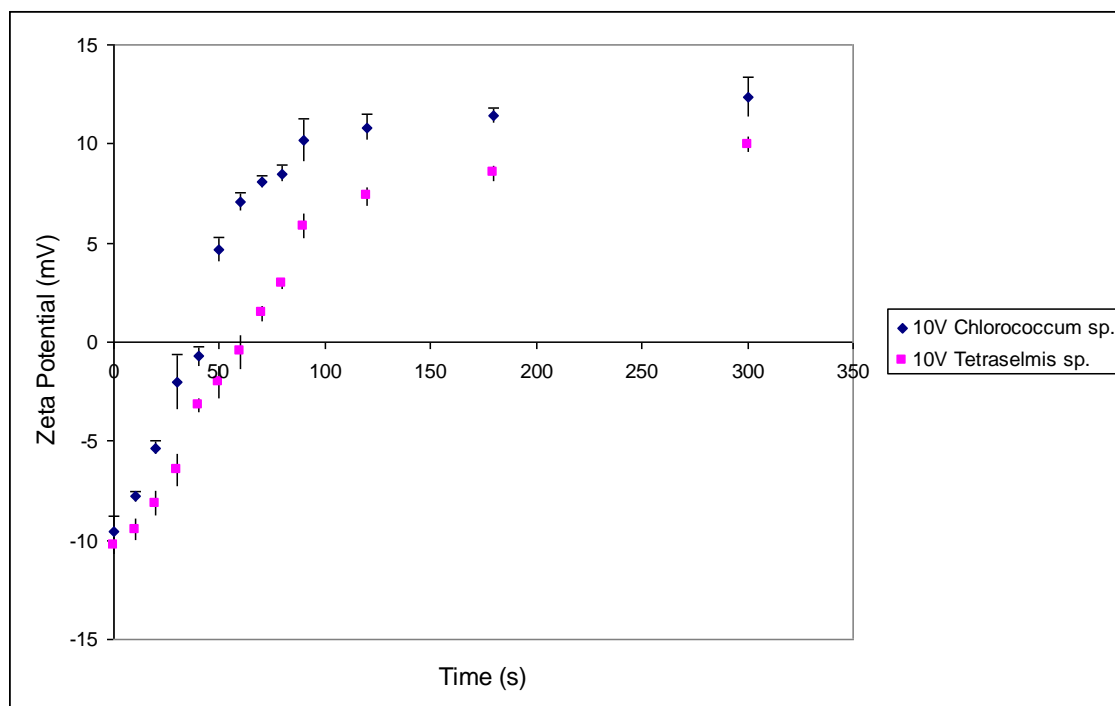
Figure 6. 14. Zeta potential change during electrocoagulation at a fixed voltage of 10 V for *Chlorococcum sp.* and *Tetraselmis sp.*, with the stainless steel 430 anode.
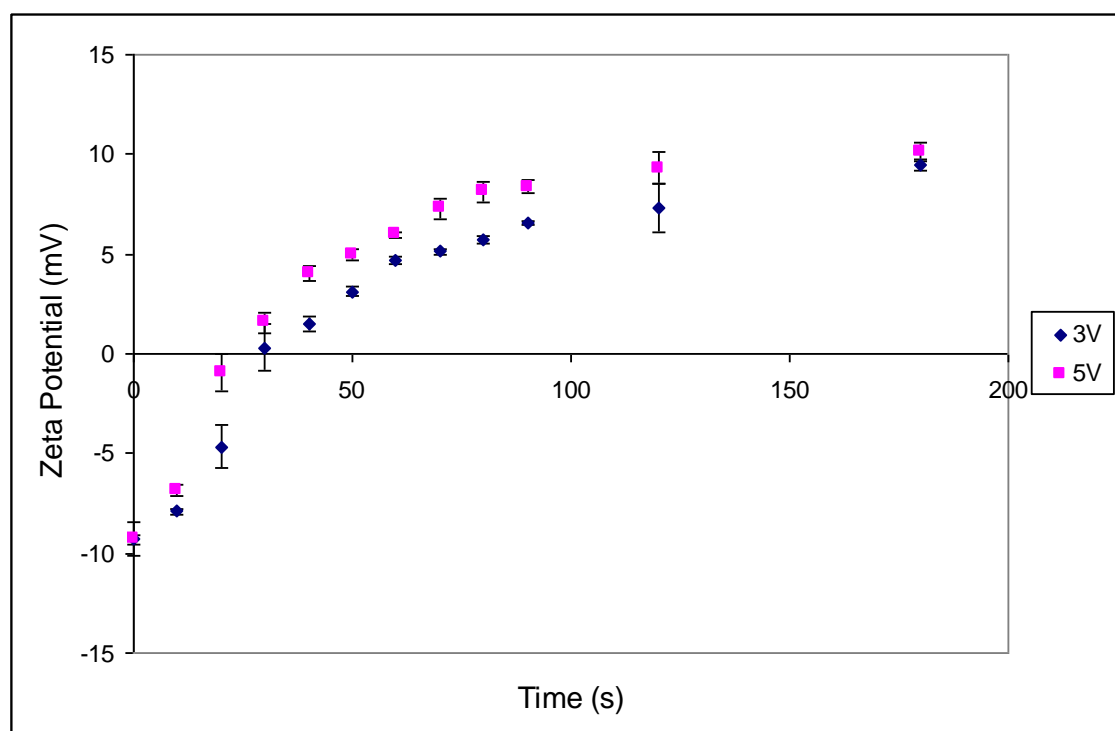
Figure 6. 15. Zeta potential change during electrocoagulation at a fixed voltage of 3 V and 5 V for *Tetraselmis sp.*, with the aluminium anode.

Once the charge of the microalgae cells have been neutralised by the dissolved anode ion species, coagulation can occur. The coagulation of microalgae will be dependent on the ability of the neutralised particles to collide with each other to form flocs. The number of collisions will be directly related to the amount of mixing occurring in the system.

Another way to analyse the coagulation process is to plot the zeta potential measured after electrocoagulation as a function of the mass of metal dissolved. Figures 6.16 to 6.18 show an increase in electropositive zeta potential of the microalgae with increasing metal ions dissolved into the system. The zeta potential measurements are seen to plateau to a constant value once the saturation point has been reached. This is not seen for the 3 and 5 V results with the stainless steel 430 anode because the zeta potential data is only measured up to 180 s. Since the concentration of microalgae remains the same for each experiment, a given mass of metal dissolved into the system is expected to cause a constant change in the zeta potential independent of the rate of dissolution. This observation was observed in the aluminium anode electrocoagulation results, but not for the stainless steel 430 anode. The stainless steel 430 results indicate that a slower dissolution rate (i.e. when the voltage is low) may use the dissolved cations more efficiently.
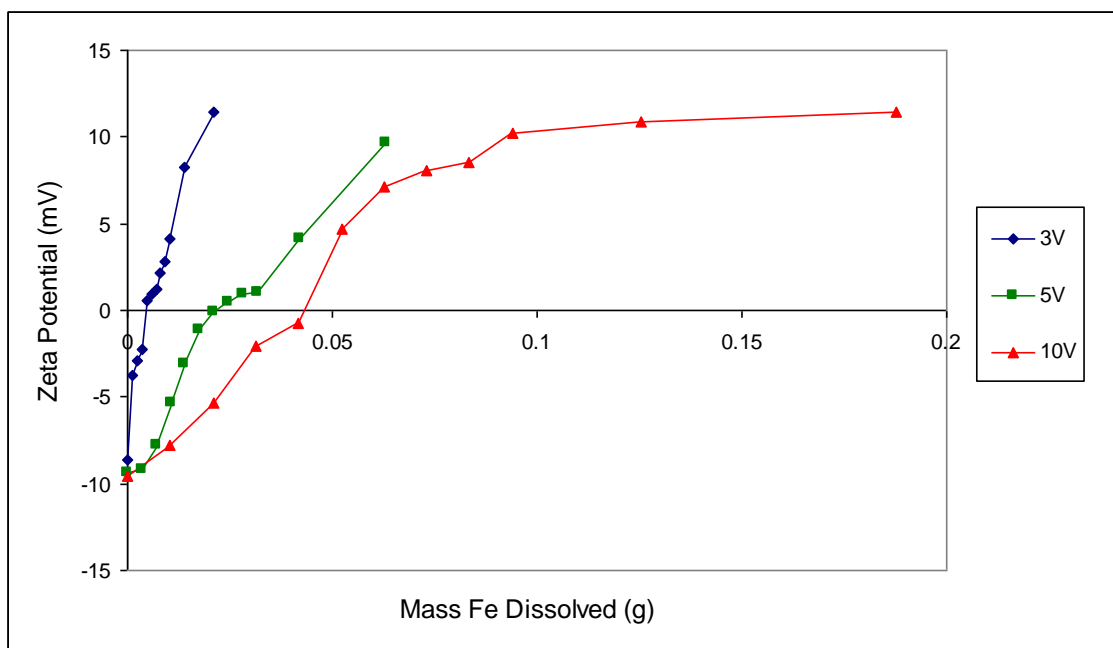
Figure 6. 16. Zeta potential versus iron dissolved for electrocoagulation of *Chlorococcum sp.* with the stainless steel 430 anode.
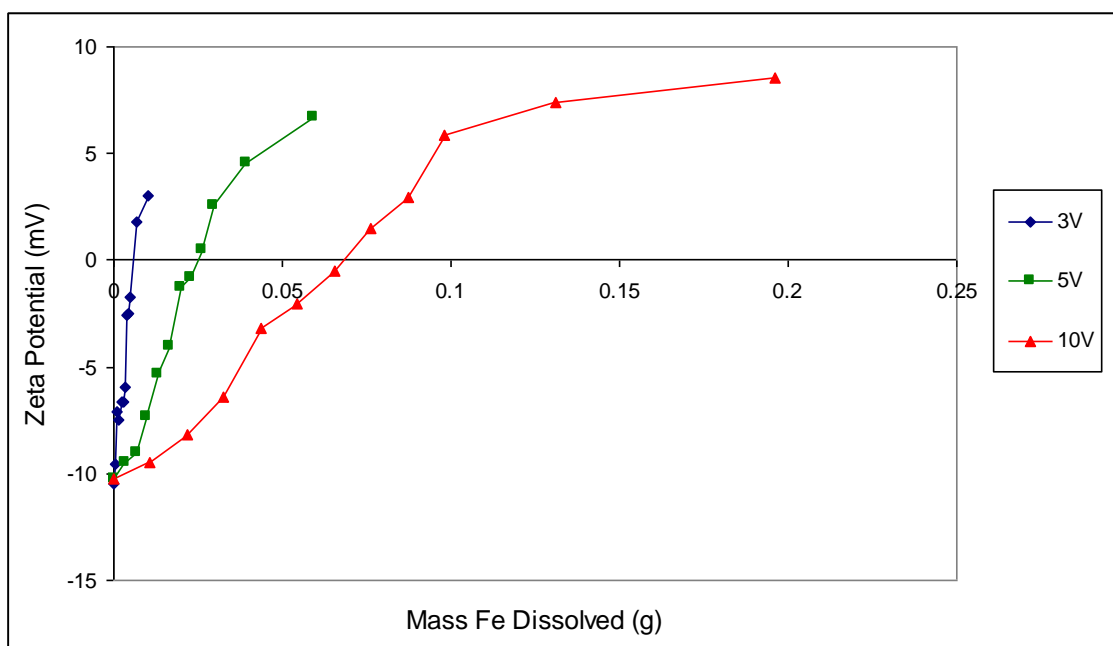
Figure 6. 17. Zeta potential versus iron dissolved for electrocoagulation of *Tetraselmis sp.* with the stainless steel 430 anode.
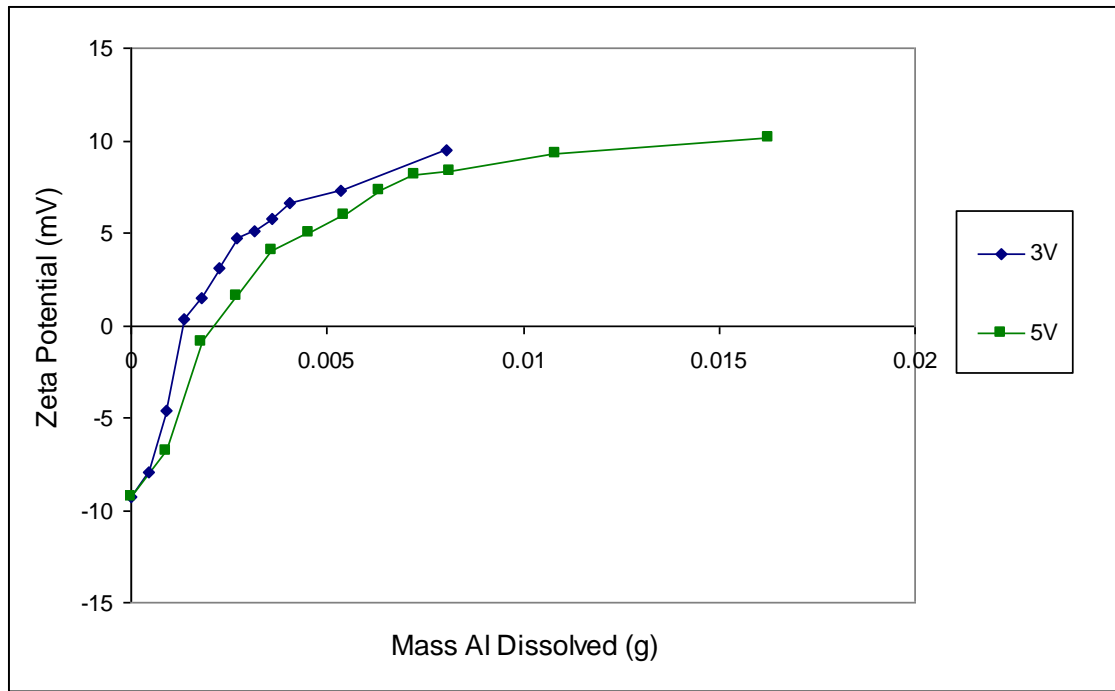
Figure 6. 18. Zeta potential versus aluminium dissolved for electrocoagulation of *Chlorococcum sp.* with the aluminium anode.

A mass balance on the dissolving anode metal was performed on the system. Performing a mass balance on the system enabled the determination of the percentage of total metal ion species required for coagulation to occur. From the law of conservation of mass, the total amount of metal dissolving from the anode material must equal that in the system, as described by the following equation (assuming no metal species settles at the bottom of the batch cell):

$$m_{total\ dissolved\ metal} = m_{dissolved\ metal\ in\ floated\ layer} + m_{dissolved\ metal\ in\ solution} \quad (6.17)$$

Where m refers to the mass of metal (g).

The results from the mass balance indicate the percentage of metal ion used for coagulation and how much metal is needed per gram of microalgae recovered. It was observed that with increasing time, the percentage of metal used to coagulate the microalgae increased. This increase may be due to equilibrium between the microalgae surface and the solution. The more cations forced into solution, the more they are adsorbed onto a fixed amount of microalgae, until saturation occurs.

143

Table 6.2 shows the mass balance results for iron in the electrocoagulation system. These results correspond well with the recovery data presented in chapter 5 which showed that up to a run time of 360 s at 5 V, the recovery of microalgae continued to increase. The mass of microalgae in the floated layer also agrees with these results, showing a continuing increase in microalgae mass with time.

Table 6. 2. Mass balance of iron in the system at 5 V, with *Chlorococcum sp*.

Time (s)	Fe Dissolved from Anode Experimentally (g)	Mass Fe in Floated Layer (g)	Mass Fe in Supernatant (g)	Total Mass Fe in System (g)	% Fe Used in Coagulation	Mass Algae in Floated Layer (g)	Mass Fe/ Mass Algae in Floated Layer
60	0.01	0.00	0.01	0.01	0.00	0.01	0.00
120	0.03	0.00	0.03	0.03	3.63	0.03	0.03
240	0.06	0.01	0.05	0.06	17.4	0.09	0.11
360	0.09	0.03	0.06	0.09	36.9	0.15	0.23

Table 6.3 shows the mass balance results for aluminium in the electrocoagulation system. It can be seen from this table that the percentage of aluminium used for coagulation increases with time and then plateaus to a constant value. This agrees with the recovery data presented in chapter 5 and the zeta potential data presented earlier, illustrating that once a saturation point is reached, there can be no more adsorption of metal ions onto the microalgae surface; hence further coagulation can not occur. The saturation point is observed between 120 and 240 s. For that particular voltage and concentration of microalgae, there is no need to electrocoagulate beyond the saturation point because there is more than enough aluminium dissolved in the system.

Table 6. 3. Mass balance of aluminium in the system at 5 V, with *Chlorococcum sp.*

Time (s)	Al Dissolved from Anode Experimentally (g)	Mass Al in Floated Layer (g)	Mass Al in Supernatant (g)	Total Mass Al in System (g)	% Al Used in Coagulation	Mass Algae in Floated Layer (g)	Mass Al/ Mass Algae in Floated Layer
60	0.01	0.00	0.01	0.01	35.1	0.11	0.03
120	0.02	0.01	0.01	0.02	57.0	0.14	0.07
240	0.03	0.02	0.01	0.03	66.3	0.15	0.15
360	0.05	0.04	0.02	0.05	65.3	0.15	0.24

6.4.2 Stirring Effects on Coagulation

The dissolved ions from the anode must be adsorbed onto the surface of the microalgae for charge neutralisation and coagualtion to occur. Just as with alum flocculation, the surface reaction is facilitated by mixing within the electrocoagulation cell. Mass transfer can occur due to the migration of ions conducting the electric current, free convection generated by buoyancy driven flow, and forced convection driven by bubbles or mechanical stirring.

Zeta potential measurements were taken after electrocoagulation in a half cell set up where a permeable membrane was added in order to separate the anode and cathode sides of the electrocoagulation cell (please refer to Appendix A.3.4 for details). The permeable barrier allowed for the passage of metal ions, but not microalgae or gas bubbles. Figure 6.19 shows the zeta potential measurements after electrocoagulation with stainless steel 430 anode without mixing, and mixing at a speed of 400 rpm. It can be seen that without mixing, the zeta potential on the cathode side becomes more electropositive with time where as the zeta potential on the anode side remains constant. The expected result when electrocoagulation is performed on a microalgae system is that the zeta potential becomes more electropositive with time. This observation was made for the microalgae on the

cathode side of the half cell. The hydrogen gas which is produced at the cathode creates adequate mixing and mass transfer of ferrous ions to the microalgae cells, allowing coagulation to occur. It can be seen that when mixing is applied to the anode side of the electrocoagulation cell, the zeta potential measurements follow the expected trend. This observation can be explained by the increase in interactive mass transfer of microalgae with mixing. When there is no mixing on the anode side, the mass transfer of ferrous ions to the microalgae is so low that neutralisation of the microalgae by the iron species dissolved from the anode does not occur. However, when the anode side is mixed during electrocoagulation, there is sufficient agitation to aid in the mass transfer of the microalgae, which results in collisions between the iron species and microalgae cells, leading to effective ion attachment and neutralisation.

It was also observed that for the stainless steel anode set up, the microalgae only floated to the surface on the cathode side. This is because the hydrogen bubbles could not pass through the membrane and therefore could only attach to microalgae flocs on the cathode side, demonstrating that the recovery of microalgae by flotation relies on hydrogen bubble collisions with the flocculated microalgae.
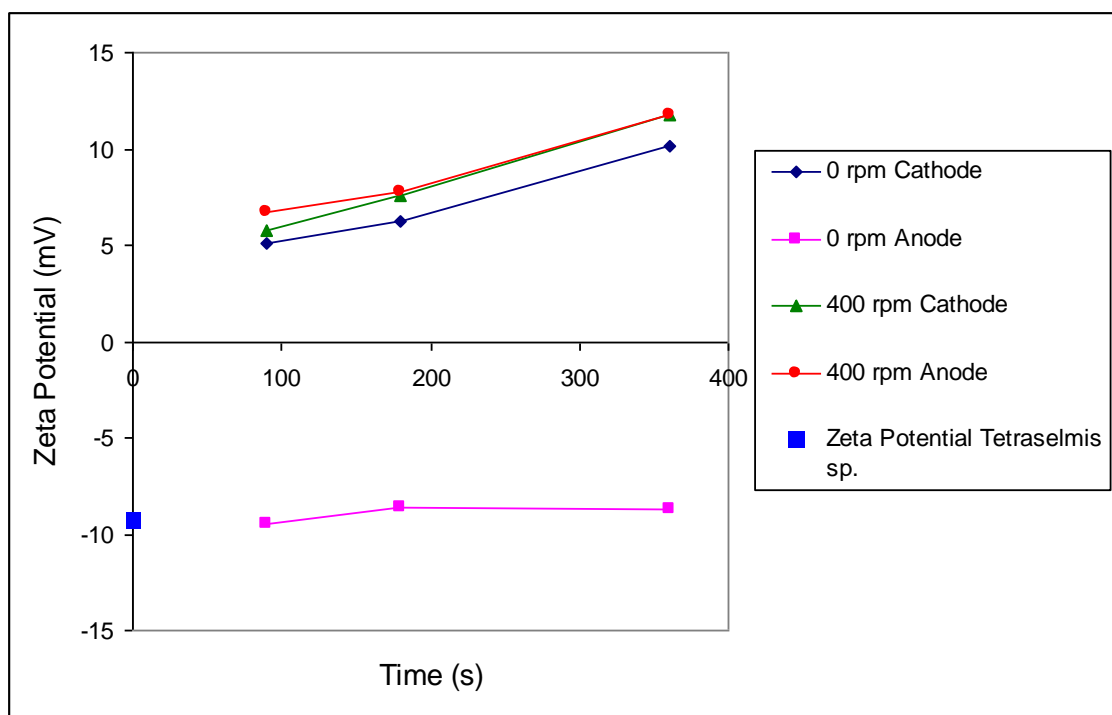
Figure 6. 19. Zeta potential measurements at the anode and cathode after electrocoagulation with a separating membrane, at 5V for *Tetraselmis sp.*, with the stainless steel 430 anode.

Half cell experiments were also conducted for electrocoagulation with the aluminium anode. The results in figure 6.20 show that the zeta potential on both sides becomes more electropositive with time without additional mixing in the system. The difference in results from the stainless steel 430 anode can be attributed to the evolution of oxygen at the aluminium anode which provides adequate stirring to aid in metal binding onto the microalgae surface. The production of oxygen is constant and not affected by the voltage. This is known because the dissolution of aluminium is linear with time as observed from the experimental results, and would not be seen if the oxygen reaction was competing with the aluminium production reaction.
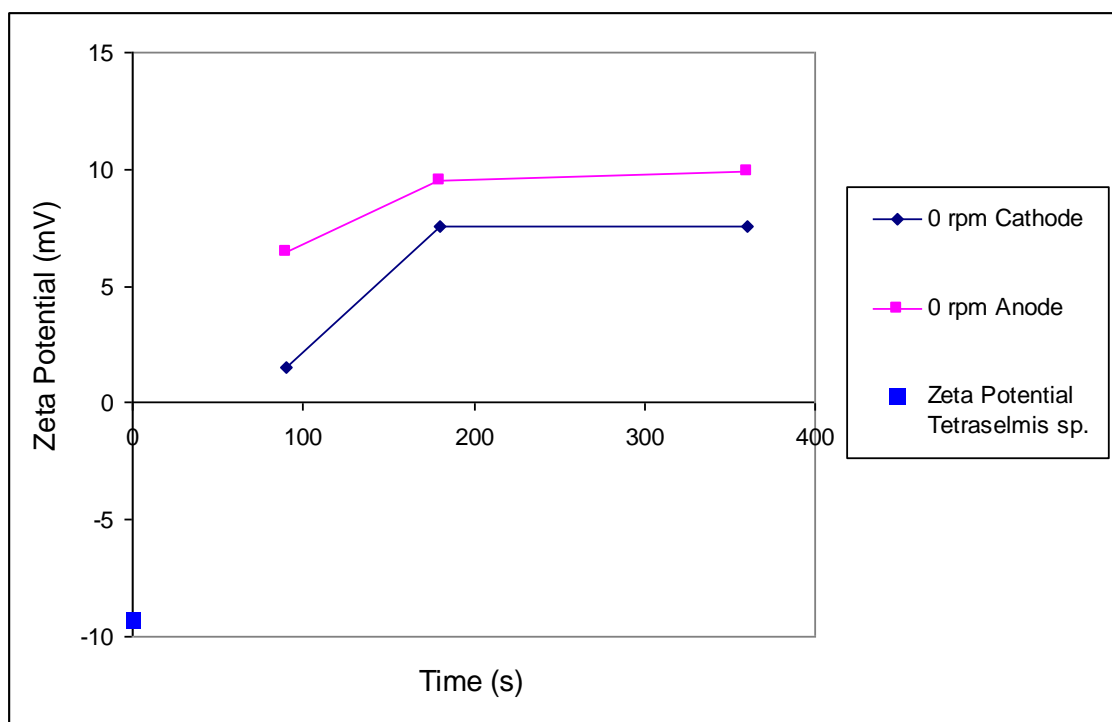
Figure 6. 20. Zeta potential measurements from the anode and cathode after electrocoagulation with a separating membrane (half cell), at 5V for *Tetraselmis sp.*, with the aluminium anode.

The membrane separation is also used to demonstrate that the microalgae do not have to come into contact with the anode for charge neutralisation and coagulation to occur, since the zeta potential increases on the cathode side. This proves that coagulation occurs in bulk solution and not at the cathode surface or in the vicinity of the electrode surface.

A lag in microalgae recovery is observed at short run times for electrocoagulation at low voltages (2 V for the aluminium anode and 3 V for the stainless steel 430 anode). Figure 6.21 shows the percentage recovery of microalgae for electrocoagulation at 3 V with and without additional mixing introduced into the system. The figure shows that with additional stirring, the recovery of microalgae is significantly improved and this lag in recovery does not occur. It should be noted that the microalgae used for this particular experiment was very dilute (0.1 g/L). Therefore, it was possible to achieve higher recoveries at lower run times as the amount of metal dissolved and hydrogen introduced into the system remained the same while the amount of microalgae to be coagulated was significantly less.

148

From the previously presented results on the changing zeta potential of the microalgae with time, it can be seen that at low voltage and short run times there is still adequate amounts of metal binding to the microalgae, illustrated by the increase in the electropositive charge of the microalgae. These conditions give no microalgae flotation, meaning coagulation does occur but with no bubble attachment to the flocs. From the predicted amount of microalgae coagulation with time (section 6.6.2), it can be seen that even at low times, a small percentage of microalgae will coagulate. Therefore, it can be concluded that the recovery lag is due to the need to build up enough bubble/floc collisions in order to achieve flotation.
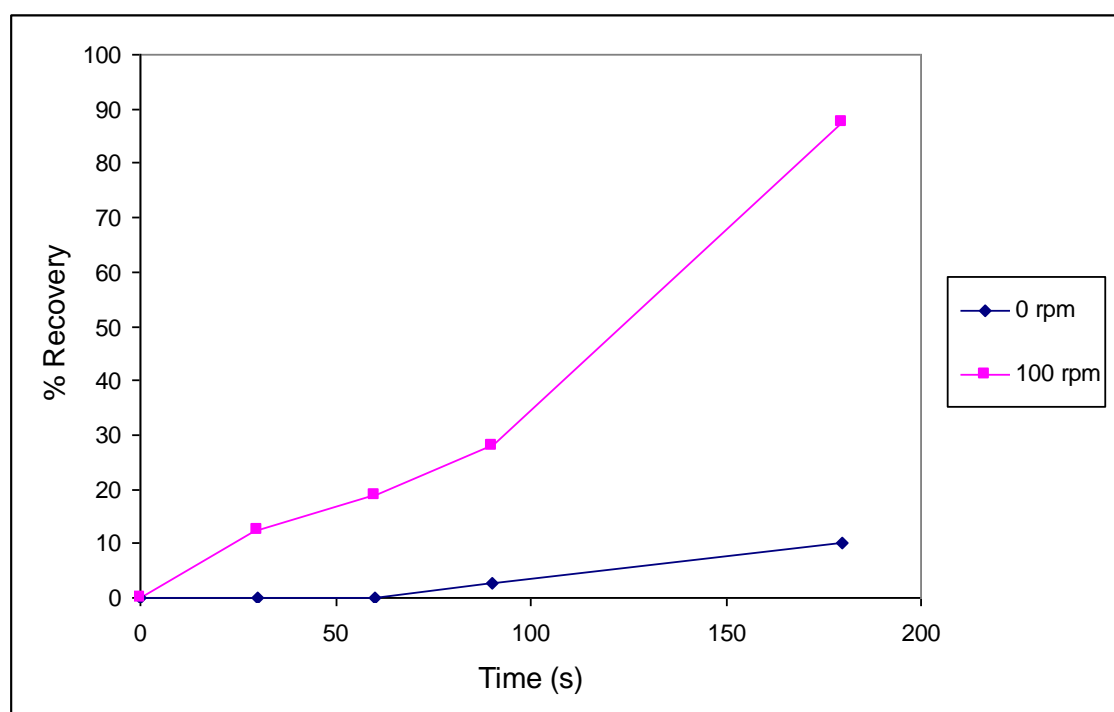
Figure 6. 21. Percentage recovery of *Chlorococcum sp.* at 3 V with and without stirring, using the stainless steel 430 anode.

The important finding to note from the stirring experimental results is that stirring has a significant effect on microalgae mass transfer and recovery. Increased mixing in the system will increase the distribution of particles within the system and hence increase the probability of collisions between the particles. This causes an increased rate of adsorption of metal to microalgae and an increased rate of attachment of hydrogen bubbles to flocs.

6.5 Flotation and Recovery of Microalgae

6.5.1 Flotation of Microalgae Flocs from Experimental Work

Microalgae flotation due to hydrogen bubble attachment was documented using a high speed camera. Hydrogen bubbles produced from the cathode attach to the microalgae flocs and carry them to the surface of the system. Figure 6.22 and 6.23 show the interaction between hydrogen bubbles and microalgae flocs at different time intervals after the application of current had been turned off in the system. It can be seen from the figure that a number of hydrogen bubbles (seen as the very small dark circles) are required to attach to the much larger microalgae flocs (grey shapes) in order to carry them to the surface. It can be seen from the time difference between the images that the hydrogen bubble - microalgae floc aggregates rise quickly. These images confirm the flotation of the bubble floc complex to the surface by hydrogen bubbles.
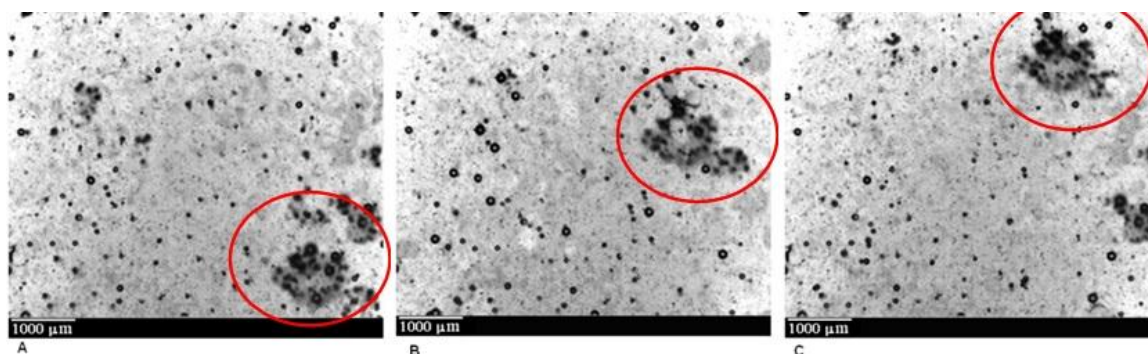
Figure 6. 22. Hydrogen bubble – *Chlorococcum sp*. floc interaction at different times A) 0 s, B) 0.4 s and C) 0.8 s after the current was turned off, with the stainless steel 430 anode. (Main bubble – microalgae complexes are circled in each figure).
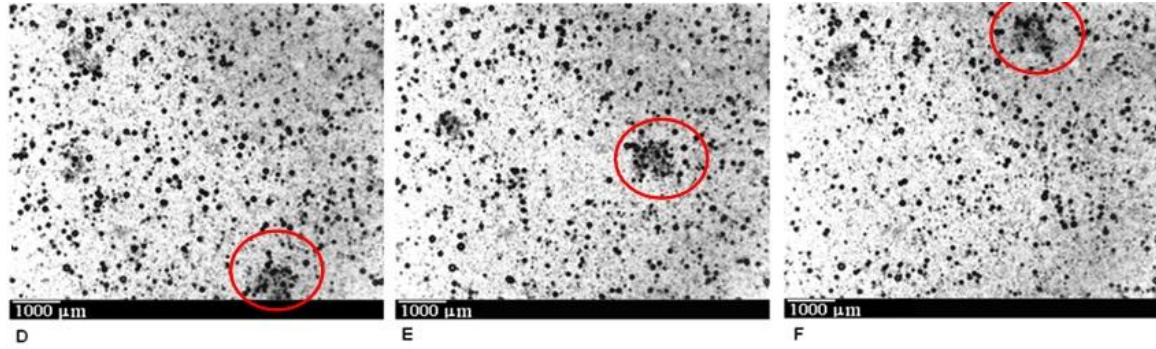
Figure 6. 23. Hydrogen bubble – *Tetraselmis sp.* floc interaction at different times D) 0.4 s, E) 0.7 s and F) 0.8 s after the current was turned off, with the stainless steel 430 anode. (Main bubble – microalgae complexes are circled in each figure).

6.5.2 Analysis of Hydrogen in the System

The images and data obtained from the high speed camera along with analysis with Image J software enabled the analysis of hydrogen bubbles produced at the cathode (please refer to Appendix A.2.8 for calculations). Figures 6.24 and 6.25 show the percentage of microalgae recovery versus the percentage of floated microalgae, taken as the volume of microalgae that floated as a percentage of the total batch volume. The figures show a positive correlation between recovery and the volume of floc. Figures 6.26 and 6.27 show the recovery of microalgae versus percentage of bubbles used for flotation. The percentage of bubbles used for flotation was calculated as a percentage of the total amount of bubbles used for flotation for electrocoagulation conditions that achieved the maximum recovery.

$$\% \ Bubbles \ for \ Flotation = \frac{No. \ Floc \ Bubbles}{Maximum \ No. \ Floc \ Bubbles} \times 100 \ \% \qquad (6.18)$$

It can be seen from these figures that the recovery of microalgae increases with the amount of hydrogen bubbles in the flocculated microalgae. These results indicate that with increased recovery comes an increase in the volume of flocculated microalgae, which corresponds to a greater number of hydrogen bubbles used for flotation.
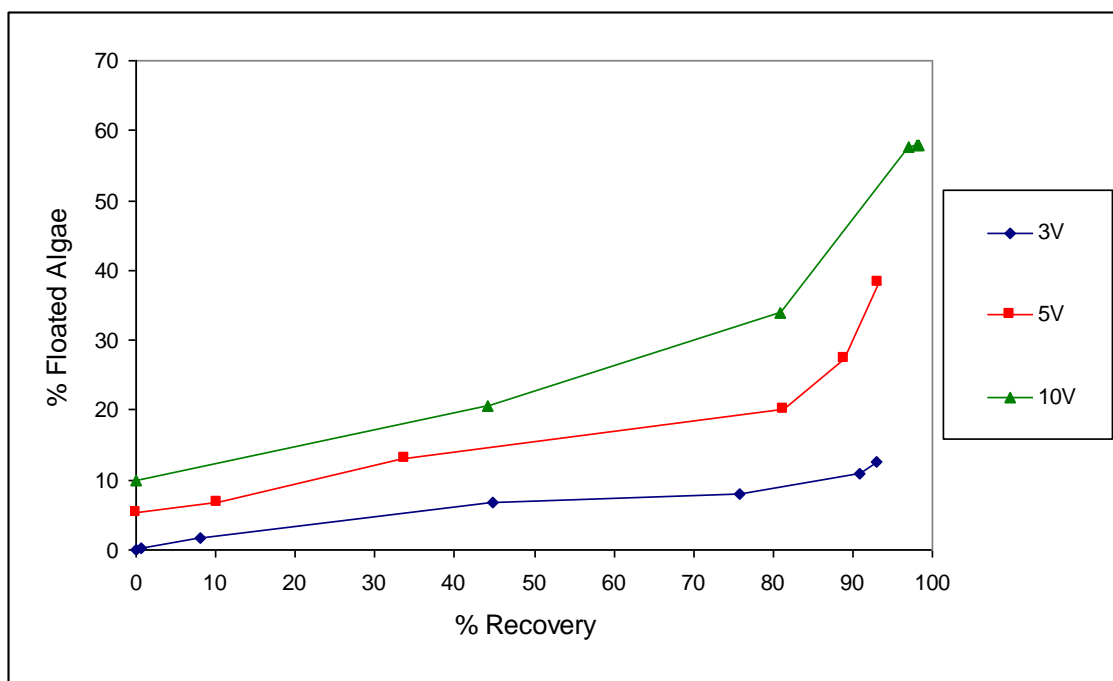
Figure 6. 24. Percentage recovery versus percentage of floated algae, for *Chlorococcum sp*. using the stainless steel 430 anode.
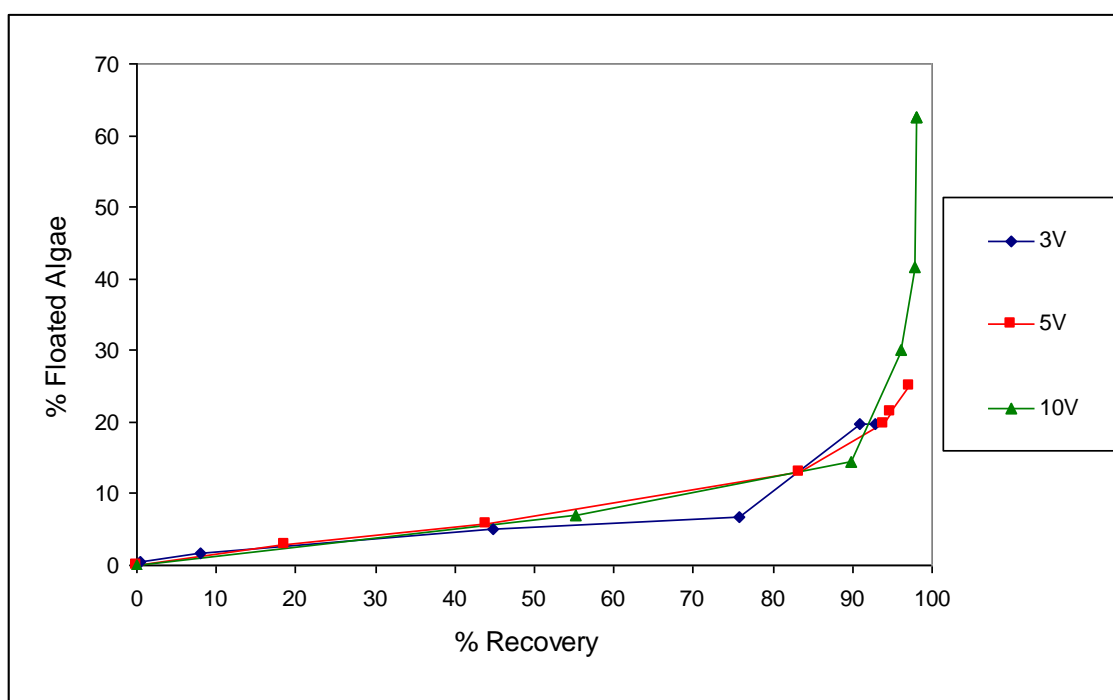
Figure 6. 25. Percentage recovery versus percentage of floated algae, for *Tetraselmis sp.* using the stainless steel 430 anode.
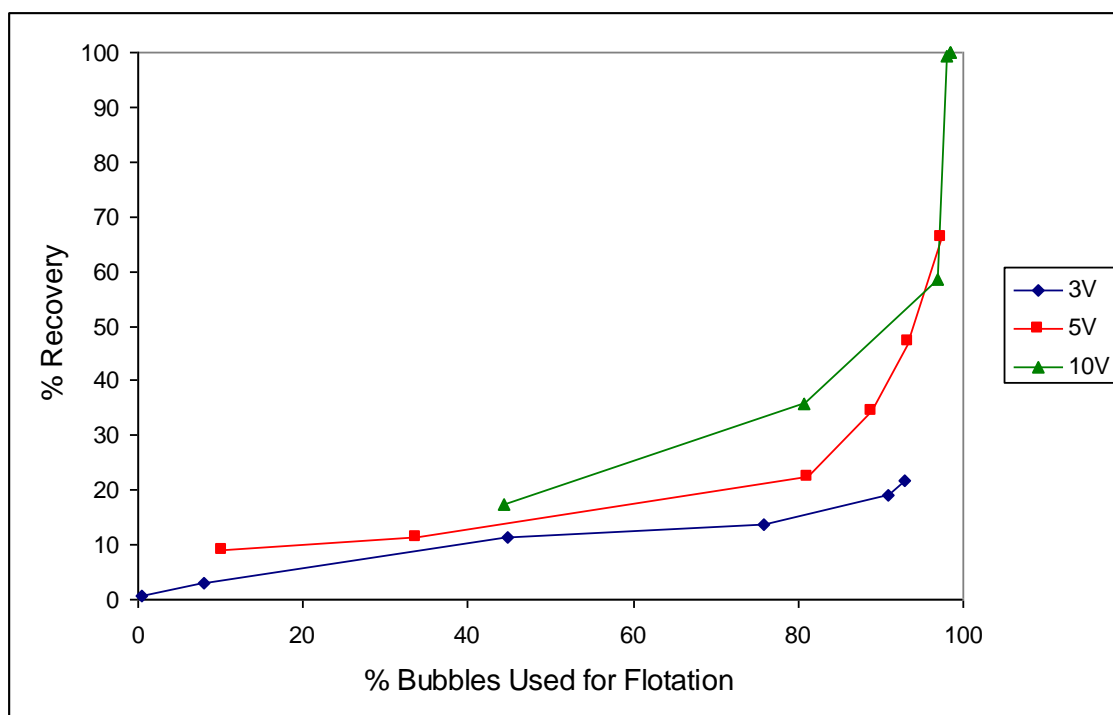
Figure 6. 26. Percentage recovery versus percentage of bubbles used for flotation (compared to total required for 100 % recovery), for *Chlorococcum sp.* using the stainless steel 430 anode.
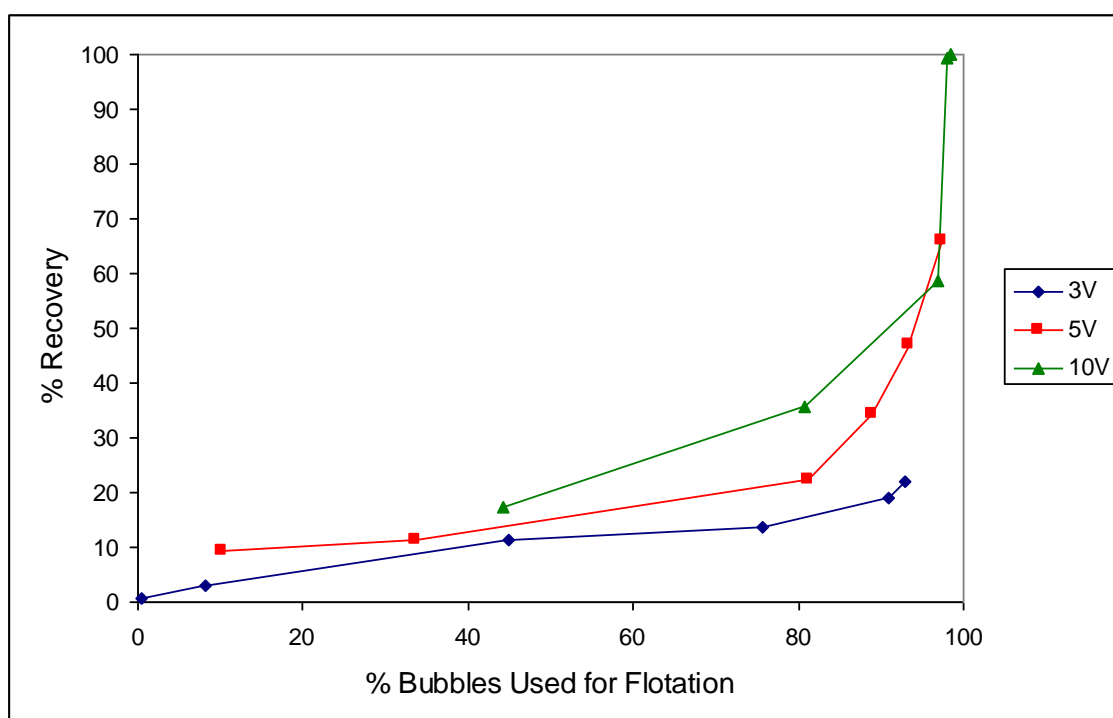
Figure 6. 27. Percentage recovery versus percentage of bubbles used for flotation (compared to total required for 100 % recovery), for *Tetraselmis sp.* using the stainless steel 430 anode.

153

Table 6.4 to 6.7 show the fraction of hydrogen used for flotation, as a percentage of the total hydrogen gas produced. It can be seen from these tables that hydrogen is produced in large excess, with generally less than 10 % and 30 % used for flotation with the stainless steel 430 and aluminium anodes, respectively. These tables also show that the longer electrolysis goes, the lower the fraction of hydrogen bubbles used for flotation. This indicates that the wastage is at the end, because the hydrogen is produced at a constant rate, but there is an ever diminishing number of flocs with no bubbles attached.

Table 6. 4. Hydrogen evolution from stainless steel 430 anode for electrocoagulation with *Chlorococcum sp.*

Voltage (V)	Time (s)	Total Volume H_2 (m^3)	Volume H_2 Used for Flotation (m^3)	% H_2 Used for Flotation
3	90	9.15E-06	2.17E-07	2.38
	600	6.10E-05	5.22E-06	8.55
	1200	1.22E-04	8.26E-06	6.77
5	90	2.75E-05	3.48E-06	12.7
	600	1.83E-04	1.30E-05	7.13
	1200	3.66E-04	2.50E-05	6.83
10	90	8.24E-05	6.52E-06	7.92
	600	5.49E-04	3.76E-05	6.85
	1200	1.10E-03	3.78E-05	3.44

Table 6. 5. Hydrogen evolution from stainless steel 430 anode for electrocoagulation with *Tetraselmis sp.*

Voltage (V)	Time (s)	Total Volume H_2 (m^3)	Volume H_2 Used for Flotation (m^3)	% H_2 Used for Flotation
3	90	4.35E-06	3.53E-07	8.12
	600	2.90E-05	4.70E-06	16.2
	1200	5.80E-05	1.39E-05	23.9
5	90	2.59E-05	2.12E-06	8.19
	600	1.72E-04	1.40E-05	8.12
	1200	3.45E-04	1.76E-05	5.12
10	90	8.47E-05	4.94E-06	5.84
	600	5.64E-04	2.94E-05	5.21
	1200	1.13E-03	4.41E-05	3.91

Table 6. 6. Hydrogen evolution from aluminium anode for electrocoagulation with *Chlorococcum sp.*

Voltage (V)	Time (s)	Total Volume H_2 (m^3)	Volume H_2 Used for Flotation (m^3)	% H_2 Used for Flotation
2	90	5.49E-06	2.70E-06	49.1
	180	1.10E-05	3.39E-06	30.9
	600	3.66E-05	4.86E-06	13.3
3	90	1.10E-05	3.48E-06	31.6
	180	2.20E-05	5.08E-06	23.1
	600	7.32E-05	8.51E-06	11.6
5	90	2.22E-05	5.43E-06	24.5
	180	4.44E-05	8.91E-06	20.1
	600	1.48E-04	1.18E-05	7.95

Table 6. 7. Hydrogen evolution from aluminium anode for electrocoagulation with *Tetraselmis sp.*

Voltage (V)	Time (s)	Total Volume H$_2$ (m^3)	Volume H$_2$ Used for Flotation (m^3)	% H$_2$ Used for Flotation
2	90	4.35E-06	2.75E-06	63.3
	180	8.70E-06	5.18E-06	59.5
	600	2.90E-05	1.41E-05	48.7
3	90	1.10E-05	5.49E-06	50.0
	180	2.20E-05	9.88E-06	45.0
	600	7.32E-05	1.46E-05	19.9
5	90	2.22E-05	6.12E-06	27.6
	180	4.44E-05	8.94E-06	20.1
	600	1.48E-04	1.68E-05	11.4

Figure 6.28 and 6.29 show the floc rise velocity versus the volume of hydrogen bubbles used to float the flocs. The figures which have a considerable amount of scatter still show a general trend between the number of bubbles used for flotation and a higher rise velocity. (Please refer to the Appendix A.2.7 for floc rise velocity calculations).
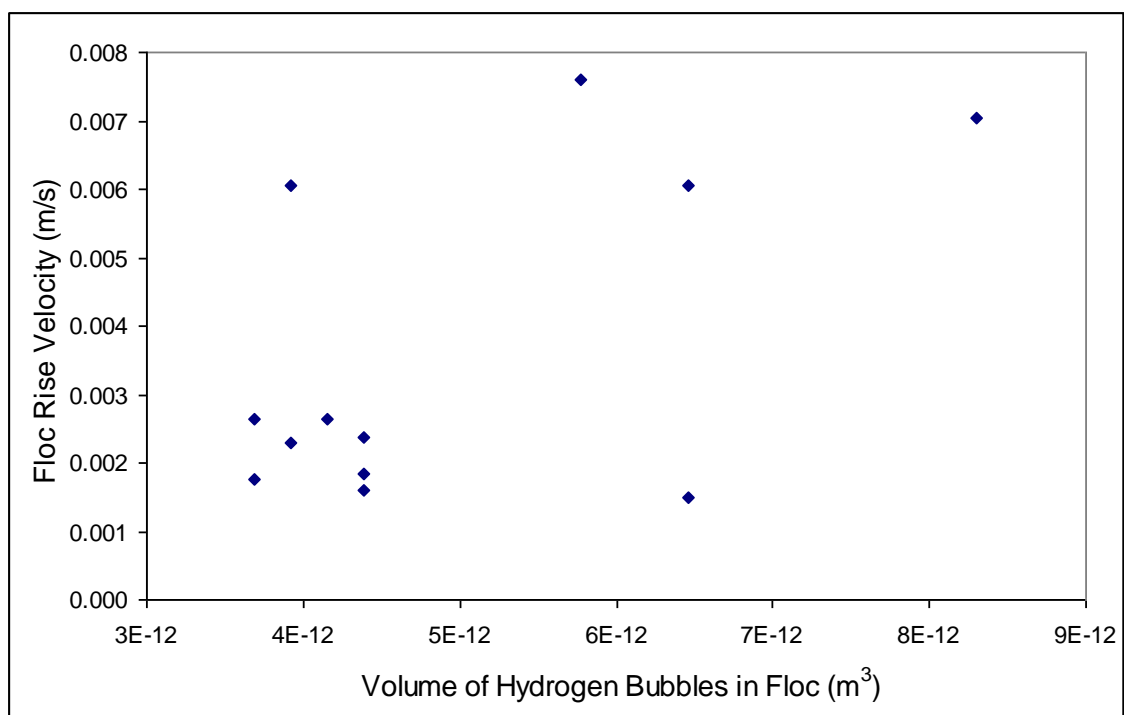
Figure 6. 28. Microalgae floc rise velocity versus bubble volume required for flotation, for *Chlorococcum sp.* with stainless steel 430 anode.
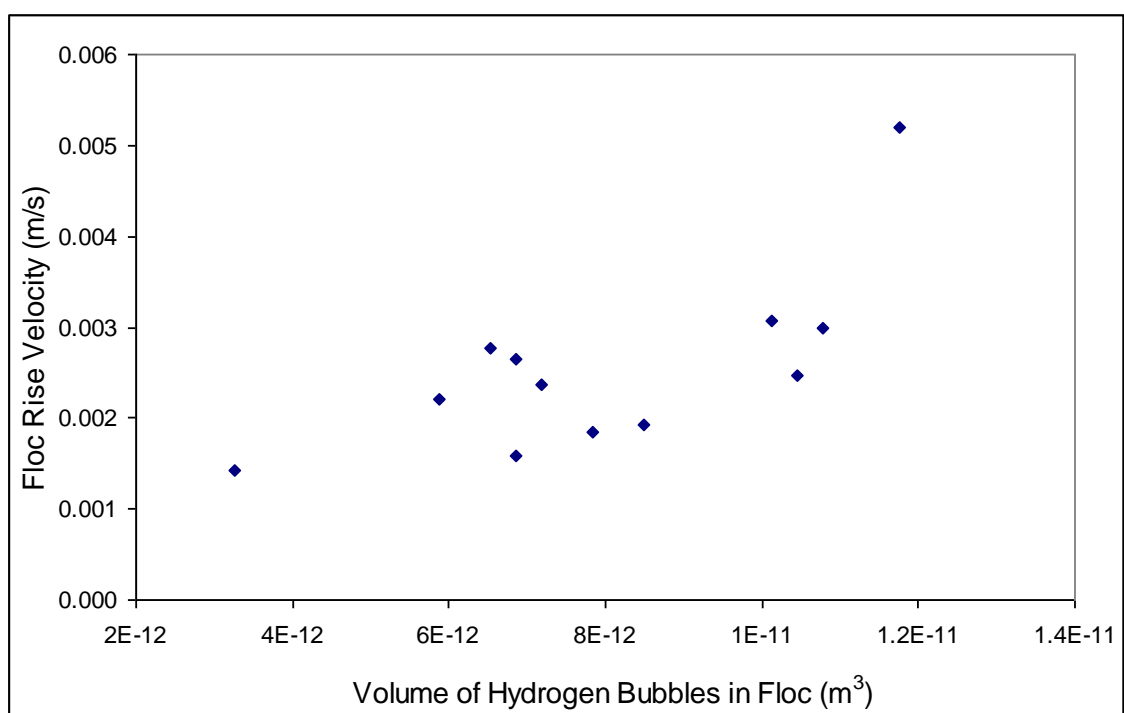
Figure 6. 29. Microalgae floc rise velocity versus bubble volume required for flotation, for *Tetraselmis sp.* with the stainless steel 430 anode

A great deal of effort was made to observe the interaction between non-flocculated microalgae cells with hydrogen bubbles. Small scale experiments using a microscope were performed and these were not able to observe any interaction between the non-flocculated microalgae and hydrogen bubbles. The conclusion drawn was that there was no interaction. It is likely that the bubbles being hydrophobic would not attach to small microalgae particles, which were hydrophilic.

6.6 Predictions by Mathematical Modelling

6.6.1 Determination of Reaction Order with respect to Microalgae Concentration

Levenspiel, O. (1999) has stated that the order of a reaction refers to the rate expression for a reaction that is found empirically. A first order reaction is dependant on the concentration of only one reactant that is consumed in the reaction. A second order reaction is dependant on either the concentration of one second order reactant, or two first order reactants. The reaction order for the electrocoagulation model was determined empirically by comparing the model parameters for different microalgae concentrations with linear and quadratic exponents.

When modelling with a linear relationship to the algae concentration (n=1), for electrocoagulation with both anode metals, the k value for *Tetraselmis sp.* was approximately double that for *Chlorococcum sp* (seen in table 6.8)*.* Changing the reaction order from linear to quadratic (n=2) resulted in the model parameter k having the same value for each microalgae system (see table 6.8). A second order reaction would place more importance on the microalgae concentration, hence when the model computed the recovery the difference in microalgae concentration did not affect the coagulation rate constant, k.

Table 6. 8. Reaction order and k values for different microalgae systems.

	Microalgae Species	Anode Material	k
1st Order	Chlorococcum sp.	Stainless steel 430	0.1
		Aluminium	3
	Tetraselmis sp.	Stainless steel 430	0.15
		Aluminium	6
2nd Order	Chlorococcum sp.	Stainless steel 430	2
		Aluminium	80
	Tetraselmis sp.	Stainless steel 430	2
		Aluminium	80

Figure 6.30 shows the recovery obtained from electrocoagulation of *Tetraselmis sp.* with the aluminium anode at concentrations of 0.3, 0.6 and 2.6 g/L, and model predictions with a first order reaction. In order to predict the recovery, when the model has a reaction order of 1, completely different k values are required. Figure 6.32 shows the recovery obtained from electrocoagulation of *Tetraselmis sp.* with the aluminium anode at concentrations of 0.3, 0.6 and 2.6 g/L, and model predictions with a second order reaction. For a reaction order of 2, the k values required by the model are the same. From the figure, it can be seen that for the three different microalgae concentrations, the data from the experimental microalgae recovery results have the same recovery rate. The second order reaction model is able to predict the recovery of microalgae successfully while keeping the same rate constant k. This result indicates that a reaction order of 2 is a better empirical fit to the experimental data.
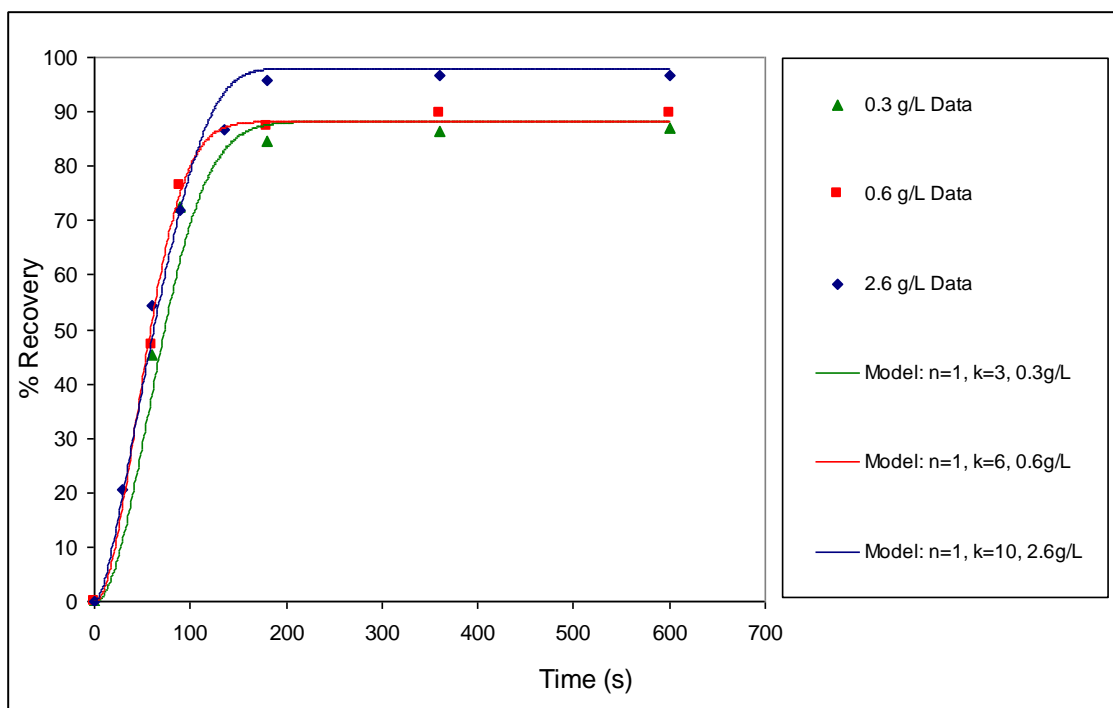
Figure 6. 30. Percentage recovery of *Tetraselmis sp.* for electrocoagulation at 5 V with different concentrations and reaction order n=1, with the aluminium anode.
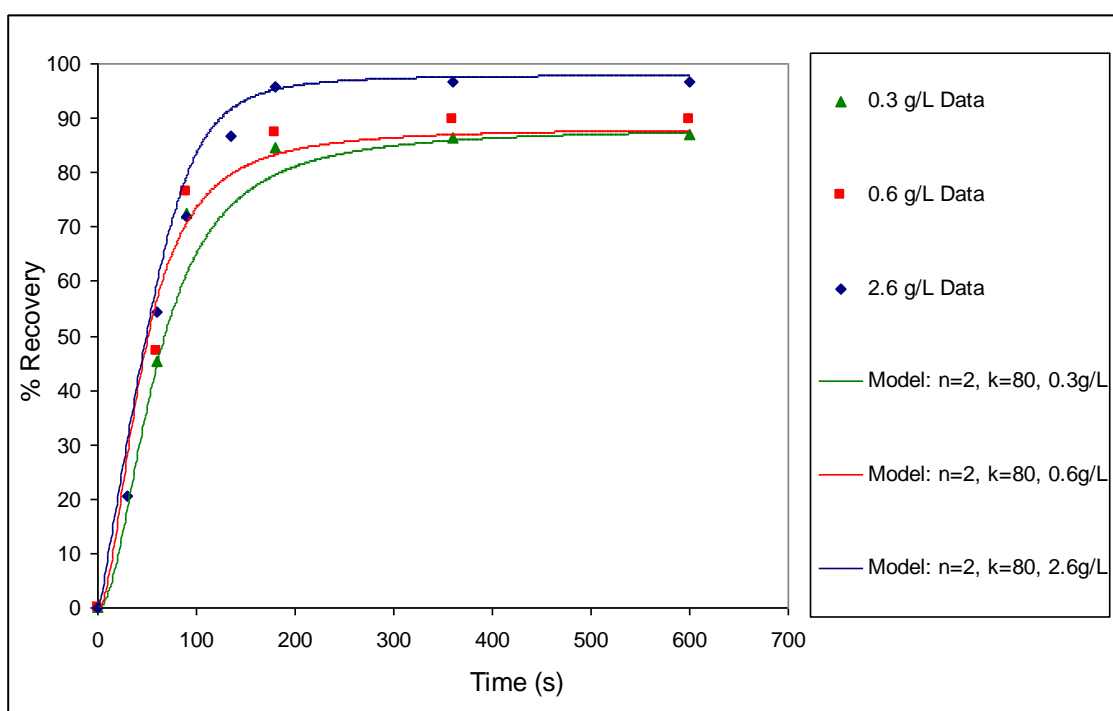
Figure 6. 31. Percentage recovery of *Tetraselmis sp.* for electrocoagulation at 5 V with different concentrations and reaction order n=2, with the aluminium anode.

The different reaction orders were also investigated for the two microalgae species. Figure 6.32 shows the experimental data and model predictions at both reaction orders, for the recovery of both microalgae species, with electrocoagulation using the stainless steel 430 anode. It can be seen from this figure that a considerably better fit is obtained with the model using a quadratic reaction order. It is noted again that the reaction order of 2 required no change in the k value regardless of the difference in concentrations between species, where as the k value for the model with a reaction order of 1 reflected the concentration of the microalgae species.
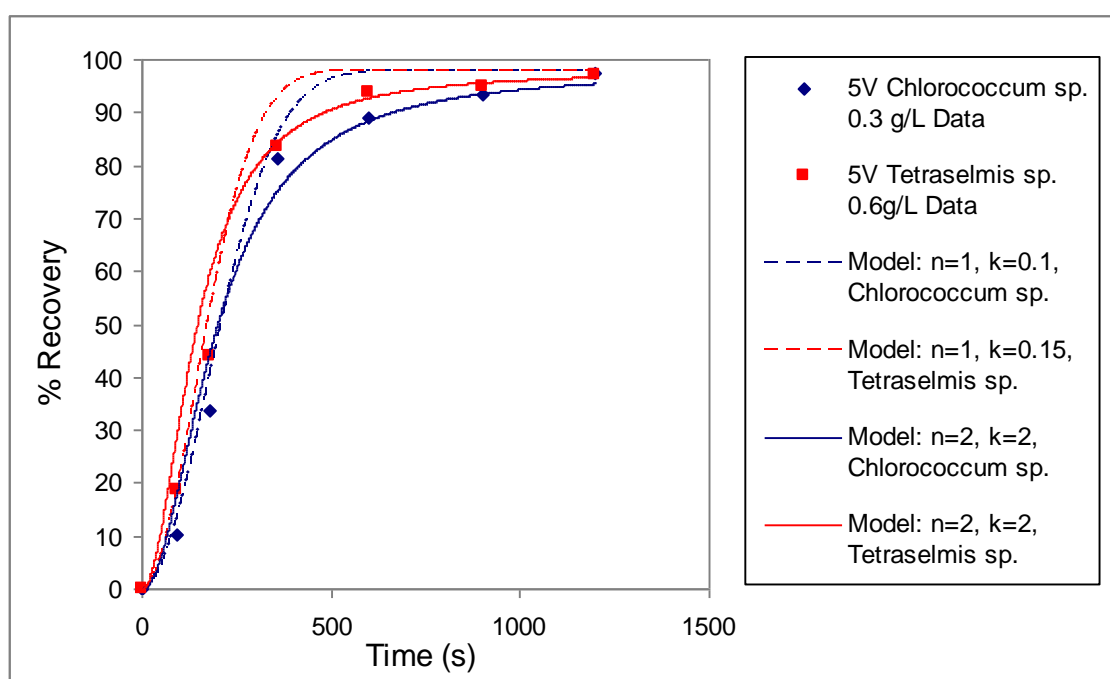
Figure 6. 32. Percentage recovery of *Chlorococcum sp.* and *Tetraselmis sp.* for electrocoagulation at 5 V with different reaction orders, with the stainless steel 430 anode.

From the empirical investigations conducted, the conclusion was made to fit the model with a secondary reaction order. The predictions of experimental results with n=2 were more accurate, and the model did not have to be adjusted for any difference in microalgae concentration.

Levenspiel, O. (1999) states that since the reaction order can be found empirically, the value does not have to be an integer. Therefore looking at all the data combined, there is a possibility that the best fit for the reaction order may lie between 1 and 2.

For the stainless steel 430 anode, the reaction order of 2 fits very well. The aluminium anode may require a reaction order of less than, but close to 2, but for consistency 2 has been adopted for both cases.

6.6.2 Coagulation Predicted by Model

The amount of microalgae that coagulates due to charge neutralisation is predicted by the mathematical model. Figures 6.33 to 6.36 show that the model predicts an increase in microalgae coagulation with time, with a subsequent plateau after the saturation point has been reached corresponding to a maximum adsorption of metal ions onto the microalgae surface.

A limitation of the model is that it does not account for mixing in the system, but instead assumes that the cell is perfectly mixed. In reality, the coagulation of the microalgae is dependent on neutralisation by metal ions, but the extent of this is determined by the amount of mixing in the system. From the experimental results, it was found that agitation in the system had a significant effect on recovery. Increasing the voltage and therefore increasing the applied current, results in an increase in production of hydrogen bubbles, which in turn increases the mixing in the system. The degree of mixing will have an effect on the value of the model parameters k and x_{21}. Mixing in the system will lead to more collisions between flocculated microalgae, hence an increased rate of metal adsorption onto the microalgae surface (resulting in a higher value of k), and a greater number of collisions between hydrogen bubbles and microalgae flocs (resulting in more hydrogen attachment at a shorter time, i.e. changing the value of $x_{<21}$), both of which will lead to a higher rate of recovery. However, turbulent mixing may disturb the upward streaming of microalgae-bubble flocs for surface recovery.

The values of parameter b (which is the quantity of metal ions required for coagulation per mass of microalgae) were calculated and given in tables 6.2 and 6.3. It can be seen from the tables that as the run time increases, b (mass of metal/mass of algae in floated layer) also increases. Therefore it was difficult to determine a

value of b that was constant for each microalgae system. There is a certain amount of metal ions which correspond to the minimum required for successful electrocoagulation. After this point, the metal ions continue to be introduced into the system but are not necessarily used. The increase observed in the b values with time can be explained by the excess binding of metal species onto the microalgae surface.
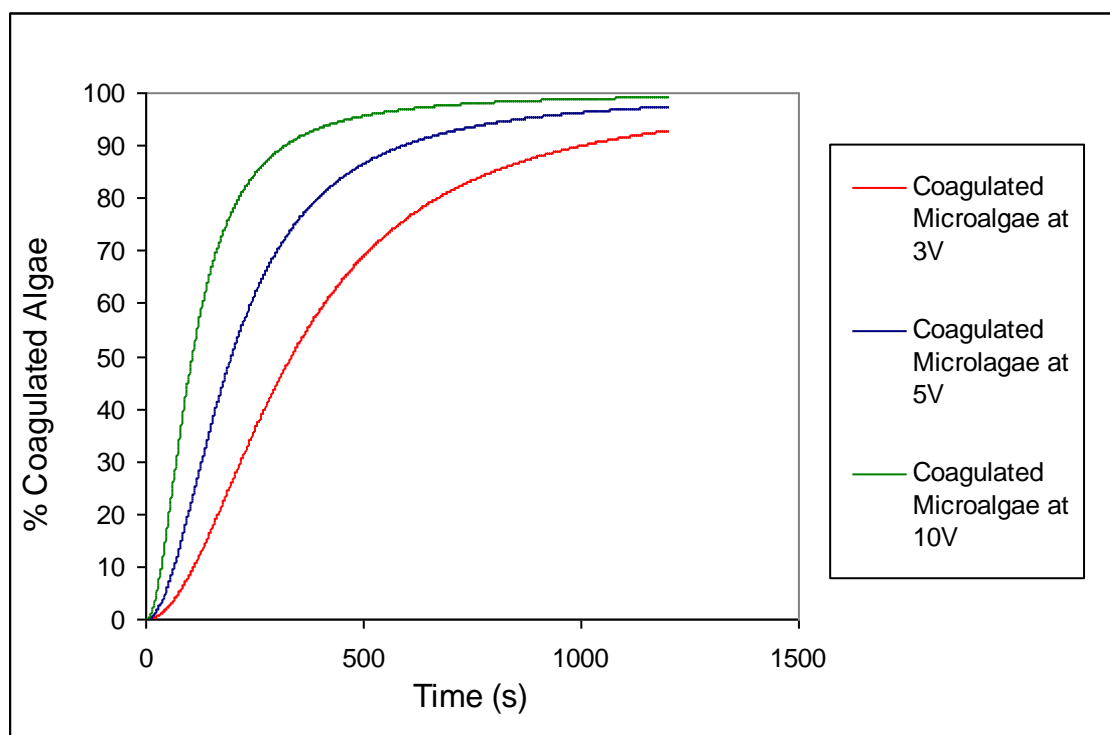
Figure 6. 33. Mass of coagulated *Chlorococcum sp.* (initial concentration of 0.3 g/L) with time for electrocoagulation with the stainless steel 430 anode.
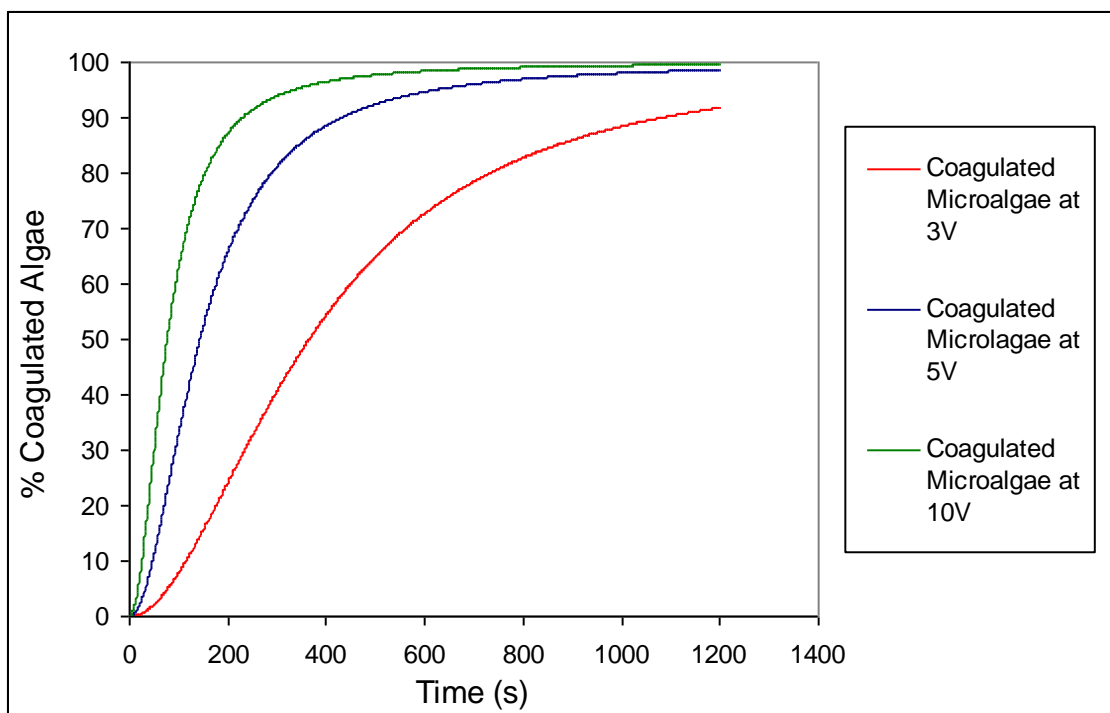
Figure 6. 34. Mass of coagulated *Tetraselmis sp.* (initial concentration of 0.6 g/L) with time for electrocoagulation with the stainless steel 430 anode.
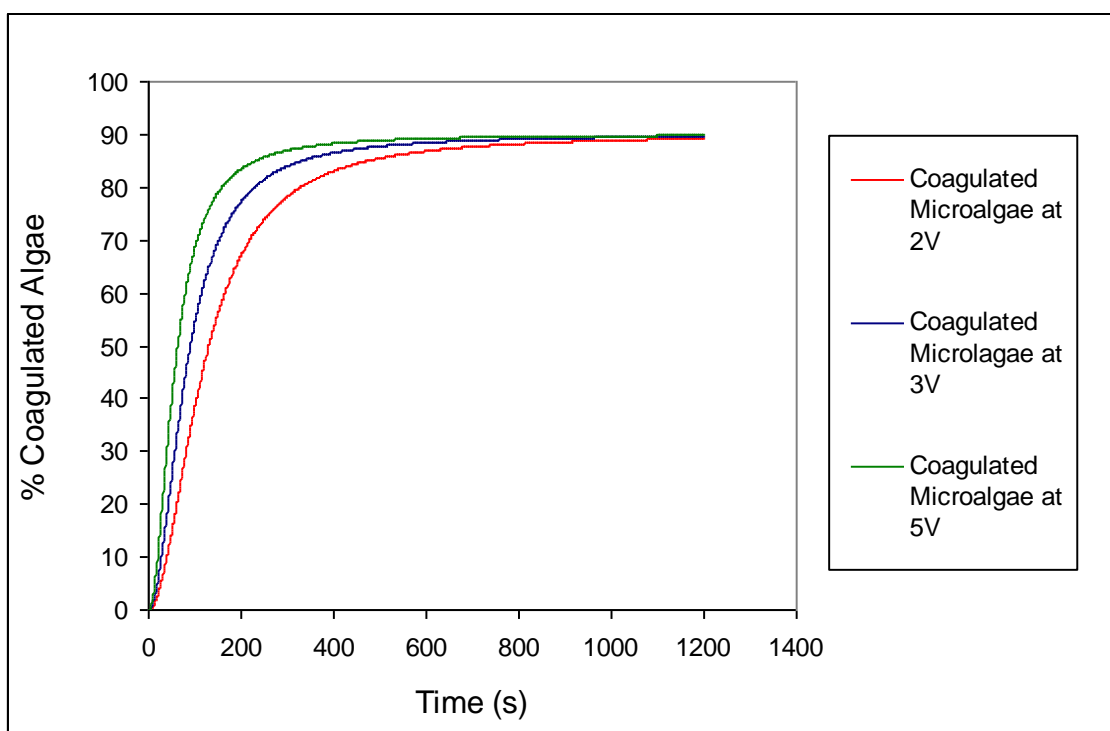
Figure 6. 35. Mass of coagulated *Chlorococcum sp.* (initial concentration of 0.3 g/L) with time for electrocoagulation with the aluminium anode.
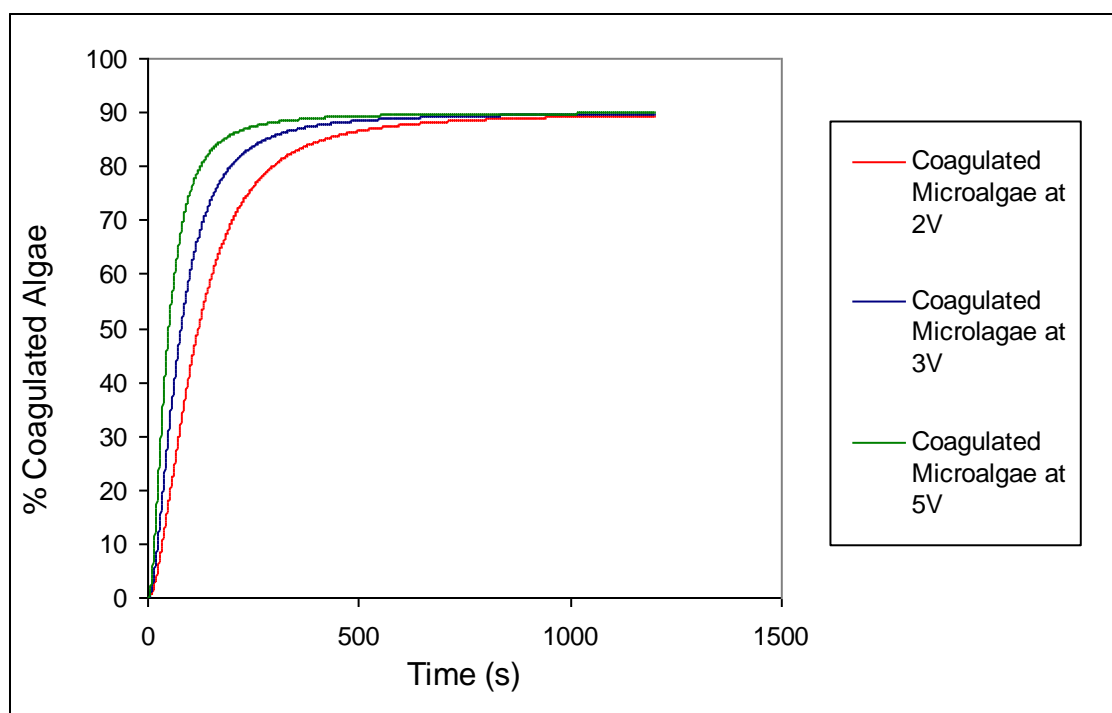
Figure 6. 36. Mass of coagulated *Tetraselmis sp.* (initial concentration of 0.6 g/L) with time for electrocoagulation with the aluminium anode.

6.6.3 Recovery of Microalgae Predicted by Model

The mathematical model developed in this study was able to predict the amount of microalgae recovery for a given voltage applied to the system. The input parameters required by the model were given in table 6.1. Along with these parameters, the model requires the current passing through the cell, the starting mass of microalgae (determined from the starting concentration of microalgae) and the fraction of microalgae that does not flocculate (determined from the experimental data for the maximum recovery obtained for each system). Figures 6.37 to 6.48 show the predicted recovery of microalgae with different applied voltage, anode material and microalgae species in comparison to the experimental data. The figures show that the model is able to predict the recovery of microalgae when the electrocoagulation conditions are given. An exception is the model result for electrocoagulation of *Chlorococcum sp.* with the stainless steel 430 anode at 3 V. The model predicts a much higher recovery to that obtained experimentally. This is not observed for the 3

V predictions with *Tetraselmis sp.* and may be due to anomalies associated with the batch of microalgae used for the experiments that gave these low recovery results.

As mentioned earlier, the main limitation of the model is that it assumes that the cell is perfectly mixed and therefore does not account for differences in the level of agitation in the system. This is evident in the model results for the 2 V aluminium anode and the 3 V stainless steel 430 anode, where there is a low level of stirring due to the low bubble generation rate at low voltages. The experimental data for these conditions show a lag in microalgae recovery with short run times, which relates to the induction period where there is a need for a build up of sufficient collisions between the particles in the system in order to achieve microalgae flotation and recovery. This result is discussed further in section 6.7.
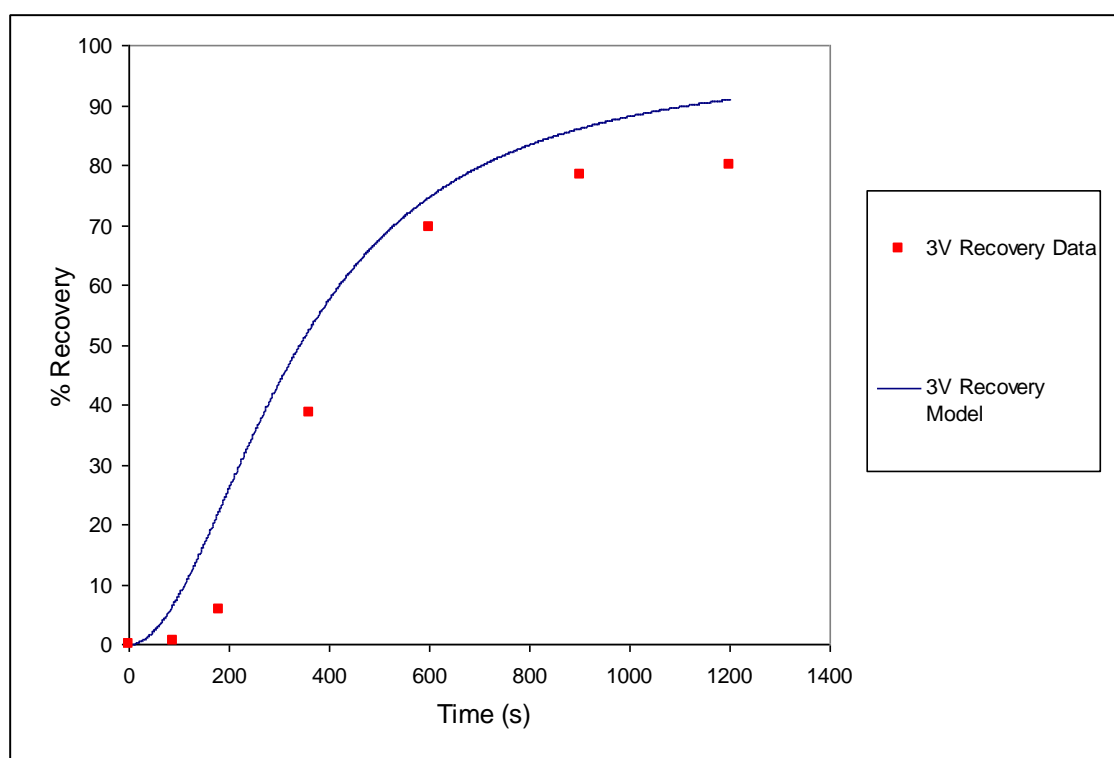
Figure 6. 37. Comparison of microalgae recovery for model and experimental data for electrocoagulation of *Chlorococcum sp.* with the stainless steel anode at 3 V.
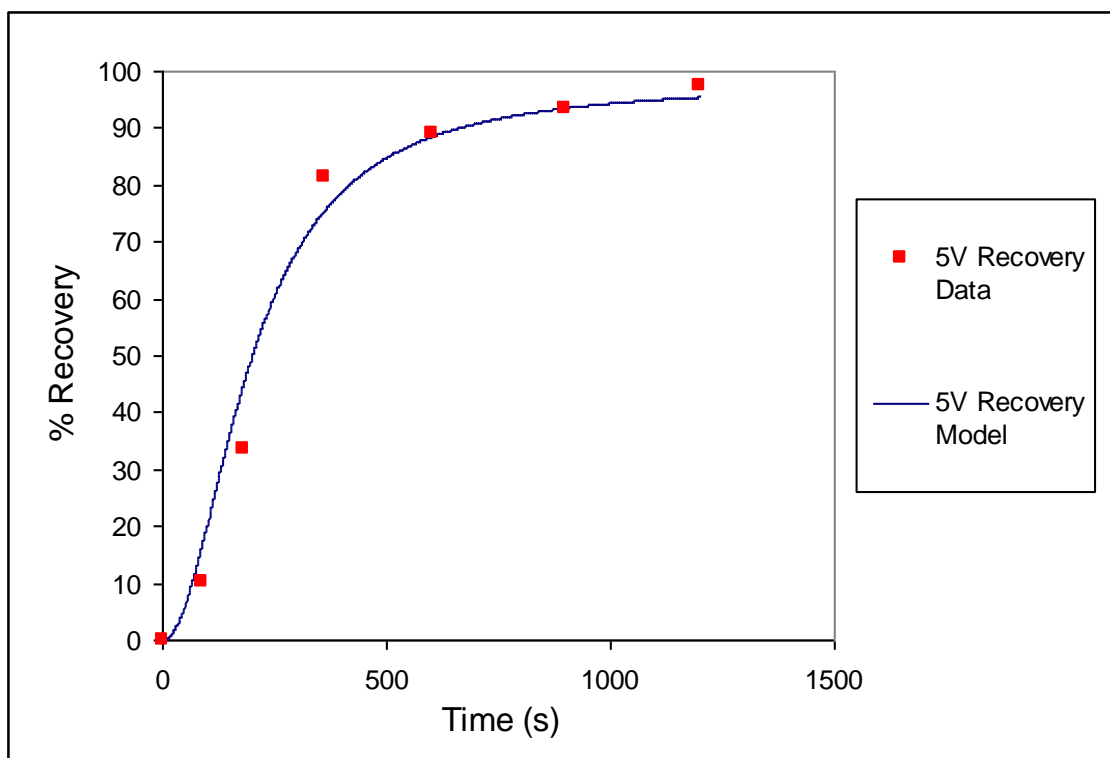
Figure 6. 38. Comparison of microalgae recovery for model and experimental data for electrocoagulation of *Chlorococcum sp.* with the stainless steel anode at 5 V.
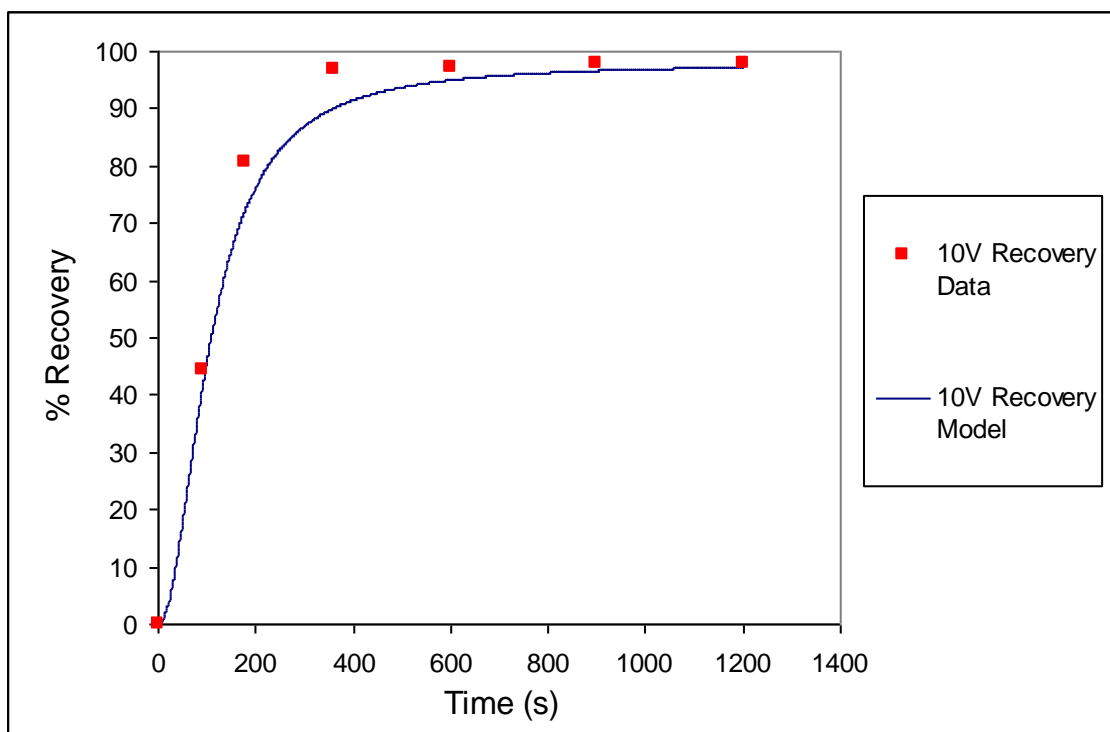
Figure 6. 39. Comparison of microalgae recovery for model and experimental data for electrocoagulation of *Chlorococcum sp.* with the stainless steel anode at 10 V.

167
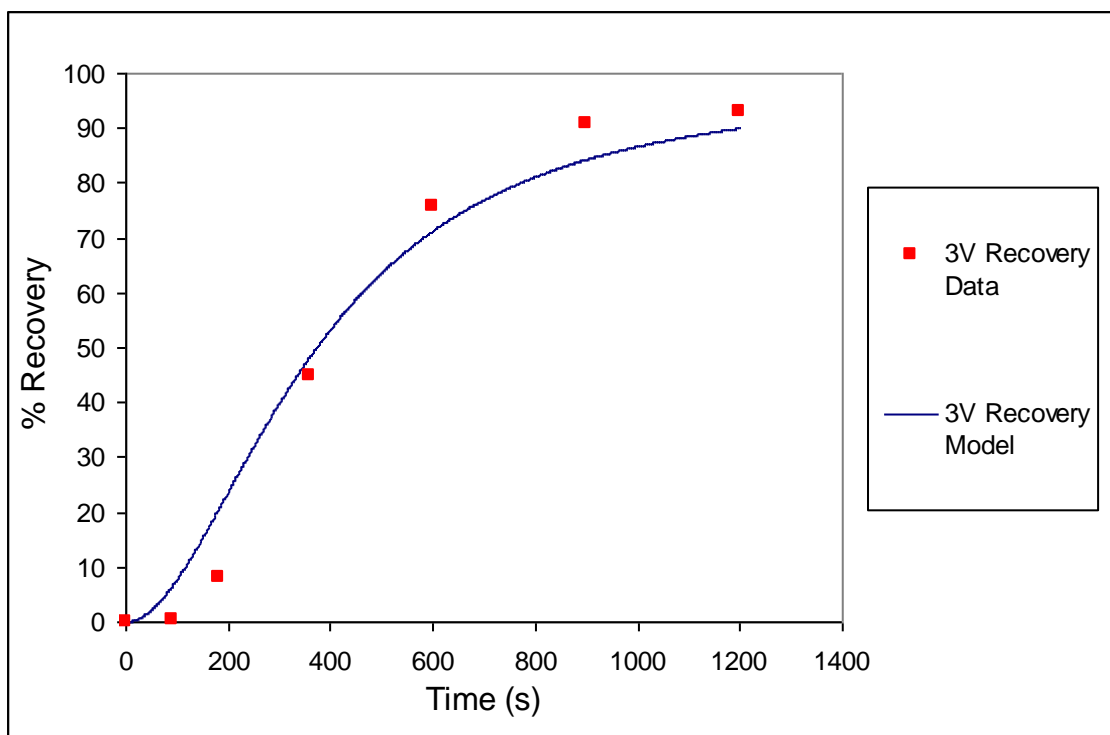
Figure 6. 40. Comparison of microalgae recovery for model and experimental data for electrocoagulation of *Tetraselmis sp.* with the stainless steel anode at 3 V.
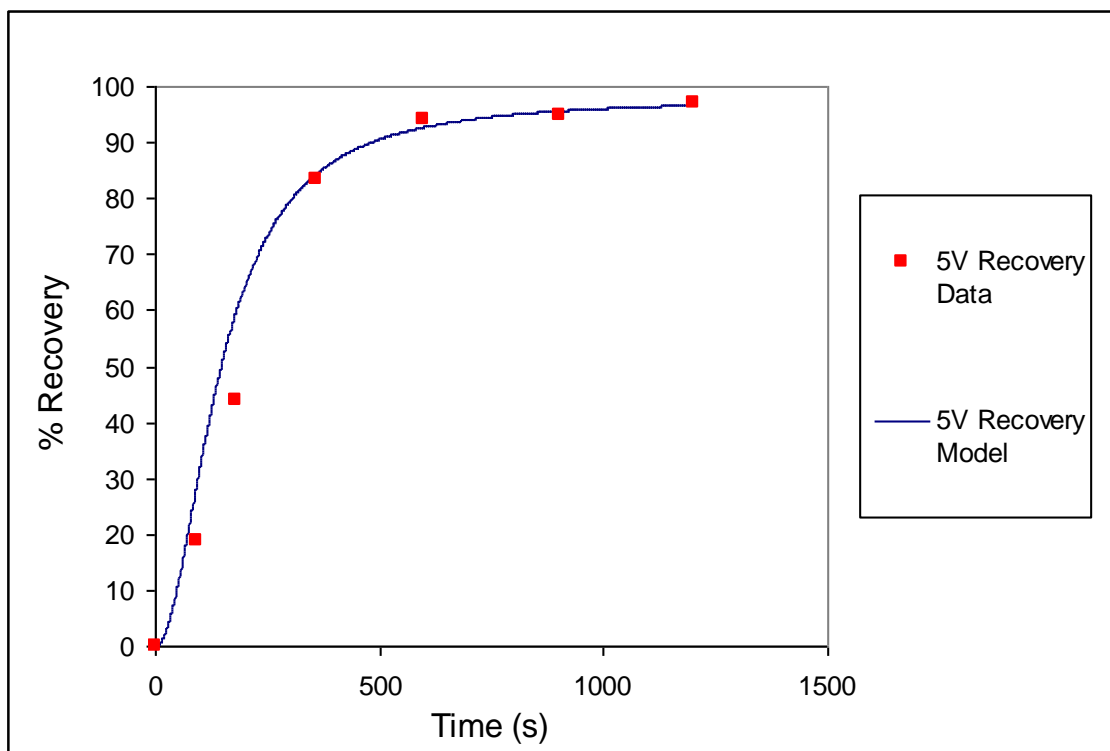
Figure 6. 41. Comparison of microalgae recovery for model and experimental data for electrocoagulation of *Tetraselmis sp.* with the stainless steel anode at 5 V.
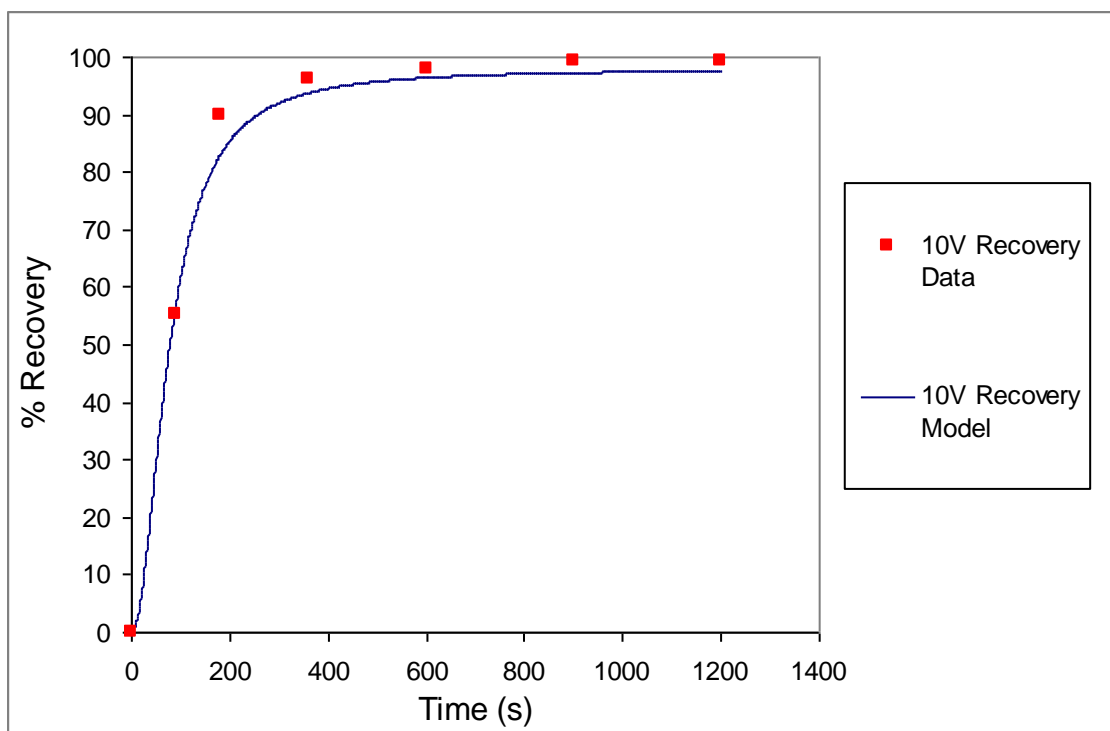
Figure 6. 42. Comparison of microalgae recovery for model and experimental data for electrocoagulation of *Tetraselmis sp.* with the stainless steel anode at 10 V.
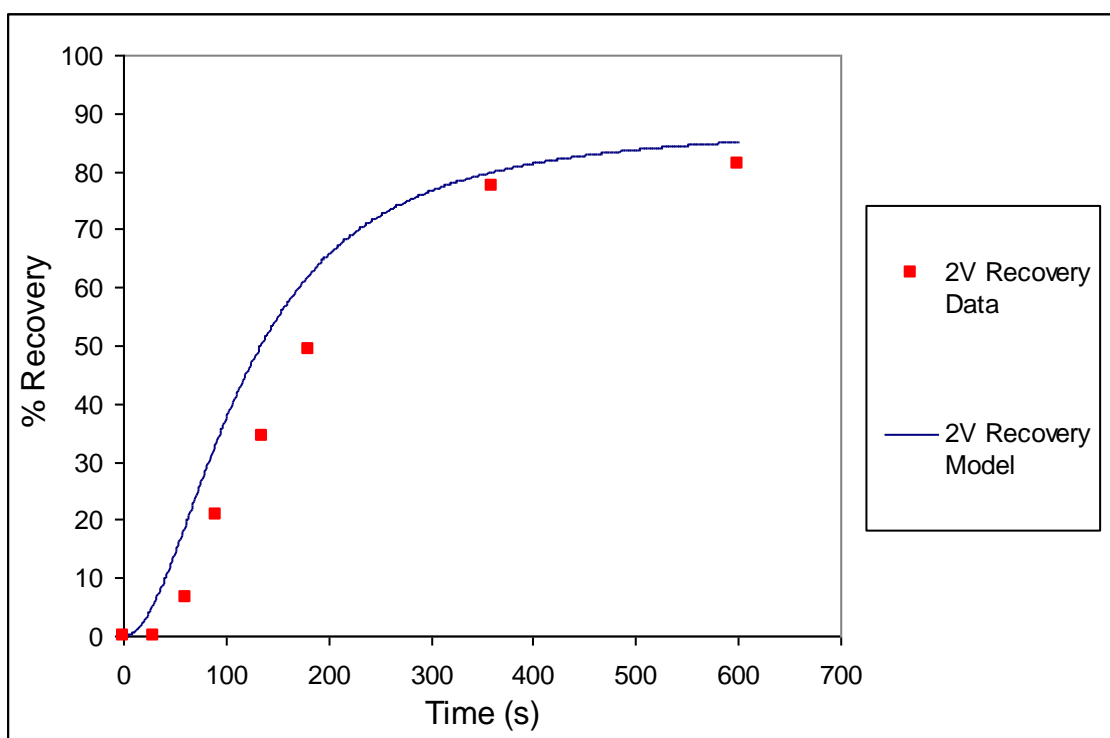
Figure 6. 43. Comparison of microalgae recovery for model and experimental data for electrocoagulation of *Chlorococcum sp.* with the aluminium anode at 2 V.
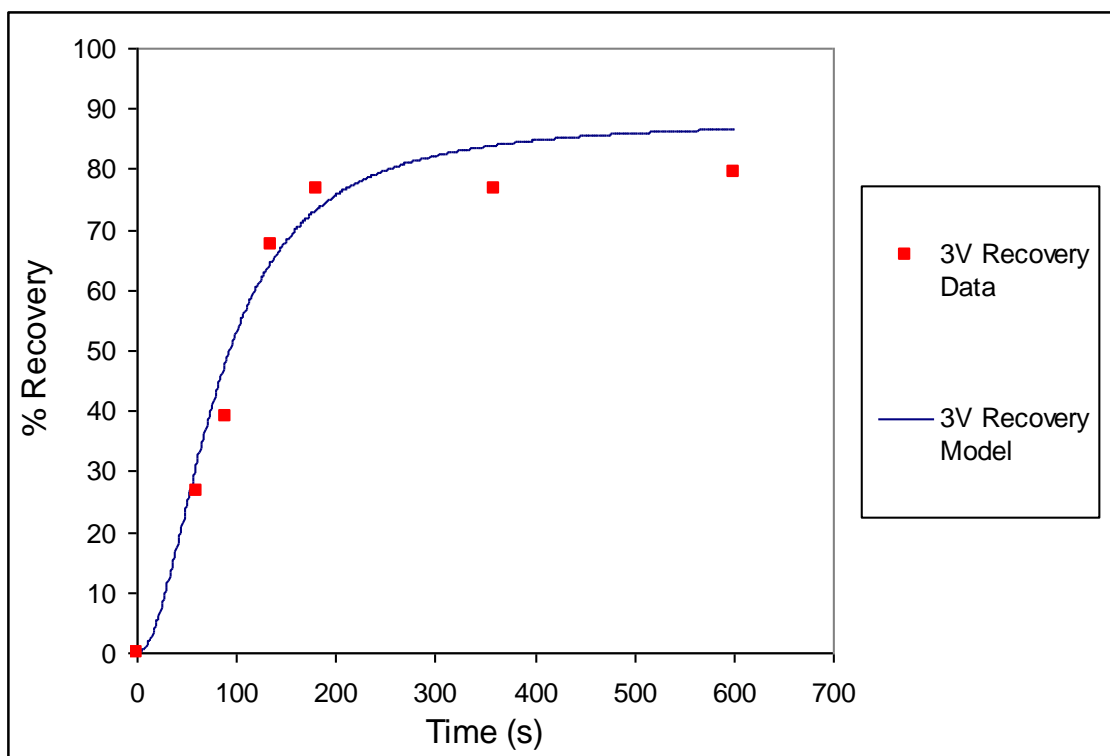
Figure 6. 44. Comparison of microalgae recovery for model and experimental data for electrocoagulation of *Chlorococcum sp.* with the aluminium anode at 3 V.
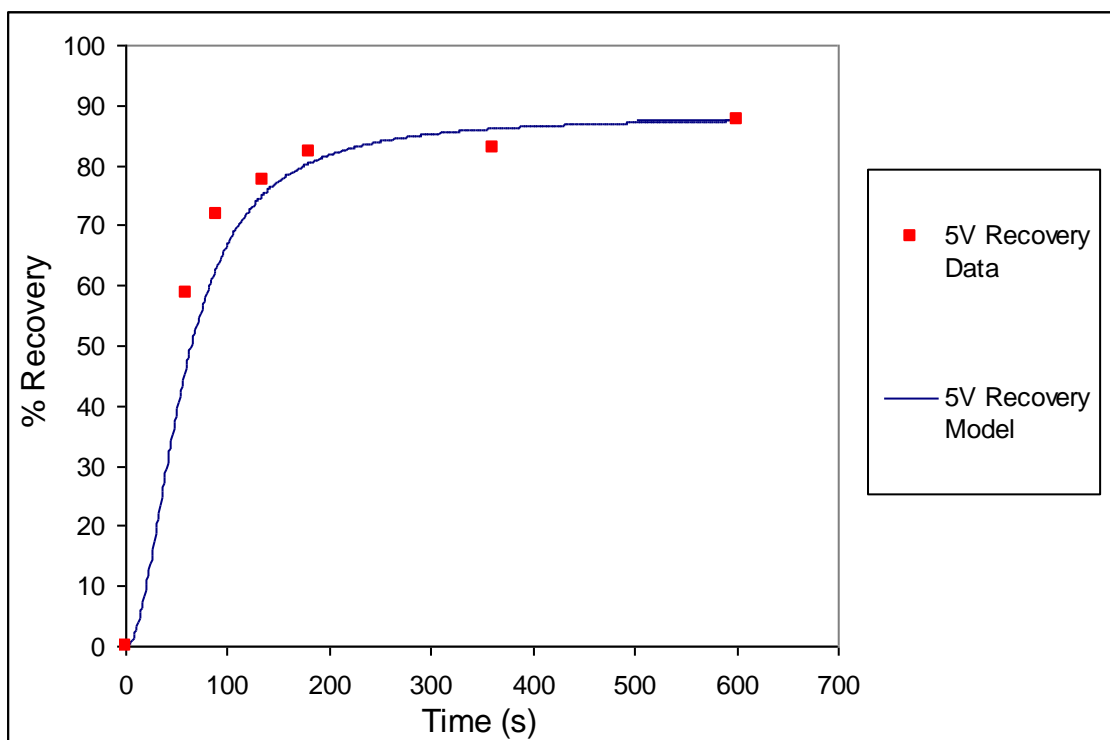
Figure 6. 45. Comparison of microalgae recovery for model and experimental data for electrocoagulation of *Chlorococcum sp.* with the aluminium anode at 5 V.
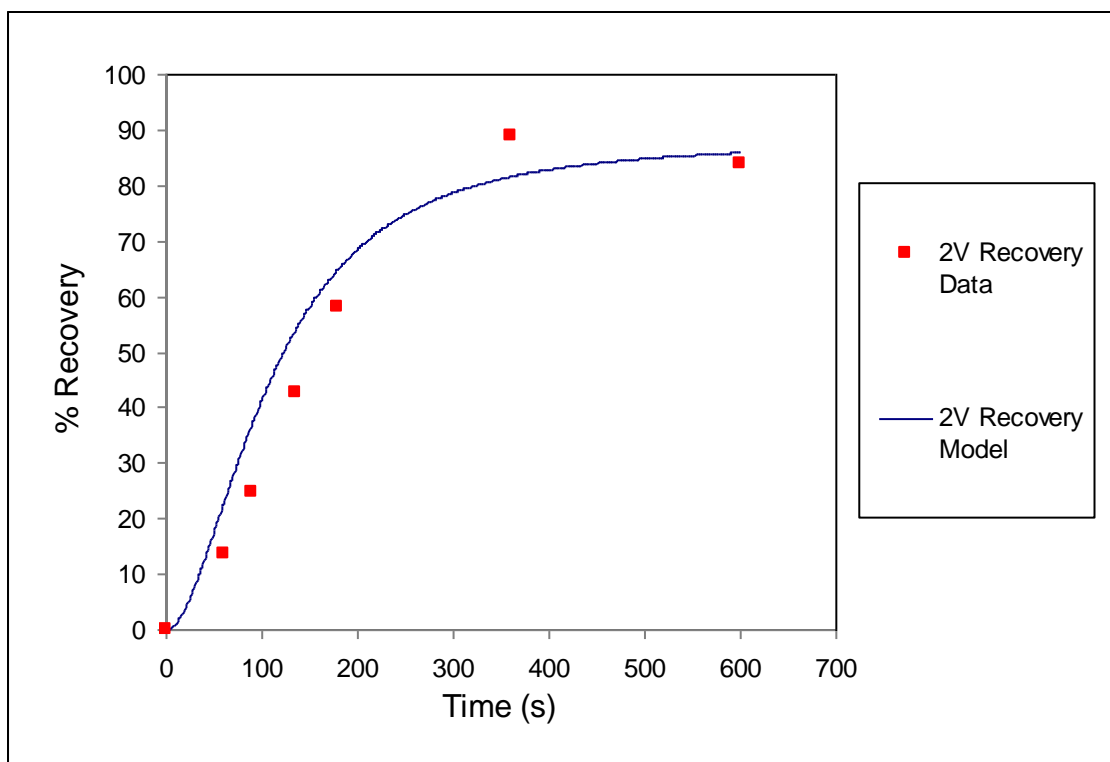
Figure 6. 46. Comparison of microalgae recovery for model and experimental data for electrocoagulation of *Tetraselmis sp.* with the aluminium anode at 2 V.
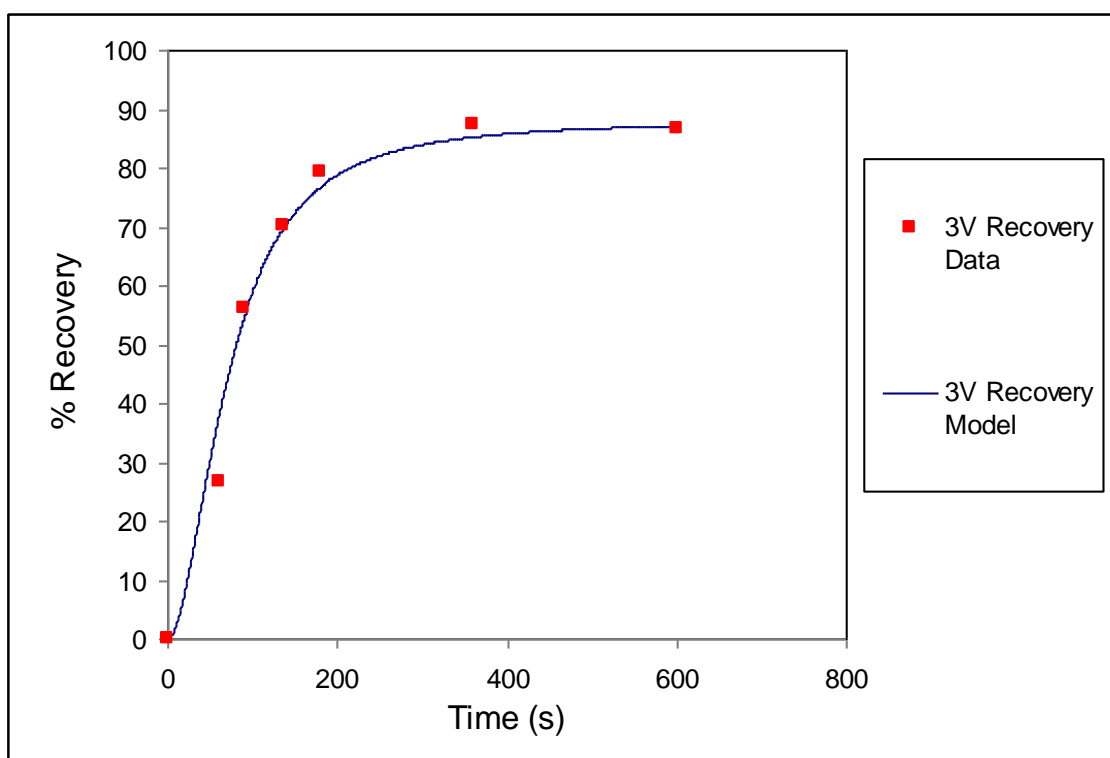
Figure 6. 47. Comparison of microalgae recovery for model and experimental data for electrocoagulation of *Tetraselmis sp.* with the aluminium anode at 3 V.
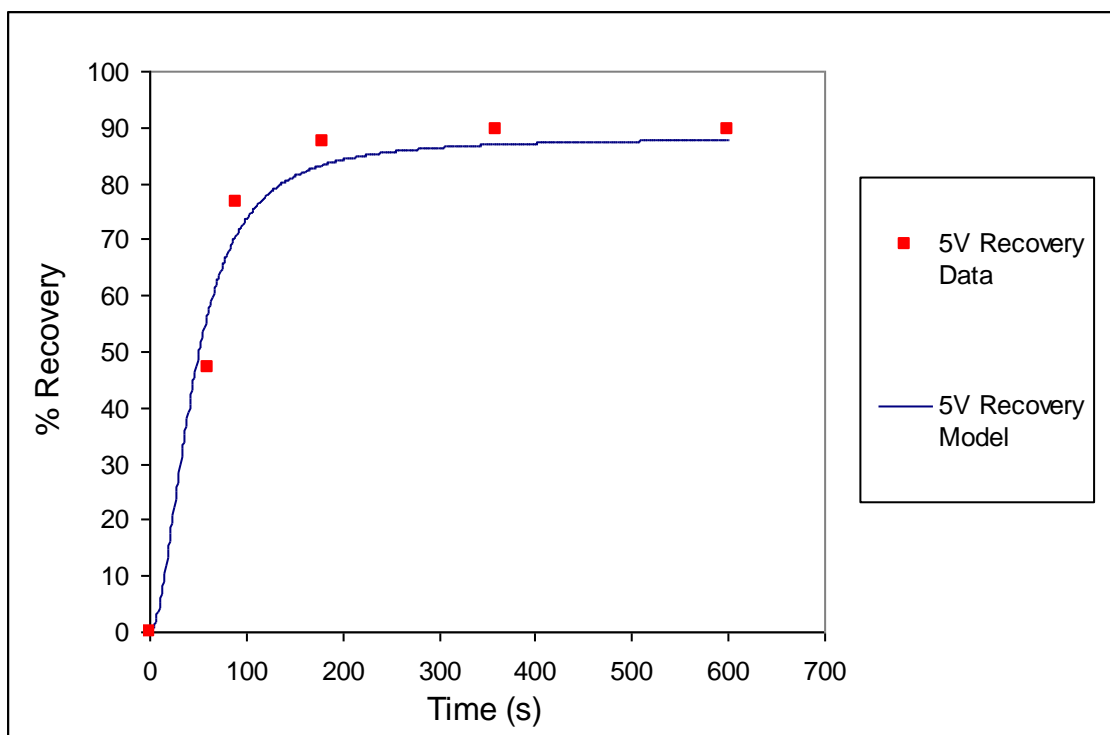
Figure 6. 48. Comparison of microalgae recovery for model and experimental data for electrocoagulation of *Tetraselmis sp.* with the aluminium anode at 5 V.

6.6.4 Unflocculated and Settled Microalgae Predicted by Model

For each electrocoagulation experiment, there is a fraction of microalgae that does not adsorb metal ions and flocculate. There is also a fraction of flocculated microalgae that does not attach to hydrogen bubbles and float. Such microalgae particulates may eventually settle to the bottom of the electrocoagulation cell. The electrocoagulation experiments were performed within a fixed time period of 15 min (which was adequate time for all flocs to float to the surface). Therefore at the end of this time period, a percentage of unflocculated microalgae would be present in the supernatant and a percentage of the unflocculated microalgae would have settled. The model does not have this time restraint and assumes that all unflocculated microalgae settles. Figures 6.49 to 6.60 show the model's predicted settled microalgae with different applied voltage, anode material and microalgae species in comparison to the experimental data. Since the experimental data was taken after a fixed time, the total experimental settled microalgae amount was taken as the sum of settled microalgae and the microalgae remaining in the supernatant.

172

From the figures, it can be seen that the model can predict the unflocculated (hence settled) microalgae.

Again, an exception is the result for electrocoagulation of *Chlorococcum sp.* with the stainless steel 430 anode at 3 V and aluminium anode at 2 V. The experimental results for this electrocoagulation condition showed lower than expected microalgae recovery at longer run times. The results also show that there is still a significant amount of microalgae in solution after longer time periods. This is due to the fact that the model assumes perfect mixing in the system. In reality, this does not occur, so it is expected that the experimental recovery is lower than that predicted by the model. A lower value of recovery in the experimental results in comparison to the model results will therefore correspond to a higher settled value.
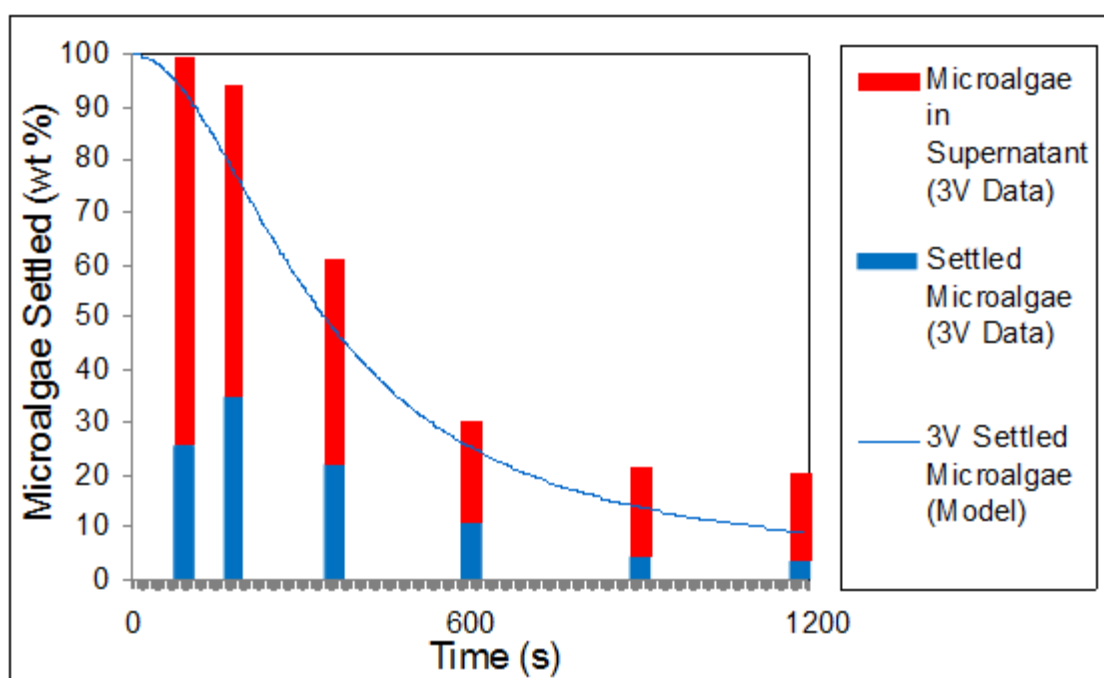
Figure 6. 49. Comparison of microalgae settling for model and experimental data for electrocoagulation of *Chlorococcum sp.* with the stainless steel anode at 3 V.
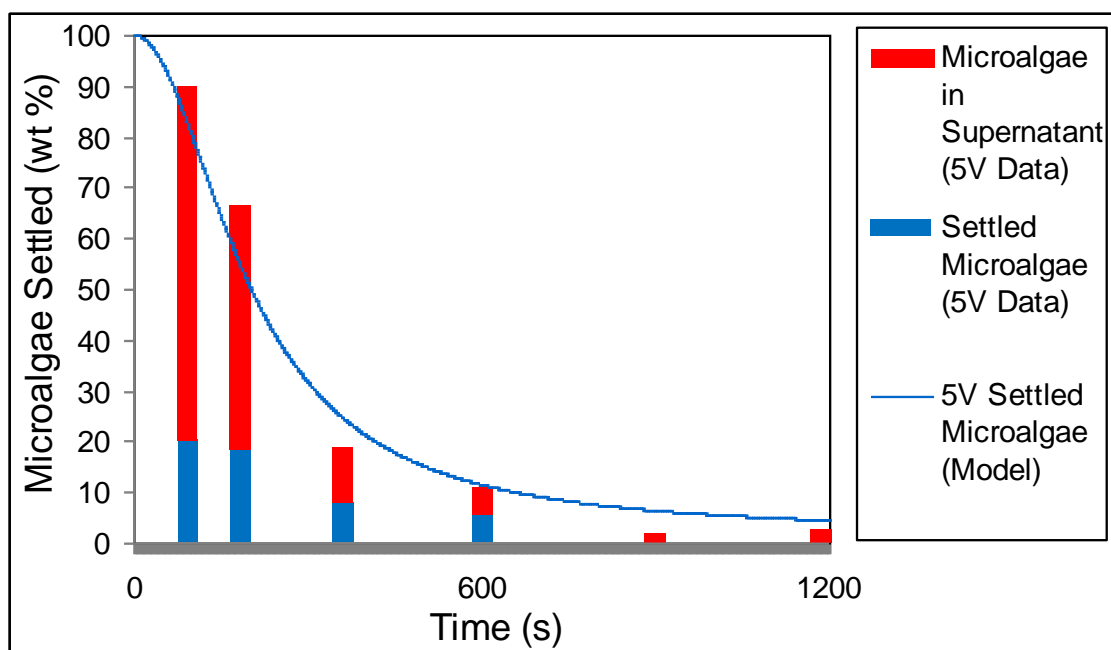
Figure 6. 50. Comparison of microalgae settling for model and experimental data for electrocoagulation of *Chlorococcum sp.* with the stainless steel anode at 5 V.
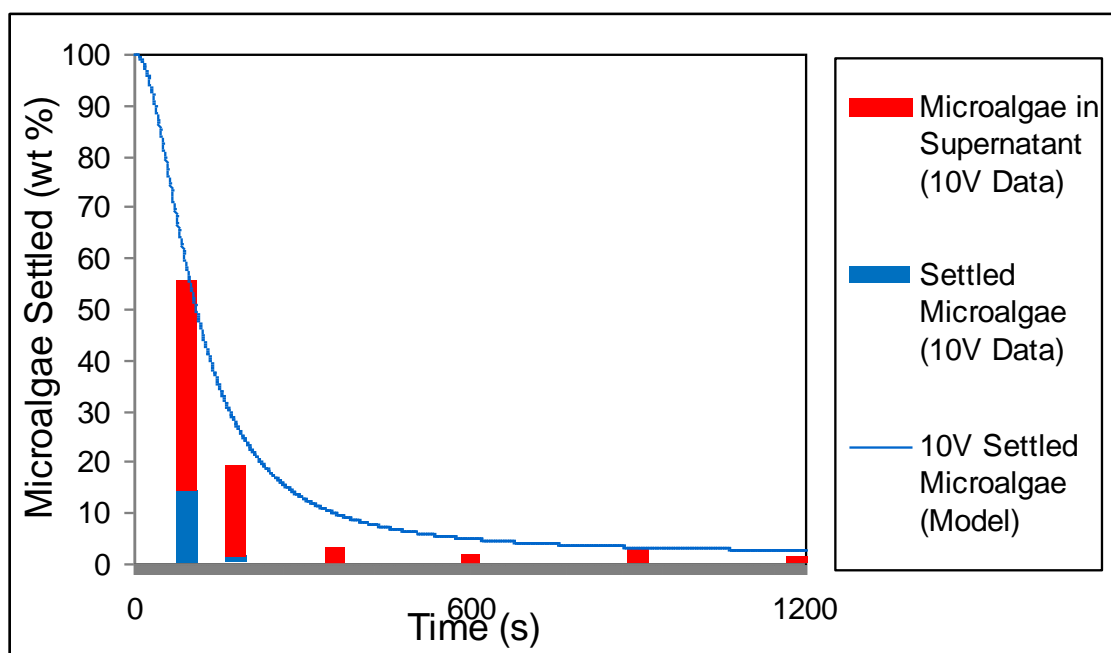
Figure 6. 51. Comparison of microalgae settling for model and experimental data for electrocoagulation of *Chlorococcum sp.* with the stainless steel anode at 10 V.
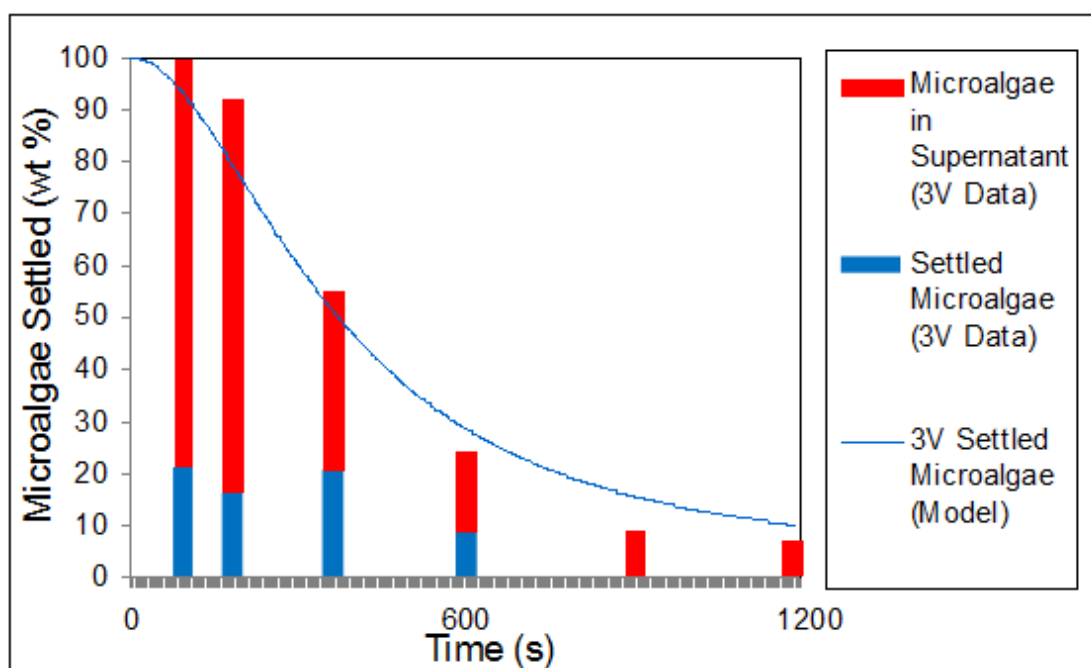
Figure 6. 52. Comparison of microalgae settling for model and experimental data for electrocoagulation of *Tetraselmis sp.* with the stainless steel anode at 3 V.
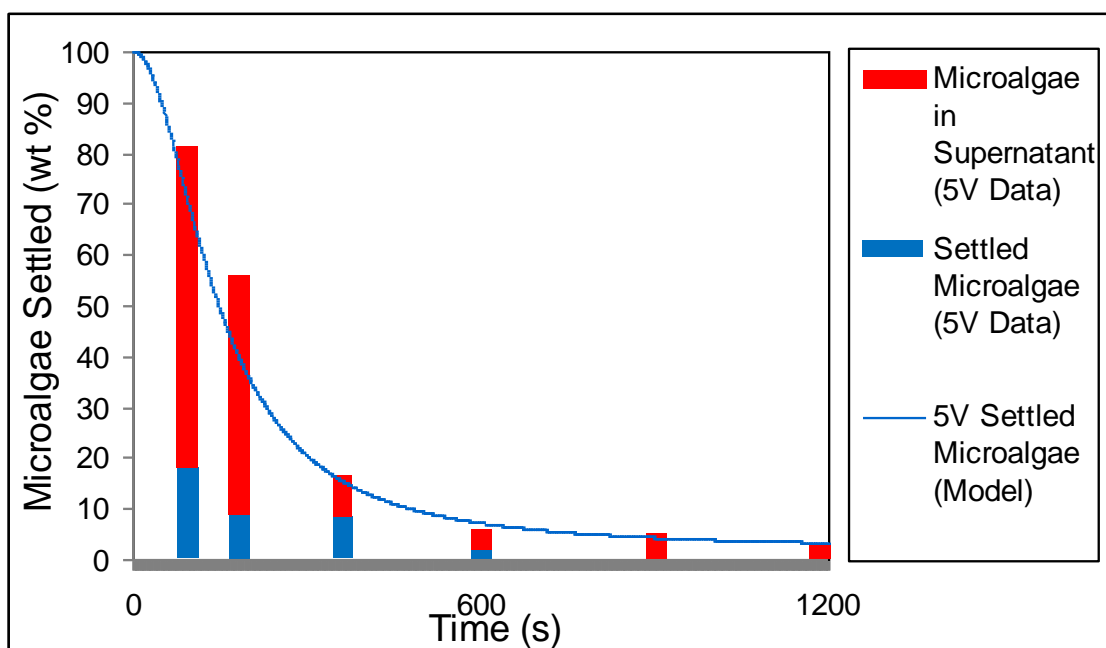
Figure 6. 53. Comparison of microalgae settling for model and experimental data for electrocoagulation of *Tetraselmis sp.* with the stainless steel anode at 5 V.

175
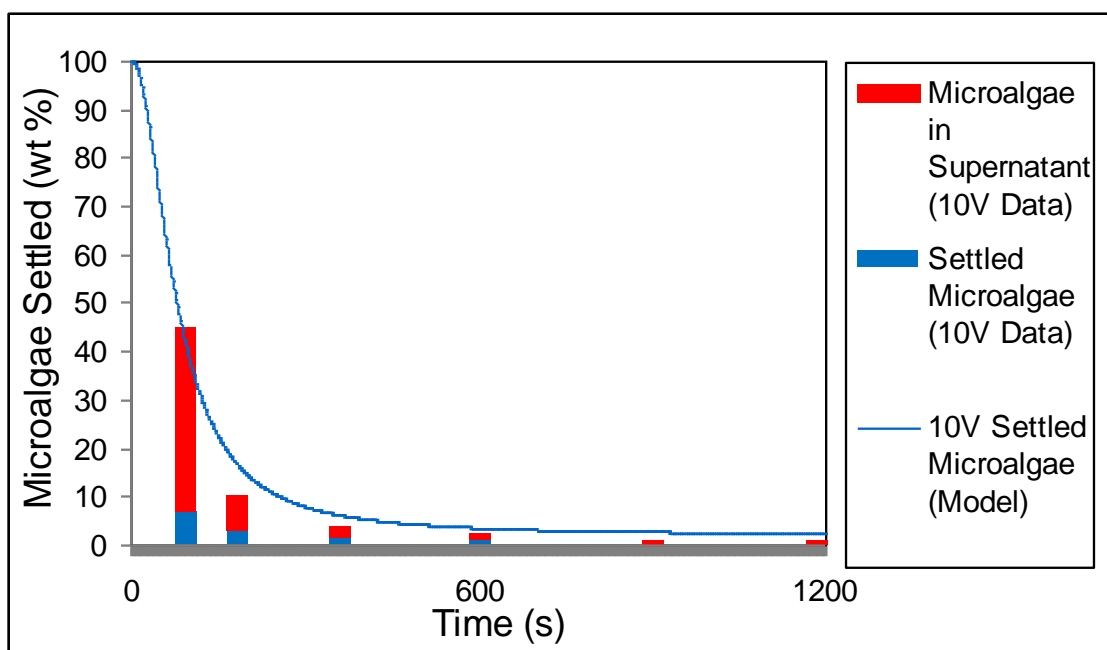
Figure 6. 54. Comparison of microalgae settling for model and experimental data for electrocoagulation of *Tetraselmis sp.* with the stainless steel anode at 10 V.
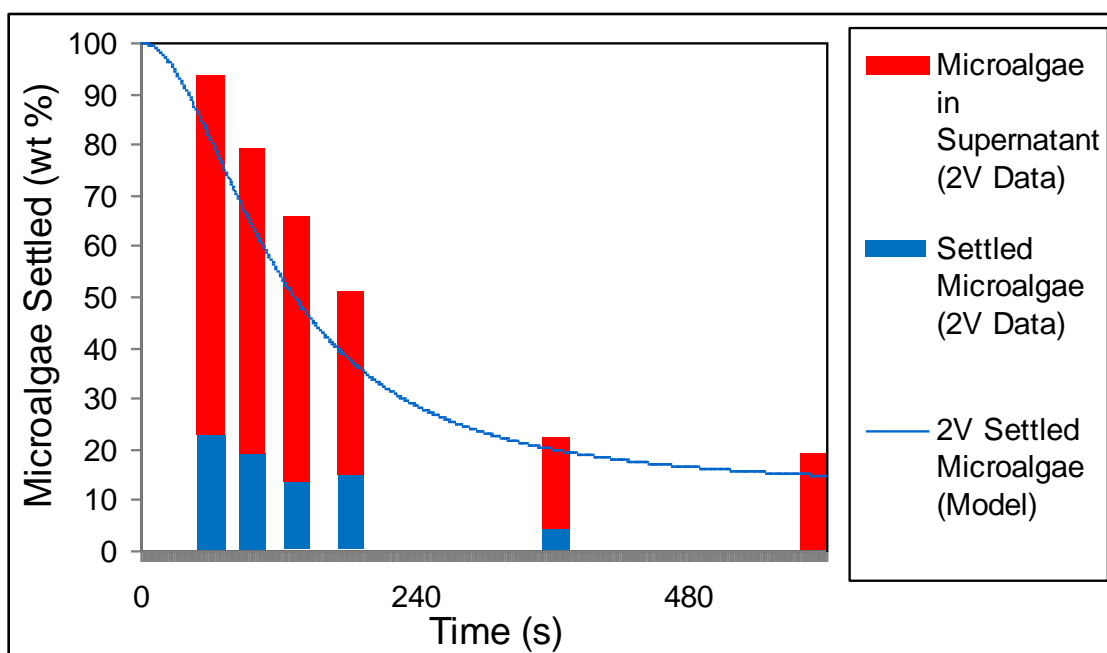
Figure 6. 55. Comparison of microalgae settling for model and experimental data for electrocoagulation of *Chlorococcum sp.* with the aluminium anode at 2 V.
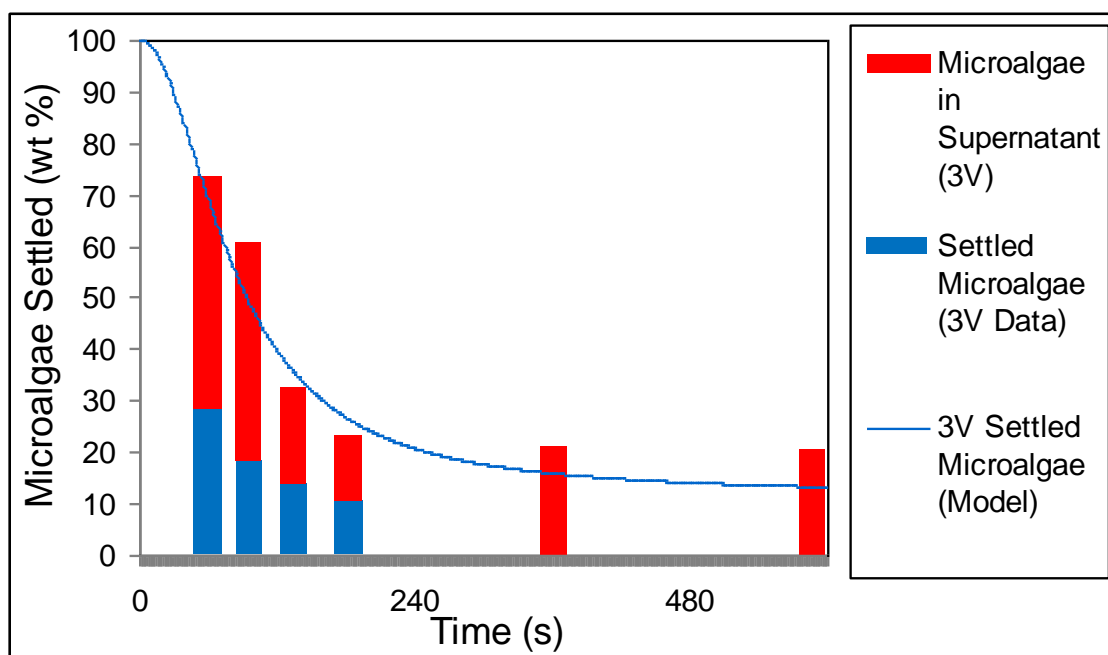
Figure 6. 56. Comparison of microalgae settling for model and experimental data for electrocoagulation of *Chlorococcum sp.* with the aluminium anode at 3 V.
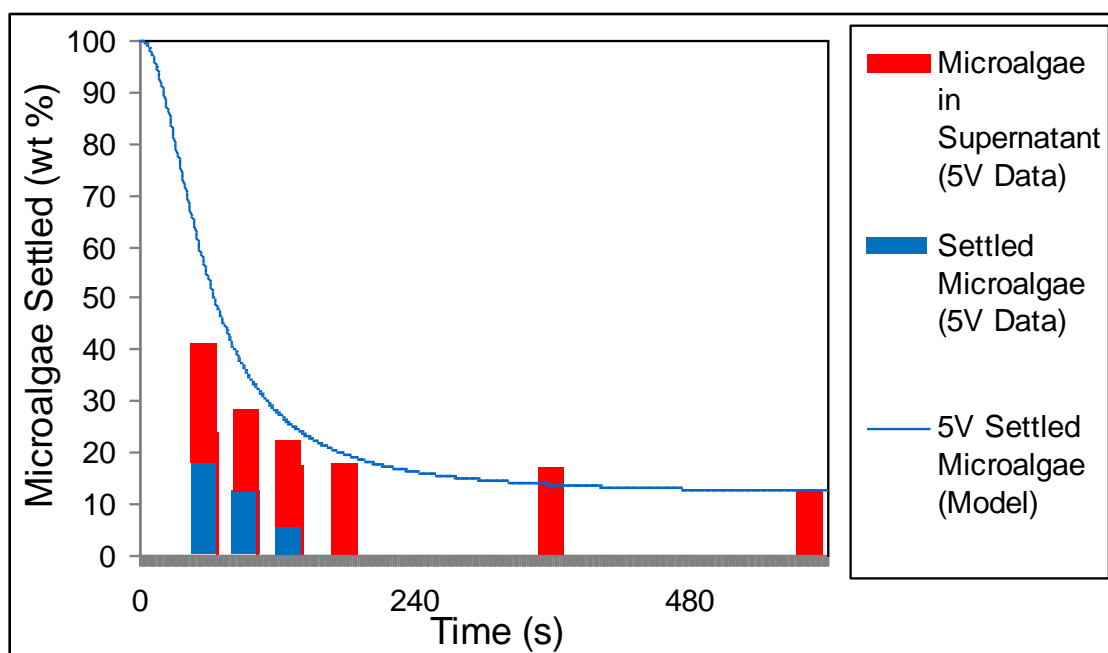
Figure 6. 57. Comparison of microalgae settling for model and experimental data for electrocoagulation of *Chlorococcum sp.* with the aluminium anode at 5 V.
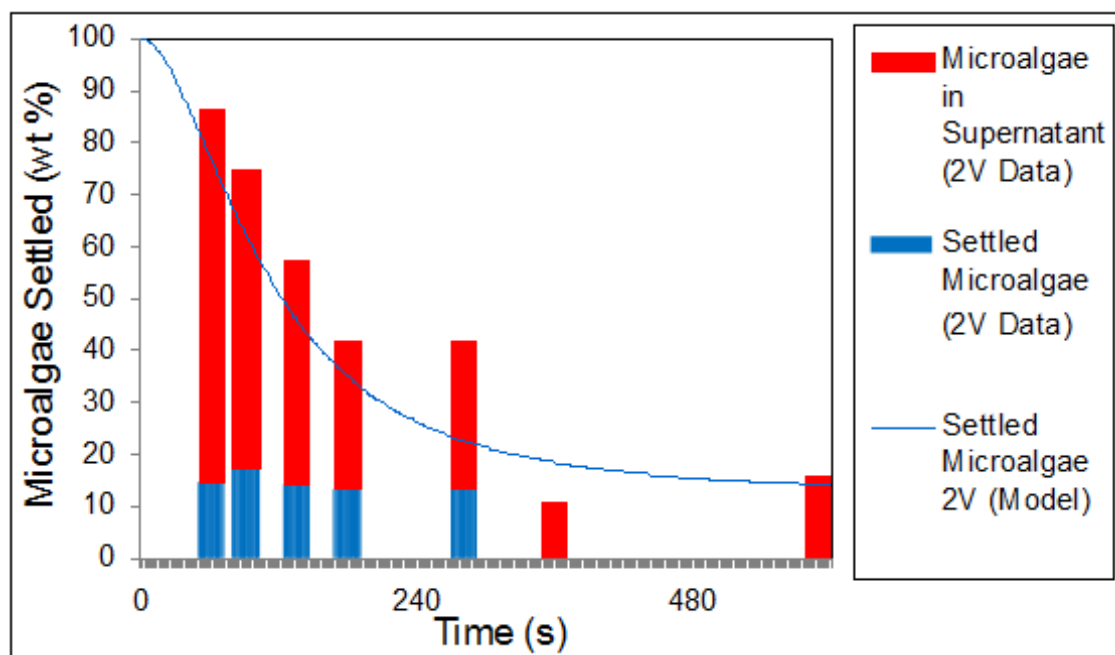
Figure 6. 58. Comparison of microalgae settling for model and experimental data for electrocoagulation of *Tetraselmis sp.* with the aluminium anode at 2 V.
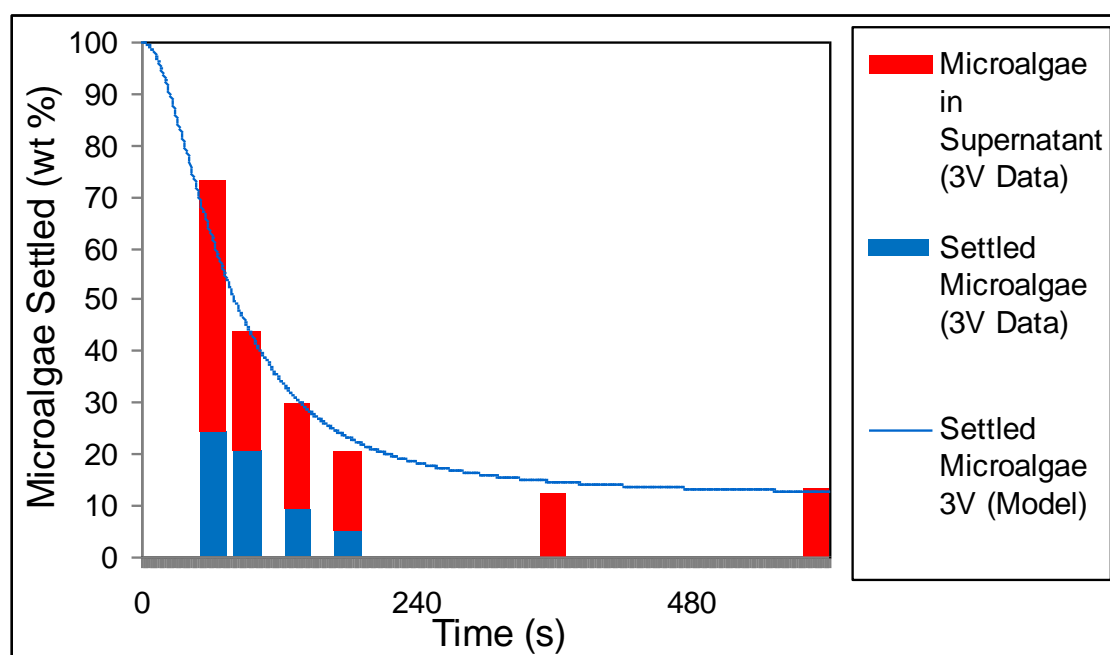
Figure 6. 59. Comparison of microalgae settling for model and experimental data for electrocoagulation of *Tetraselmis sp.* with the aluminium anode at 3 V.

178
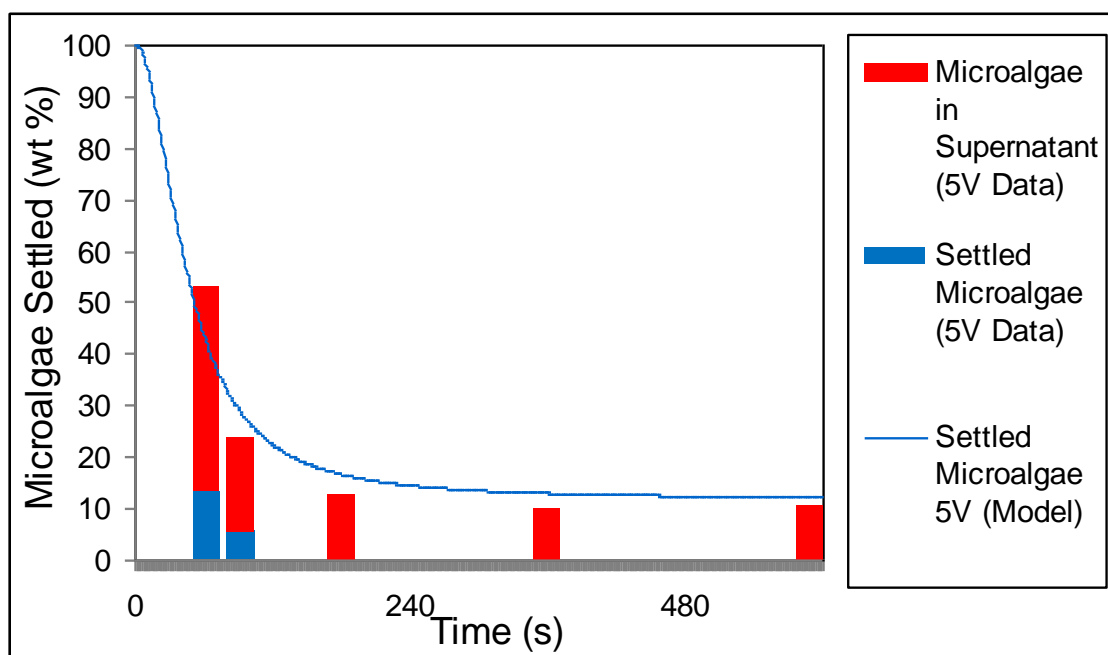
Figure 6. 60. Comparison of microalgae settling for model and experimental data for electrocoagulation of *Tetraselmis sp.* with the aluminium anode at 5 V.

6.7 Rate Limiting Step and Electrocoagulation Efficiency

6.7.1 Electrocoagulation Rate Limiting Step

The two main factors that influence the amount of recovery of microalgae is the use of the metal cation as a coagulant and the hydrogen gas as a flotation agent.

Separation of microalgae by electrocoagulation is partly dependant on the ability of the metal cation to adsorb to the microalgae surface. Without this step, the microalgae can not coagulate. The influence of the rate of metal adsorption onto the microalgae surface was investigated using the mathematical model. Figure 6.61 and 6.62 show the predicted recovery for electrocoagulation of *Chlorococcum sp.* with the stainless steel anode at 3 V and 10 V. From figures 6.61 and 6.62, it can be seen that increasing the rate constant k, gives faster recovery at lower run times, enabling the maximum recovery to be achieved in significantly shorter times.

179
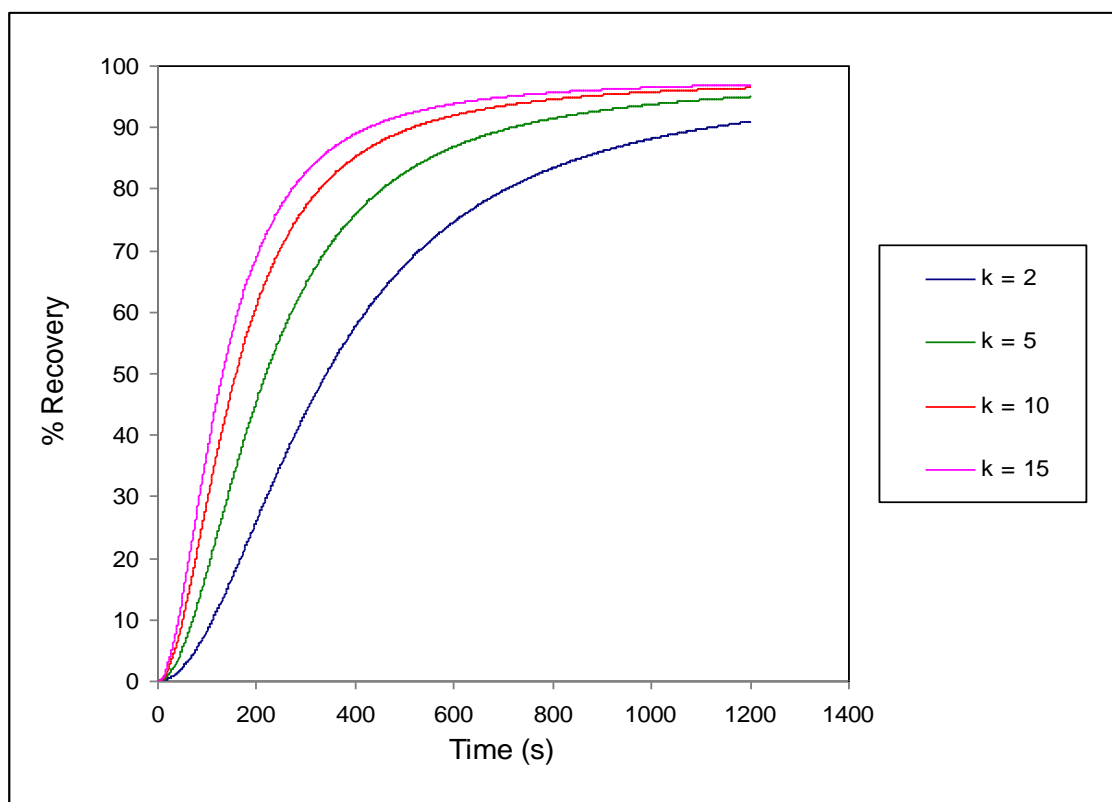
Figure 6. 61. Predicted recovery from model versus time with varying k values (all other parameters unchanged), for electrocoagulation of *Chlorococcum sp*. with the stainless steel anode at 3 V.
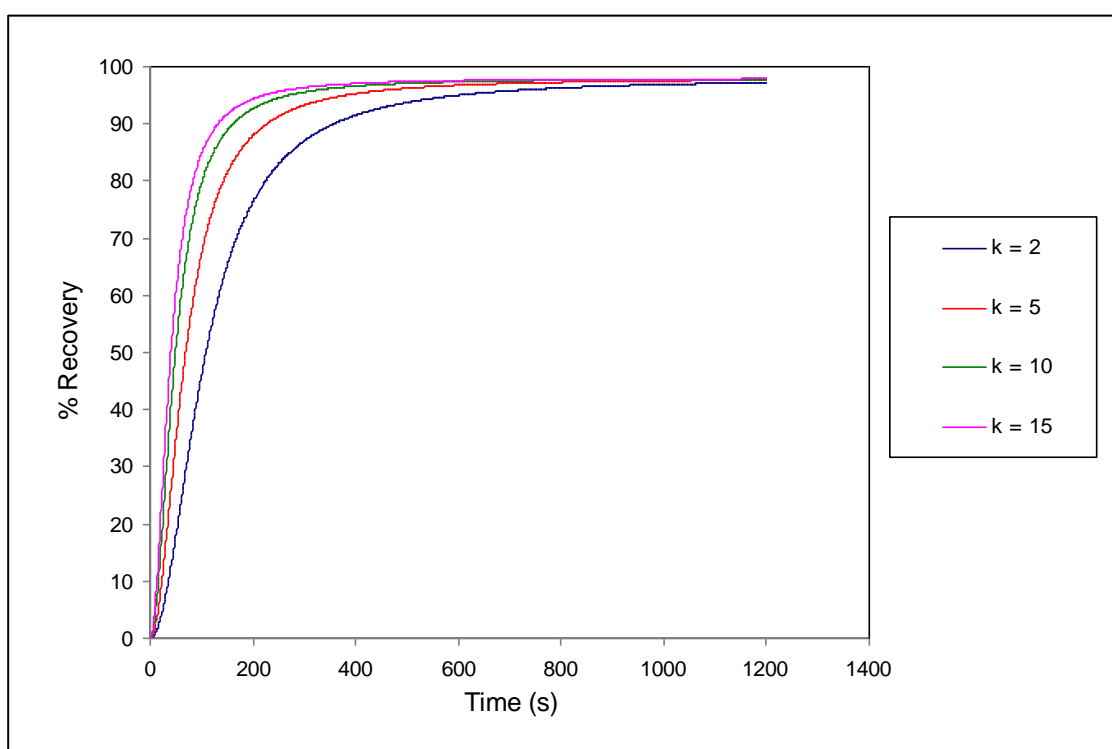
Figure 6. 62. Predicted recovery from model versus time with varying k values (all other parameters unchanged), for electrocoagulation of *Chlorococcum sp*. with the stainless steel anode at 10 V.

The model can also be used to investigate the amount of microalgae recovery possible when a greater percentage of hydrogen bubbles are able to attach to the flocs. The value of x_{max} in equation 6.14 will determine the maximum amount of hydrogen gas attached to the microalgae flocs at a given time. The time at which the hydrogen starts to float the flocculated microalgae will is used to determine x_{max}. Figure 6.63 and 6.64 show the predicted recovery for electrocoagulation of *Chlorococcum sp.* at different starting times for flotation, with the stainless steel anode at 3 V and 10 V. It can be seen from the figures that decreasing the flotation starting time in equation 6.14 results in an increase in the proportion of hydrogen gas used for flotation, which leads to more hydrogen gas attached to the flocs, seen by an increase in the rate of recovery of microalgae. However, the degree to which the flotation starting time has an effect on the recovery does not have as large an impact as changing the k value.
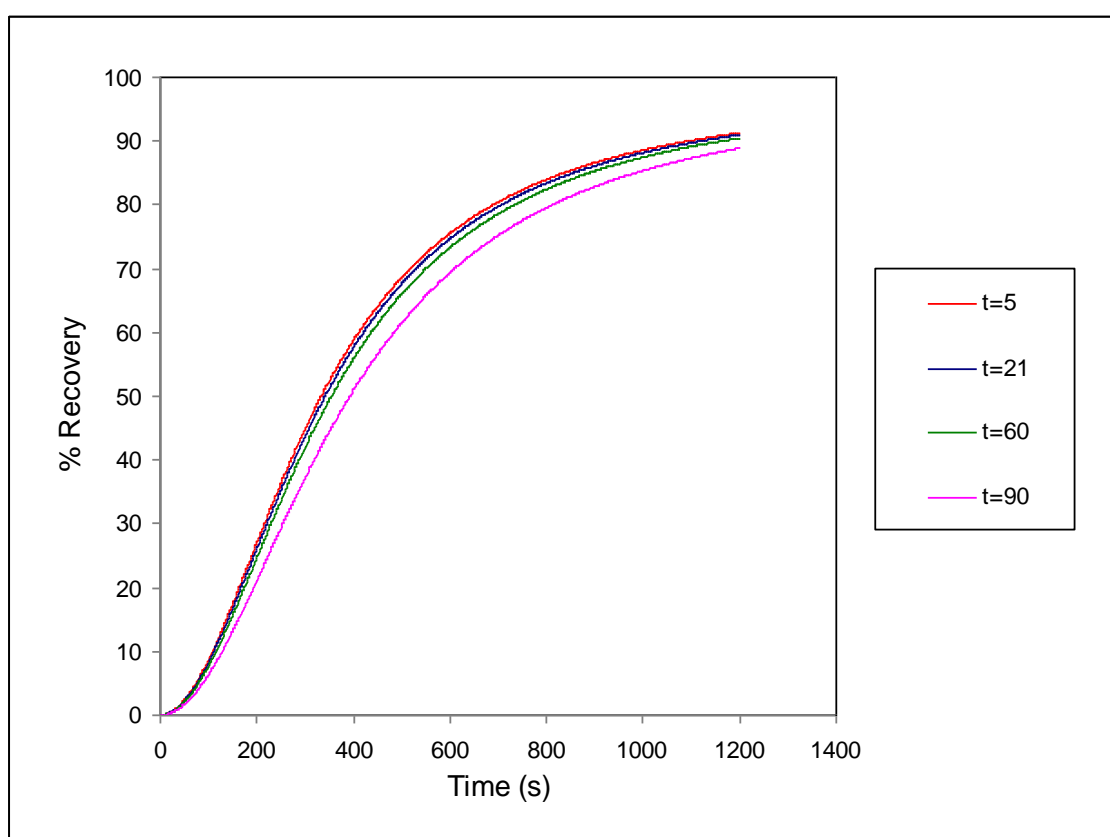
Figure 6. 63. Predicted recovery from model versus time with varying flotation start time values (all other parameters unchanged), for electrocoagulation of *Chlorococcum sp.* with the stainless steel anode at 3 V.
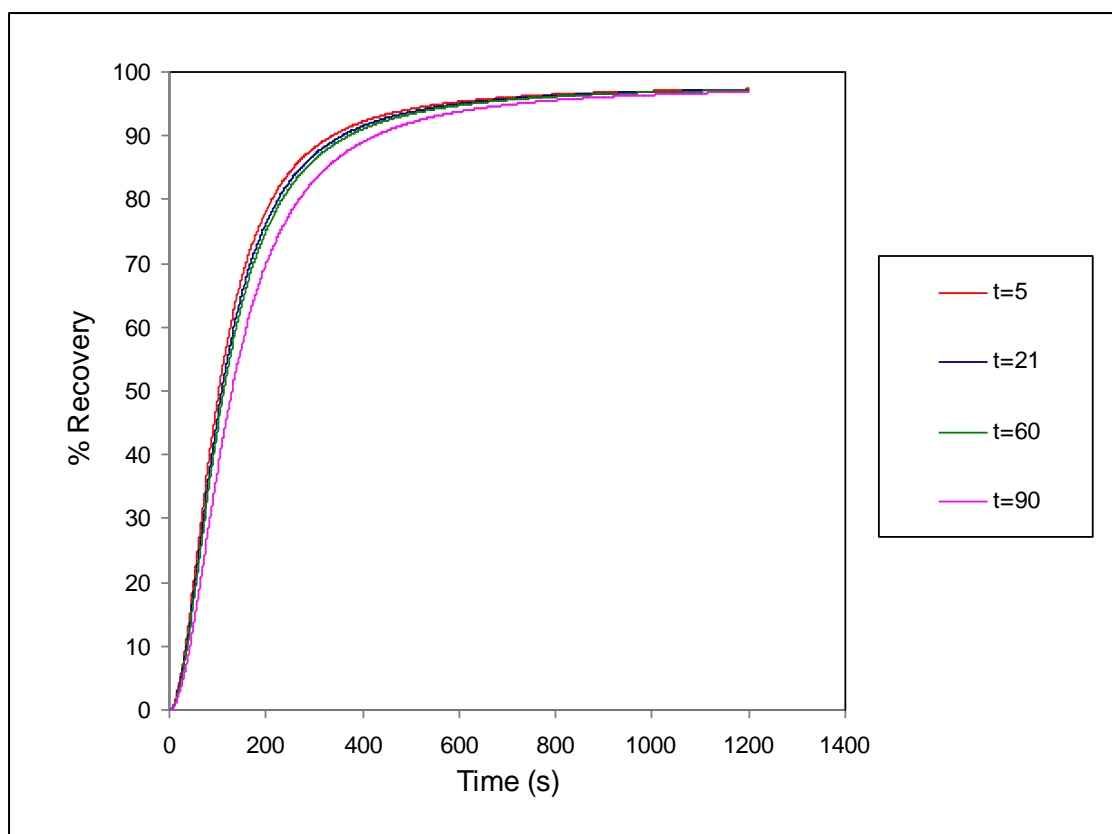
Figure 6. 64. Predicted recovery from model versus time with varying flotation start time values (all other parameters unchanged), for electrocoagulation of *Chlorococcum sp*. with the stainless steel anode at 3 V.

Based on the predictions made by the model and the information gathered from the experimental results, it is clear that electrocoagulation as a recovery technique relies on both the coagulation and flotation of microalgae. Both these steps are dependent on the amount of mass transfer i.e. stirring that is present in the system. It was shown in section 6.4.2 that increasing the stirring of the electrocoagulation system caused a significant increase in the recovery of microalgae. This stirring effect was modelled by increasing the value of k. Figure 6.65 shows that adjusting the model with a 10 fold increase in the value of k results in recovery of microalgae that matches the recovery when the system is stirred. This result emphasises the importance of the parameter k. Therefore, it can be concluded that the rate limiting step is the degree to which coagulation of microalgae occurs due to metal ion adsorption.
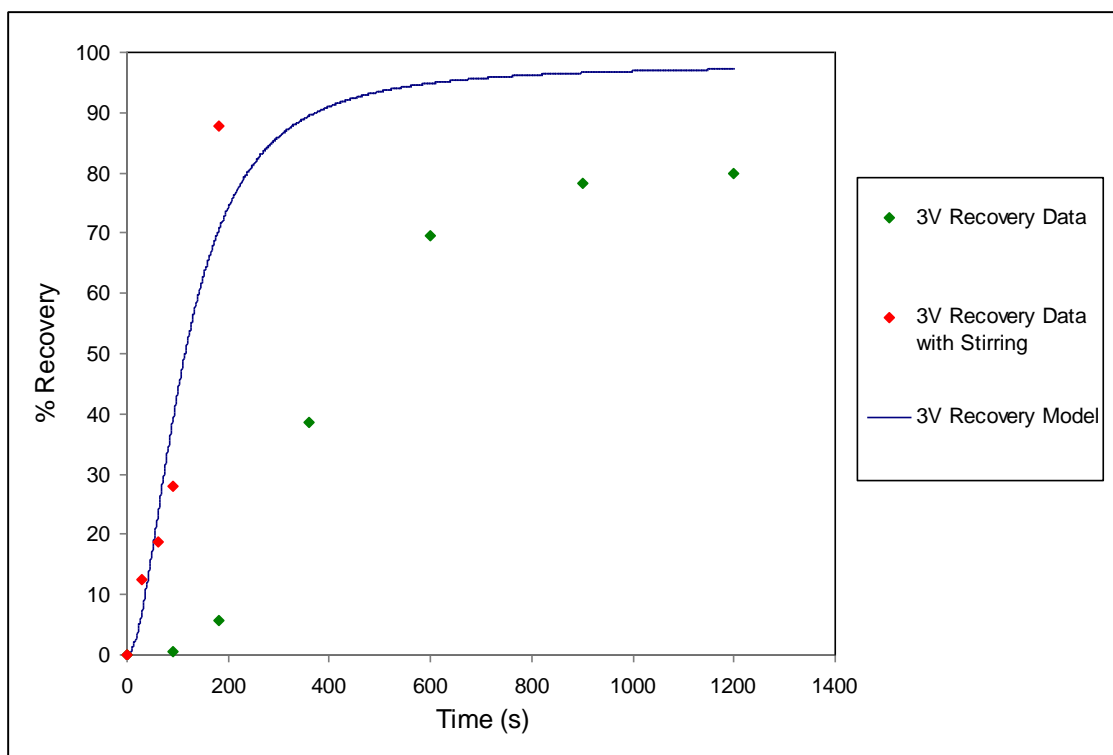
Figure 6. 65 . Predicted recovery from model for electrocoagulation with stirring (k = 20), for *Chlorococcum sp.* with the stainless steel 430 anode at 3 V.

6.7.2 Inefficiencies of Electrocoagulation and Comparison to Alum Flocculation

Like electrocoagulation, flocculation with cationic flocculants also uses charge neutralisation as the mechanism of action for microalgae recovery. Alum flocculation is similar to electrocoagulation with aluminium anodes as both techniques use a positive aluminium ion species as the means of charge neutralisation and coagulation. The main difference being the energy input required for electrocoagulation and the fact that the alum flocculated microalgae does not have a means to float to the surface of the system. From the results presented in chapter 4, it was observed that flocculation of microalgae with alum was able to achieve almost 100 % recovery (99 % with *Chlorococcum sp.* and 91 % with *Tetraselmis sp.*). The maximum recovery obtained for electrocoagulation with aluminium anodes was 88 % with *Chlorococcum sp.* and 89 % with *Tetraselmis sp*. During electrocoagulation, the pH at the cathode becomes basic due to H^+ ions being converted into hydrogen gas. At the anode, the pH becomes acidic due to OH^- ions forming $Al(OH)_m^{n+}$ species.

The overall pH change was seen to decrease with time as shown in the results in chapter 5. The inability to reach 100 % recovery may be due to the drop in pH associated with the longer run times.

There are two main inefficiencies of the electrocoagulation process. The first is the excess metal produced at the anode. The electrocoagulation results have shown that the addition of aluminium ions into the system will continue to neutralise and flocculate microalgae until the saturation point is reached. All metal ions produced from that point onwards are in excess and remains in solution. This observation was also made in the alum flocculation experiments, where the recovery was seen to plateau after a certain dosage. This inefficiency can be overcome by determining the saturation point of the microalgae and adding the corresponding amount of aluminium species into the system. For alum flocculation, this would simply mean adjusting the addition of alum that gives the maximum recovery at the lowest dose (before the recovery starts to plateau). However, for electrocoagulation, the process is more complex and involves improving the mass transfer of the metal ions in order to achieve faster flocculation. If there are more collisions between the microalgae cells and the metal ions, there will be faster neutralisation and hence faster flocculation. This can be achieved with stirring. It can be assumed that alum flocculation has adequate stirring to accomplish fast mass transfer, as the jar stirrer protocol involves a fast mix at 100 rpm for 1 min followed by a slow mix at 60 rpm for 4 min.

The second inefficiency is the low level of attachment of hydrogen bubbles to flocs. As explained in the previous section, the percentage of hydrogen gas attached to the flocs can affect the recovery of microalgae. This inefficiency can be observed in particular at low voltage and run times (seen from the lag in recovery). During these conditions, the hydrogen bubbles produced are wasted due to the low mixing conditions. This can be overcome by introducing additional stirring into the system. Stirring will increase the rate of microalgae coagulation and also increase the attachment of hydrogen bubbles, resulting in a higher recovery.

If the electrocoagulation process could be optimised in order to achieve an increased rate of coagulation and a high proportion of hydrogen gas used to float the flocs, the process would be more efficient and comparable with alum flocculation. As will be discussed in chapter 7, this would lead to savings in the energy costs and associated carbon dioxide emissions compared to conventional centrifugation dewatering and alum flocculation. Figures 6.66 and 6.67 show the recovery of microalgae versus the energy required per mass of flocculated microalgae. These figures can be used to determine the optimal electrocoagulation energy conditions, i.e. the lowest energy input per mass of flocculated microalgae corresponding to the highest recovery. For electrocoagulation using the aluminium anode, the optimal condition is 2 V with a run time of 360 s.
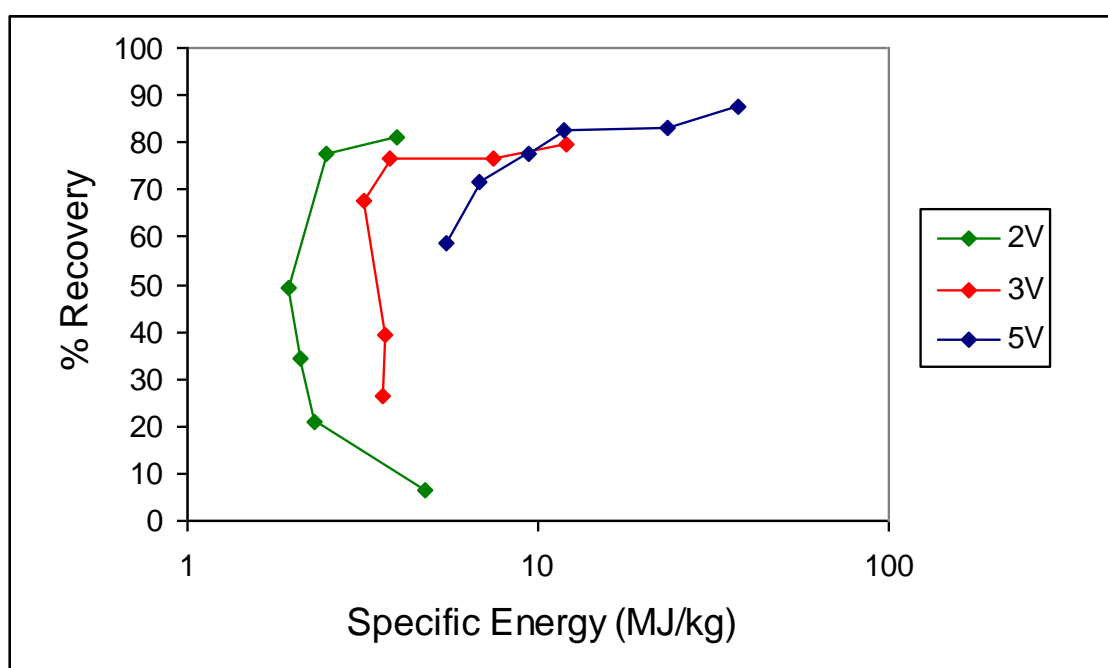
Figure 6. 66. Percentage recovery of microalgae versus energy required per kg of flocculated microalgae, for electrocoagulation of *Chlorococcum sp.* with the aluminium anode.
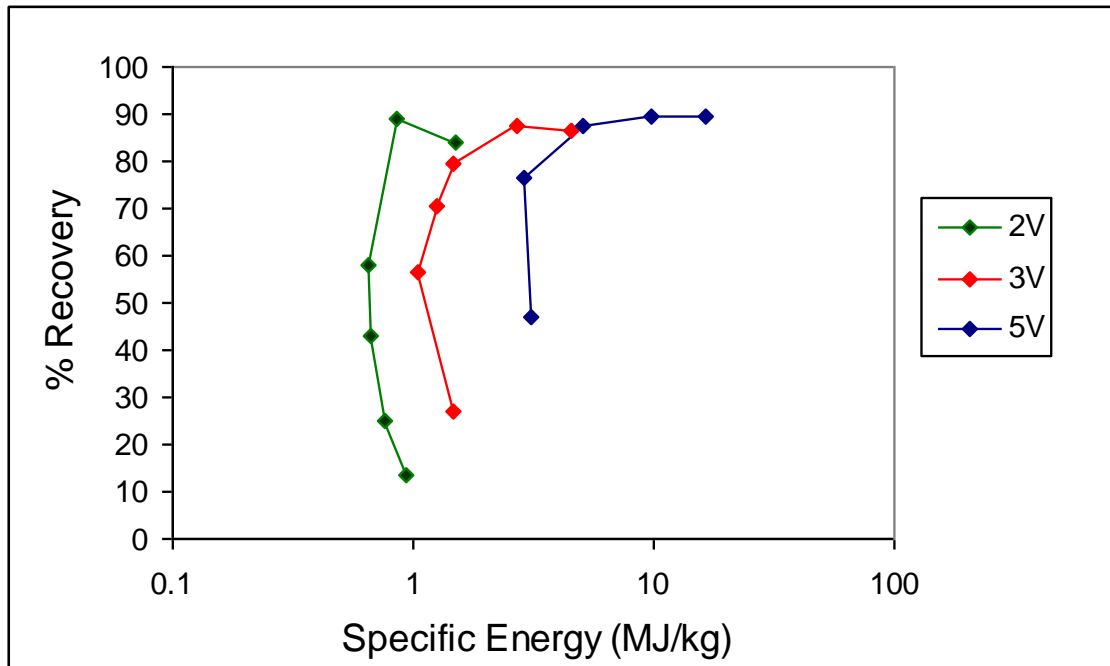
Figure 6. 67. Percentage recovery of microalgae versus energy required per kg of flocculated microalgae, for electrocoagulation of *Tetraselmis sp.* with the aluminium anode.

As discussed earlier, if stirring was added to the system, the rate of coagulation and hydrogen bubble attachment can be increased, giving an increased amount of microalgae recovery. At the optimum energy condition of 2 V, the mathematical model can be used to show that the microalgae recovery can reach the maximum value of 88 % (assuming that the optimum k and x_t values correspond to conditions that incorporate the additional stirring). Figure 6.68 shows results predicted by the model with electrocoagulation of *Chlorococcum sp.* at 2 V. It can be seen that for electrocoagulation at 2 V (using model parameters k = 500 and flotation starting at 5 s), the maximum recovery can be obtained at 360 s.
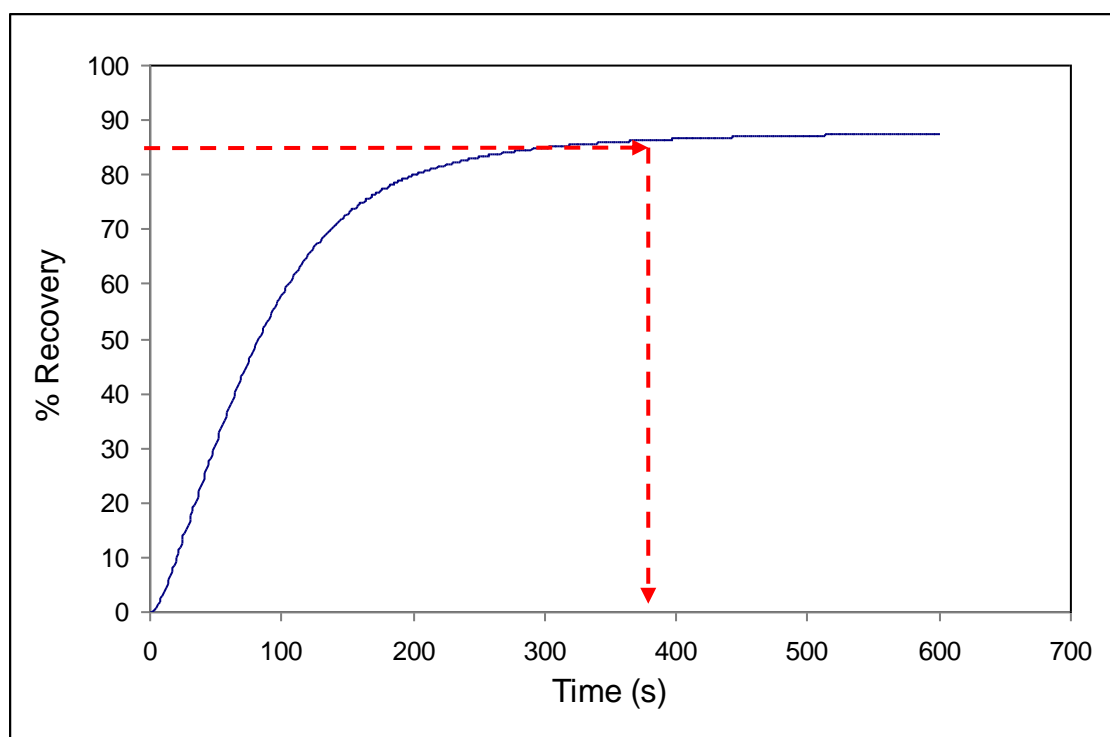
Figure 6. 68. Percent recovery versus time predicted by model for electrocoagulation of *Chlorococcum sp.* at 2 V with the aluminium anode (k = 500 and flotation starting at 5 s).

6.8 Electrocoagulation Experimental Conclusions

This research explored the batch electrocoagulation of two marine species of microalgae. Successful recovery was obtained for both microalgal species with both the aluminium and stainless steel 430 anodes. The results showed that although the highest maximum recovery of microalgae was achieved with the stainless steel 430 anode. Electrocoagulation with the aluminium anode was more efficient, being able to reach the maximum recovery at a faster rate.

This research involved the investigation of work that aimed at closing the research gaps found with electrocoagulation studies to date. The mechanisms of the electrocoagulation process were demonstrated and proven in this work and was found to agree with what has been previously presented by other researchers. This includes evidence of the adsorption of coagulating species onto the microalgae surface and microalgae floc/bubble attachment. A mathematical model was developed that was able to predict successfully the percentage of flotation and

187

recovery of microalgae and the percentage of settled microalgae for a given electrocoagulation condition. The coagulation model was first order with respect to the metal ion concentration, but second order with respect to the algae concentration. The rate limiting step of the electrocoagulation process was found to be the microalgae coagulation reaction which was compromised by insufficient agitation.

Electrocoagulation was found to be successful in recovering algae but not very efficient. Although high recovery values can be obtained, the electrocoagulation conditions which give these recovery values produce excess metal ions and hydrogen gas which is directly related to surplus use of current, hence the energy related to the process is unnecessarily high. Excess metal ions produced in the system means that there is an unnecessary consumption of metal, which will increase the cost of materials required for the process. These inefficiencies can be reduced by introducing additional stirring into the system. Stirring will increase the rate of coagulation and hydrogen bubble attachment resulting in higher recovery of microalgae. Furthermore, the batch nature of the process means that the use of electricity and the dissolution of metal towards the end of the electrolysis process are only achieving a small additional recovery and the development of a continuous process may overcome these inefficiencies.

Alum flocculation has a similar coagulation mechanism to electrocoagulation with the aluminium anode. The optimum energy per kg flocculated microalgae was calculated and modelled assuming the conditions included additional mixing in the system. The following chapter will investigate and compare the energy, costs and carbon dioxide emissions associated with these dewatering techniques at optimum conditions.

CHAPTER 7 ENERGY, CARBON DIOXIDE EMISSIONS AND COST EVALUATION OF DEWATERING TECHNOLOGIES

7.1 Scope of Dewatering Assessment

Life cycle assessment is a technique that is used to assess the environmental aspects and potential impacts that are associated with a product life cycle. This involves looking into the relevant inputs and outputs of a system and evaluating the potential impacts that are associated with these inputs and outputs. These environmental aspects are studied throughout the life of the product i.e. from raw material acquisition to the manufacture of the product through to its use and eventual disposal.

A life cycle assessment of microalgae for biodiesel production conducted by Sander, K. and Murthy, G.S. (2010) outlined that for every 24 kg of microalgae biodiesel produced, 34 kg of co products were produced. The unit process that resulted in the highest energy demand were harvesting and dewatering. The total energy input without the use of solar drying were 3292 MJ when dewatering with a filter press and 6194 MJ for the centrifuge dewatering process. Table 7.1 presents the energy demand and carbon dioxide emissions associated with the different stages of biodiesel production from microalgae, on the basis of 24 kg of biodiesel for dewatering with centrifugation and natural gas drying. The dryer requires 3.56 MJ/kg of water removed and the dry algae produced has a density of 1000 kg/m^3. The life cycle assessment illustrated the significance of the dewatering stage of the process and that there was a need for the improvement of dewatering technologies to make microalgae biodiesels less energy intensive and more commercially viable.

Table 7. 1. Energy demand and carbon dioxide emissions for different unit processes in the production of biodiesel from microalgae, on a basis of 24 kg biodiesel (Sander, K. and Murthy, G. S. 2010).

Unit Process	Energy Demand (MJ)	CO_2 Emissions (kg)
Growth and Culturing	15.43	0.00
Harvesting: centrifuge / natural gas dryer	5743.32	398.48
Separation/Lipid Extraction	165.03	6.33
Transportation	8.79	0.65
Biodiesel Conversion	36.02	3.18
Biodiesel Transport and Distribution	9.66	0.66

Life cycle assessment data combined with experimental data from this research was used to determine the energy requirements, carbon dioxide emissions and costs for the selected dewatering technologies. Figure 7.1 shows the process flow diagram for microalgae sourced biodiesel.
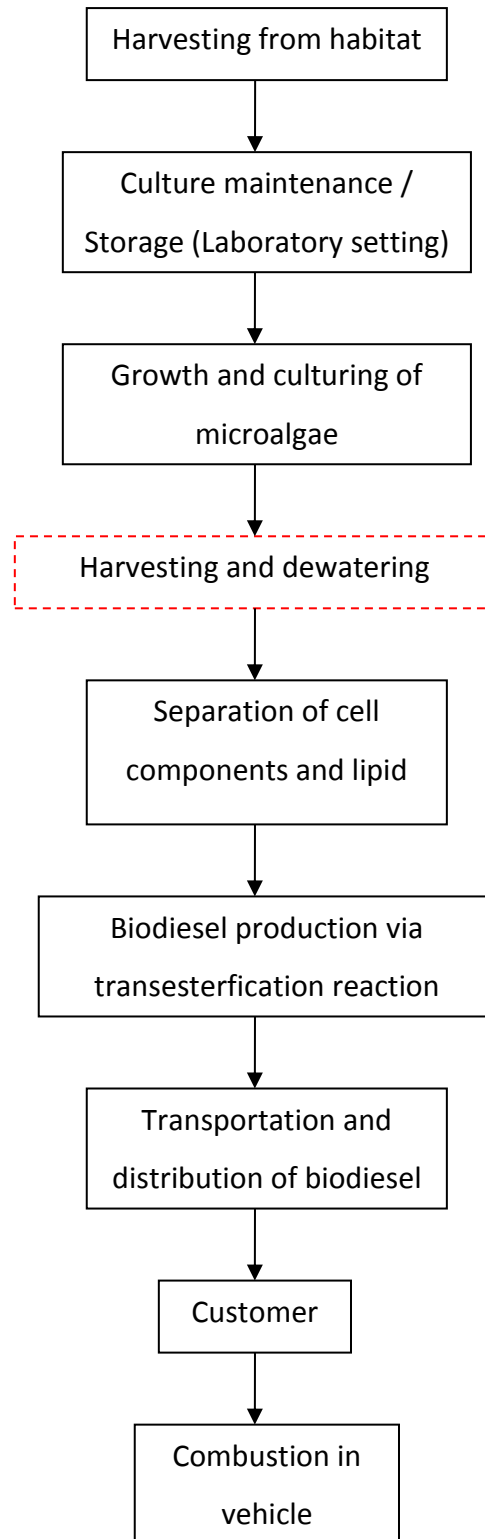
Figure 7. 1. Process flow diagram of microalgae sourced biodiesel.

The chosen dewatering technologies were centrifugation as a single harvesting step, as it is the most conventional method used in the industry, batch electrocoagulation with aluminium anodes coupled with centrifugation and alum flocculation coupled with centrifugation. Figure 7.2 shows a block diagram of each dewatering method. Aluminium anodes were chosen over stainless steel 430 anodes for several reasons which were concluded based on the experimental work presented in chapter 6. From the work detailed in chapter 6, it was found that coagulation of microalgae occurred at a faster rate with aluminium anodes, seen from the Zeta potential results showing microalgae becoming more electropositive at a faster rate. The maximum recovery of microalgae was obtained at shorter run times with aluminium anodes. The mass of aluminium dissolved was also measured to be lower than the mass of iron dissolved from the stainless steel 430 anode at the same electrocoagulation conditions.

A)

Dilute Algae → [Centrifuge] → Concentrated Algae

↓

Extremely Dilute Algae

B)

Dilute Algae → [Electrocoagulation (Step 1)] → [Centrifuge (Step 2)] → Concentrated Algae

↓ Extremely Dilute Algae   ↓ Extremely Dilute Algae

C)

Dilute Algae → [Alum Flocculation (Step 1)] → [Centrifuge (Step 2)] → Concentrated Algae

↓ Extremely Dilute Algae   ↓ Extremely Dilute Algae
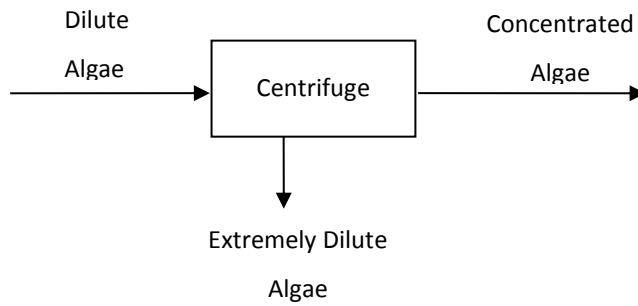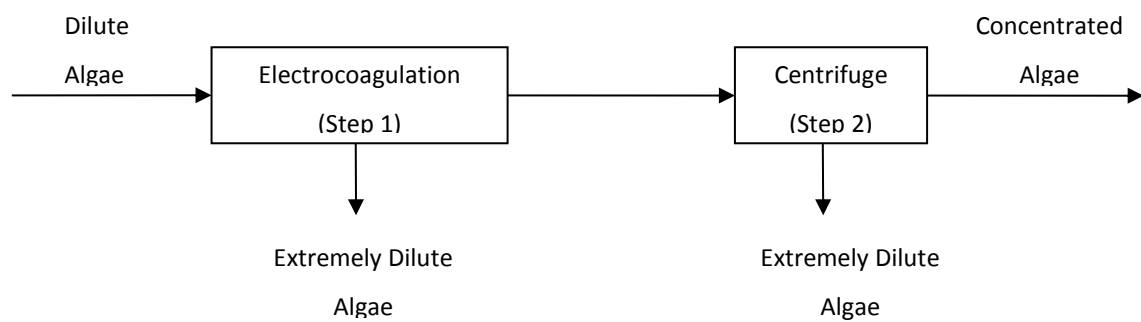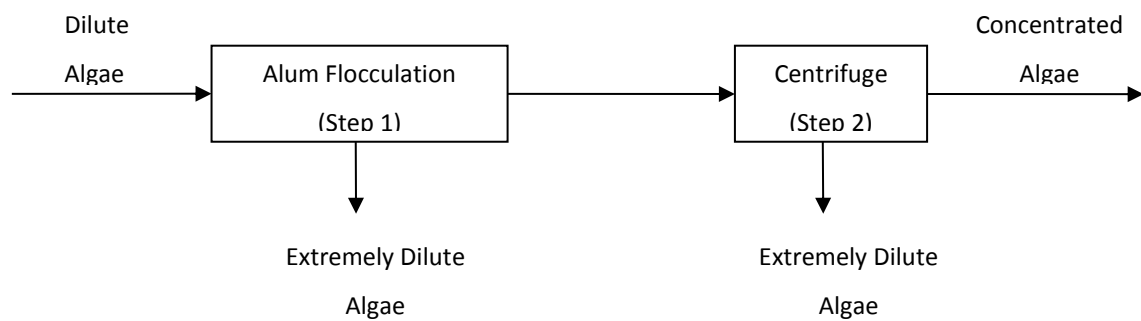
Figure 7. 2. Block diagram of one - step dewatering of microalgae via: A) centrifugation, and two-step dewatering of microalgae via: B) Electrocoagulation and centrifugation, C) Alum flocculation and centrifugation.

The goal of this work was to determine baseline information on the energy input, carbon dioxide emissions and costs related to the three dewatering techniques chosen for analysis, i.e. centrifugation, electrocoagulation with aluminium anodes and alum flocculation. The functional unit (the measure of performance of the functional outputs of the system) was chosen as 1000 kg of microalgae mass in the

final slurry. The microalgae was to be taken from a concentration of 0.3 – 1 g/L (0.03 – 0.1 % TSS) to 120 g/L (12 % TSS).

7.2 Techno Economic Assessment of Dewatering Techniques

7.2.1 Assumptions

The following assumptions have been made to facilitate the analysis:

- The recovery from each dewatering method is either based on literature or taken from experimental data from this research.

- The final algae slurry has a concentration of approximately 12 % TSS or 120g/L (Shelef, G. et al. 1984).

- The centrifuge is able to concentrate algae up to a concentration factor of 120 (Mohn, F. H. 1980).

- The Hall Heroult process is used to produce aluminium metal for the anodes.

- The Bayer Process is used to make aluminium hydroxide to produce alum.

- The sulphuric acid used to produce alum is made from the contact process.

- Electricity consumed is generated from black coal with associated environmental impacts given by Norgate, T.E. and Rankin, W.J. (2001).

- Electrocoagulation energy required is based on the optimum conditions determined in section 6.7.2 in chapter 6.

- Aluminium metal dissolution and requirements are based on the batch experimental data.

- Alum flocculation dosage requirements are based on the batch experimental data.

7.2.2 System Boundary

The system boundary for this research includes only the harvesting and dewatering step of the biodiesel production process, outlined in a red dotted line in figure 7.1. Natural gas drying was not included in the system boundary due to the fact that

some lipid extraction systems don't require a drying system. The drying stage may be common to all three systems and there are a number of drying methods available, including techniques which are more energy efficient such as superheated steam drying.

7.2.3 Data Sources

The data sources used for this research are presented in table 7.2.

Table 7. 2. Data sources for energy, carbon dioxide and cost analysis.

Unit Process		Data Source [Reference]
Electricity price	$ 0.19/kWh	Penwell Power Engineering (2011)
Aluminium price	$ 2.2/kg	Metal News (2011)
Alum price	$ 0.17/kg	Alibaba 2012
Centrifugation final concentration	120 g/L	Shelef, G. et al. (1984)
Centrifuge energy requirement	1 kWh/m^3	Shelef, G. et al. (1984)
Electrocoagulation energy requirement	0.69 kWh/kg	Batch experimental data
Electrocoagulation concentration factor	x 6.3	Batch experimental data
Alum flocculation concentration factor	x 1.5	Batch experimental data
Energy to produce aluminium	58.61 kWh/kg	Norgate, T.E. and Rankin, W.J. (2001)
Energy to produce alum	3.06 x 10^{-4} kWh/kg	Arpke, A. and Hutzler, N. (2006)
Energy to produce aluminium hydroxide	4.5 kWh/kg	Aluminium Industry 2012
Energy to produce sulphuric acid	0.3 kWh/kg	Outotec 2012

7.3 Process Descriptions

Dewatering the freshly harvested microalgae is accomplished via a single or two-step dewatering process, as shown earlier in figure 7.2. The chosen dewatering technologies include:

- Centrifugation

- Electrocoagulation with aluminium anodes coupled with centrifugation

- Alum flocculation coupled with centrifugation

7.4 Discussion of Data

The results of the research of dewatering energy, carbon dioxide emissions and costs are summarised in table 7.3 for microalgae starting with a concentration of 0.3 g/L, which is the approximate concentration of the *Chlorococcum sp.* used in the batch electrocoagulation studies. Please refer to Appendix A.2.6 for detailed calculations.

For all dewatering methods, the energy and cost associated with raw material production was included. For microalgae dewatering by electrocoagulation, the energy and cost of aluminium production for the anode material was taken into account. The process of producing aluminium is most commonly performed by the Hall-Heroult process. For alum flocculation, the energy and cost associated with aluminium hydroxide and sulphuric acid production was taken into account. Aluminium hydroxide and sulphuric acid are reacted to produce alum. Aluminium hydroxide can be produced via the Bayer process, and sulphuric acid is produced in the contact process with single adsorption using sulphur, oxygen and water. Figure 7.3 and 7.4 show block diagrams depicting the aluminium and alum production process.
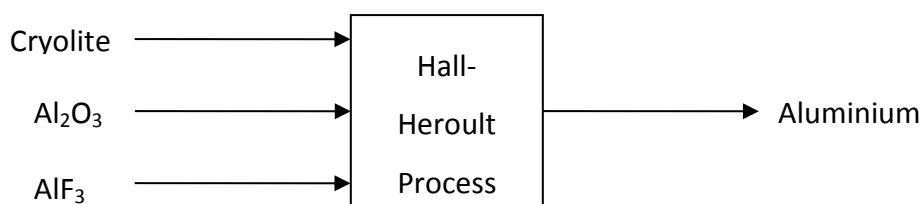
Figure 7. 3. Block diagram of simplified aluminium production process.
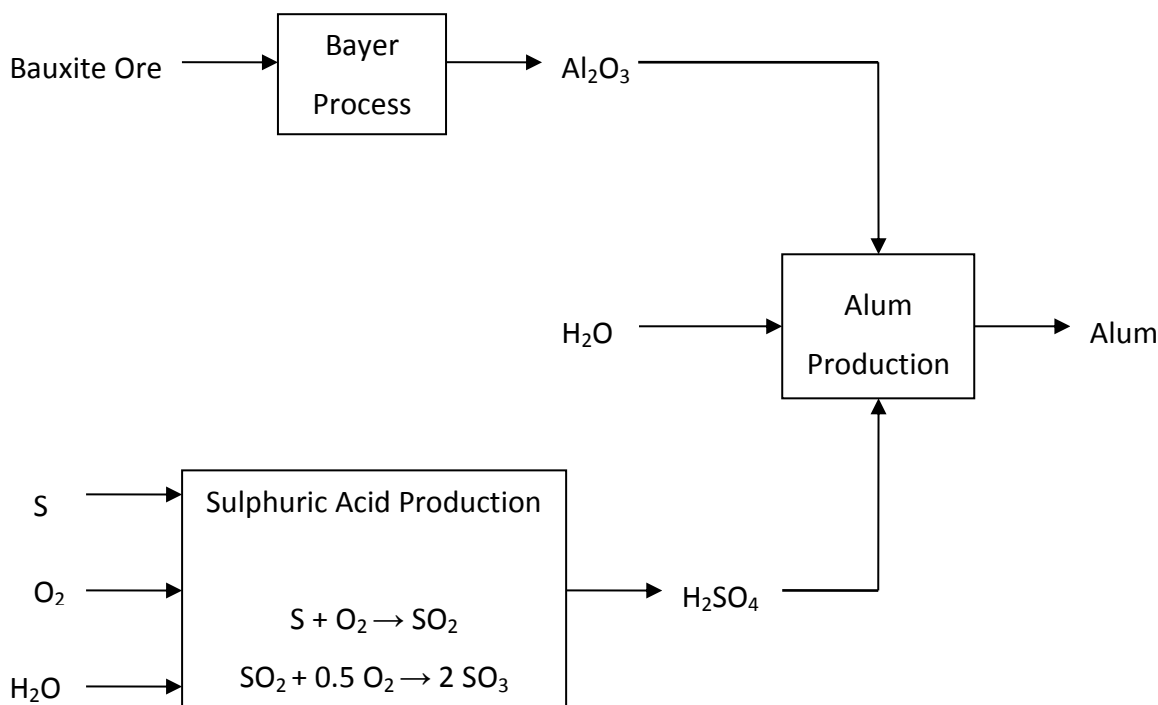
Figure 7. 4. Block diagram of alum production process.

Many studies have been conducted on the efficiency of electrocoagulation and alum flocculation as a dewatering technique, however these studies only take into account the energy and costs associated with the operation and do not take into account the energy and costs associated with raw material production. Vandamme, D. et al. (2011) obtained greater than 80 % recovery of marine microalgae with aluminium electrocoagulation consuming energy at 0.3 kWh/kg under optimum conditions. Can, O.T. et al. (2006) conducted studies on the removal of COD from wastewater with alum flocculation and electrocoagulation with aluminium anode. Electrocoagulation required an energy demand of 1.2 kWh/kg COD and an operating

cost of \$0.31/kg COD. Alum flocculation required an energy demand of 0.02 kWh/kg COD and an operating cost of \$0.08 /kg COD.

Table 7. 3. Dewatering energy demand, carbon dioxide emissions and costs for two-step dewatering processes using microalgae at concentration 0.3 g/L.

Unit Process		Energy Demand (MJ)	CO_2 Emissions (kg)	Cost (USD)
Centrifuge	Centrifugation	13300	3790	687
Electrocoagulation / Centrifuge	Centrifugation	2120	602	109
	Al production	32000	3090	1980
	Electrocoagulation	3140	17.0	162
	Total	37200	3700	2250
Alum Flocculation / Centrifuge	Centrifugation	2670	758	137
	Alum flocculation	2.2E-01	6.4E-02	1.2E-02
	Alum production	1010	286	30.0
	Total	3670	1040	167

Table 7.3 shows a breakdown of the energy demand, carbon dioxide emissions and cost for each dewatering process explored. The results in table 7.3 show that the energy required, carbon dioxide emitted and cost are all the highest for the electrocoagulation/centrifugation dewatering technique. Literature has stated that electrocoagulation is a promising technique due to the low energy requirement, however after incorporating the energy and costs associated with the anode material production, the resulting energy demand and costs are increased significantly. The alum flocculation/centrifuge process seems by far the most attractive, showing significantly lower values for each parameter in comparison to the other processes. Early alum flocculation studies would have deemed this method of dewatering unsuitable for marine microalgae species due to the high dosages required. However, from the results obtained in this research (presented in chapter

4), the dosage of alum lies within a reasonable limit, which allows for the reconsideration of alum flocculation as an industrial microalgae dewatering technique. From the experimental results obtained in this research, the doses required for polyelectrolyte flocculation were also very low (2 - 10 mg/L). If the energy and cost to produce the polyelectrolytes (sufficient data was not attainable to perform actual calculations) are similar to that of alum, flocculation with polyelectrolytes would also be a viable option.

Electrocoagulation has shown immense potential to dewater microalgae effectively at low energy requirements and costs. The results in this research show that although electrocoagulation does require little energy to achieve successful dewatering, the energy and cost required to make aluminium for the electrode material is very high, amounting to 88 % of the total energy and cost, for this specific case. In order to make electrocoagulation a more feasible technique, the amount of electrode material required must be reduced. A continuous electro-coagulation process would require less electrode material due to the fact that there would be no time wasted for the induction period that requires a build up of sufficient metal cations and bubbles in the system to achieve successful recovery. A continuous flow study was conducted by Emamjomeh, M.M. and Sivakumar, M. (2009) on electrocoagulation with an aluminium anode for the removal of fluoride from wastewater. The electrocoagulation energy consumption was found to be $0.06 /m^3 of wastewater treated. The aluminium consumption was found to be $0.19 /m^3 of wastewater treated, which amounted to 52.8 % of the total costs. The operational cost was calculated between $0.36 and $0.61 /m^3 of treated water when the initial fluoride concentration was 5 mg/L.

Since this research concentrates on batch electrocoagulation, a reduction in electrode material can only occur by the use of microalgae with a higher starting concentration (assuming the rate of coagulation and hydrogen bubble attachment was maintained). This is because a higher concentration of microalgae would require a smaller volume to recover the same final mass of microalgae, which would reduce the number of batches, hence reduce the overall mass of aluminium metal dissolving

from the anode and the amount of aluminium required for electrocoagulation. The model can be used to predict the recovery of microalgae at a concentration of 1 g/L (figure 7.5). From these predictions, the energy required per mass of recovered microalgae can be calculated. Figure 7.6 shows the recovery of microalgae versus the energy required per mass of flocculated microalgae. Figure 7.6 can be used to determine the optimal electrocoagulation energy condition, i.e. the lowest energy input per mass of flocculated microalgae corresponding to the highest recovery. The optimal condition is 2 V with a run time of 360 s.
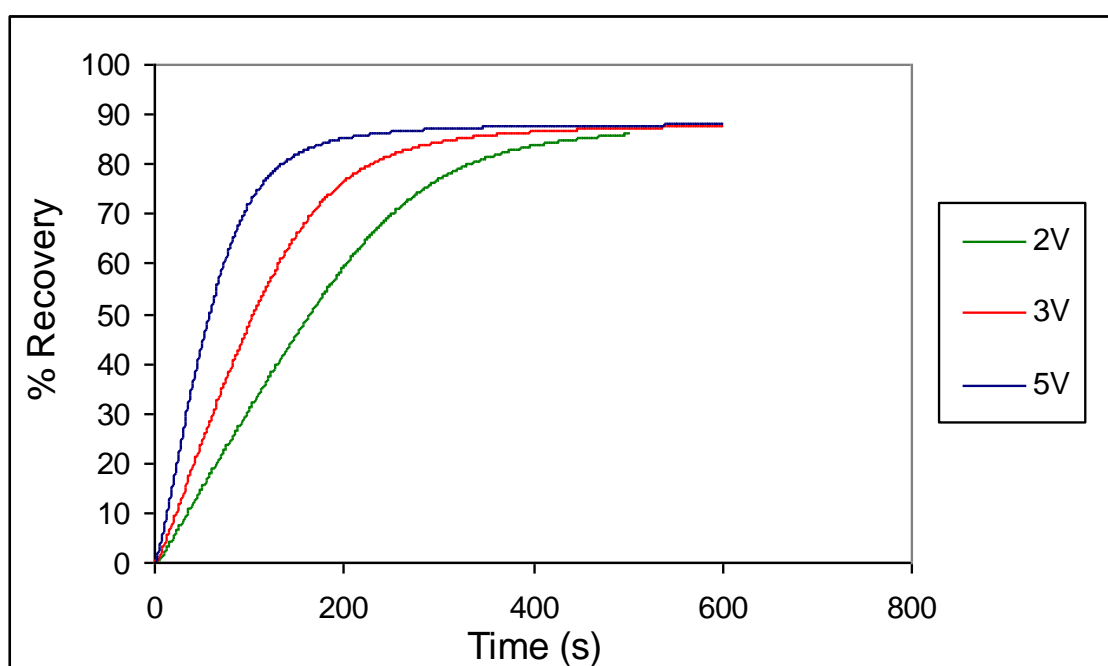
Figure 7. 5. Percentage recovery of *Chlorococcum sp.* at a concentration of 1 g/L, predicted by model, using the aluminium anode.
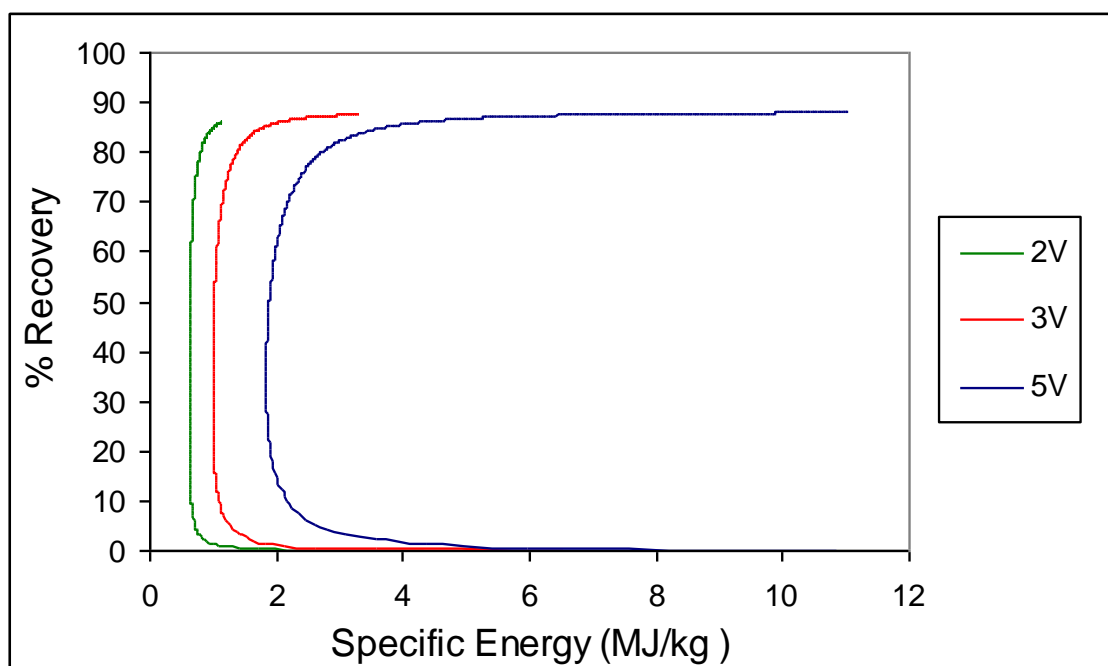
Figure 7. 6. Percentage recovery of microalgae predicted by model versus energy required per kg of flocculated microalgae, for electrocoagulation of *Chlorococcum sp.* at concentration 1 g/L, with the aluminium anode.

Table 7.4 presents a summary of energy required, carbon dioxide emitted and cost for the two-step dewatering processes with a microalgae starting concentration of 1 g/L. It can be seen from the table that increasing the starting microalgae concentration significantly reduces the values for each parameter. Alum flocculation coupled with centrifugation is still the most attractive process, showing by far the lowest energy demand, cost and carbon dioxide emissions.

Table 7. 4. Dewatering energy demand, carbon dioxide emissions and costs for two-step dewatering processes using microalgae at concentration 1 g/L.

Unit Process		Energy Demand (MJ)	CO$_2$ Emissions (kg)	Cost (USD)
Centrifuge	Centrifugation	4000	1140	206
Electrocoagulation / Centrifuge	Centrifugation	635	181	32.7
	Al production	9590	927	594
	Electrocoagulation	3140	17.0	162
	Total	13400	1120	788
Alum Flocculation / Centrifuge	Centrifugation	800	228	41.2
	Alum flocculation	6.7E-02	1.9E-02	3.5E-03
	Alum production	1010	286	30.0
	Total	1810	513	71.2

CHAPTER 8 CONCLUSIONS

8.1 Summary of Major Findings and Concluding Comments

This research investigated two dewatering techniques; flocculation and electrocoagulation. As part of this investigation the two dewatering techniques are compared to determine their optimum recovery conditions, as well as to evaluate their potential to reduce the energy consumption and cost involved in commercialising the production of microalgae sourced biodiesel.

The research gaps that were identified in the literature review in chapter 2 relate to the optimum separation of marine microalgae from saline media and are presented in 8.1.1 for microalgae flocculation and 8.1.2 for microalgae electrocoagulation along with the associated conclusions. Batch experiments were conducted at various experimental conditions using two quite different marine microalgae species; *Chlorococcum sp.* and *Tetraselmis sp.*

8.1.1 Flocculation of Microalgae

Flocculation of microalgae was carried out with two main types of flocculants; polyelectrolyte/polymer flocculants and inorganic aluminium sulphate (alum). Early flocculation studies conducted on marine microalgae showed success with only cationic polyelectrolytes. Alum flocculation with marine microalgae species was shown to be effective but only at very high flocculant doses. The main research gaps in microalgae flocculation was that there was minimal research conducted on marine microalgae flocculation and there had been no monitoring of the flocculation process in real time. The results from this research have been contradictory to previous studies and have shown that adequate flocculation is possible with cationic, anionic and non-ionic polyelectrolytes with recoveries up to 90 % and optimum doses ranging between 2 and 10 mg/L. It was also found that contrary to literature, the dose of alum required to flocculate marine microalgae successfully was

204

comparable to that required when used in freshwater. Alum flocculation was able to achieve recoveries above 90 % at optimum doses under 100 mg/L. In addition to these results, it was possible to monitor the flocculation process in real time using the FBRM. This allowed for a detailed analysis of microalgae flocculation, specifically looking at the rate that the microalgae cells agglomerate and the distribution of the different particle size ranges in the system. The efficiency of each polyelectrolyte flocculant was also quantified using the FBRM, allowing for another means of comparison aside from the recovery results.

8.1.2 Electrocoagulation of Microalgae

Microalgae dewatering by electrocoagulation was found to be successful with both marine microalgae species. In agreement with literature, a trend was observed where the amount of microalgae recovered increased with increasing applied voltage and electrocoagulation run time. Three anode materials were investigated and compared on their ability to induce microalgae coagulation and hence recovery. Microalgae was recovered at a faster rate using the aluminium anode, however the highest recovery was obtained using the stainless steel 430 anode. The maximum recovery obtained was 99, 90 and 38 % for electrocoagulation with the stainless steel 430, aluminium and carbon anodes, respectively.

The major research gap in electrocoagulation literature was that the theory of the electrocoagulation, which has been reported extensively, has not been supported by a significant amount of data. There is data lacking on the dissolving anode metal such as mass balances in the system, valency of dissolving species, the percent of metal ions required for coagulation and the amount of metal remaining in the recovered microalgae. There have also been no investigations done on the hydrogen bubbles in the system or a thorough mathematical model developed that can predict microalgal recovery. Literature to date has focused mainly on the amount of recovery obtained with electrocoagulation, the efficiency of electrode material and the energy demand of the process. The mechanisms involved in the dewatering

method have been stated loosely, but with no quantitative analysis to demonstrate closure.

In this electrocoagulation work, each stage in the process of electrocoagulation was successfully proven and the experimental results were able to outline further findings and conclusions on the electrocoagulation process. The dissolution of the metal anode was analysed and the valency of the dissolved metal species was confirmed. Charge neutralisation and coagulation of microalgae was verified from zeta potential measurements. The results showed that with increasing run time, the microalgae became increasingly electropositive in charge, indicating that the metal ion had adsorbed to the microalgae surface and charge neutralisation had occurred. A mass balance on the system was carried out to determine the percentage of metal ion used for coagulation and how much metal was needed per gram of microalgae recovered.

Half cell experiments were carried out by the addition of a permeable membrane that divided the electrocoagulation cell in half. With the half cell set up using the stainless steel 430 anode, charge neutralisation of microalgae did not occur. It was determined that stirring was required in order to increase the mass transfer and thus collisions between microalgae and metal ions in order to induce metal ion adsorption and charge neutralisation. The membrane separation results demonstrated that the microalgae do not have to come into contact with the anode for charge neutralisation and coagulation to occur. This proves that coagulation occurs in bulk solution and not at the anode or cathode surfaces or in the vicinity of these surfaces.

A lag in microalgae recovery was observed at short run times for electrocoagulation at low voltages. By introducing additional stirring into the system, the recovery of microalgae was significantly improved and the lag in recovery did not occur. It was concluded that the recovery lag was due to the need to increase the frequency of bubble/floc collisions in order to achieve flotation. The key finding from the stirring experiments was that stirring had a significant effect on mass transfer in more than

one way. Agitation leads to an increase in the distribution of particles within the system and hence increases the probability of collisions between the particles. This results in both an increased rate of adsorption of metal to microalgae and an increased rate of attachment of hydrogen bubbles to flocs.

The flotation of microalgae flocs was documented using a high speed camera which was able to capture the attachment of hydrogen bubbles to the flocs and their subsequent flotation to the surface of the system. An analysis on the hydrogen produced at the cathode was performed and it was found that the hydrogen used to float the microalgae flocs was only a small percentage of the total hydrogen produced. The recovery of microalgae was seen to increase with the amount of hydrogen bubbles in the flocculated microalgae, which indicated that with increased recovery comes an increase in the volume of flocculated microalgae, which corresponds to a greater number of hydrogen bubbles used for flotation.

A mathematical model was developed that enabled the prediction of the amount of microalgae coagulation, recovery and settling. The mathematical model consisted of a rate based reaction, which was second order with respect to the algae concentration and first order with respect to the metal ion concentration. It also considered the equilibrium between settling and flotation of the microalgae based on the density of the complex of flocculated algae with entrapped hydrogen bubbles. Two main inefficiencies of the electrocoagulation process were determined. The first was the excess metal produced at the anode and the second was the low level of attachment of hydrogen bubbles to flocs. These inefficiencies can be partly overcome by introducing additional stirring into the system. Stirring will increase the rate of microalgae coagulation and also increase the attachment of hydrogen bubbles, resulting in a higher recovery for shorter electro-coagulation times.

The model is able to show which steps in the electrocoagulation process had the greatest influence on microalgae recovery. From these results, the rate limiting step of the electrocoagulation process was determined to be the rate of coagulation of microalgae, induced by metal adsorption onto the microalgae surface. As stated

previously, no work to date has been published that has quantitatively investigated the mechanisms involved in electrocoagulation. Therefore until now, the inefficiencies and rate limiting step of the process had not been quantified.

8.1.3 Comparison of Energy Consumption, Carbon Dioxide Emissions and Material Costs

The mathematical model was also used to investigate the recovery of microalgae at optimum conditions. Assuming that ideal mixing conditions could be introduced to the system, the model predicted a maximum recovery of microalgae at 360 s for electrocoagulation with aluminium anodes at 2 V (the condition that corresponded to having the lowest energy consumption and highest recovery).

Alum flocculation and aluminium electrocoagulation dewatering were compared at the optimum conditions for both processes. For both processes, the charge neutralisation mechanisms involved with flocculation were similar. These dewatering methods were coupled with centrifugation in a two step dewatering process and the energy consumption, carbon dioxide emissions and material costs were calculated and compared to dewatering with centrifugation on its own. The life cycle energy consumption and the related carbon dioxide emissions and the purchasing costs of the raw materials (aluminium and alum) were also taken into consideration in this comparative study. Alum flocculation was found to be the most promising dewatering technique having the lowest life cycle energy consumption and related carbon dioxide emissions and material costs. Electrocoagulation required low energy for its operation as a dewatering process, but the overall process was highly energy intensive, due to the energy demand associated with aluminium production.

8.1.4 Concluding Comments

The overall conclusion to this research is that both flocculation and electrocoagulation are able to successfully dewater marine microalgae at a low energy requirement. Alum flocculation is the more promising technique, owing to

the extremely low power consumption, material costs and carbon dioxide emissions related to the life cycle of the material used in this process. Batch electrocoagulation is not realistically feasible for commercial use due to the high energy demand for the sacrificial aluminium anode production. However if the overall process can be fine-tuned to reduce the consumption of aluminium, it could lead to a more positive comparison.

8.2 Future Investigations

Future investigations that stem from this research are directed at modifying and optimising the coagulation and flotation mechanisms of the electrocoagulation process. Future work may be directed at optimising the electrocoagulation process by introducing agitation into the system without a significant increase in power consumption. In addition to this, future work may involve the exploration of cheaper alternative anode materials in order to reduce the overall costs and also the use of a continuous process for electrocoagulation, which should be more energy efficient. In a continuous process for electrocoagulation, there would be no induction or lag time and the hydrogen produced during that period would not be wasted. Another important factor that would need to be considered in a continuous system would be whether the supernatant media could be returned to the bioreactor thus conserving salt, or whether the metal ions from the anode would have a disruptive effect on the growth of the algae. An additional optimisation of the continuous electrocoagulation process that could be investigated is the combination of continuous electrocoagulation and flocculation. As mentioned in chapter 2, studies have been conducted that looked into dewatering using the combined process of electrocoagulation and flocculation. The addition of a flocculant before electrocoagulation was found to result in significant improvements in recovery as well as reduced electrical consumption and decreased operating costs.

REFERENCES

Akers, R. J. (1975). *Flocculation*. London, The institution of chemical engineers.

Alfafara, C. G., Nakano, K., Nomura, N., Igarashi, T. and Matsumura, M. (2002). "Operating and scale-up factors for the electrolytic removal of algae from eutrophied lakewater." *Journal of chemical technology and biotechnology*, Vol. 77, pp. 871 - 876.

Alibaba. (2012). "Alibaba manufacturers and suppliers." Retrieved 03/01/12, from http://www.alibaba.com/product-gs/341650116/aluminium_sulphate_Al2_SO4_3.html?s=p.

Aluminium Industry. (2012). "Energy consumption in bayer process." Retrieved 17/03/12, from https://docs.google.com/viewer?a=v&q=cache:ok3hVFcHgAAJ:www.pcra.org/english/latest/book/14-Chapter%2520-%252014.pdf+energy+for+bayer+process+kwh&hl=en&gl=au&pid=bl&srcid=ADGEESj2QdU0d2T_E8sWi7CH4IBgCiFu9SBlxy-jwRoCL5KPR3NC_VP2moj-8lVuHIGrz3AqBc1IWvieDEpwMlAGT8GYKHvdaieNaTjr8kEMoJIJ8pCQUscTOwgRXegaAFGgEptn8cma&sig=AHIEtbT3LrHr1Wra7HQad9U3QYw8BmO_7A.

Antoni, D., Zverlov, V. V. and Schwarz, W. H. (2007). "Biofuels from microbes." *Applied microbiology biotechnology*, Vol. 77, pp. 23 - 35.

Aragon, A. B., Padilla, R. B. and Fiestas Ros de Ursinos, J. A. (1992). "Experimental study of the recovery of algae cultured in effluents from the anaerobic biological treatment of urban wastewaters." *Resources, Conservation and Recycling*, Vol. 6, pp. 293 - 302.

Arenz, R. F., Lewis, W. M. and Saunders, J. F. (1996). "Determination of chlorophyll and dissolved organic carbon from reflectance data for Colorado reservoirs." *International journal of remote sensing*, Vol. 17, No. 8, pp. 1547 - 1566.

Arpke, A. and Hutzler, N. (2006). "Domestic water use in the united states: a life cycle approach." *Journal of industrial ecology*, Vol. 10, No. 1-2, pp. 169 - 184.

Ayoub, G. M., Lee, S. and Koopman, B. (1986). "Seawater induced algal flocculation." *Water research*, Vol. 20, No. 10, pp. 1265 - 1271.

Azarian, G. H., Mesdaghinia, A. R., Vaezi, F., Nabizadeh, R. and Nematollahi, D. (2007). "Algae removal by electro-coagulation process, application for treatment of the effluent from an industrial wastewater treatment plant." *Iranian journal of public health*, Vol. 36, No. 4, pp. 57 - 64.

Bare, W. F. R., Jones, N. B., E.J., M. and (975) (1975). "Algae removal using dissolved air flotation." *Jounrla of water pollution control federation*, Vol. 47, pp. 153 - 169.

Becker, E. (1995). *Microalgae biotechnology and microbiology*. Cambridge, UK, Cambridge university press.

Benemann, J. and Oswald, W. J. (1996). Systems and economic analysis of microalgae ponds for conversion of carbon dioxide to biomass, 4th Quarterly Technical Progress Report. Report CONF-9409207-2**:** 105 - 109.

Bernhardt, H. and Clasen, J. (1991). "Flocculation of micro-organisms." *Journal of water supply: research and technology - aqua*, Vol. 40, No. 2, pp. 76 - 87.

Bernhardt, H. and Clasen, J. (1994). "Investigations into the flocculation mechanisms of small algal cells." *Journal of water supply: research and technology - aqua*, Vol. 43, No. 5, pp. 222 - 232.

Bilanovic, D. and Shelef, G. (1988). "Flocculation of microalgae with cationic polymers - effects of medium salinity." *Biomass*, Vol. 17, pp. 65 - 76.

Black, A. P. and Chen, C. (1967). "Electrokinetic behaviour of aluminium species in dilute dispersed kaolinite systems." *Journal of the american waterworks association*, Vol. 59, No. 9, pp. 1173 - 1183.

Blanco, A., Fuente, E., Negro, C. and Tijero, J. (2002). "Flocculation monitoring: focused beam reflectance measurement as a measurement tool." *The canadian journal of chemical engineering*, Vol. 80, pp.

Borowitzka, M. A. (1992). "Algal biotechnology products and processes - matching science and economics." *Journal of applied pshychology*, Vol. 4, pp. 267 - 279.

Briley, D. S. and Knappe, D. R. U. (2002). "Optimising ferric sulfate coagulation of algae with streaming current measurements." *American Water Works Association Journal*, Vol. 94, No. 2, pp. 80 - 92.

Bukhari, A. A. (2008). "Investigation of the electro-coagulation treatment process for the removal of total suspended solids and turbidity from municipal water." *Bioresource technology*, Vol. 99, pp. 914 - 921.

Bull, J. J. and Collins, S. (2012). "Algae for biofuel: will the evolution of weeds limit the enterprise?" *International journal of organic evolution*, Vol. 9, pp. 2983 - 2987.

Can, O. T., Kobya, M., Demirbas, E. and Bayramoglu, M. (2006). "Treatment of the textile wastewater by combined electrocoagulation." *Chemosphere*, Vol. 62, pp. 181 - 187.

Canizares, P., Martinez, F., Jimenez, C., Saez, C. and Rodrigo, M. A. (2008). "Coagulation and electrocoagulation of oil-in-water emulsions." *Journal of hazardous materials*, Vol. 151, pp. 44 - 51.

Chen, G. (2004). "Electrochemical technologies in wastewater treatment " *Separation and Purification Technology*, Vol. 38, pp. 11 - 41.

Chen, Y. M., Liu, J. C. and Ju, Y. (1998). "Flotation removal of algae from water." *Colloids and surfaces*, Vol. 12, pp. 49 - 55.

Chisti, Y. (2007). "Biodiesel from microalgae." *Biotechnology advances*, Vol. 25, pp. 294 - 306.

Chisti, Y. (2008). "Biodiesel from microalgae beats bioethanol." *Trends in biotechnology*, Vol. 26, No. 3, pp. 126 - 131.

Chung, Y., Choi, Y. C., Choi, Y. H. and Kang, H. S. (2000). "A demonstration scaling-up of the dissolved air flotation." *Water research*, Vol. 34, No. 3, pp. 817 - 824.

Danquah, M. K., Ang, L., Uduman, N., Moheimani, N. and M., F. G. (2009). "Dewatering of microalgal culture for biodiesel production: exploring polymer flocculation and tangential flow filtration." *Journal of chemical technology and biotechnology* Vol. 84, pp. 1078 - 1083.

Danquah, M. K., Harun, R., Halim, R. and Forde, G. (2010). "Cultivation medium design via elemental balancing for tetraselmis suecica." *Journal of chemical and biochemical engineering*, Vol. 24, No. 3, pp. 361 - 369.

De La Noue, J. and De Pauw, N. (1988). "The potential of microalgal biotechnology: a review of production and uses of microalgae." *Biotechnology advances*, Vol. 6, pp. 725 - 770.

Demirbas, A. and Demirbas, F. M. (2011). "Importance of algae oil as a source of biodiesel." *Energy conversion and management,* Vol. 52, No. 1, pp. 163 - 170.

Demirbas, A. and Karslioglu, S. (2007). "Biodiesel production facilities from vegetable oils and animal fats." *Energy sources*, Vol. 29, pp. 133 -141.

Dones, R., Heck, T. and Hirschberg, S. (2004). "Greenhouse gas emissions from energy systems: comparison and overview." *Encyclopedia of energy*, Vol. 3, pp. 77 - 95.

Edzwald, J. K. (1993). "Algae, bubbles, coagulants and dissolved air flotation." *Water science technology*, Vol. 27, No. 10, pp. 67 - 81.

Emamjomeh, M. M. and Sivakumar, M. (2009). "Fluoride removal by a continuous flow electrocoagulation reactor." *Journal of Environmental Management*, Vol. 90, pp. 1204 - 1212.

Evans, D. F. and Wennerstrom, H. (1999). *The colloidal domain, where physics, chemistry, biology and technology meet*. New York, John Wiley & Sons, Inc.

Everett, D. H. (1988). *Basic principles of colloid science*. Cambridge, Uk, The royal society of chemistry.

Folkman, Y. and Wachs, A. M. (1973). "Removal of algae from stabilisation pond effluents by lime treatment." *Water research*, Vol. 7, pp. 419 - 435.

Franco, M. C., Buffing, M. F., Janssen, M., Lobato, C. V. and Wijffels, R. H. (2011). "Performance of Chlorella sorokiniana under simulated extreme winter conditions." *Journal of Applied Phycology*, Vol. DOI: 10.1007/s10811-011-9687-y, pp.

Friedman, A. A., Peaks, D. A. and Nichols, R. L. (1977). "Algae separation from oxidation pond effluents." *Journal of water pollution control federation*, Vol. 49, No. 1, pp. 111 - 119.

Fuglestvedt, J., Berntsen, T., Myhre, G., Rypdal, K. and Skeie, R. B. (2008). "Climate forcing from the transport sectors." *Proceedings of the National Academy of Sciences*, Vol. 105, No. 2, pp. 454 - 458.

Fukuda, H., Kondo, A. and Noda, H. (2001). "Biodiesel fuel production by transesterfication of oils." *Journal of Bioscience and Bioengineering* Vol. 92, No. 5, pp. 405 - 416.

Gao, S., Du, M., Tian, J., Yang, J., Yang, J., Ma, F. and Nan, J. (2010a). "Effects of chloride ions on electro-coagulation-flotation process with aluminium electrodes for algae removal." *Journal of hazardous materials*, Vol. 182, pp. 827 - 834.

Gao, S., Yang, J., Tian, J., Ma, F., Tu, G. and Du, M. (2010b). "Electro-coagulation-flotation process for algae removal." *Journal of hazardous materials*, Vol. 177, pp. 336 - 343.

Ghernaout, D., Badis, A., Kellil, A. and Ghernaout, B. (2008). "Application of electrocoagulation in Escherichia coli culture and two surface waters." *Desalination*, Vol. 219, pp. 118 - 125.

Gregory, J. (1989). "Fundamentals of flocculation." *CRC critical reviews in environmental control*, Vol. 19, No. 3, pp. 185 - 230.

Grima, E. M., Belarbi, F. G., Fernandez, A., Medina, A. R. and Chitsi, Y. (2003). "Recovery of microbial biomass and metabolites: process options and economics." *Biotechnology advances*, Vol. 20, pp. 491 - 515.

Halim, R., Gladman, B., Danquah, M. K. and Webley, P. A. (2011). "Oil extraction from microalgae for biodiesel production." *Bioresource technology*, Vol. 102, No. 1, pp. 178 - 185.

Haynie, D. T. (2008). *Biological Thermodynamics*. Cambridge, Cambridge university press.

Henderson, R., Parsons, S. A. and Jefferson, B. (2008). "The impact of algal properties and pre-oxidation on solid-liquid separation of algae." *Water research*, Vol. 42, pp. 1827 - 1845.

Higgins, M. J. and Novak, J. T. (1997). "Characterisation of exocellular protein and its role in bioflocculation." *Journal of environmental engineering*, Vol. 123, No. 5, pp. 479 - 586.

Holt, P. K., Barton, G. W. and Mitchell, C. A. (2005). "The future for electrocoagulation as a localised water treatment technology." *Chemosphere*, Vol. 59, pp. 355 - 367.

Holt, P. K., Barton, G. W., Wark, M. and Mitchell, C. A. (2002). "A quantitative comparison between chemical dosing and electrocoagulation." *Colloids and surfaces A: physiochemical and engineering aspects*, Vol. 211, pp. 233 - 248.

Hossain, A. B. M. S., Salleh, A., Boyce, A. N., Chowdhury, P. and Naqiuddin, M. (2008) "Biodisel fuel production from algae as renewable energy". *American journal of biochemistry and biotechnology,* Vol. 4, No. 3, pp. 250 - 254.

Hunter, R. J. (2001). *Foundations of colloid science*. New York, Oxford university press.

Jimenez, C., Talavera, B., Saez, C., Canizares, P. and Rodrigo, M. A. (2010). "Study of the production of hydrogen bubbles at low current densities for electroflotation processes." *Journal of chemical technology and biotechnology*, Vol., pp.

Khemis, M., Leclerc, J., Tanguy, G., Valentin, G. and Lapicque, F. (2006). "Treatment of industrial liquidwastes by electrocoagulation: Experimental investigations and an overall interpretation model." *Chemical Engineering Science*, Vol. 61, pp. 3602 - 3609.

Knuckey, R. M., Brown, M. R., Robert, R. and Frampton, D. M. F. (2006). "Production of microalgal concentrates by flocculation and their assessment as aquaculture feeds." *Aquacultural engineering*, Vol. 35, pp. 300 - 313.

Kobya, M., Hiz, H., Senturk, E., Aydiner, C. and Demirbas, E. (2006). "Treatment of potato chips manufacturing wastewater by electrocoagulation." *Desalination*, Vol. 190, pp. 201 - 211.

Lee, A. K., Lewis, D. M. and Ashman, P. J. (2009). "Microbial flocculation, a potentiall low cost harvesting technique for marine microalgae for the production of biodiesel." *journal of applied phycology*, Vol. 21, pp. 559 - 567.

Lee, S. H., Lee, S. O., Jang, K. L. and Lee, T. H. (1995). "Microbial flocculant from Arcuadendron sp. TS-49." *Biotechnology letters*, Vol. 17, No. 1, pp. 95 - 100.

Lee, S. J., Kim, S. B., Kim, J. E., Kwon, G. S., Yoon, B. D. and Oh, H. M. (1998). "Effects of harvesting method and growth stage on the flocculation of the green alga botryococcus braunii." *Letters in applied microbiology*, Vol. 27, pp. 14 - 18.

Lee, W. and Pyun, S. (1999). "E€ects of hydroxide ion addition on anodic dissolution of pure aluminium in chloride ion-containing solution." *Electrochimica Acta*, Vol. 44, pp. 4041 - 4049.

Levenspiel, O. (1999). *Chemical reaction engineering*. New York, Wiley.

Li, X., Xu, H. and Wu, Q. (2007). "Large-scale biodiesel production from microalga Chlorella protothecoides through heterotrophic cultivation in bioreactrs." *Biotechnology and bioengineering*, Vol. 98, No. 4, pp. 764 - 771.

Lian, B., Chen, Y., Zhao, J., Teng, H., Zhu, L. and Yuan, S. (2008). "Microbial flocculation by Bacillus mucilaginosus: applications and mechanisms." *Bioresource technology*, Vol. 99, No. 11, pp. 4825 - 4831.

Ma, F. and Hanna, M. A. (1999). "Biodiesel production: a review." *Bioresource technology*, Vol. 70, pp. 1 - 15.

Matis, K. A., Gallios, G. P. and Kydros, K. A. (1993). "Separation of fines by flotation techniques." *Separation technology*, Vol. 3, pp. 76 - 90.

McGarry, M. G. (1970). "Algal flocculation with aluminum sulfate and polyelectrolytes." *Water pollution control federation*, Vol. 42, No. 5, pp. R191-R201.

McGarry, M. G. and Tongkasame, C. (1971). "Water reclamation and algae harvesting." *Water pollution control federation*, Vol. 43, No. 5, pp. 824 - 835.

Metal News. (2011). "Metal Prices & News on the Internet."   Retrieved 20/12/11, from http://www.metalprices.com/FreeSite/metals/stainless_flat_product/stainless_flat_product.asp#.

Metal News. (2011). "Metal Prices & News on the Internet."   Retrieved 27/10/11, from http://www.metalprices.com/#.

Middlebrooks, E. J., Porcella, D. B., Gearheart, R. A., Marshall, G. R., Reinold, J. H. and Grenney, W. J. (1974). "Effects of temperature on oil refinery waste toxicity." *Journal of water pollution control federation*, Vol. 46, No. 12, pp. 2675.

Mohn, F. H. (1980). "Experiences and strategies in the recovery of biomass from mass cultures of microalgae." *Algae biomass*, Vol., pp. 547 - 571.

Mollah, M. Y. A., Morkovsky, P., Gomes, J. A. G., Kesmez, M., Parga, J. and Cocke, D. L. (2004). "Fundamentals, present and future perspectives of electrocoagulation." *Journal of hazardous materials*, Vol. B114, pp. 199 - 210.

Moraine, R., Shelef, G., Meydan, A. and Levi, A. (1979). "Algal single cell protein from wastewater treatment and renovation process." *Biotechnology and bioengineering*, Vol. 21, pp. 1191 - 1207.

Moraine, R., Shelef, G., Sandbank, E., Bar-moshe, Z. and Shvartzburd, L. (1980). *Recovery of sewage-borne algae: flocculation, flotation, and centrifugation techniques*. Amsterdam, New York, Oxford, Elsevier/ North holland biomedical press.

Mouedhen, G., Feki, M., De Petris Wery, M. and Ayedi, H. F. (2008). "Behavior of aluminum electrodes in electrocoagulation process." *Journal of hazardous materials*, Vol. 150, pp. 124 - 135.

Mouedhen, G., Feki, M., De Petris Wery, M. and Ayedi, H. F. (2008). "Behaviour of aluminium electrodes in electrocoagulation process." *Journal of hazardous materials*, Vol. 150, pp. 124 - 135.

Murgananthan, M., Raju, G. B. and Prabhakar, S. (2004). "Removal of sulfide, sulfate and sulfite ions by electro coagulation." *Journal of hazardous materials*, Vol. 109, pp. 37 - 44.

Norgate, T. E. and Rankin, W. J. (2001). Greenhouse gas emissions from aluminium production – a life cycle approach. Proceedings of the international symposium on greenhouse gases in the metallurgical industries: policies, abatement and treatment, Toronto, Canada.

NorthernGraphite. (2011). "Graphite price." Retrieved 20/12/11, from http://www.northerngraphite.com/index.php/graphite-labs/graphite-price/.

Oh, H., Lee, S. J., Park, M., Kim, H. S., Kim, H. C., Yoon, J. H., Kwon, G. and Yoon, B. D. (2001). "Harvesting of chlorella vulgaris using a bioflocculant from paenibacillus sp. AM49." *Biotechnology letters*, Vol. 23, pp. 1229 - 1234.

Outotec. (2012). "More out of ore." Retrieved 17/03/12, from https://docs.google.com/viewer?a=v&q=cache:uuO6QtSrrlcJ:www.outotec.com/39417.epibrw+energy+sulphuric+acid+kWh&hl=en&gl=au&pid=bl&srcid=ADGEESjUms3J7pLAyWFybNfQm-C-c-2Kme_n1fOGm8U-cqndEDTE6EQQk07Fihz9pd3J7AEoY11TbapiJrz9W_TO58_3Zq6kiijchvTcFlLP4X0W22A-1gGddT9rL6MV5iXB8auacDNP&sig=AHIEtbRTQWGHFsUvRZWAIOslynGZvL4jfA.

PenWell. (2011). "Power Engineering." Retrieved 12/08/11, from http://www.power-eng.com/index.html.

Petrusevski, B., Bolier, G., Van Breemen, A. N. and Alaerts, G. J. (1995). "Tangential flow filtration: a method to concentrate freshwater algae " *Water research*, Vol. 29, No. 5, pp. 1419 - 1424.

Petrusevski, B., Van Breemen, A. N. and Alaerts, G. J. (1996). "Effect of permanganate pre-treatment and coagulation with dual coagulants on algae removal in direct filtration." *Journal of water supply: research and technology - aqua*, Vol. 45, No. 5, pp. 316 - 326.

Phoochinda, W., White, D. A. and Briscoe, B. J. (2004). "An algal removal using a combination of flocculation and flotation processes." *Environmental Technology*, Vol. 25, pp. 1385 - 1395.

Pieterse, A. J. H. and Cloot, A. (1997). "Algal cells and coagulation, flocculation and sedimentation processes." *Water science technology*, Vol. 36, No. 4, pp. 111 - 118.

Poelman, E., De Pauw, N. and Jeurissen, B. (1997). "Potential of electrolytic flocculation for recovery of microalgae." *Resources, conservation and recycling*, Vol. 19, pp. 1 - 10.

Pourbaix, M. (1966). *Atlas of electrochemical equilibria in aqueous solutions*. Oxford, Pergamon Press Ltd.

Pushparaj, B., Pelosi, E., Torzillo, G. and Materassi, R. (1993). "Microbial biomass recovery using a synthetic cationic polymer." *Bioresource technology*, Vol. 43, pp. 59 - 62.

Rossignol, N., Vandanjon, L., Jaouen, P. and Quemeneur, F. (1999). "Membrane technology for the continuous separation microalgae: culture medium: compared performances of cross-flow microfiltration and ultrafiltration." *Aquacultural engineering*, Vol. 20, pp. 191 - 208.

Rubio, J., Souza, M. L. and Smith, R. W. (2002). "Overview of flotation as a wastewater treatment technique." *Minerals engineering* Vol. 15, pp. 139 - 155.

Sander, K. and Murthy, G. S. (2010). "Life cycle analysis of algae biodiesel." *International jounral of life cycle assess*, Vol. 15, pp. 704 - 714.

Schweitzer, P. A. (2007). *Fundamentals of metallic corrosion – atmospheric and media corrosion metals*. Boca Raton, CRC Press.

Scott, S. A., Davey, M. P., Dennis, J. S., Horst, I., Howe C. J., Lea-Smith, D. J. and Smith, A. G. (2010). "Biodiesel from algae: challenges and prospects", *Current opinion in biotechnology.* Vol. 21, No. 3, pp. 277 - 286.

Semerjian, L. and Ayoub, G. M. (2003). "High-pH-magnesium coagulation-flocculation in wastewater treatment." *Advances in environmental research*, Vol. 7, pp. 389 - 403.

Shelef, G., Sukenik, A. and Green, M. (1984). Microalgae harvesting and processing: a literature review.

Shirvani, T., Yan, X., Inderwildi, O. R., Edwards, P.P., King, D. A. (2011). "Life cylce energy and greenhouse gas analysis for algae-derived biodiesel." *Energy and environmental science*, Vol. 4, pp. 3773.

Sinnott, R. K. (2005). *Chemical Engineering Design*. Oxford, Elsvier Butterworth-Heinemann.

Stechemesser, H. and Dobias, B., editors (2005). *Coagulation and flocculation*. Florida, CRC Press.

Stephenson, A. L., Kazamia, E., Dennis, J.S., Howe, C.J., Scott, S. A., Smith, A. G. (2010). "Life-cycle assessment of potential algal biodiesel production in the United Kingdom: a comparison of raceways and air-lift tubular bioreactors." *Energy fuels*, Vol. 24, pp. 4062 - 4077.

Stumm, W. and Morgan, J. J. (1981). *Aquatic chemistry*. New York, Wiley Interscience.

Sukenik, A., Bilanovic, D. and Shelef, G. (1988). "Flocculation of microalgae in brackish and sea waters." *Biomass*, Vol. 15, pp. 187 - 199.

Sukenik, A. and Shelef, G. (1984). "Algal Autoflocculation-Verification and Proposed Mechanism." *Biotechnology and bioengineering*, Vol. 26, No. 2, pp. 142 - 147.

Tenney, M. W., Echelberger, J., W.F., S. and R.G., P., J.L. (1969). "Algal Flocculation with Synthetic Organic Polyelectrolytes." *Applied microbiology* Vol. 18, No. 6, pp. 965 - 971.

Tilton, R. C., Murphy, J. and Dixon, J. K. (1972). "The flocculation of algae with synthetic polymeric flocculants." *Water research*, Vol. 6, pp. 155 - 164.

Toeda, K. and Kurane, R. (1991). "Microbial flocculant from alcaligenes cupidus KT201." *Agricultural and biochemistry* Vol. 55, pp. 2793 - 2799.

Tricot, M. (1984). "Comparison of experimental and theoretical persistence length of some polyelectrolytes at various ionic strengths." *Macromolecules*, Vol. 17, pp. 1698 - 1704.

Trompette, J. L. and Vergnes, H. (2009). "On the crucial influence of some supporting electrolytes during electrocoagulation in the presence of aluminium electrodes." *Journal of hazardous materials*, Vol. 163, pp. 1282 - 1288.

Van Vuuren, L. R. J. and Van Duuren, F. A. (1965). "Removal of algae from wastewater maturation pond effluent." *Journal of water pollution control federation*, Vol. 37, No. 9, pp. 1256 - 1262.

Vandamme, D., Pontes, S. C. V., Goiris, K., Foubert, I., Pinoy, L. J. J. and Muylaert, K. (2011). "Evaluation of electro-coagulation-flocculation for harvesting marine and freshwater microalgae." *Biotechnology and bioengineering*, Vol. doi: 10.1002/bit.23199, pp.

Vlaski, A., van Breemen, A. N. and Alaerts, G. J. (1997). "The role of particle size and density in dissolved air flotation and sedimentation." *Water science technology*, Vol. 36, No. 4, pp. 177 - 189.

Wang, C., Chou, W. and Kuo, Y. (2009). "Removal of COD from laundry wastewater by electrocoagulation/electroflotation." *Journal of hazardous materials*, Vol. 164, pp. 81 - 86.

Wilde, E. W., Beneman, J. R., Weissman, J. C. and Tillett, D. M. (1991). "Cultivation of algae and nutrient removal in a waste heat utilisation process." *Journal of applied pshychology*, Vol. 3, pp. 159 - 167

Wright, L. (2006). "Worldwide commercial development of bioenergy with a focus on energy crop-based projects " *Biomass and bioenergy*, Vol. 30, No. 8 - 9, pp. 706 - 714.

Zaroual, Z., Azzi, M., Saib, N. and Chainet, E. (2006). "Contribution to the study of electrocoagulation mechanism in basic textile effluent." *Journal of hazardous materials*, Vol. 131, pp. 73 - 78.

APPENDIX

A.1 Detailed Methods

A.1.1 Dry Weight Concentration of Microalgae

To determine the dry weight concentration of the microalgae, the following steps were taken:

1. Weigh filter paper.
2. Filter a set volume of microalgae. E.g. 30 ml microalgae.
3. Rinse filter cake with 50 ml deionised water.
4. Rinse filter cake with 0.65 M ammonium formate.
5. Dry overnight at 60 °C.
6. Weigh filter paper and algal biomass.
7. Calculate concentration of algae based on microalgae volume and mass obtained.

Ammonium formate is used in order to remove the salt from the sea water media, since the salt adds to the weight of the sample and gives inaccurate results. The ammonium formate reacts to form ammonium chloride which then evaporates in the oven.

A.1.2 Calibration Curve for Calculation of Microalgae Concentration

A calibration curve was used in order to determine the concentration of the microalgae samples throughout the experimental work. This saved time, because once the dry weight concentration of that particular batch of microalgae was determined, it was then possible to determine the concentration of the microalgae with simple UV-VIS absorbance data and the calibration curve. To create the calibration curve, the following steps were taken:

1. Dilute samples of algae with sea water in dilutions of 0.1, 0.2, 0.4, 0.6, 0.8, 1 (where the dilution 0.1 refers to 10% algae, 90% sea water).
2. Measure the dry weight concentration of the microalgae at no dilution using the method in section A.1.1.
3. Measure the absorbance of the samples at 570 nm using a UV-VIS spectrophotometer.
4. Plot absorbance vs. concentration to obtain calibration curve. Since concentration and absorbance has a linear trend, the concentrations of each dilution could be calculated by simple multiplication of the original dry weight microalgae concentration with the dilution factor.

A.1.3 Harvesting of Microalgae

Harvesting of the microalgae was performed while the microalgae was in the stationary phase of growth, which is approximately 8 - 10 days after addition of fresh culture media. The growth of microalgae can be modelled in 4 phases: lag phase (no growth), exponential growth phase (microalgae grows exponentially), stationary phase (microalgae growth plateaus) and death phase. The reason the microalgae was harvested at the stationary phase is because at this stage, the concentration of biomass is at a steady value. Therefore continual harvesting at the same phase of microalgae growth would ensure a relatively constant composition of microalgae culture and biomass concentration. Studies by Danquah, M.K. et al. (2010) on the same *Tetraselmis sp.* culture used in this research have shown that the stationary phase is reached after approximately 8 - 10 days. From figure A.1, it can be seen that after 8 days, the concentration of microalgae steadies to a constant value.
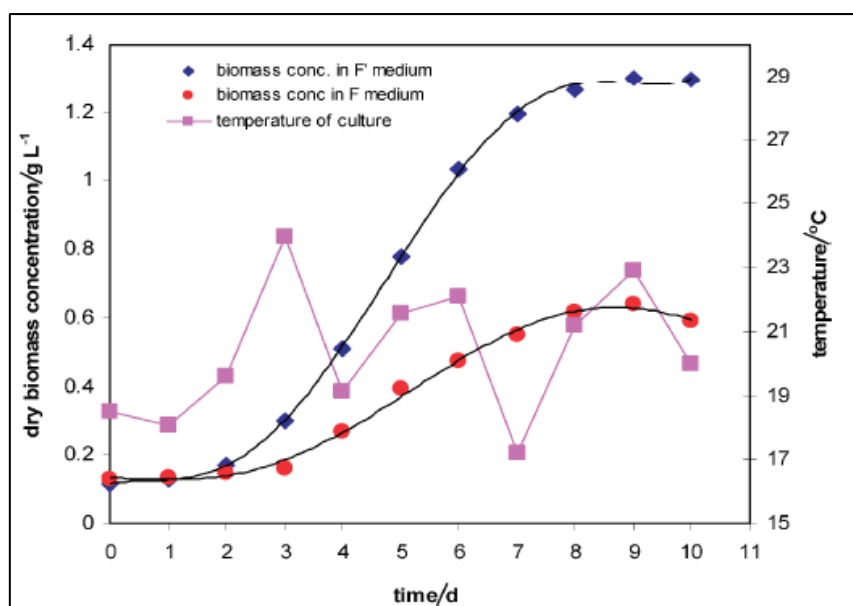
Figure A. 1. Biomass concentration of *Tetraselmis sp.* with time (Danquah, M. K. et al. 2010).

The total volume of the bioreactor was 100 L. With every harvest, 40 L of microalgae was removed from the bioreactor for experimental use, and 40 L of culture media was added. After each harvest, the dry weight concentration, pH and conductivity of microalgae was determined. If the results obtained for a single harvest were consistent with those obtained for previous harvests, the microalgae from the current harvest was deemed to be uniform and in the correct growth phase. Experiments were only conducted on microalgae that satisfied these conditions.

The following steps were taken to perform a harvest:

1. Prepare 40 L culture medium, with the entire formulation being dissolved in 0.2 μm sterile filtered natural water. The culture medium contains:

- 30 g/L aquarium salt

- 250 mg/L $NaNO_3$

- 18.0 mg/L KH_2PO_4

- 9.0 mg/L iron(III) citrate $C_6H_5O_7Fe$

- 9.0 mg/L citric acid $C_6H_8O_7$

- 0.200 mg/L $MnCl_2.4H_2O$

- 0.023 mg/L $ZnSO_4.7H_2O$

- 0.011 mg/L $CoCl_2.6H_2O$

- 0.005 mg/L $CuSO_4.5H_2$

- 0.008 mg/L $Na_2MoO_4.2H_2O$

- 0.00065 mg/L H_2SeO_3

- traces of vitamin B12, biotin and thiamine

2. Pump 40 L of microalgae from bioreactor

3. Pump 40 L culture medium into bioreactor

A.1.4 Absorbance Measurements with UV-VIS-2450 Spectrophotometer

The absorbance of microalgae was used to determined the dry weight concentration and hence the recovery of microalgae after dewatering. For both flocculation and electrocoagulation, the absorbance of microalgae was measured after the experiment was conducted. This absorbance reading relates to the concentration of microalgae, because the more concentrated the microalgal solution, the more chlorophyll (green colour pigment) there will be, which corresponds to a higher absorbance reading. The experiments were conducted in triplicate to ensure reproducibility of the data, and the error calculated (see Appendix A.2.4). From the constructed calibration curve (see Appendix A.1.2), the dry weight concentration can be calculated (see Appendix A.2.1). The choice of wavelength corresponds to the absorbance wavelength of the green pigment chlorophyll. Green light absorbs at wavelengths between 490 – 570 nm. Arenz, R.F. et al. (1996) state that a wavelength of 570 nm corresponds to the maximum absorbance of green chlorophyll. Therefore, all absorbance measurements were conducted at 570 nm.

A.1.5 Determination of Optimum Flocculant Dose

The optimum flocculant dose was determined by performing flocculation jar stirrer tests on the microalgae at a range of doses. The optimum dose was chosen as the dose which gave the highest microalgal removal. Figures A.2 to A.8 show the results obtained giving optimum doses for polyelectrolyte and alum flocculants with both *Chlorococcum sp.* and *Tetraselmis sp.*
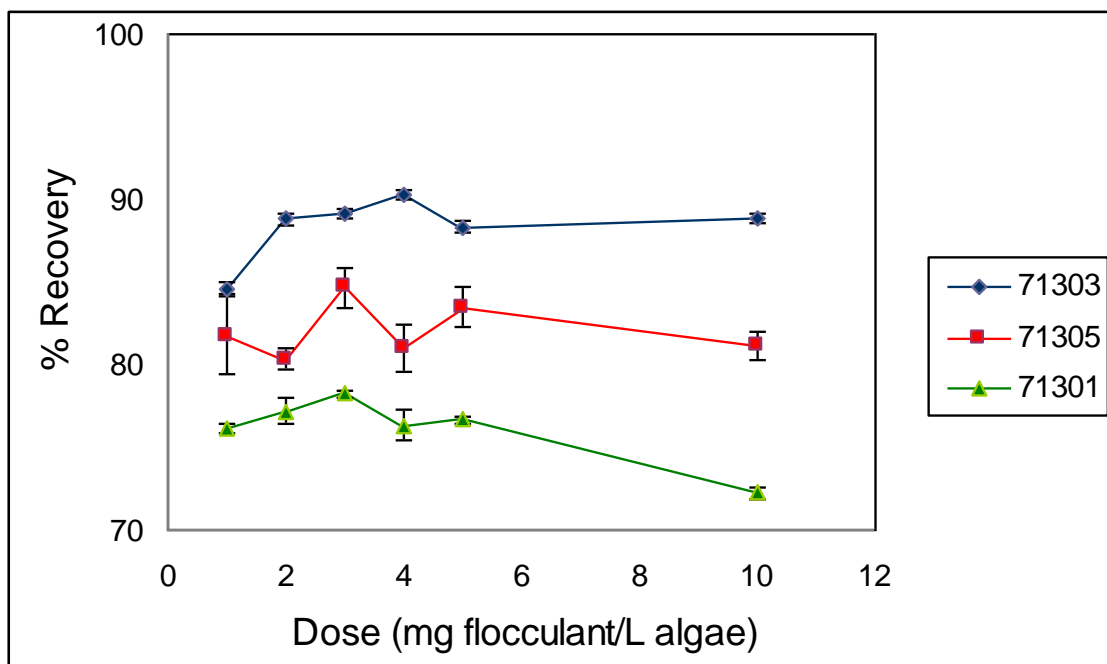
Figure A. 2. Optimum dose curve for cationic polyelectrolytes with *Chlorococcum sp.*
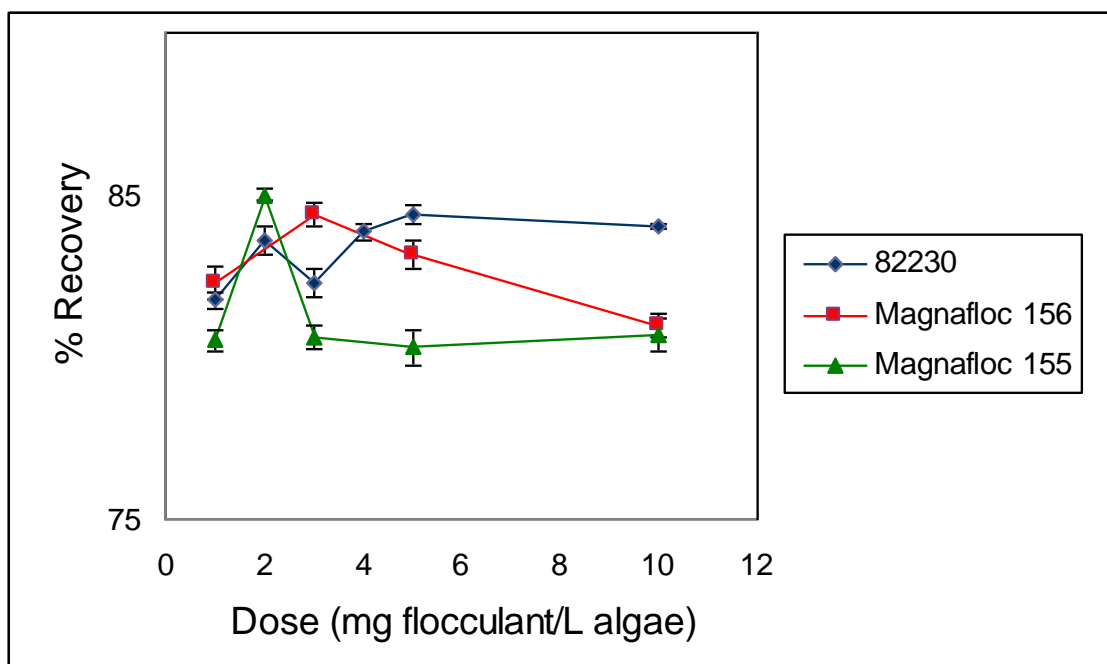
Figure A. 3. Optimum dose curve for anionic polyelectrolytes with *Chlorococcum sp.*
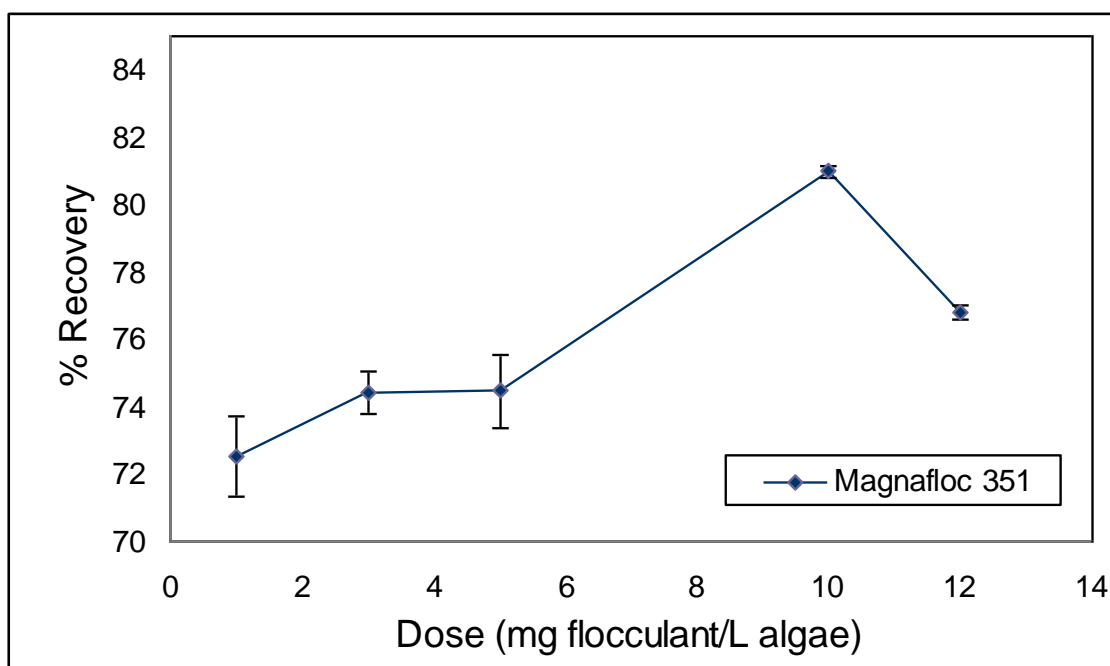
Figure A. 4. Optimum dose curve for non-ionic polyelectrolytes with *Chlorococcum sp.*
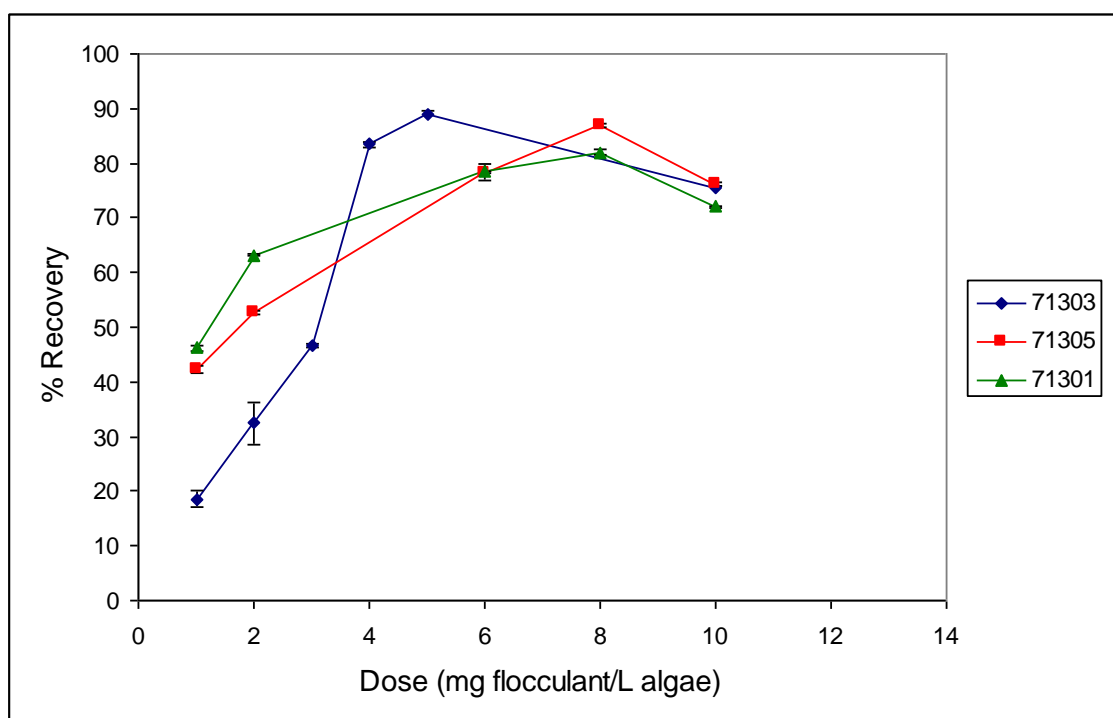
Figure A. 5. Optimum dose curve for cationic polyelectrolytes with *Tetraselmis sp.*
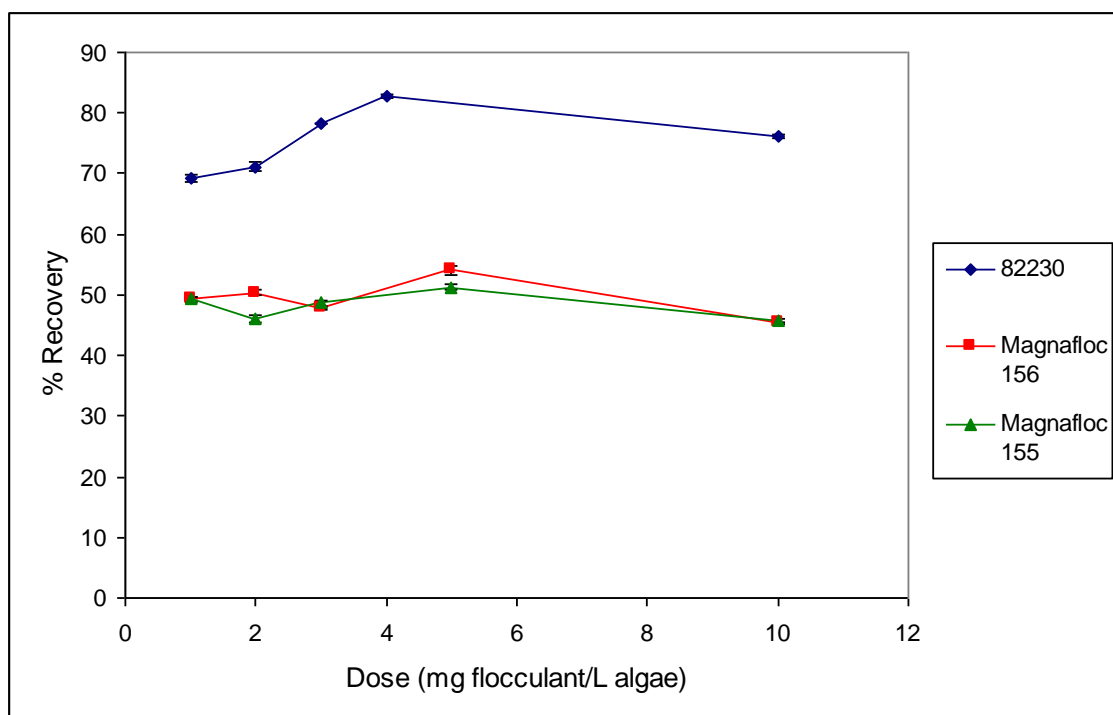
Figure A. 6. Optimum dose curve for anionic polyelectrolytes with *Tetraselmis sp.*
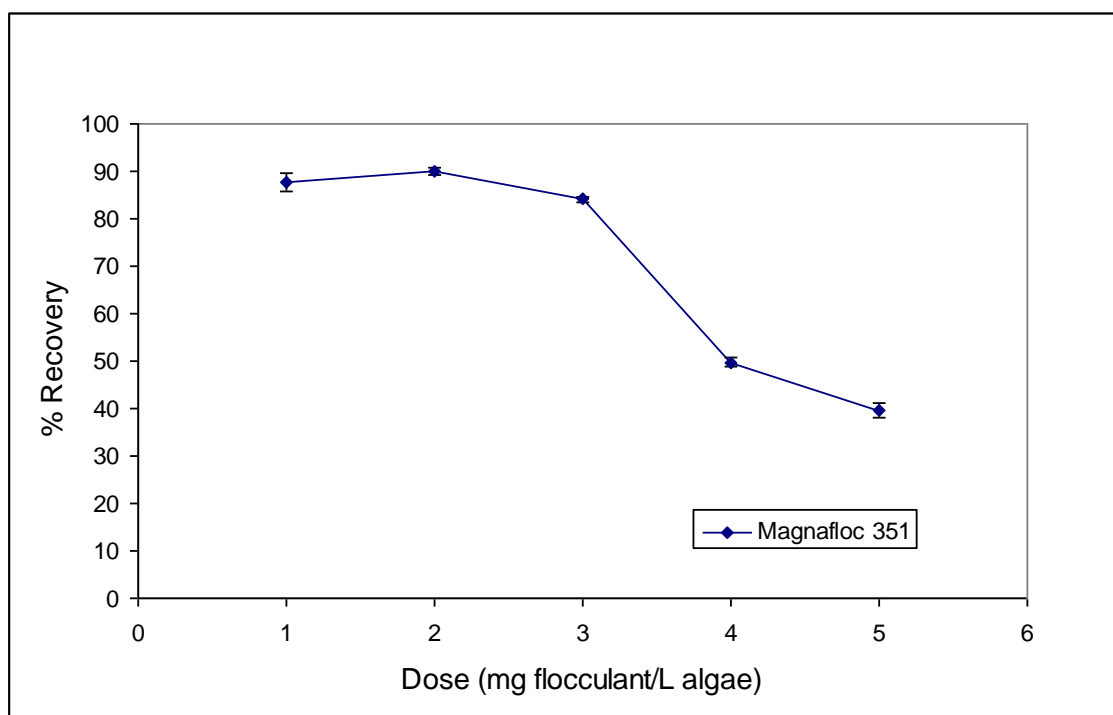
Figure A. 7. Optimum dose curve for non-ionic polyelectrolytes with *Tetraselmis sp.*
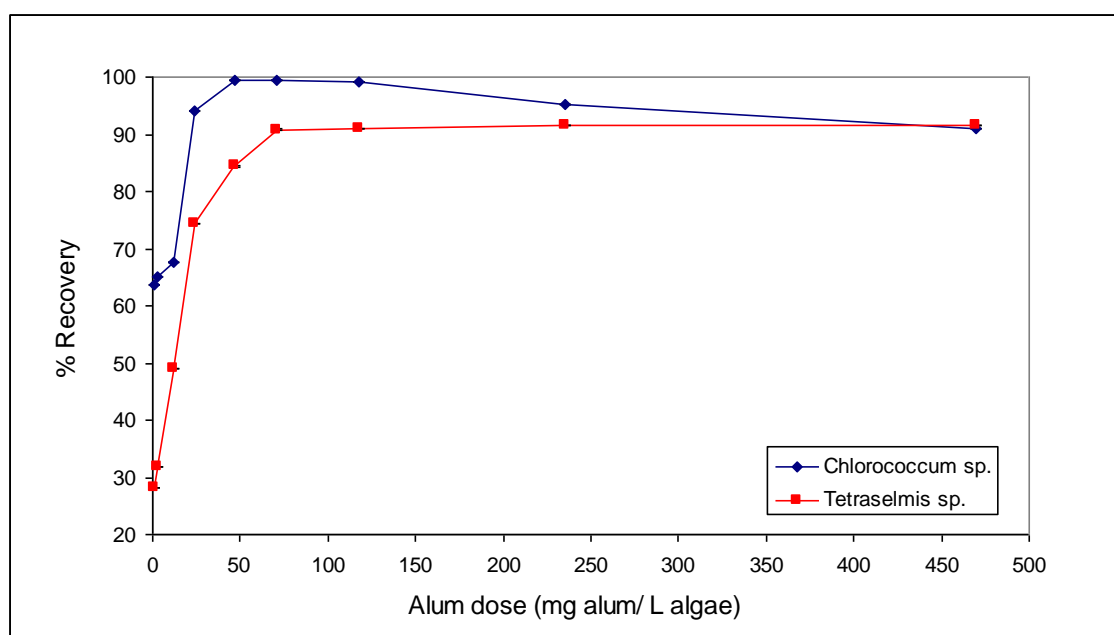
Figure A. 8. Optimum dose curve for alum with *Chlorococcum sp.* and *Tetraselmis sp.*

A.1.6 Rotating Electrode Electrocoagulation

A rotating electrode set up was created in order to observe the effects of increased microalgae mass transfer on recovery. A cylindrical anode was made from stainless steel 430 with the same surface area as the flat plate electrodes used in all other electrocoagulation experiments. These experiments were conducted at the research laboratories in the department of Materials Engineering, Monash University as they had the rotating experimental set up that was required. Limitations of this laboratory however, was that the total system could not handle using voltages above 2V. Therefore the electrocoagulation experiments had to be conducted at 2 V. The experiments conducted included varying the rotation of the anode from 0 – 500 rpm and determining the corresponding microalgae recovery obtained. Figure A.9 shows a schematic diagram of the experimental set up.
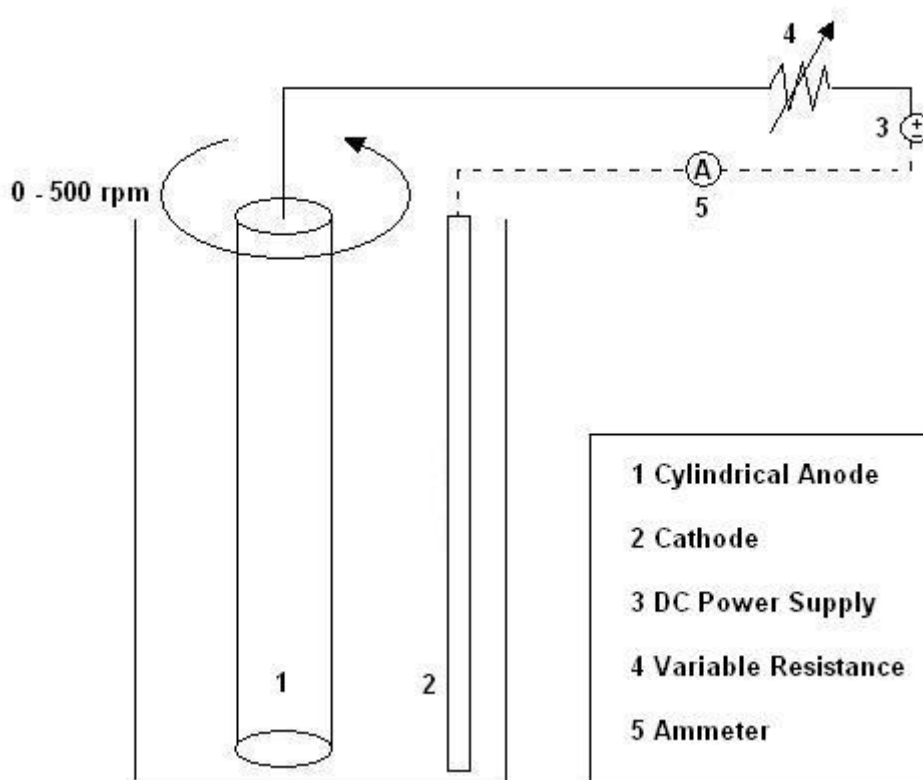
Figure A. 9. Schematic diagram of rotating electrode experimental set up.

A.1.7 Concentrating Microalgae

The microalgae was concentrated to a higher concentration for electrocoagulation work (section 6.6.1). The following steps were performed to concentrate the microalgae:

1. Put microalgae into a 5 or 10 L beaker.

2. Allow microalgae to settle for a period of 24 h. The microalgae will settle to the bottom of the beaker.

3. Decant the salt water media. The decanted volume will depend on the final concentration of the microalgae.

4. Resuspend the microalgae and determine the dry weight following the protocol outlined in A.1.1.

A.2 Calculations

A.2.1 Dry Weight Concentration and Construction of the Calibration Curve

Using *Tetraselmis sp.* data as the example data:

1. Determine dry weight of microalgae:

Trial	1	2	3	Average
Filter Paper (g)	0.21	0.20	0.20	
Filter paper + Algae (g)	0.22	0.21	0.21	
Dry Algae (g)	0.01	0.01	0.01	0.01

Volume of algae = 30 ml

Mass of algae = 0.01 g

Concentration of algae = 0.3 g/L

2. Dilute the microalgae in the correct dilutions and measure absorbance at 570 nm with a UV-VIS spectrophotometer.

Dilution factor	Algae Concentration (g/L)	Absorbance (nm)			Average Abs. (nm)
		1	2	3	
0.1	0.030	0.072	0.073	0.072	0.072
0.2	0.061	0.135	0.132	0.131	0.133
0.4	0.122	0.24	0.243	0.248	0.244
0.6	0.183	0.358	0.361	0.359	0.359
0.8	0.244	0.516	0.521	0.519	0.519
1	0.304	0.603	0.644	0.638	0.628

3. Plot absorbance vs. concentration and obtain the equation for the line of best fit.

Calibration Curve
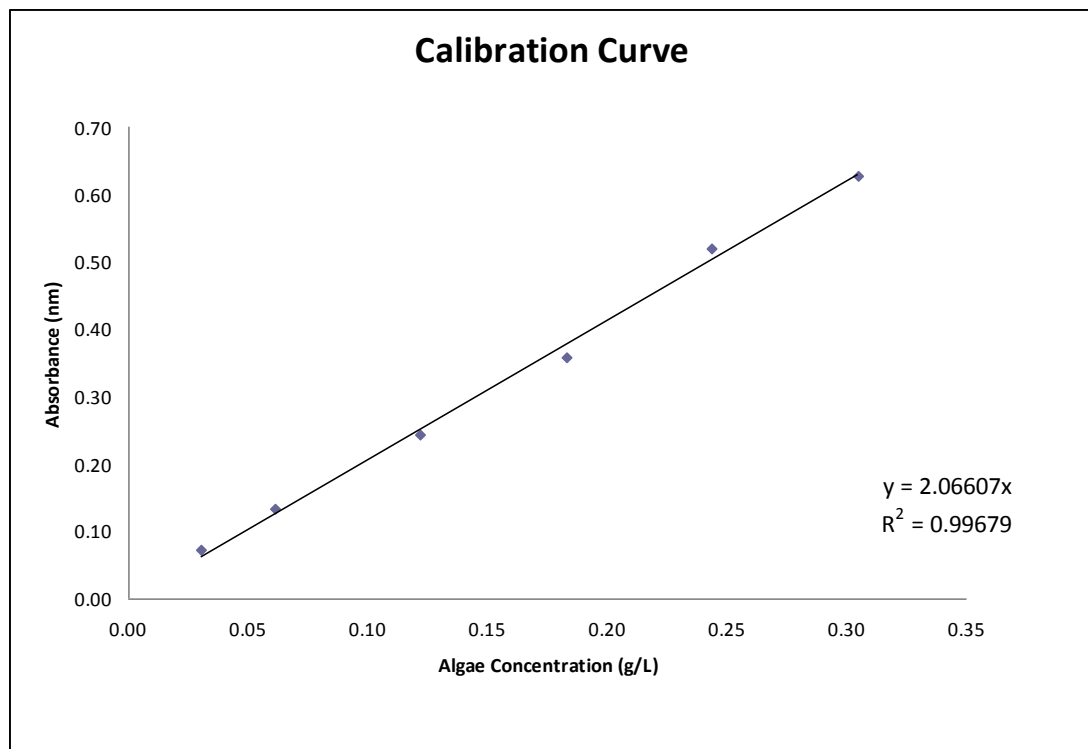
y = 2.06607x
R^2 = 0.99679

Equation for line of best fit:

Absorbance = 2.06607 x Concentration

4. Use the equation to calculate the concentration of microalgae from experimental absorbance data.

Absorbance of algae from experimental data = 1.526

Concentration of algae = 1.526/2.06607 = 0.739 g/L

A.2.2 Theoretical Metal Dissolution

Theoretical mass equation:

$$w = \frac{itM}{zF}$$

(A.1)

Where w is the quantity of electrode material dissolved (g), i is the current (A), t is the time in s, M is the relative molar mass of the electrode concerned (g/mol), z is the number of electrons in the oxidation/reduction reaction, F is the Faradays constant.

Sample calculation:

Calculating the theoretical mass of aluminium:

i = 1.3 A

n = 3

M = 26.98 g/mol

F = 96500 coulombs

Using the equation A.1 to calculate the mass at a given time:

Time (s)	Theoretical mass (g)
60	0.007
120	0.015
240	0.029
360	0.044

A.2.3 Power Requirement for Electrocoagulation

Using *Chlorococcum sp.* with aluminium anode as the sample data:

To determine the power input for electrocoagulation:

$$P = voltage \times current \qquad\qquad (A.2)$$

Where P is the power in W.

Using equation A.2 and experimental data we can calculate the power input for a given voltage:

Voltage (V)	Current(A)	Power (W)
2	0.24	0.48
3	0.48	1.45
5	0.97	4.87

To determine the power input per kg of algae:

$$Power\ Input(kWh/kg) = \frac{Power\ Input(W)\Big/1000 \times t(s)\Big/3600}{Mass\ Alg\,ae\ \mathrm{Re}moved(kg)} \qquad (A.3)$$

The mass of algae removed is determined experimentally as the mass of algae that floats to the surface of the cell after electrocoagulation at a given voltage and time. For electrocoagulation at 2 V and 90 s:

$$Power\ Input = \frac{0.48/1000 \times 90/3600}{1.86 \times 10^{-5}}$$
$$= 0.64\ kWh/kg$$

To determine the change in mass, dM, calculate the difference in mass at time t (s) and time t – 1(s):

$$dM(kg) = mass_t(kg) - mass_{t-1}(kg) \qquad (A.4)$$

For electrocoagulation at 2 V, t =90 s, t-1 = 60 s:

$$dM = 1.86 \times 10^{-5} - 6.04 \times 10^{-6}$$
$$= 1.26 \times 10^{-5} kg$$

To determine the change in energy, dE:

$$dE(kWh) = \frac{Power\ Input(W)}{1000} \times \frac{t_n(s) - t_{n-1}(s)}{3600} \qquad (A.5)$$

For electrocoagulation at 2 V, t =90 s, t-1 = 60 s:

$$dE = \frac{0.48}{1000} \times \frac{90 - 60}{3600}$$
$$= 4 \times 10^{-6} kWh$$

Using equations A.2 to A.5 and experimental data we can calculate the power input for a given voltage in kWh/kg, the change in mass and the change in energy:

Time(s)	Mass Removed (kg)	kWh/kg algae	dM	dE	dE/dM
0	0	0	0	0	0
30	0	0	0	4.00E-06	0
60	6.04E-06	1.32	6.04E-06	4.00E-06	0.66
90	1.86E-05	0.64	1.26E-05	4.00E-06	0.32
135	3.10E-05	0.58	1.23E-05	6.00E-06	0.49
180	4.43E-05	0.54	1.33E-05	6.00E-06	0.45
360	6.98E-05	0.69	1.65E-05	2.40E-05	1.45
600	7.30E-05	1.1	1.68E-05	3.20E-05	1.9

A.2.4 Experimental Error

All experiments were performed in triplicate and the standard deviation and error was calculated.

$$Error = \frac{\sigma}{\sqrt{n}}$$ (A.6)

Where σ is the standard deviation and n is the number of samples, in all cases for this research, n = 3.

Using data from a flocculation jar stirrer test for *Chlorococcum sp.* with flocculant 71303 as an example to calculate the error:

Dose (mg/L)	Trial 1	Trial 2	Trial 3	St. Dev	Error
3	0.251	0.254	0.246	0.004	0.002
4	0.206	0.211	0.209	0.003	0.001
5	0.241	0.243	0.240	0.002	0.001
10	0.230	0.232	0.235	0.003	0.001

A.2.5 Mathematical Model

A.2.5-1 Calculation of Parameter b

The parameter b used in the mathematical model describes the average mass ratio of metal ions that are used for coagulation per gram of algae.

$$b = \left[\frac{m_{metal}(g)}{m_{algae}(g)} \right]$$
(A.7)

A.2.5-2 Critical Density Calculation (ρ_C)

Stokes law was used in order to determine the critical density which determines whether a floc will float or settle. The critical density is defined as the initial density of the floc minus the change in density of a settling particle (taken from Stokes law).

Stokes law:

$$v = \frac{2r^2(\rho_{sphere} - \rho_{fluid})g}{9\mu}$$
(A.8)

Where v is the velocity of the particle (m/s), r is the radius of the particle (m), ρ_{sphere} and ρ_{fluid} are the densities of the particle and fluid, g is gravity (m/s^2) and μ is the viscosity of the fluid (Ns/m^2).

The velocity values for each floc were taken as the average velocities of floating flocs determined from experimental data. The density of floc was assumed to be equal to the density of sea water.

Using equation A.8, the critical density was calculated:

	Chlorococcum sp.	Tetraselmis sp.
Velocity (m/s)	3.62E-03	2.54E-03
Radius (m)	1.55E-04	1.66E-04
Viscosity (Ns/m2)	1.08E-03	1.08E-03
$\rho_{sphere} - \rho_{fluid}$ (kg/m3)	75	46
ρ_{fluid} (kg/m3)	1020	1020
ρ_C	945	974

A.2.5-3 Density of Flocs (ρ_{floc})

The density of the flocs were calculated in the MATLAB program. The program calculates a value of the floc density at each ΔC step size, for each time point i.e. for time from 0 to 1200 s (with 1000 steps) and a ΔC step size of 100, there will be a matrix of size 1000 x 100, as shown below:

$$\rho_{floc} = \begin{bmatrix} \rho_{t=0,\Delta C=0} & \cdot & \cdot & \cdot & \rho_{t=0,\Delta C=100} \\ & \cdot & & & \cdot \\ & \cdot & & \cdot & \cdot \\ & \cdot & & \cdot & \cdot \\ \rho_{t=1200,\Delta C=0} & \cdot & \cdot & \cdot & \rho_{t=1200,\Delta C=100} \end{bmatrix}$$

The floc densities at each time can be plotted versus the percent of algae that coagulates. Figure A.10 is a plot obtained from MATLAB showing the change in density of flocs at time 120 s, 480 s, 900 s and 1200 s. It can be seen from the graph that when there is no algae coagulated, which also corresponds to the mass of hydrogen produced being zero, the density of flocs is the same as the density of algae (1020 kg/m^3). As time increases, more algae will coagulate due to metal ion

adsorption and more hydrogen is produced to float flocs. The density can be seen to decrease with time and percentage algae coagulation.
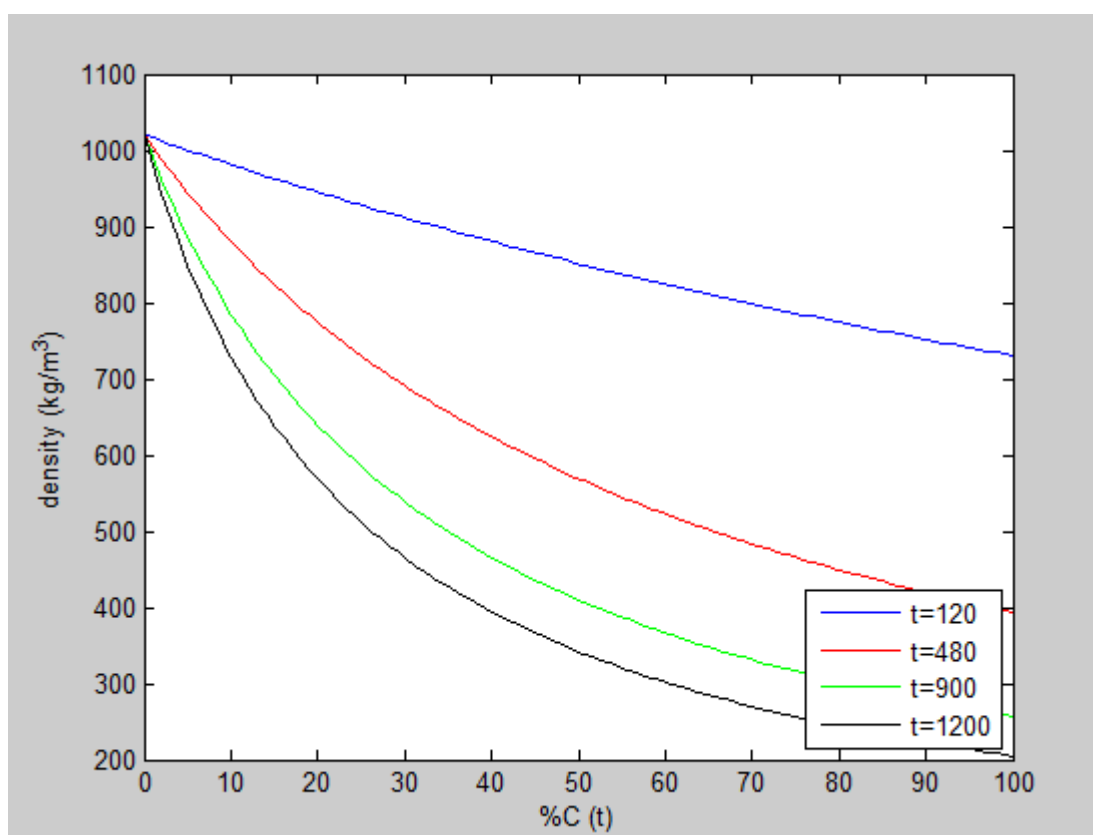
Figure A. 10. Floc density versus precent coagulated algae at different times, obtained from MATLAB. For *Chlorococcum sp.* with stainless steel 430 anode and 3.8 A (5 V).

A.2.5-4 MATLAB Program Code

The following code was used in order to obtain the mathematical models predicted recovery and settling values. Each microalgae species had a different critical density and each anode material had different parameters for metal dissolution calculations. The inputs required for the MATLAB code (highlighted in yellow) are the values for k, b, current applied to the system, initial mass of algae and y, the fraction of algae that does not flocculate. The following table lists the inputs for each system:

	Microalgae System			
	Chlorococcum sp.		Tetraselmis sp.	
	Stainless steel 430	Aluminium	Stainless steel 430	Aluminium
Current at 2V (A)	-	0.24	-	0.19
Current at 3V (A)	0.40	0.48	0.20	0.39
Current at 5V (A)	1.13	0.97	1.13	0.88
Current at 10V (A)	3.80	-	3.80	-
k	2	80	2	80
b	0.05	0.03	0.05	0.03
y	0.02	0.10	0.02	0.10

The following code was used to calculate the floated and settled microalgae at given electrocoagulation conditions. The code below is specifically for electrocoagulation of *Chlorococcum sp.* with the stainless steel 430 anode. However, the user can change highlighted inputs in order to change the code to suit the other systems.

When the input parameters are entered and the code run, the output is an array of the mass of coagulated algae and floated algae with time. The total settled algae can be calculated simply by subtracting the coagulated and floated algae from the starting mass of algae.

MATLAB code:

```matlab
function xfecc

t=0:(1200/1000):1200;
[tt,y2]=solverf2(t,[0.09,0,0]);
% Initial mass of algae, at time t=0 (g)
C=y2(:,2)*1000;
Fd=96500; % Faradays constant
mH=1; % Molecular weight of hydrogen ion (g/mol)
ZH=1; % Valency of hydrogen ion
ab=mH./(ZH.*Fd); % Constant used for H2 dissolution
cur=0.4; % Current applied (A)
yy=cur.*ab*t; %total H2 produced at any time
pmax=6.23E-6./yy(21).*yy; %fraction of H2 used
% 6.23E-6 is the mass H2/mass algae calculated to achieve the
critical floc density of 945kg/m3

rho0=1020000;
rhoH2=80;
d=yy;
prob=linspace(0,1,100);
rho=zeros(length(C),length(prob));
float=zeros(length(C));
for i=1:length(C)
    for j=1:length(prob)
        p=prob(j).*pmax(i);
        rho(i,j) = ((1+p)./((1./rho0)+(p./rhoH2)))./1000;
        if float(i)<1E-12;

            if rho(i,j)<945;
                float(i)=1-prob(j);
            end
        end
    end
end

plot(prob*100,rho(101,:),'b',prob*100,rho(401,:),'r',prob*100,rho(751
,:),'g',prob*100,rho(length(t),:),'k')
xlabel('%C (t)');
```

```matlab
ylabel('density (kg/m^3)');
legend('t=120','t=480','t=900','t=1200','Location','SouthEast');
rec=float(i)'.*C./1000;
xlswrite('modelfe.xls', rec,'rec');
end
function [t,y] = solverf2(tspan,y0)
[t,y] = ode45(@ecmodel2,tspan,y0);
xlswrite('modelfe.xls', y(:,2),'C');
end


function yp = ecmodel2(t,y)
Fd=96500; % Faradays constant
k1=2; % Rate constant of dC/dt
mm=55.845; % Molecular weight of metal ion (g/mol)
ZM=2.2; % Valency of metal ion (based on adjustment for chromium)
aa=mm./(ZM*Fd); % Constant used for metal dissolution
cur=0.4; %current applied (A)
A0=0.09; % Initial mass of algae, at time t=0 (g)
y=a3=0.02; % Percent of algae that does not flocculate
b=0.05; % mass of metal ions used for coagulation per mass algae

yp1=-k1.*((y(1)-(A3.*A0))).^2.*((cur.*t.*aa)-(a.*(A0.*(1-A3)-(y(1)-
(A0.*A3))))));
yp2=k1.*((y(1)-(A3.*A0)).^2).*((cur.*t.*aa)-(a.*(A0.*(1-A3)-(y(1)-
(A0.*A3))))));
yp3=(cur.*mH)./(ZH.*Fd);
yp=[yp1;yp2;yp3];

end
```

A.2.6 Energy Requirements, Carbon Dioxide Emissions and Costs for Dewatering Technologies

The following calculations were done to determine the energy required, carbon dioxide emitted and costs associated with the three dewatering processes investigated.

The carbon dioxide emissions were calculated based on the amount of electrical energy required for each process. For coal based electricity, 1023.81 g CO_2 is produced per kWh (Dones, R. et al. 2004).

The cost of electricity was taken as 18.55 US cents/kWh (PenWell 2011).

The cost of aluminium was taken as $2.27 USD/kg (Metal News 2011).

The cost of alum was taken as 17 US cents/kg (Alibaba 2012).

A.2.6-1 Centrifugation
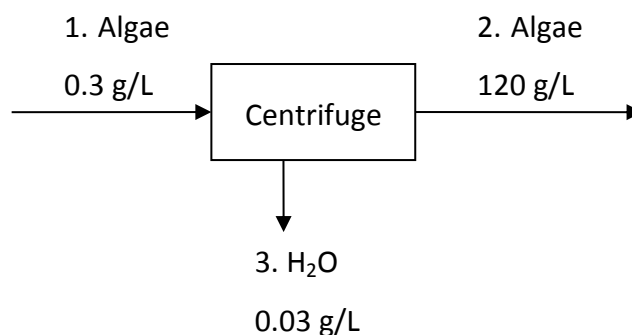
Figure A. 11. Flow diagram for the dewatering of microalgae using centrifugation.

The centrifuge can recover 90 % of microalgae (Moraine, R. et al. 1980). Based on this recovery percentage, with a basis of 1000 kg of algae at 0.3 g/L, the process volume required is 3703703.70 L.

The equipment of choice was the self cleaning plate centrifuge due to its high reliability and performance ability. For a self cleaning plate centrifuge, the operating energy required is 1 kWH/m^3 (Mohn, F. H. 1980).

With a feed volume of 3703703.70 L (3703.70 m^3), the energy required to centrifuge the microalgae is calculated to be 13333.33 MJ (3703.70 kWh).

A balance on the centrifuge system gives:

Stream No.	1	2	3
Concentration (g/L)	0.30	120.00	0.03
Mass (g)	1111111	1000000	111111
Volume (L)	3703703.70	8333.33	3695370.37

Using the CO_2 emissions and electricity price data given previously, the following was calculated:

	Energy (MJ)	CO_2 Emissions(kg)	Cost (USD)
Centrifuge	13333.33	3791.89	687.00

A.2.6-2 Electrocoagulation / Centrifugation

Figure A. 12. Flow diagram for the dewatering of microalgae using a two-step process including electrocoagulation and centrifugation.

The data used to determine the energy and aluminium required for electrocoagulation was taken from the experimental data from this research.

For a basis of 1000 kg of microalgae at a concentration of 0.3 g/L:

The energy required for optimal recovery was based on that for *Chlorococcum sp.* at optimal conditions determined from chapter 6. These conditions were for 88 % microalgae recovery (the maximum obtainable for *Chlorococcum sp.* with the aluminium anode) with electrocoagulation at 2 V for 360 s, which requires 0.69 kWh per kg algae.

The dissolution rate of aluminium was calculated from Faradays law for electrocoagulation of aluminium anode at 2 V (figure A.13). This plot shows the amount of aluminium that dissolves from the anode with time. Using the equation of best fit, it was possible to determine the amount of aluminium that would dissolve in 360 s.
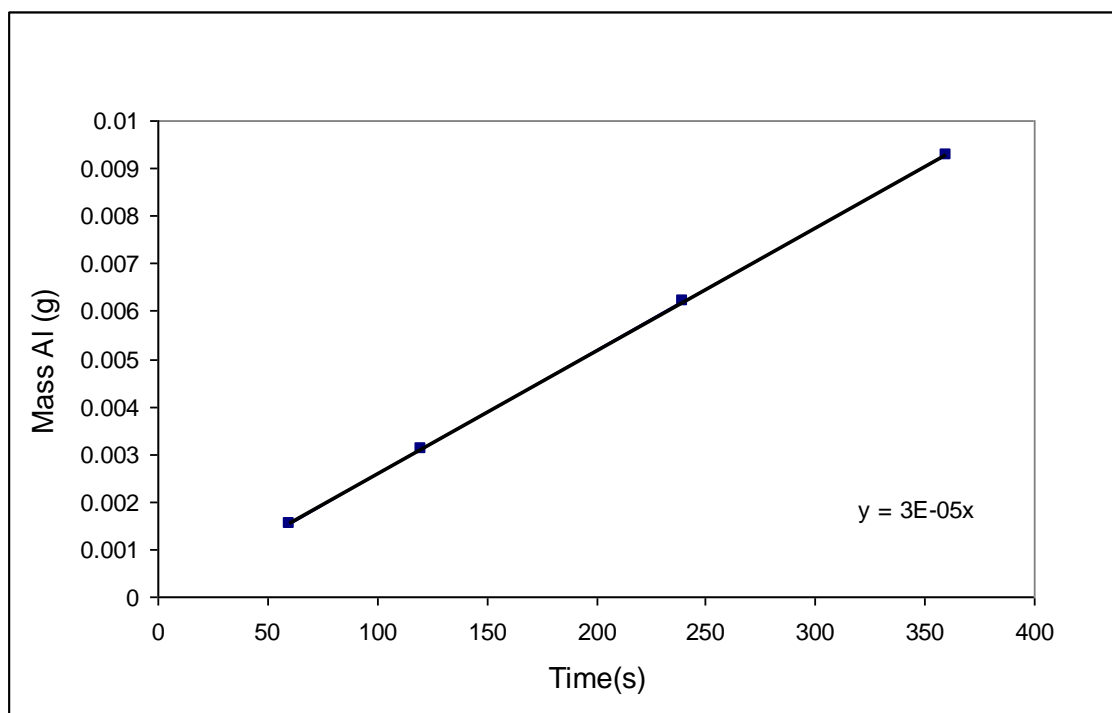
Figure A. 13. Mass of aluminium dissolved with time for electrocoagulation of *Chlorococcum sp.* at 2 V.

Mass of aluminium dissolved from anode (g) = 3 x 10^{-5} x time (s)

= (3 x 10^{-5} x 360) = 0.01 g aluminium dissolved per batch

Electrocoagulation can recover 88 % of microalgae (from experimental data). Based on this recovery percentage, with a basis of 1000 kg of algae at 0.3 g/L, the process volume required is 4208754 L. To electrocoagulate 1000 kg of algae with a volume of 4208754 L, with a batch cell volume of 300 ml, the number of batches equals 14029181. For 4208754 batches, with 0.01 g aluminium dissolving from the anode per batch, the amount of aluminium required is 151.52 kg. The mass of microalgae in the feed stream is 1262.62 kg, calculated based on the concentration and volume of microalgae. Therefore, the energy required to electrocoagulate 1262.62 kg of microalgae is 3136.36 MJ (871.21 kWh).

Aluminium is generally produced by the Hall-Heroult process. This process requires approximately 13.64 kWh of electrical energy per kg of aluminium produced. Therefore, to produce 151.52 kg of aluminium, 31969.70 MJ (8880.47 kWh) of electrical energy is required.

A balance on the electrocoagulation/centrifuge system gives:

Stream No.	1	2	3	4	5
Concentration (g/L)	0.30	1.89	0.04	226.80	0.19
Mass (g)	1262626	1111111	151515	1000000	111111
Volume (L)	4208754	587889	3620865	4409	583480

Using the CO_2 emissions, aluminium production energy requirements, aluminium price data and electricity price data, the following was calculated:

	Energy (MJ)	CO_2 Emissions (kg)	Cost (USD)
Electrocoagulation	3136.4	17.0	161.6
Aluminium production	31969.7	3090.9	1980.1
Centrifuge	2116.4	601.9	109.1
Total 2-step process	**37222.5**	**3709.8**	**2250.7**

A.2.6-3 Alum Flocculation / Centrifugation
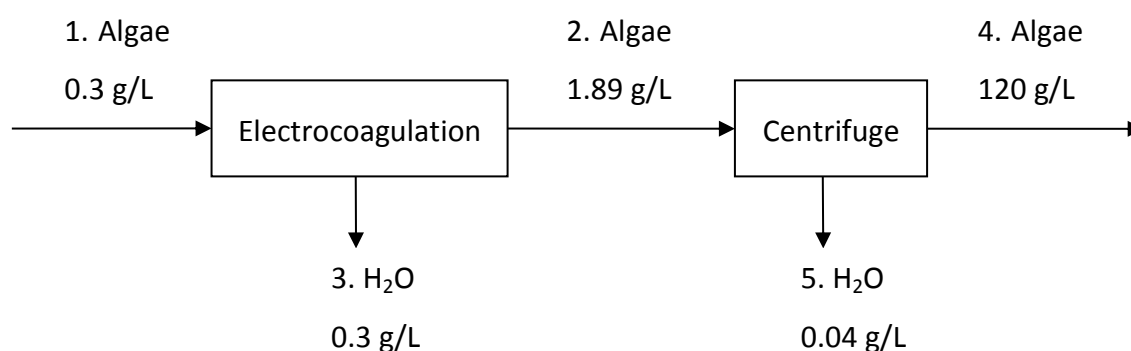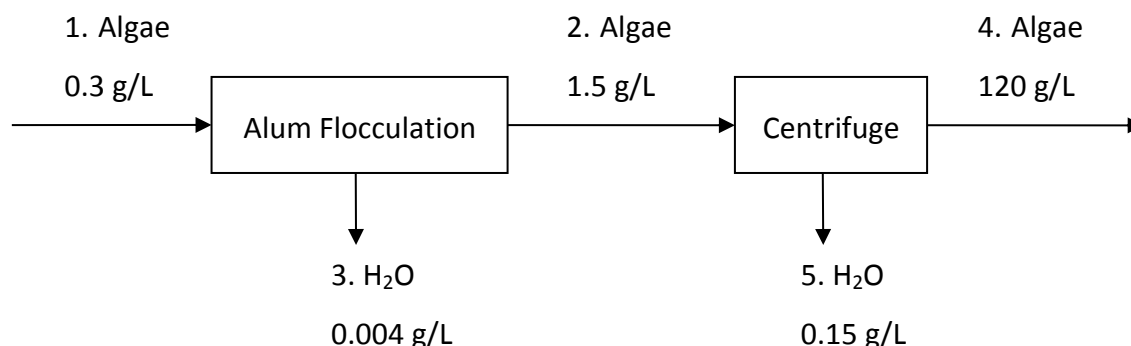

Figure A. 14. Flow diagram for the dewatering of microalgae using a two-step process including alum flocculation and centrifugation.

The optimum dosage of alum flocculation was taken from experimental data as 47 mg/L (optimal dose of *Chlorococcum sp.* see Chapter 5 for details). A dose of 47 mg/L of alum corresponds to 0.157 g alum per g algae (this dose has been adjusted to suit algae of concentration 0.3 g/L). To achieve a final recovery of 1000 kg of algae, 3741114.85 L of algae must be flocculated with alum, which requires 176 kg of alum. The electrical energy required to produce alum is 0.04 kWh/m^3 (Arpke, A. and Hutzler, N. 2006). The energy required to produce alum i.e. the energy required to mix aluminium hydroxide and sulphuric acid, is 0.04 kWh/m^3. To produce 176.21 kg of alum, 0.05 MJ (0.01 kWh) of electrical energy is required.

The energy required to make the raw materials for alum was also taken into account. The energy demand for aluminium hydroxide production via the Bayer process is 16.24 MJ/kg of aluminium hydroxide (Aluminium Industry 2012). The energy demand for sulphuric acid production via the Contact process is 1 MJ/kg of sulphuric acid (Outotec 2012). A mass balance was performed in order to determine the energy required to produce aluminium hydroxide and sulphuric acid. Figure A.15 shows a simplified flow diagram for the production of alum.
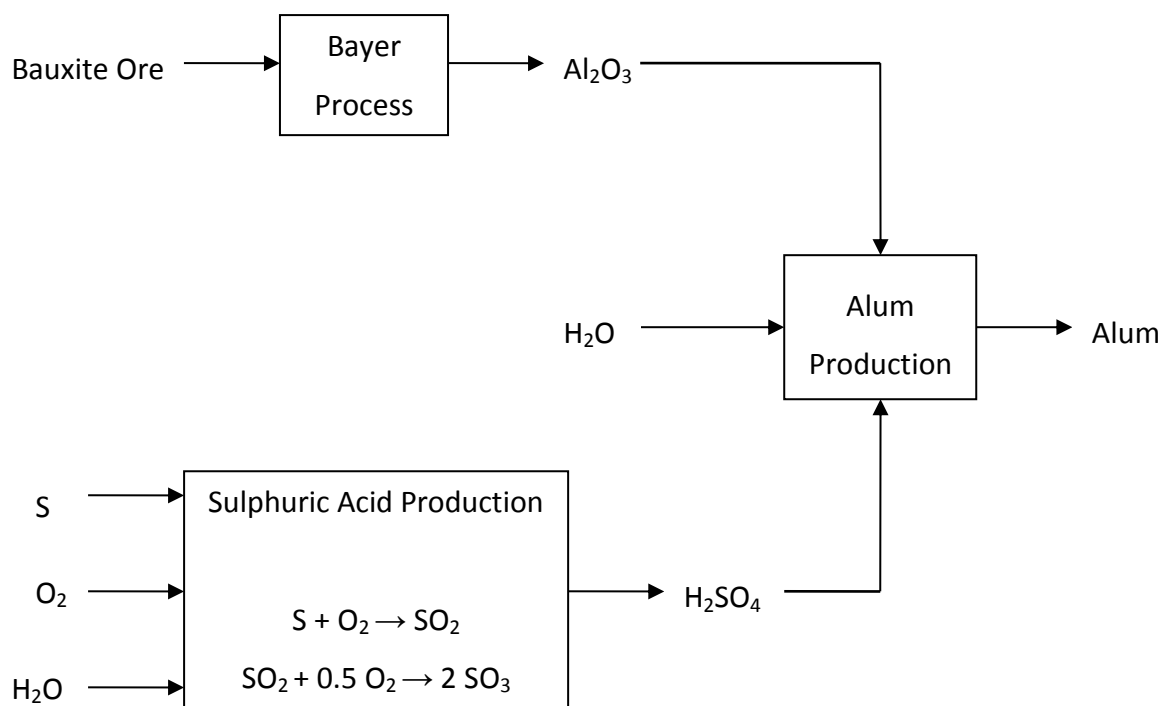
Figure A. 15. Flow diagram for the production of alum.

The balance over the system yields:

	Aluminium Hydroxide	Sulphuric Acid	Alum
Amount (mol)	57112	77735.8	176207
Mass (g)	3172.89	793.22	264.41
Molecular weight (g/mol)	18	98	666.42
Energy (MJ)	927.5	77.74	0.05
CO_2 Emissions (kg)	263.77	22.11	0.02

Therefore, the total energy demand for alum production is 1005.29 MJ (279.25 kWh) and the total mass of carbon dioxide emitted is 285.90 kg.

Alum flocculation requires mixing energy. For one batch, there is a fast mix at 100 rpm for 1 min followed by a slow mix at 60 rpm for 4 min. The mixing energy was calculated by determining the mixing power consumption of the stirrer blades at the two speeds for the total mixing time (Sinnott, R. K. 2005). The shaft power required to drive an agitator can be estimated using the power number:

$$N_p = \frac{P}{D^5 N^3 \rho}$$
(A.9)

Where D is the agitator diameter (m), N is the agitator speed (s^{-1}), ρ is the fluid density (kg/m^3) and P is the shaft power (W).

Equation A.9 can be rearranged to solve for the shaft power. The power number can be obtained by using a power correlation for a single three bladed propeller and the Reynolds number.

$$Re = \frac{D^2 N \rho}{\mu}$$
(A.10)

Where μ is the viscosity of the fluid (Ns/m^2)

	p/D	D/D$_T$
Curve 1	1·8	0·30
Curve 2	1·4	0·33
Curve 3	1·0	0·33
Curve 4	1·0	0·40

Figure A. 16. Power correlation for a single three bladed propeller (Sinnott, R. K. 2005).

Using curve 4 (as it had the best fit for the given conditions) from figure A.16 and the calculated Reynolds number for the algae, the power number and finally the shaft power can be determined.
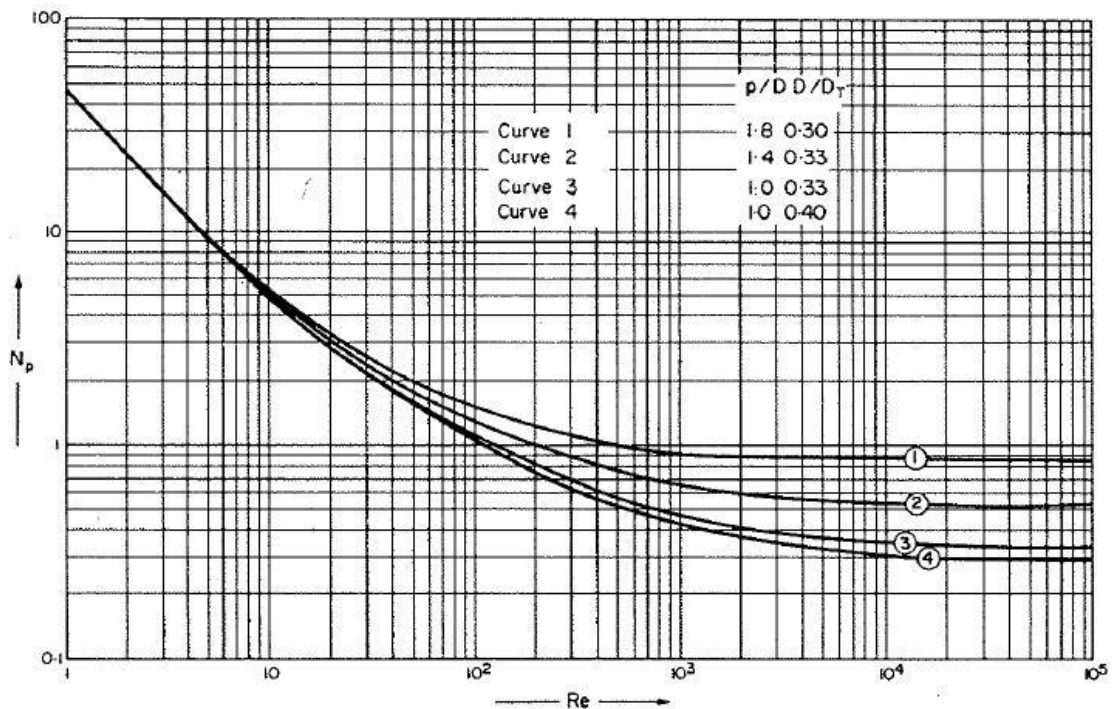
	100rpm 1 min - Fast Mix	60rpm 4 min - Slow Mix
D (m)	0.05	0.05
N (rev/s)	1.67	1.00
ρ_{fluid} (kg/m^3)	1020.00	1020.00
μ_{fluid} (Ns/m^2)	0.00	0.00
Reynolds Number	3935.19	2361.11
Power Number	0.35	0.38
P (W)	5.16E-04	1.21E-04
P (MW)	5.16E-10	1.21E-10
Total time - batches x time (s)	224466891.13	897867564.53
Power for all batches (MJ)	0.12	0.11

Total energy for alum flocculation: 0.23 MJ

A balance on the alum flocculation/centrifuge system gives:

Stream No.	1	2	3	4	5
Concentration (g/L)	0.3	1.5	0.0037	120	0.15
Mass (g)	1122334	1111111	11223	1000000	111111
Volume (L)	3741114.85	740740.7	3000374	8333.33	732407.41

Using the CO_2 emissions, aluminium production energy requirements, aluminium price data and electricity price data, the following was calculated:

	Energy (MJ)	CO$_2$ Emissions (kg)	Cost (USD)
Alum flocculation	2.25E-01	6.39E-02	1.16E-02
Alum production	1005.29	285.90	29.96
Centrifuge	2666.67	758.38	137.41
Total 2-step process	**3672.18**	**1044.34**	**167.37**

A.2.6-4 Dewatering with Microalgae Concentration 1 g/L

For the dewatering processes using microalgae at a concentration of 1 g/L, all calculations performed to obtain the data for energy demand, carbon dioxide

emissions and costs were performed in the same manner as for microalgae with a concentration of 0.3 g/L detailed above. The only difference being the starting concentration of microalgae, which reduced the volume of microalgae used in the dewatering process.

A.2.7. Rise Velocity of Floc

The rise velocity of the flocs were determined from analysis of the Image J software. The software enabled the calculation of distance travelled by the floc in relation to the time interval when the images were taken. The analysis gave the following data:

For *Chlorococcum sp.*:

Time = 0s	Time = 0.05s	Time = 0.1s	Velocity 1 (m/s)	Velocity 2 (m/s)	Average Velocity (m/s)
0	371.26	388.52	7.43E-03	7.77E-03	7.60E-03
0	123.08	140.66	2.46E-03	2.81E-03	2.64E-03
0	70.30	79.12	1.41E-03	1.58E-03	1.49E-03
0	70.88	105.80	1.42E-03	2.12E-03	1.77E-03
0	290.13	316.04	5.80E-03	6.32E-03	6.06E-03
0	290.13	316.04	5.80E-03	6.32E-03	6.06E-03
0	70.33	88.35	1.41E-03	1.77E-03	1.59E-03
0	105.86	124.33	2.12E-03	2.49E-03	2.30E-03
0	132.16	131.87	2.64E-03	2.64E-03	2.64E-03
0	131.87	105.86	2.64E-03	2.12E-03	2.38E-03
0	342.97	360.87	6.86E-03	7.22E-03	7.04E-03
0	70.33	114.29	1.41E-03	2.29E-03	1.85E-03

For *Tetraselmis sp.*:

Time = 0s	Time = 0.05s	Time = 0.1s	Velocity 1 (m/s)	Velocity 2 (m/s)	Average Velocity (m/s)
0	123.39	96.70	2.47E-03	1.93E-03	2.20E-03
0	123.39	140.66	2.47E-03	2.81E-03	2.64E-03
0	136.25	139.96	2.73E-03	2.80E-03	2.76E-03
0	70.33	123.08	1.41E-03	2.46E-03	1.93E-03
0	67.10	75.31	1.34E-03	1.51E-03	1.42E-03
0	131.87	175.82	2.64E-03	3.52E-03	3.08E-03
0	70.88	87.91	1.42E-03	1.76E-03	1.59E-03
0	146.15	153.01	2.92E-03	3.06E-03	2.99E-03
0	251.25	269.32	5.03E-03	5.39E-03	5.21E-03
0	131.87	114.29	2.64E-03	2.29E-03	2.46E-03
0	123.08	114.29	2.46E-03	2.29E-03	2.37E-03
0	96.70	87.91	1.93E-03	1.76E-03	1.85E-03

Average velocity for *Chlorococcum sp.* flocs = 3.62E-03 m/s

Average velocity for *Tetraselmis sp.* flocs = 2.54E-03 m/s

A.2.8 Hydrogen Evolution and Bubble Calculations

A.2.8-1 Hydrogen Evolution

The volume of hydrogen evolved from the cathode was determined using the theoretical mass equation (equation A.1).

For the two optimum recovery conditions of *Chlorococcum sp.* used as example calculations:

- 5 V, 600 s, 89 % microalgae recovery
- 5 V, 1200 s, 97 % microalgae recovery

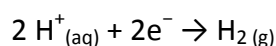The mass of hydrogen is calculated to be:

m(H^+, t = 600 s) = 0.0075 g

m(H^+, t = 1200 s) = 0.0150 g

The amount of H^+ can then be calculated using the molecular weight (where amount is mass/molecular weight):

n(H^+, t = 600 s) = m/M = 0.0075 mol

n(H^+, t = 1200 s) = m/M = 0.0150 mol

$$2\ H^+_{(aq)} + 2e^- \rightarrow H_{2\ (g)}$$

From the hydrogen evolution equation(above), the amount of hydrogen ions is double that of hydrogen gas.

Therefore the amount of hydrogen gas calculates to be:

n(H_2, t = 600 s) = 0.0075/2 = 0.0038 mol

n(H_2, t = 1200 s) = 0.0150/2 = 0.0075 mol

The ideal gas law is then used to determine the volume of hydrogen gas evolved:

$$PV = nRT \hspace{4cm} \text{(A.11)}$$

$$V = \frac{nRT}{P}$$

Where P is the pressure (atm), V is the volume (L), n is the amount of gas (mol), R is the universal gas constant (0.00821 L.atm/mol.K) and T is the temperature (K).

V(H_2, t = 600 s) = 0.092 L = 9.22 x 10^{-5} m^3

V(H_2, t = 1200 s) = 0.185 L = 1.85 x 10^{-4} m^3

A.2.8-2 Number of Bubbles Required for Flocculation

It is assumed that all hydrogen gas is used to produce the bubbles and that the bubbles are 100 % hydrogen.

From the images of electrocoagulation obtained from the high speed camera and the use of Image J software, it was possible to determine the average hydrogen bubble radius.

Average bubble radius (*Chlorococcum sp.* experiments) = 3.80×10^{-5} m

Average bubble radius (*Tetraselmis sp.* experiments) = 4.27×10^{-5} m

The volume of one bubble can be calculated from the volume of a sphere:

$$V(sphere) = \frac{4\pi r^3}{3}$$ (A.12)

V(bubble, *Chlorococcum sp.*) = 2.31×10^{-13} m^3

V(bubble, *Tetraselmis sp.*) = 3.27×10^{-13} m^3

From the Image J software analysis, an average floc volume was calculated.

Average floc volume, *Chlorococcum sp.* = 2.28×10^{-11} m^3

Average floc volume, *Tetraselmis sp.* = 3.40×10^{-11} m^3

The number of flocs for a specific electrocoagulation condition was calculated as:

$$No\ flocs = \frac{Total\ floc\ volume}{Average\ floc\ volume}$$ (A.13)

From the Image J software analysis, an average number of bubbles per floc was calculated.

Average number of bubbles in *Chlorococcum sp.* flocs = 21.5

Average number of bubbles in *Tetraselmis sp.* flocs = 24.5

The number of bubbles in the flocculated matter for a specific electrocoagulation condition was calculated as:

$$No\ bubbles = No\ flocs \times Average\ no\ bubbles$$ (A.14)

A.2.8-3 Percentage of Hydrogen used for Flotation

The percentage of hydrogen bubbles that were used for flotation was calculated as the fraction of hydrogen gas in the flocculated matter in comparison to the total hydrogen produced.

The total mass of hydrogen produced was determined using the method outlined in section A.2.8-1. The hydrogen used in flotation was calculated using the volume of floc matter measured for each experimental electrocoagulation run. Using the measured volume of floc matter, the number of bubbles in the floc was calculated. The volume and mass of the bubbles was then determined from the number of bubbles in the floc matter and the average volume of one bubble.

$$\%\ H_2\ used\ for\ floation = \left(\frac{Mass\ H_2\ in\ floc}{Total\ mass\ H_2} \right) \times 100\% \tag{A.15}$$

A.3 Supporting Results

A.3.1 Polyelectrolyte Flocculation Mixing Conditions

The mixing conditions for polyelectrolyte flocculants were obtained by performing flocculation experiments on various mixing speeds and durations to achieve the best results. The following table shows a list of the different mixing conditions tested for polyelectrolyte flocculant 82230.

Table A. 1. Polyelectrolyte flocculant mixing conditions.

Test No.	1st Mixing Condition		2nd Mixing Condition	
	Speed (rpm)	Time (sec)	Speed (rpm)	Time (sec)
0	no flocculation (control)			
1	100	120	100	600
2	100	300	50	300
3	80	120	50	600
4	80	300	50	300
5	100	600	50	600
6	80	600	50	300
7	200	10	50	600
8	200	10	50	300
9	300	10	50	300
10	80	120	20	600
11	100	120	20	600

The performance of the flocculant was determined by turbidity measurements taken after the sample had settled for 30 min. The numbers listen in table A.1 associated to each mixing condition correspond to the numbers on the x axis on figure A.17, which shows the performance of the polyelectrolyte at each condition. From the figure, it can be seen that condition 7 gives the best flocculation results (i.e. the highest removal of microalgae and therefore lowest turbidity measurement). Therefore, the

polyelectrolyte flocculation experiments conducted in this research were performed with a fast mix of 200 rpm for 10 sec, followed by a slow mix of 50 rpm for 10 min.
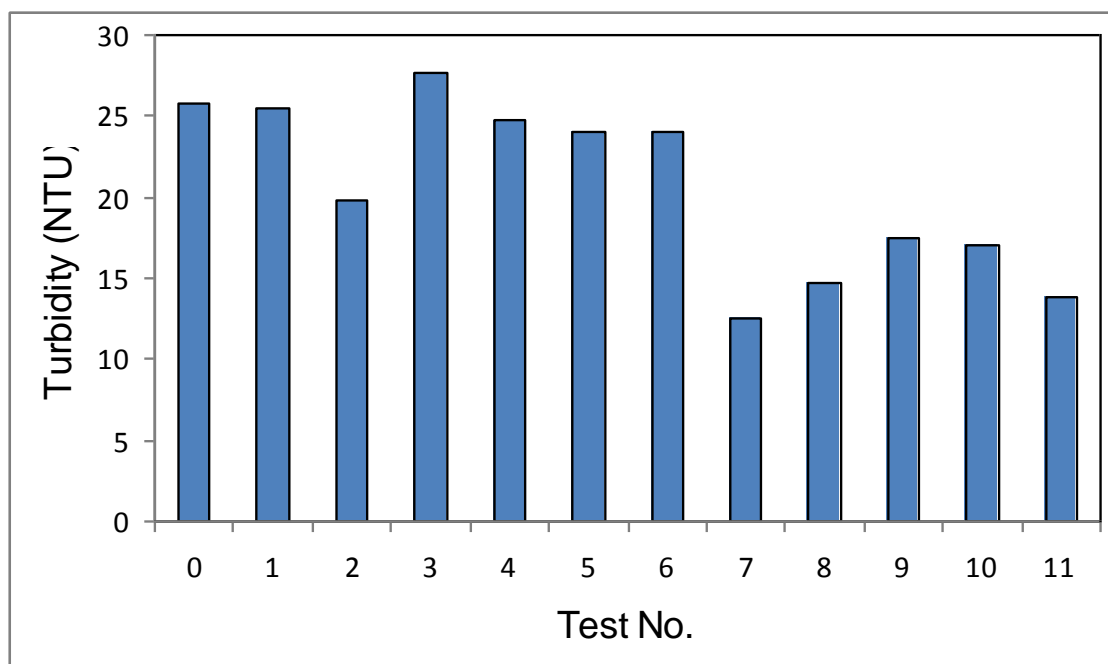

Figure A. 17. Turbidity of solution after flocculation with 82230 at varying mixing conditions.

A.3.2 Metal Dissolution from Anode

ICP analysis for metals concentrations in the microalgae before and after electrocoagulation was performed by a certified external laboratory company.

The following table shows a metals concentration result for:

Sample 1 - fresh algae with no electrocoagulation

Sample 2 - algae after electrocoagulation with stainless steel 430 anode

Sample 3 - algae after electrocoagulation with aluminum anode

Table A. 2. ICP metals analysis results.

Client Sample ID			#1	#2	#3
Sample Matrix			Other	Other	Other
mgt-LabMark Sample No.			10-No11624	10-No11625	10-No11626
Date Sampled			Nov 30, 2010	Nov 30, 2010	Nov 30, 2010
Test/Reference	PQL	Unit			
Alkali Metals					
Calcium	5	mg/kg	4900	1400	650
Potassium	5	mg/kg	6000	2200	2300
Sodium	5	mg/kg	270	180	140
Heavy Metals					
Aluminium	10	mg/kg	240	140	137000
Iron	5	mg/kg	3300	67000	2900
Chromium	5.0	mg/kg	< 5	12000	23
Lead	5	mg/kg	< 5	< 5	34
Nickel	5.0	mg/kg	< 5	130	7.6

From table A.2, we can see that sample 2 shows much higher levels of iron compared to sample 1. These results confirm that for the stainless steel anode, iron is the major dissolving species.

From table A.2, we can see that sample 3 shows much higher levels of aluminium compared to sample 1. These results confirm that for the aluminium anode, aluminium is the dissolving species.

A.3.3 Colour of Ferrous Iron Dissolution

The colour of iron precipitates does not affect the overall results. The absorbance of the floated layer, supernatant and settled layer was measured. It was possible to determine the mass of microalgae in each layer. The concentration and starting volume of microalgae made it possible to know the mass expected in the total system. Even though the iron precipitates are green in colour, and the UV-VIS spectrophotometer detects green colour at 570 nm, an overall mass balance was performed on the system confirmed that there wasn't an increase in mass caused by iron precipitates, i.e. the mass of algae in the floated layer, supernatant and settled later summed to equal the total mass in the system. The problem of coloured precipitates does not occur for the aluminium anode. Figure A.18 shows that the aluminium anode produces aluminium precipitates with no colour.
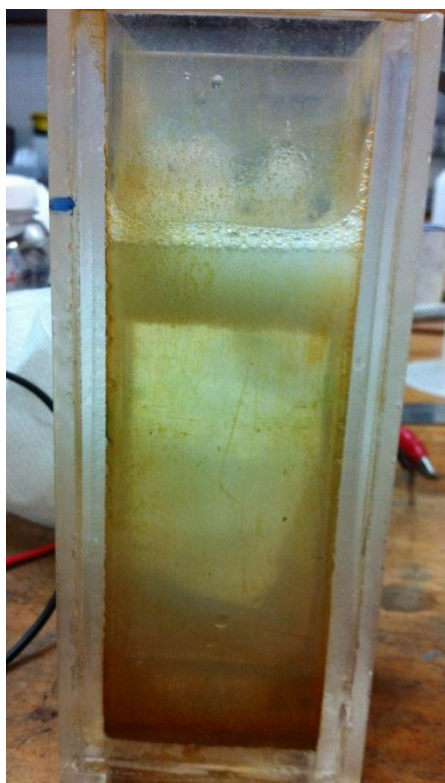
Figure A. 18. Electrocoagulation performed on salt water media, with aluminium anode.

A.3.4 Half Cell Electrocoagulation

The half cell electrocoagulation experiments involved using a porous filter paper membrane to separate the anode and cathode sides of the electrocoagulation cell. Figure A.19 shows a schematic diagram of the half cell. Electrocoagulation experiments were performed with the usual protocol with the membrane in place. After electrocoagulation, the zeta potential of each side was measured. Experiments were also performed with a mixer placed on the anode side of the cell. This mixer was set at 400 rpm and was operating only while the current was applied.
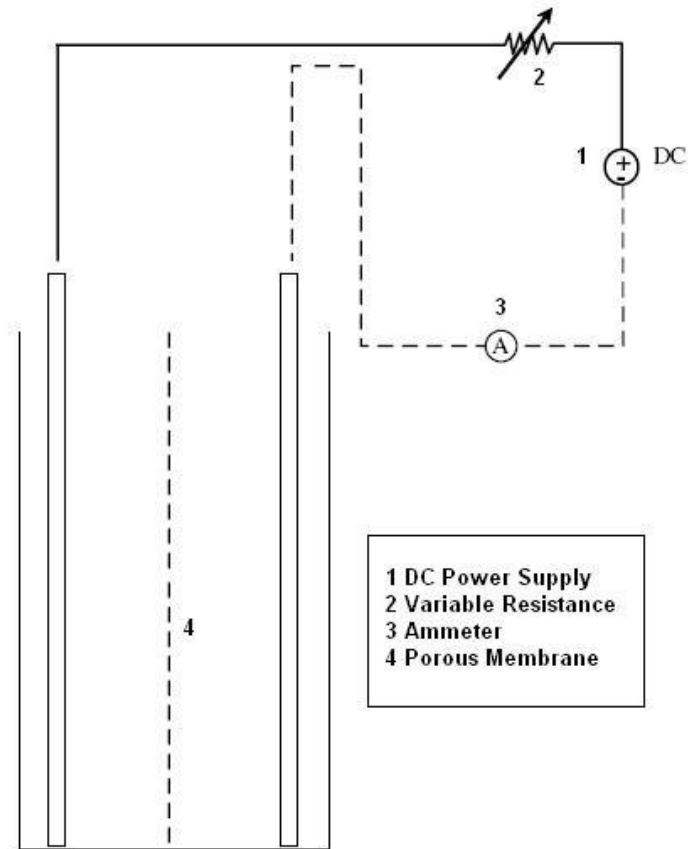
Figure A. 19. Schematic diagram of electrocoagulation half cell.

Figure A.20 shows a birds-eye view of the batch half cell after electrocoagulation with stainless steel 430 cathode and anode, with no mixing. From the figure, it can be seen that the left hand side (anode, +), the algae does not float to the surface, and on the right hand side (cathode, -) the algae does float to the surface. The hydrogen bubbles are also visible on the cathode side.
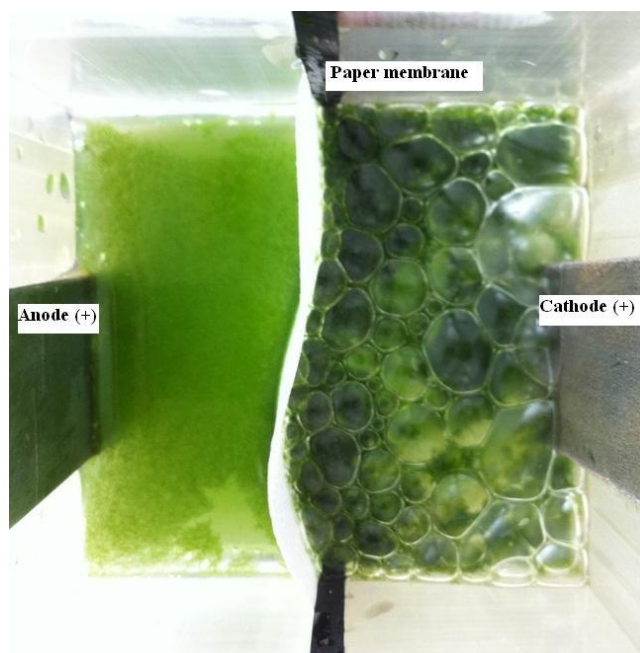
Figure A. 20. After electrocoagulation with the half cell set up.

A.3.5 Electrochemical Series

The electrochemical series is built up by arranging various redox equilibria in order of their standard electrode potentials (redox potentials). The most negative E° values are placed at the top of the electrochemical series, and the most positive at the bottom. The difference in the positions of equilibrium causes the number of electrons which build up on the metal electrode and the platinum of the hydrogen electrode to be different. This produces a potential difference which is measured as a voltage. Metals at the top of the series are good at giving away electrons. They are good reducing agents. The reducing ability of the metal increases as you go up the series. The more negative the E° value, the more the position of equilibrium lies to the left, i.e. the more readily the metal loses electrons. The more negative the value, the stronger reducing agent the metal is.

Table A. 3. A selected part of the electrochemical series.

Equilibrium	E° (volts)
$Li^+_{(aq)} + e^- \rightleftharpoons Li_{(s)}$	-3.03
$K^+_{(aq)} + e^- \rightleftharpoons K_{(s)}$	-2.92
$Ca^{2+}_{(aq)} + 2e^- \rightleftharpoons Ca_{(s)}$	-2.87
$Na^+_{(aq)} + e^- \rightleftharpoons Na_{(s)}$	-2.71
$Mg^{2+}_{(aq)} + 2e^- \rightleftharpoons Mg_{(s)}$	-2.37
$Al^{3+}_{(aq)} + 3e^- \rightleftharpoons Al_{(s)}$	-1.66
$Zn^{2+}_{(aq)} + 2e^- \rightleftharpoons Zn_{(s)}$	-0.76
$Fe^{2+}_{(aq)} + 2e^- \rightleftharpoons Fe_{(s)}$	-0.44
$Pb^{2+}_{(aq)} + 2e^- \rightleftharpoons Pb_{(s)}$	-0.13
$2H^+_{(aq)} + 2e^- \rightleftharpoons H_{2(g)}$	0
$Cu^{2+}_{(aq)} + 2e^- \rightleftharpoons Cu_{(s)}$	+0.34
$Ag^+_{(aq)} + e^- \rightleftharpoons Ag_{(s)}$	+0.80
$Au^{3+}_{(aq)} + 3e^- \rightleftharpoons Au_{(s)}$	+1.50

A.3.6 Mini Electrocoagulation Cell

A mini cell (figure A.21) was used in order to observe the bubble/floc complexes and the change in hydrogen bubble size with pH. Figure A.22 shows a schematic diagram of the mini cell. The electrodes used ferritic stainless steel and were set up both vertically and horizontally in order to observe the rising bubble/floc aggregates. Figure A.23 shows the schematic set up used in order to capture images with the

MotionPro high speed camera. Figures A.24 and A.25 show actual images of the camera set up and lens used.

The set up of the mini cell was slightly different to the batch electrocoagulation cell used in the main experiments; the mini cell could only hold 7 ml of sample, and the electrodes were orientated in a side on position, not front on as was used in the batch experiments. These differences in cell set up would give different results as the surface area of electrode will influence the nucleation of hydrogen bubbles. However, these results are only used qualitatively in order to observe the bubble floc interactions.
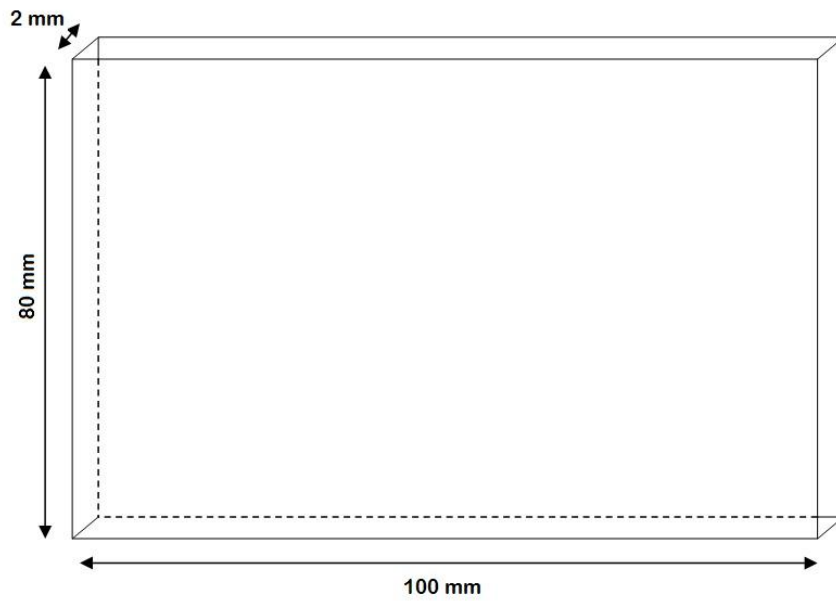

Figure A. 21. Mini electrocoagulation cell.

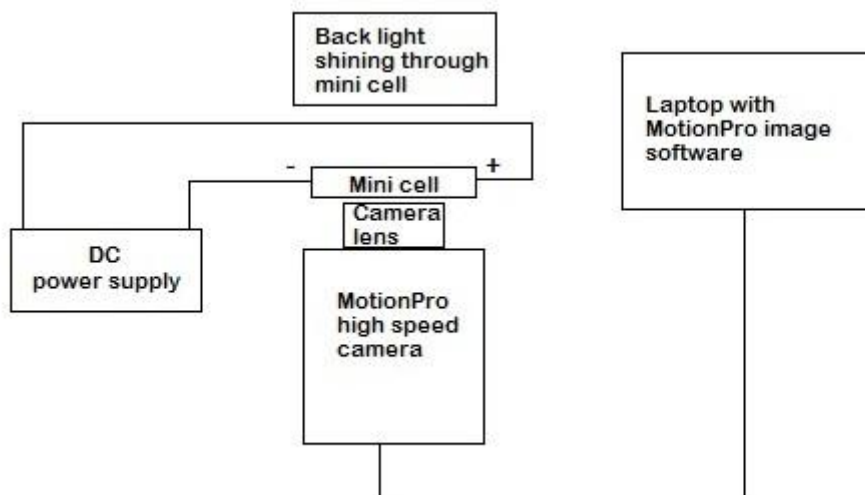Figure A. 22. Schematic diagram of mini cell.

Figure A. 23. Schematic diagram of mini cell and high speed camera set up.

Figure A. 24. Mini cell and high speed camera.

Figure A. 25. Lens used for high speed camera.

A.3.7 Effect of Batch Volume of Microalgae Recovery

Figures A.26 and A.27 show the microalgal recovery as a function of electrolysis time for varying liquid volumes with electrocoagulation at a constant current density of 1190 A/m^2. The results show that changes in volume do not have a significant effect on microalgal recovery, if the current density is kept constant.
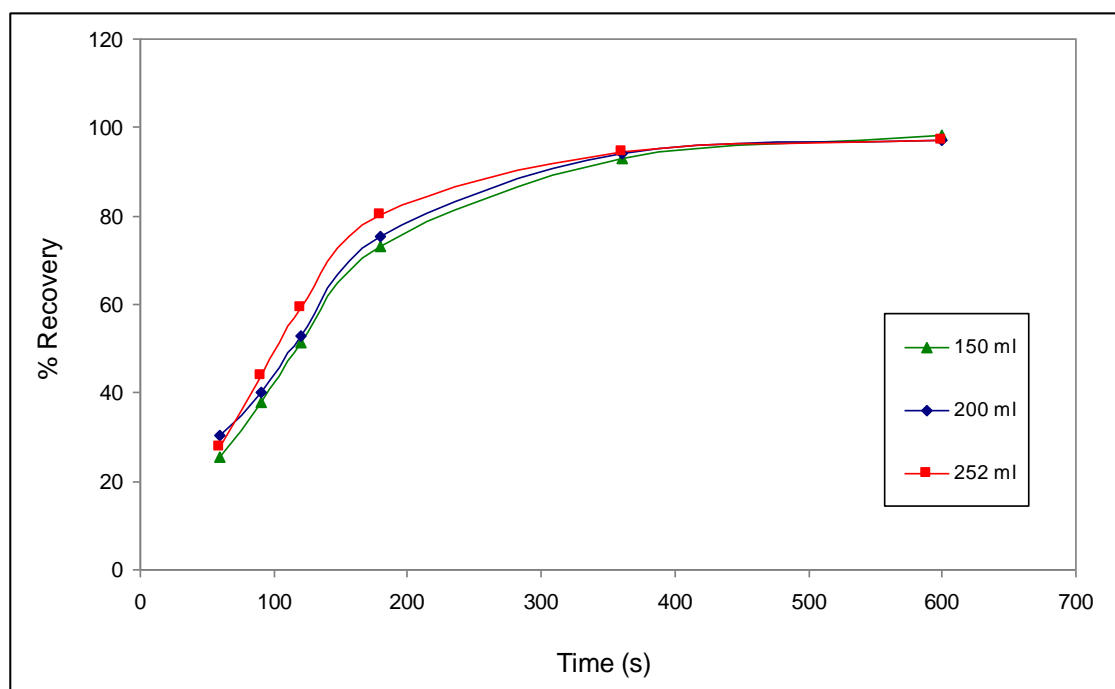

Figure A. 26. Microalgae recovery as a function of electrolysis time for varying sample volumes with electrocoagulation at a constant current density of 1190 A/m^2, with *Chlorococcum sp*. with the aluminium anode.[1]
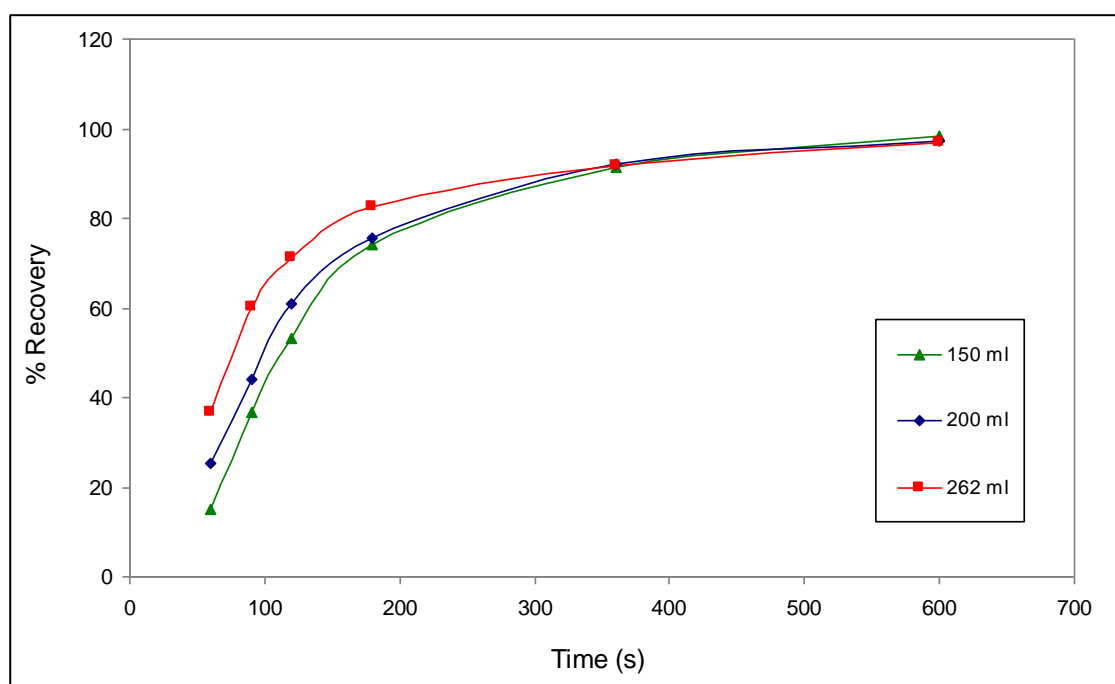
Figure A. 27. Microalgae recovery as a function of electrolysis time for varying sample volumes with electrocoagulation at a constant current density of 1190 A/m^2, with *Tetraselmis sp.* with the aluminium anode.[1]

A.4 Published Work

A.4.1 Publications

Danquah, M.K., Ang, L., Uduman, N., Moheimani, N., Forde, G., (2009), "Dewatering of microalgae culture for biodiesel production: exploring polymer flocculation and tangential flow filtration", *Journal of chemical technology and biotechnology,* Vol 48, pp. 1078 – 1083.

Uduman, N., Qi, Y., Danquah, M.K., Hoadley, F.A., (2010), "Dewatering of microalgal cultures: A major bottleneck to algae-based fuels", *Journal of renewable and sustainable energy*, Vol 2, 012701.

Uduman, N. Qi, Y., Danquah, M.K., Hoadley, F.A., (2010), "Marine microalgae flocculation and focused beam reflectance measurement", *Chemical engineering journal,* Vol 162, pp. 935 – 940.

Uduman, N. Bourniquel, V., Danquah, M.K., Hoadley, F.A., (2011), "A parametric study of electrocoagulation as a recovery process of marine microalgae for biodiesel production", *Chemical engineering journal,* Vol 174, No 1, pp. 249 – 257.

A.4.2 Pending Publications

Uduman, N., Danquah, M.K., Hoadley, F.A., (2012), "Microalgae dewatering - technology advancement using electrocoagulation", *Modern energy storage, conversion and transmission.*

Uduman, N. and Hoadley, F.A., (2012), "Modelling batch electrocoagulation of marine microalgae", *Chemical engineering journal*.